UNIVERSIDAD
DE GRANADA

February 2025

Doctoral Thesis

PhD Programme in Fundamental and Systems Biology

MicroRNAs in parasite-host interaction:
Cooperative effect and biomedical applications

José María Medina Muñoz

Supervisor:

Michael Hackenberg

Editor: Universidad de Granada. Tesis Doctorales
Autor: José María Medina Muñoz
ISBN: 978-84-1195-846-2
URI: https://hdl.handle.net/10481/106330

Abstract

Ixodes ricinus, the European castor bean tick, is a hard-bodied parasitiform mite that relies on blood feeding for survival and reproduction. It is widely distributed across Europe and Northern Africa and is responsible for transmitting several pathogens, including *Borrelia burgdorferi*, the causative agent of Lyme borreliosis. The increasing prevalence of tick-borne diseases in recent years, exacerbated by climate change and habitat modifications, poses significant public health and economic concerns. The ability of ticks to successfully parasitize their hosts is largely attributed to their saliva, which contains bioactive molecules capable of manipulating different host defense mechanisms, including the immune system, wound healing processes, and blood coagulation. Recent studies propose non-coding RNAs (ncRNAs) present in saliva, such as microRNAs (miRNAs), as potential modulators of the tick-host interface.

miRNAs are highly conserved non-coding genes present in virtually all metazoans. Their functional product consists of small RNA molecules (21–23 bp) that regulate gene expression negatively and post-transcriptionally. Their importance in cellular homeostasis has been extensively demonstrated through functional assays and is also evident in the apparent causal involvement of miRNAs in various pathologies. Recent findings suggest that miRNAs can function cooperatively, enhancing their regulatory effects. Long non-coding RNAs (lncRNAs), in turn, have been proposed to act as miRNA sponges, possessing the ability to sequester miRNAs via target regions on the lncRNAs themselves, adding another layer of complexity to the process of gene regulation.

This thesis aims to determine the functional importance of miRNAs and lncRNAs in the parasitism and blood-feeding processes carried out by *I. ricinus*. To achieve this, we comprehensively analyzed the transcriptomic dynamics *of I. ricinus* during active parasitism, assessing the role of gene products, miRNAs, and lncRNAs in the tick-host interface through an extensive bioinformatics approach. The ultimate goal is to establish a foundation for the development of novel clinical and pest control strategies.

During the course of this thesis, we collaborated on the generation of a new reference genome assembly for *I. ricinus*. The use of this new reference genome, along with multiple datasets from various tissues, such as salivary glands, midgut, saliva, and even the whole tick body, allowed us to improve the annotation of miRNAs and lncRNAs.

To analyze the potential functional impact of tick miRNAs on the host, we designed a new computational workflow that integrates miRNA target site prediction and the functional characterization of regulated genes. Target prediction incorporates target sequence conservation profiles based on position and recent findings on the importance of the TNRC6 protein in the synergistic cooperation of miRNAs in gene silencing.

By applying the aforementioned workflow, we could demonstrate that integrating target sequence conservation into miRNA target prediction drastically reduces the number of predicted targets. We found that conserved predicted target genes were functionally enriched in pathways highly relevant to host defense. In addition to this, we successfully detected cooperative target regions for tick salivary miRNAs in host genes that were abundant in skin cells of the host and involved in key processes at the tick-host interface, such as immunity, wound healing, nociception, and mechanosensation. We also demonstrated that these tick miRNAs are present and protected in extracellular vesicles, which increases their potential to interact with host cells.

To study how lncRNAs can influence the parasitism of *I. ricinus*, we generated a *de novo* assembled reference transcriptome from tick salivary gland and midgut samples. These samples were collected at different time points from sister ticks that were either unfed, fed on naïve hosts, or fed on hosts that had been previously exposed to ticks and, therefore, sensitized to tick parasitism. The specific samples allowed us to analyze the transcriptional dynamics occurring under these different conditions over time in non-coding RNAs and, additionally, in coding RNAs.

By means of this analysis, we observed significant differences between the specific groups of ticks and found that genes differentially expressed over time are involved in key biological processes, including glycosylation and protein folding, which play crucial roles in tick adaptation to parasitism and in the evasion of the host immune response.

Several lncRNAs were identified as potential host miRNA sponges, with the capability to inhibit the action of host miRNAs involved in critical processes against parasitism. One of these lncRNAs emerges as the most promising candidate, as it was detected in extracellular vesicles and it has the capability to impair glycosylation processes in hosts, which are essential for host immunity, and signaling processes of extracellular matrix receptors.

Overall, this thesis aims to establish a foundation for future research and clinical advancements, such as the development of therapeutic miRNAs and antimiRs. Continued investigation, particularly in biological validation and host response analysis, will be crucial to complement the bioinformatically driven results presented in this thesis. This knowledge will be essential in ultimately reducing the public health and economic impact of *I. ricinus* on our society.

Graphical abstract

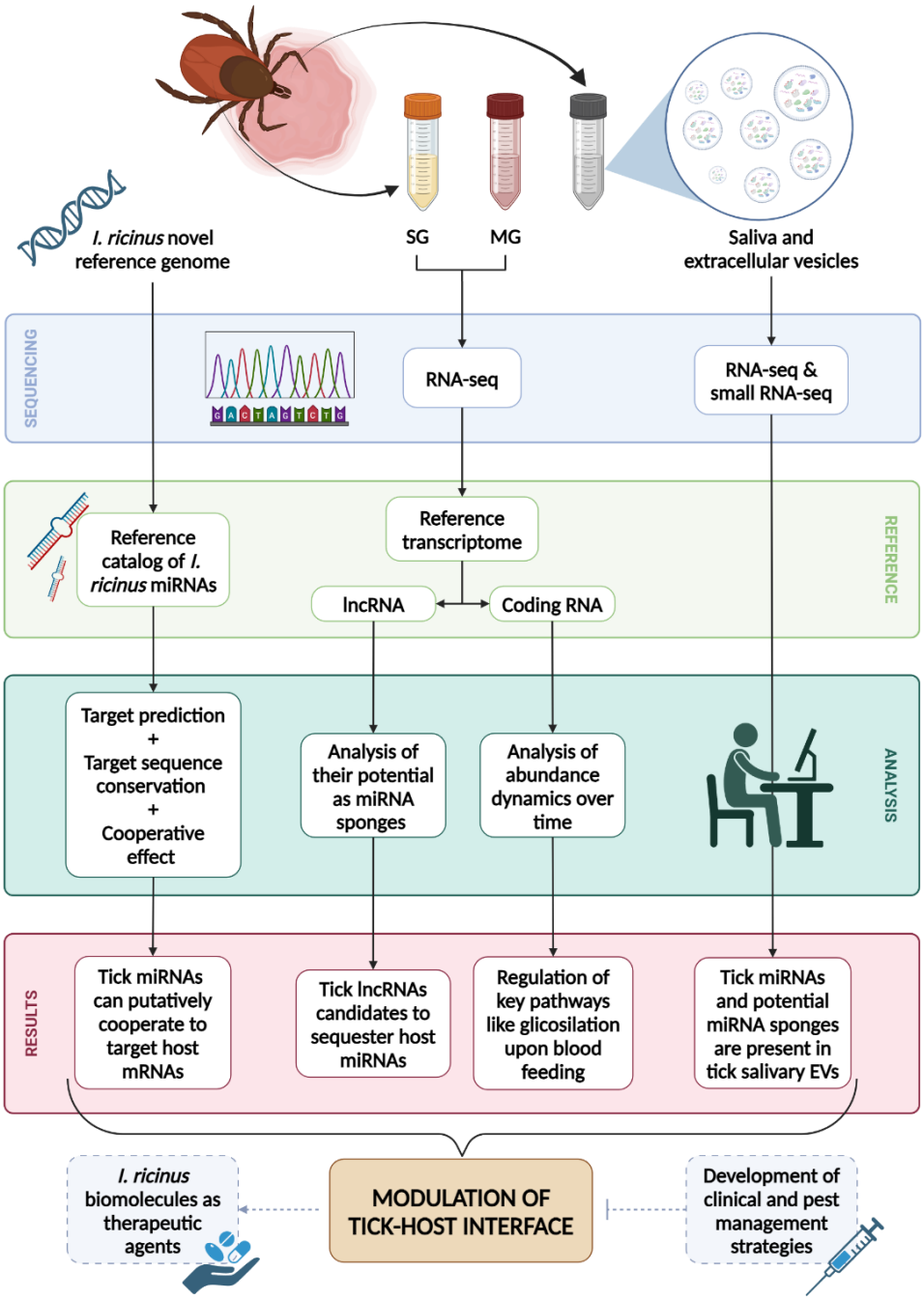

Resumen

Ixodes ricinus, la garrapata del ricino europea o garrapata común, es un ácaro parasitiforme de cuerpo duro que depende de la hematofagia para su supervivencia y reproducción. Está ampliamente distribuida por Europa y el norte de África y es responsable de transmitir varios patógenos, incluidos *Borrelia burgdorferi*, el agente causante de la enfermedad de Lyme. La creciente prevalencia de enfermedades transmitidas por garrapatas en los últimos años, exacerbada por el cambio climático y las consiguientes modificaciones de su hábitat, plantea importantes preocupaciones en términos de salud pública y economía. La capacidad de las garrapatas para parasitar con éxito a sus hospedadores se atribuye en gran medida a su saliva, que contiene moléculas bioactivas capaces de manipular diferentes mecanismos de defensa del hospedador, incluyendo el sistema inmune o los procesos de cicatrización de heridas y coagulación de la sangre. Estudios recientes proponen que los ARNs no codificantes (ARNncs) presentes en la saliva, incluyendo los micro-ARNs (miARNs), son posibles moduladores de la interfaz garrapata-hospedador.

Los miARNs son genes no-codificantes altamente conservados y presentes en prácticamente todos los metazoos. Su producto funcional son pequeñas moléculas de ARN (entre 21-23 pb) que regulan la expresión génica de forma negativa y post-transcripcional. Su importancia en la homeostasis celular ha sido ampliamente demostrada mediante ensayos funcionales y queda patente también en la aparente implicación causal de los miARNs en diferentes patologías. Hallazgos recientes sugieren que los miARNs pueden funcionar de manera cooperativa, potenciando sus efectos regulatorios. Por su parte, se ha propuesto que los ARN largos no codificantes (ARNlncs) actúan como esponjas de miARNs, con la capacidad de secuestrar miARNs a través de regiones diana

en los propios ARNlncs, lo que añade otra capa de complejidad al proceso de regulación génica.

Esta tesis tiene como objetivo determinar la importancia funcional de miARNs y ARNlncs en el proceso de parasitismo y hematofagia realizado por *I. ricinus*. Para ello, analizamos de manera exhaustiva la dinámica transcriptómica de *I. ricinus* durante el proceso de parasitismo, evaluando el papel de los productos génicos, miARNs y ARNlncs en la interfaz garrapata-hospedador mediante un enfoque bioinformático extenso. El objetivo final de la tesis es establecer una base para el desarrollo de nuevas estrategias clínicas y de control de plagas.

Durante el transcurso de esta tesis se colaboró en la generación de un nuevo ensamblado de referencia del genoma de *I. ricinus*. El uso del nuevo genoma de referencia y de múltiples conjuntos de datos de diversos tejidos como las glándulas salivales, el intestino medio, la saliva, e incluso el cuerpo completo de la garrapata, nos permitió mejorar las anotaciones de miARNs y ARNlncs.

Para analizar el posible impacto funcional de miARNs de la garrapata en el hospedador, se diseñó un nuevo flujo de trabajo computacional que integra la predicción de sitios diana de miARNs y la caracterización funcional de los genes regulados. La predicción de dianas incluye la incorporación de perfiles de conservación de la secuencia diana en función de la posición y hallazgos recientes sobre la importancia de la proteína TNRC6 en la cooperación sinérgica de miARNs en el silenciamiento génico.

Aplicando el flujo de trabajo descrito arriba, se ha podido demostrar que integrar la conservación de las secuencias diana en la predicción de las dianas de los miARNs reduce drásticamente el número de secuencias dianas predichas. Además, observamos que los genes con secuencias diana conservadas están funcionalmente enriquecidos en procesos altamente relevantes para la defensa del hospedador frente al parasitismo. Sumado a

esto, detectamos con éxito regiones cooperativas para miARNs de la garrapata en genes abundantes en células dérmicas del hospedador y relacionados con procesos clave en la interfaz garrapata-hospedador, como la respuesta inmunitaria, cicatrización de heridas, nocicepción y mecanosensación. También demostramos que estos miARNs de la garrapata están presentes en vesículas extracelulares de diferentes tamaños, lo que aumenta su potencial para interactuar con las células del hospedador.

Para estudiar cómo los ARNlncs pueden influir en el parasitismo de *I. ricinus*, generamos un transcriptoma de referencia ensamblado *de novo* a partir de muestras de glándulas salivales e intestino medio de garrapata. Estas muestras se obtuvieron de en diferentes puntos temporales de garrapatas hermanas que o bien no estaban alimentadas, o bien estaban alimentadas en hospedadores vírgenes, o bien alimentadas en hospedadores previamente expuestos a garrapatas y, por lo tanto, sensibilizados al parasitismo por garrapata. Estas muestras, a su vez, nos permitieron analizar la dinámica transcripcional que sucede en estas diversas condiciones a lo largo del tiempo en ARN no codificantes y de forma adicional en ARN codificantes.

Mediante este análisis, observamos diferencias significativas entre estos grupos de garrapatas y encontramos que los genes diferencialmente expresados a lo largo del tiempo están involucrados en procesos biológicos clave, incluidos la glicosilación y el plegamiento de proteínas. Estos procesos desempeñan roles cruciales en la adaptación de la garrapata al parasitismo y en la evasión del sistema inmune del hospedador.

Varios ARNlncs fueron identificados como posibles esponjas de miARNs del hospedador, con la capacidad de inhibir la acción de los miARNs del hospedador involucrados en procesos críticos contra el parasitismo. Uno de estos ARNlncs destaca como el candidato más prometedor, ya que fue detectado en vesículas extracelulares y tiene la capacidad de afectar los

procesos de glicosilación en los hospedadores, lo cual es esencial para la inmunidad del hospedador, así como los procesos de señalización de los receptores de la matriz extracelular.

En general, esta tesis trata de consolidar una base para futuras investigaciones y avances clínicos, como el uso de miARNs terapéuticos y antimiRs. La investigación continua, especialmente en la validación biológica y el análisis de la respuesta del hospedador, será crucial para complementar los resultados impulsados por la bioinformática y presentados en esta tesis. Este conocimiento será esencial para reducir finalmente el impacto de *I. ricinus* en la salud pública y la economía de nuestra sociedad.

Contents

Figure index

Table index

List of abbreviations

Abbreviation	Meaning
AGO	Argonaute
BUSCO	Benchmarked Universal Single-Copy Ortho
ceRNAs	Competing endogenous RNA
circRNA	Circular RNA
CV	Coefficient of variation
DC	Digestive gut cell
DE	Differentially expressed
DEG	Differentially expressed gene
eRNA	Enhancer RNA
EV	Extracellular vesicle
FDR	False discovery rate
FPKM	Fragments per kilobase per million fragments mapped
GO	Gene ontology
HCA	Hierarchical clustering analysis
lEV	Large extracellular vesicle
lncRNA	Long non-coding RNA

Abbreviation	Meaning
m7G	7-methylguanosine
mEV	Medium extracellular vesicle
MG	Midgut
miRNA	MicroRNA
mRNA	Messenger RNA
ncRNA	Non-coding RNA
PCA	Principal component analysis
piRNA	Piwi-interacting RNA
PPI	Protein-protein interaction
pre-miRNA	Precursor miRNA
pri-miRNA	Primary miRNA
RBP	RNA-binding protein
RISC	RNA-induced silencing complex
RPM	Reads per million
rRNA	Ribosomal RNA
sEV	Small extracellular vesicle
SG	Salivary gland
siRNA	Small interfering RNA
SN	Supernatant

Abbreviation	Meaning
sncRNA	Small non-coding RNA
snoRNA	Small nucleolar RNA
snRNA	Small nuclear RNA
SPF	Specific pathogen-free
TBD	Tick-borne disease
TBP	Tick-borne pathogens
TERC	Telomerase RNA
tRNA	Transfer RNA
tsRNA	tRNA-derived small RNA
UTR	Untranslated region
WB	Whole body
XPO	Exportin

Chapter 1.

Introduction

Ticks are parasitic arthropods that depend on blood feeding for survival and reproduction, playing a critical role in the transmission of pathogens that affect human and animal health [1,2]. Ticks, or *Ixodida*, form one of the seven orders of the subclass *Acari [3]*. This order is further divided into three families: the *Ixodidae*, or 'hard' ticks, which contain around 900 species; the *Argasidae*, or 'soft' ticks, with approximately 200 species; and the somewhat unique *Nutalliellidae*, represented by a single species [4]. Their capacity to transmit a wide array of diseases, including Lyme borreliosis and tick-borne encephalitis, underscores their medical and veterinary importance [5]. Over recent decades, the global prevalence of tick-borne diseases has risen dramatically, attributed to the expansion of tick habitats influenced by climate change and human-induced environmental transformations such as deforestation, urbanization, and international trade [6].

The feeding mechanism of hard ticks is a complex process, involving immune evasion, inhibition of blood coagulation and effective attachment to their hosts. By using their chelicerae to breach the skin layers, ticks firmly anchor themselves with their hypostomes, causing localized damage to blood vessels and haemorrhagic lesions [7,8]. This prolonged interaction at the skin interface facilitates pathogen transmission [9].

The economic impact of ticks is substantial, particularly in the livestock sector. For example, *Rhipicephalus microplus* alone accounts for annual losses exceeding 2.5 billion USD in tropical and subtropical regions [10]. Additionally, climate change and habitat encroachment have increased human exposure to ticks, leading to a notable rise in tick-borne disease cases and heightened societal concern over the lack of effective control measures and potential long-term health implications [11]. Additionally, ticks are emerging as a significant public health concern due to their increasing presence in urban green spaces, which are frequented by people for recreation [12]. This expansion into urban areas elevates the risk of human exposure to tick-borne diseases, such as Lyme disease and tick-borne encephalitis [12]. A striking example of this challenge is the invasion of multiple U.S. states by *Haemaphysalis longicornis* [13].

Despite advancements in biotechnology, chemical acaricides remain the predominant method for tick control. However, their extensive use has led to environmental contamination and growing tick resistance to acaricides, highlighting the urgent need for alternative, sustainable solutions [14]. Emerging strategies, such as the development of anti-tick vaccines, increasingly rely on insights gained from genomic and transcriptomic studies. Sequencing efforts for species such as *Ixodes scapularis*, *Ixodes persulcatus*, *Rhipicephalus microplus*, *Rhipicephalus sanguineus*, *Hyalomma asiaticum*, and *Dermacentor silvarum* have marked significant progress in understanding tick biology and behavior [15]. Moreover, next-generation sequencing technologies have revolutionized the field, enabling comprehensive genome analyses and detailed exploration of transcriptomes [16]. Studies of tick transcriptomes have uncovered tick miRNAs which play key roles in modulating host immune responses and facilitating successful blood feeding, paving the way for innovative anti-tick interventions [17–19].

1.1. *Ixodes ricinus*, the European hard tick: Biology and Ecology

Ixodes ricinus, commonly known as the castor bean tick, is a prostriate hard tick belonging to the family *Ixodidae* and subfamily *Ixodinae*, within the subgenus *Ixodes*. *I. ricinus* is distributed across northern, western, central, and eastern Europe, with sparse populations in southern regions [20]. It is also found in mountainous areas of northern Africa, demonstrating its adaptability to diverse habitats [21]. Initial studies on this species were conducted in the United Kingdom during the 1930s and 1940s, marking the beginning of scientific interest in its biology and its role as both a pest affecting domestic animals and a vector of three significant diseases [22]: louping-ill in sheep, caused by a flavivirus; tick-borne fever in sheep and cattle, caused by the intracellular bacterium *Anaplasma phagocytophilum*; and redwater fever (bovine babesiosis) in cattle, caused by the erythrocytic parasite *Babesia divergens*. Today, *I. ricinus* has become one of the most extensively studied vectors of disease in Europe. Infectious diseases transmitted by this tick are a growing public health concern across many European countries. Figure 1 shows the current known distribution of *I. ricinus* in Europe and Northern Africa. The European Center for Disease Prevention and Control predicts a rising incidence of tick-borne diseases (TBDs) in the near future [23].

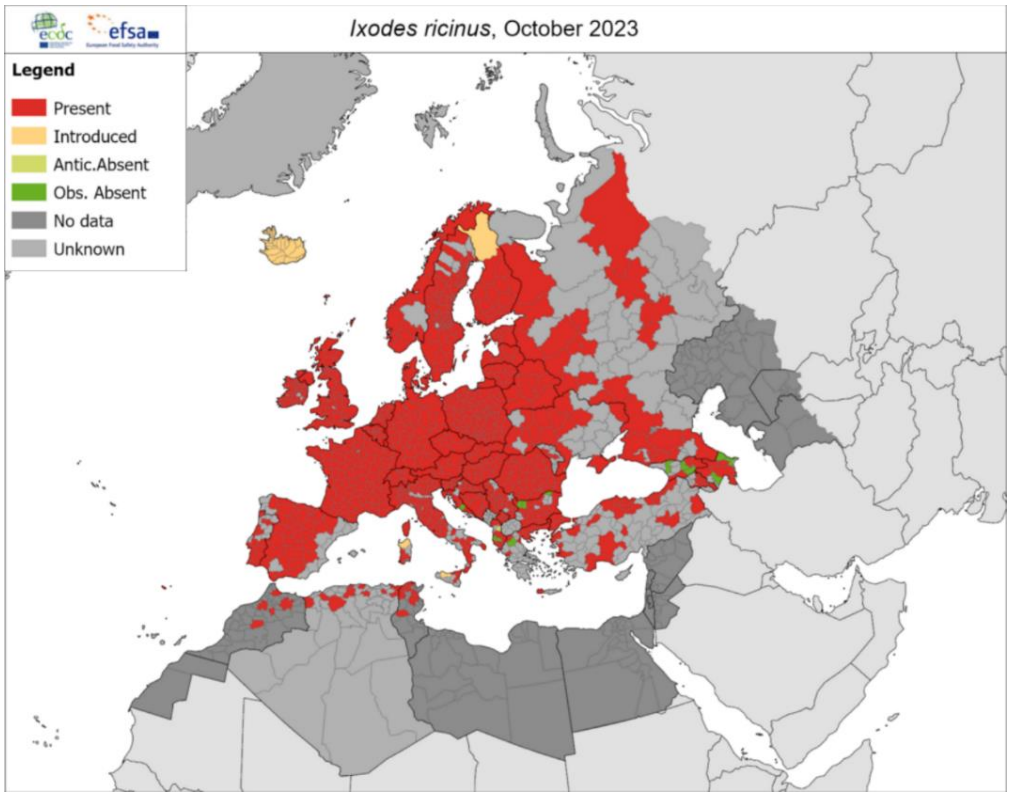

Figure 1. Currently known distribution of* Ixodes ricinus *in European and proximal countries, as of October 2023. *Adapted from [24].*

This section will provide an overview of essential information about *I. ricinus*, covering its anatomy, life cycle, host range, and its role in transmitting various pathogens for the purpose of improving the understanding of the thesis results. By analyzing these aspects, we can better comprehend the role of the specific arthropod vector in the spread of diseases that pose a significant and growing health risk.

1.1.1. Anatomy of *Ixodes ricinus*

Ixodes ricinus has an ovoid or pear-shaped body, typically brownish red in color, with the female's abdomen turning light grey when engorged [4]. In terms of size,

the adult male measures between 2.4 and 2.8 mm in length, while the female ranges from 3.0 to 3.6 mm [25]. However, when engorged, the female can exceed 1 cm in length [4]. From a morphological perspective, *I. ricinus* is divided into three primary parts: the head, body, and legs [3]. Figure 2 provides an overview of the anatomical parts of *I. ricinus*, which will be discussed in more detail below.

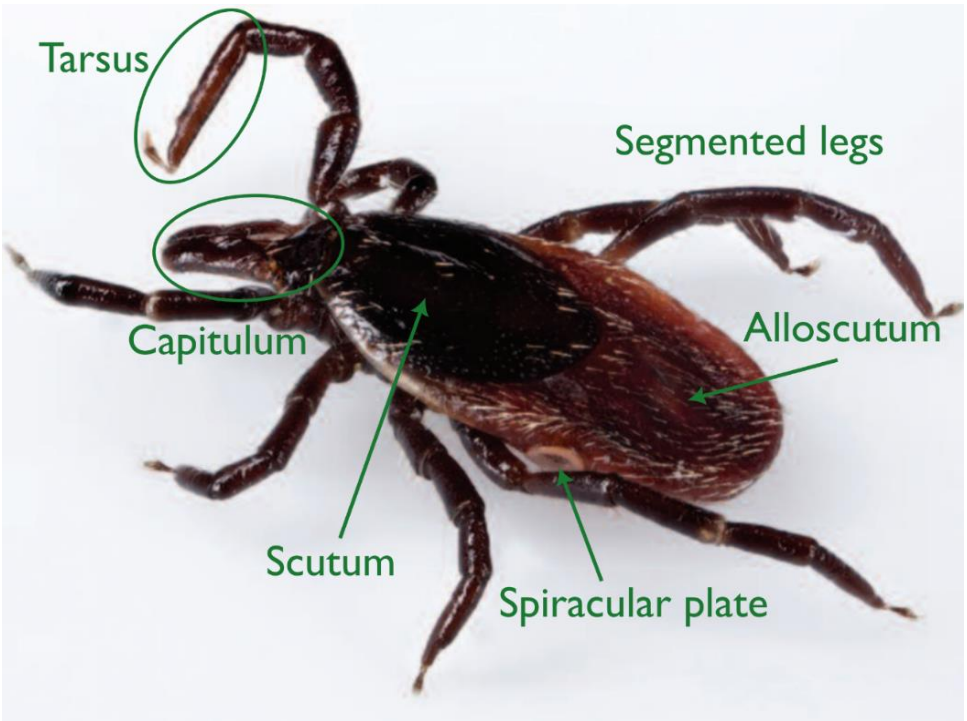

Figure 2. Dorsal view of* Ixodes ricinus *with key anatomical parts labeled. *Adapted from [4].*

The head and mouthparts of ticks are referred to as the *Capitulum*, with the *Basis Capitulum* serving as a support structure [4]. The *Auriculae*, small spurs on the side of the *Capitulum*, aid in anchoring the tick to the host and are important for species identification; in *I. ricinus*, they appear as dark divergent triangles [26]. The mouthparts contain various essential structures for blood

feeding, including sensory *palps*, cutting *chelicerae*, and a syringe-like *hypostome* used for blood extraction [4].

Regarding the body, the frontal region of mites is called the *podosoma* and the posterior *opisthosoma*, but in ticks, these sections are merged [3]. As hard ticks, the body of *I. ricinus* is covered by a protective chitinous cover, named *Scutum [27]*. In males, the *Scutum* covers the entire body, while in females, it only partially covers the body [4]. This allows the uncovered part of the body, known as the *Alloscutum*, to expand during blood feeding [28]. Scapular grooves run down the *Scutum*, and lateral grooves encircle its rim [27]. Ventrally, the genital opening is located between the 3rd and 4th pairs of legs, and males have additional hard plates around the genitals and anus, with the anus surrounded by a groove [27].

I. ricinus has four pairs of segmented legs attached to the frontal *podosoma* region [4]. The final segment of the legs, known as the *tarsus*, is long and tapering on the frontal legs of *I. ricinus [4]*. Additionally, the front legs feature long spurs, which are sharp hooks that assist in attaching to the host [4].

Among the internal organs of *I. ricinus*, several belong to the digestive tract: the preoral canal, which acts as an extension of the mouth; the pharynx; the esophagus; and the midgut, which stores and digests the host's blood meal; and the hindgut, which comprises the intestine, the rectal sac, and the rectum [29]. As an accessory organ to the digestive track, the Malpighian tubules consolidate nitrogenous wastes and transport them to the rectal sac [30].

I. ricinus has paired salivary glands located in the antero-lateral regions, with saliva passing through salivary ducts into the host tissue at the bite site [31]. Thus, these glands and the saliva they produce will play a crucial role in modulating the tick-host interaction, making them a central focus of this thesis.

I. ricinus respiratory system features an extensive tracheal network that opens via two lateral spiracular plates [32]. The tick's open circulatory system includes a heart situated dorsally along the mid-sagittal line [31]. Ticks lack a distinct brain and ventral nerve cord; instead, the central nervous system's ganglia form a structure called synganglion, a highly condensed, fused nerve mass, covered by a vascular sheath known as the periganglionic sheath [29]. Ticks also have peripheral nerves and sensory organs that provide environmental information and adaptability [29].

In females, the reproductive system includes the genital aperture, a two-part vagina, seminal receptacle, oviducts, ovaries, and two accessory glands: the lobular and tubular glands [31]. Additionally, females have the Gené's organ, which produces wax to coat eggs during oviposition [29].

The male reproductive system comprises the male accessory gland, vas deferens, and testes, connected to the genital aperture via the ejaculatory duct [31]. During reproduction, the male produces a capsule containing sperm, the spermatophore, which is manually transferred to the female's genital aperture using his mouthparts [33].

1.1.2. Life cycle of *Ixodes ricinus*

The life cycle of *I. ricinus* typically lasts 2-3 years in warmer southern regions, or 4-6 years in the cooler northern and central European climates [34]. Aside from climate conditions, the life span of *I. ricinus* is intricately tied to both host availability and other environmental conditions. *I. ricinus* typically inhabits lowland, humid biotopes, including unmanaged grasslands, heaths, forest edges, woodlands, and broadleaf forests, where dense undergrowth provides suitable conditions for survival and questing [35]. Most of the tick's life is spent off-host, either unfed (resting or questing), engorged in a developmental

diapause, or developing to the next stage following a bloodmeal (engorged or moulting) [34]. In contrast, the feeding phases as a whole comprise less than 1% of the life cycle (approximately 2-3 weeks) [34]. The tick's life cycle consists of four key stages: egg, larva, nymph, and adult. Each of the three active life stages must take a bloodmeal to develop to the next life stage (larva, nymph) or to produce and lay eggs in the case of an adult female [34].

I. ricinus larvae and nymphs are highly opportunistic in seeking a host. They actively climb low vegetation, where they wait in ambush, ready to attach to passing hosts [4]. After completing their bloodmeal, engorged larvae and nymphs seek refuge in the leaf litter, where they avoid exposure to sunlight and desiccation [34]. They can survive dry periods, especially in habitats with a stable layer of leaf litter formed by oak or beech trees, which provides consistent moisture [34]. During these off-host phases, ticks are capable of absorbing water vapor from the environment through hygroscopic salivary secretion to compensate for moisture loss [36]. However, they require high relative humidity (above 80-85%) to survive and thrive [37].

Once engorged, a process called apolysis occurs. During this process, the old integument separates from the underlying epithelium, marking the transition from the current life stage to the next [38]. After the apolysis, ticks undergo a process called moulting. During this phase, ixodid ticks temporarily lose the ability to walk and to actively absorb atmospheric water vapor [39]. Simultaneously, all ectodermal tissues undergo degeneration, followed by the development of new structures [40]. The majority of their old external chitin layer, the cuticle, is digested, while a new cuticle is formed in a highly intricate process [41,42]. The moulting process concludes with ecdysis, during which the tick's new form emerges, leaving behind the remnants of the old cuticle, known as the exuvia [34,41,42].

Following ecdysis, *I. ricinus* ticks transition to the next life stage, typically in the warmer months [34]. However, *I. ricinus* ticks that detach late in the summer may enter a developmental diapause, which can last for 9-10 months, remain in an engorged state over the winter and continue their development in the following spring [43]. The aforementioned tick's ability to survive extended periods between bloodmeals is a key aspect of its ecology, allowing *I. ricinus* to adapt to varying environmental conditions and ensure survival until the next suitable bloodmeal opportunity arises.

After a period of post-ecdysial maturation, the unfed adult tick begins its quest for a host, which can involve climbing vegetation or resting on objects up to 1.2 meters in height, waiting for the opportunity to latch onto a passing animal [34]. The questing phase can last for weeks, with the tick often retreating to more humid, sheltered areas if conditions become too dry or hot [34]. Questing behaviour ensures that ticks maximize their chances of encountering a suitable host while also managing environmental stress.

The adult male tick, unlike the females, does not feed significantly but attaches to a host primarily to mate with feeding females [44]. Off-host mating is possible assuming an accidental encounter of males with unfed females in the environment [44].

When conditions are favorable, the adult female tick completes its life cycle by laying 2,000-3,000 eggs after a successful bloodmeal [37]. This egg-laying process is temperature-dependent, ceasing below 4-5°C until warmer conditions resume [37]. Following oviposition, the female dies, marking the completion of the life cycle of *I. ricinus* [34,37]. A schematic representation of the lifecycle of *I. ricinus* is provided in Figure 3.

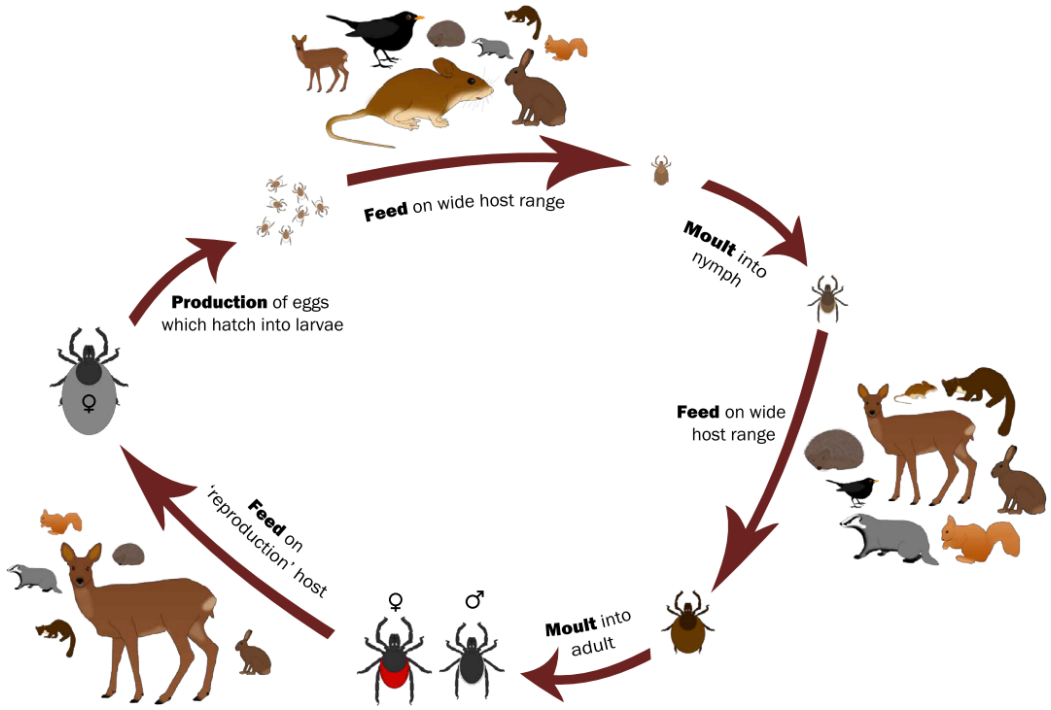

Figure 3. Overview of* Ixodes ricinus *lifecycle. *Adapted from [45].*

1.1.3. Potential hosts of *Ixodes ricinus*

I. ricinus is a highly adaptable tick species, capable of feeding on a broad spectrum of vertebrate hosts throughout its various life stages. The larval and nymphal stages are particularly opportunistic and have been recorded feeding on over 300 vertebrate species, including mammals, birds, and reptiles [46].

The adult stage of *I. ricinus* primarily feeds on large and medium-sized mammals, with a preference for species such as deer. Hedgehogs represent some of the smallest mammals to support adult ticks, but larger hosts like the deer species: *Capreolus capreolus*, *Cervus elaphus* and *Dama dama*, are critical for maintaining tick populations [47]. In the absence of deer, hares and wild boars may serve as important hosts for adult ticks [48]. Additionally, domestic livestock, including sheep and cattle, provide substantial support for

tick populations in agricultural environments, where they sustain large numbers of ticks [49].

To successfully parasitize such a wide variety of evolutionarily divergent hosts, *I. ricinus* must target conserved molecules and pathways shared across the various vertebrate host species that the specific ticks parasitize. This hypothesis has significant implications for the analyses conducted in this thesis and remarks on the importance of identifying universally conserved molecular mechanisms that mediate the parasitism of *I. ricinus*.

1.1.4. Pathogens and diseases associated with *Ixodes ricinus*

I. ricinus poses significant public health and economic challenges. As a vector of multiple pathogens, *I. ricinus* is responsible for transmitting viral, bacterial, and protozoan agents that cause serious anthropozoonotic diseases. The rise of tick populations in urban and peri-urban green spaces has heightened the risk of human exposure to infected ticks, complicating disease prevention and management strategies [12].

Some of the most significant and challenging diseases caused by pathogens transmitted by *I. ricinus* include:

1. **Lyme borreliosis**: The spirochete *Borrelia burgdorferi* sensu lato, transmitted by *I. ricinus*, causes Lyme borreliosis, the most common tick-borne disease in Europe. It manifests in various forms, including localized erythema migrans, systemic neurological involvement, and chronic arthritis. Small rodents, birds, and certain reptiles act as reservoirs for these spirochetes, sustaining transmission cycles [50,51].

2. **Tick-borne encephalitis**: Caused by the tick-borne encephalitis virus, tick-borne encephalitis is a potentially severe neuroinvasive disease endemic in Europe and Asia. *I. ricinus* is the primary vector for the western European subtype of TBEV. The virus circulates in natural cycles involving small mammals and co-feeding ticks, with occasional spillovers to humans through tick bites or consumption of unpasteurized dairy products [52].

3. **Anaplasmosis**: *Anaplasma phagocytophilum* is a bacterium that infects granulocytes, leading to human granulocytic anaplasmosis. Although clinical cases are less common in Europe compared to the U.S., the pathogen is widely prevalent in *I. ricinus* ticks and various reservoir hosts, such as roe deer and rodents [53].

4. **Babesiosis**: Protozoans of the genus *Babesia*, particularly *Babesia microti* and *Babesia divergens*, are transmitted by *I. ricinus* and cause babesiosis, a malaria-like illness. This disease poses a particular threat to immunocompromised individuals, with cattle serving as a primary reservoir for *B. divergens* [54].

5. **Rickettsioses**: Members of the spotted fever group, such as *Rickettsia helvetica* and *Rickettsia monacensis*, are transmitted by *I. ricinus*. These pathogens can cause febrile illnesses and are emerging as notable zoonotic agents in Europe [55].

6. ***Borrelia miyamotoi* infection**: *Borrelia miyamotoi* is a spirochete transmitted by *I. ricinus* ticks. Unlike Lyme borreliosis, an infection with *B. miyamotoi* leads to a relapsing fever disease characterized by recurring episodes of fever, headache, and myalgia, without the typical erythema migrans rash. Additionally, *B. miyamotoi* can be transmitted transovarially, from adult ticks to their offspring, resulting in infected

larvae capable of transmitting the pathogen to hosts, including humans [56].

7. **Neoehrlichiosis**: Caused by *Candidatus Neoehrlichia mikurensis* and transmitted by *I. ricinus*, this disease is characterized by systemic inflammation, headache, malaise, nausea, and fever. Thromboembolic and vascular events have been reported in patients with human neoehrlichiosis, although it remains unclear whether these complications arise from infected or inflamed vascular endothelial cells [57].

8. **Other Pathogens**: *I. ricinus* has also been implicated in the transmission of *Bartonella spp*. and *Francisella tularensis*. Although their public health impact is less well understood, these pathogens are considered emerging threats to both humans and livestock [51].

The wide range of diseases and tick-borne pathogens (TBPs) transmitted by *I. ricinus* remarks the importance of studying how these ticks evade host defenses, thus creating a favourable environment for the establishment of pathogens in the sites of tick bites. This thesis aims to address this challenge by providing a deeper understanding of the saliva protein components and miRNAs that may assist ticks in evading host responses, with the goal of developing anti-tick and anti-TBP strategies.

1.2. Blood feeding in *Ixodes ricinus*: Biological and biochemical aspects

1.2.1. Mouthparts and bite mechanism

The mouthparts of ixodid ticks, including *I. ricinus*, are highly specialized to facilitate blood feeding and attachment to the host. These external structures comprise a hypostome, which serves as a conduit for saliva secretion and the ingestion of blood and inflammatory exudate, and a pair of movable chelicerae [41]. The biting process begins with the chelicerae's apical digits creating an incision in the skin through lateral movements [34]. Once the incision is made, the hypostome, equipped with recurved denticles on its ventral surface, is inserted into the tissue in a ratchet-like motion [34]. This mechanism, supported by the anchoring function of reflexed cheliceral digits, ensures that the hypostome and chelicerae are fully embedded.

A critical aspect of this process is the exchange of saliva and blood that occurs at the tick-host interface. Saliva is secreted into the host tissue through the hypostome, delivering salivary molecules that modulate host immune responses, prevent coagulation, and facilitate feeding. Simultaneously, the hypostome serves as a channel for the ingestion of blood and inflammatory exudate [58]. The attachment is further stabilized by the secretion of a cement-like structure around the hypostome and the deposition of collagen, which anchor the tick securely to the host [34,58,59].

The bite of the tick generates a rapid hemostatic reaction on the host, characterized by blood clotting, platelet clumping, and vessel constriction, alongside an immune defense reaction involving complement activation, leukocyte mobilization, and inflammation as the main modules of host

homeostatic response to tick feeding [60,61]. Figure 4 provides a schematic overview of the *I. ricinus* bite, highlighting the mouthparts and organs involved in host attachment, saliva secretion, and blood intake.

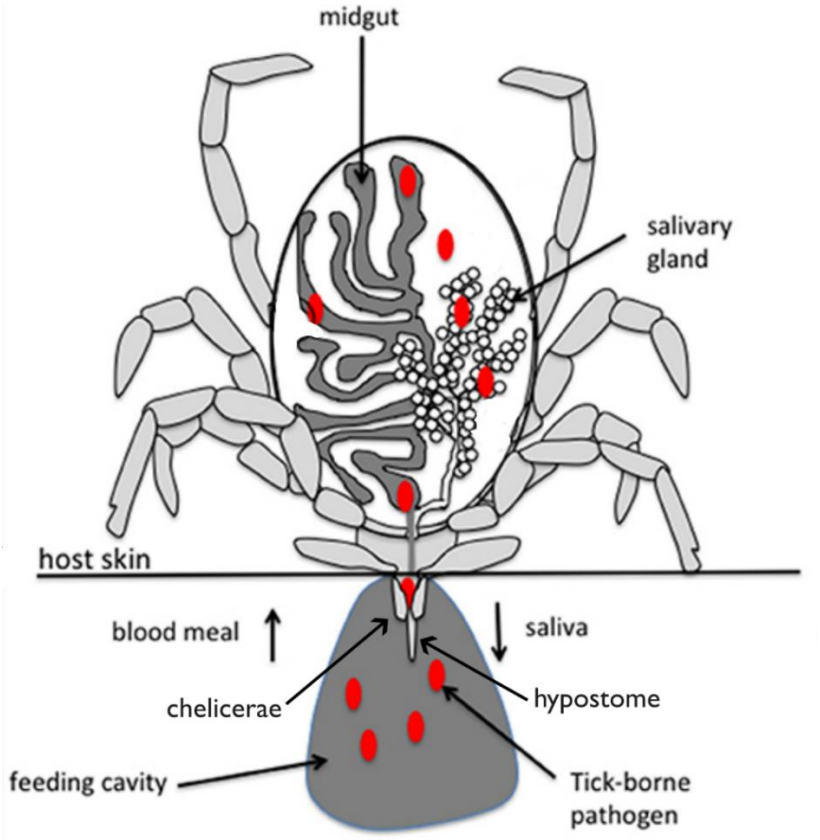

Figure 4. Schematic representation of tick blood feeding, saliva secretion, and tick-borne pathogen (TBP) injection into the host. *The diagram indicates the tick organs and structures involved in the blood-feeding process. TBPs are highlighted in red. For presentation purposes, only one-half of the digestive tract and a single salivary gland are shown. Adapted from [62].*

1.2.2. Digestive processes in the midgut

The midgut of *I. ricinus* plays a central role in the slow and intricate process of blood digestion, distinct from the rapid digestion in insect blood-feeders [63]. The tick midgut is the central section of the digestive tract where most blood

digestion and nutrient absorption occur, and it is the largest organ in the body of a tick regardless of its developmental stage [31]. The midgut consists of a ventriculus, which acts as a stomach in arthropods, and multiple pairs of branched caeca, which increase the surface area of the midgut and fill much of the female tick's body [64,65]. This gut architecture includes a lumen encased by a single epithelial layer of large digestive gut cells (DCs), covered by a peritrophic matrix that separates luminal contents from digestive cells [41]. Unlike insects, digestion in ticks occurs intracellularly in acidic vesicles within gut epithelial cells [63].

Upon ingestion, red blood cells are lysed in the lumen, releasing proteins such as hemoglobin or albumin, which comprise more than 80% of the total protein content of vertebrate blood, making them the main sources of amino acids for ticks [66]. Hemoglobin is internalized by DCs via receptor-mediated endocytosis, while albumin is internalized by non-specific fluid-phase endocytosis [66]. Hemoglobin is directed to clathrin-coated pits and taken into large endosomal vesicles, where acidic lysosomal enzymes, such as cysteine and aspartic peptidases, digest hemoglobin into peptides and amino acids [66]. On the other hand, albumin is directed to small acidic vesicles, where it will be further digested [66]. These products are utilized in several anabolic processes in the tick, including in vitellogenin synthesis for reproduction in fertilized females [65,66].

The digestion process generates heme as a byproduct, a potentially toxic molecule due to its ability to produce reactive oxygen species [67]. To counter this, ticks sequester heme in specialized organelles called hemosomes, a detoxification mechanism critical for tick survival [68].

1.2.3. The role of salivary glands

The salivary glands (SG) of *I. ricinus* perform multiple essential functions that are critical for tick survival and parasitic lifestyle. These glands play a central role during both on-host feeding periods and off-host fasting, contributing not only to the tick blood-feeding success, but also to the transmission of TBPs [62].

In ixodid ticks such as *I. ricinus*, the SGs are composed of numerous acini, which are alveoli-like rounded secretory units. Acini are categorized into four types: type I, II, III, and IV [62]. Types I, II, and III are common to both sexes, while type IV is specific to males. These acini connect to the salivary ducts, with type I primarily associated with the anterior part of the main duct and types II and III linked to more distal secondary and tertiary ducts, respectively [41,62,69]. The acini contain specialized cells responsible for various physiological and secretory activities. Agranular type I acini comprise four distinct cell types, including lamellate and peritubular cells, while granular type II and III acini house additional glandular cells that secrete biologically active molecules [41,70]. These secretions play a pivotal role in tick feeding and pathogen transmission [62].

The ixodid SGs exhibit remarkable adaptations to ensure survival and efficient parasitism. As previously mentioned, a defining feature of ixodid ticks is their ability to anchor firmly to the host using a cement cone [59]. This structure, composed of glycine-rich proteins, lipids, and carbohydrates, is secreted by type II and III acini [59]. The cement protects the tick's mouthparts and shields them from the host's immune response, facilitating prolonged feeding [59].

During feeding, ixodid ticks like *I. ricinus* can increase their body weight over 100-fold [71]. This is achieved through the uptake of large volumes of blood while simultaneously excreting excess water and ions back into the host via SGs and the secretion of saliva [71]. The type III acini play a key role in this process, with

their epithelial cells housing sodium-potassium pumps (Na+/K+-ATPase) that regulate ion and water movement, maintaining homeostasis [72].

During off-host fasting, type I acini facilitate the absorption of atmospheric moisture. These structures secrete a hygroscopic solution rich in Na+, K+, and Cl−, which absorbs environmental humidity [72,73]. This absorbed moisture is subsequently swallowed and utilized, a critical adaptation to prevent desiccation in dry environments [74].

The activation of SGs in *I. ricinus* is tightly regulated by the nervous system, specifically the synganglion [75]. The synganglion, as further discussed in Section 1.1.1, is the central nervous system of the tick, including the major peripheral nerves, and it is a highly condensed, fused nerve mass, covered by a vascular sheath known as the periganglionic sheath [29]. The synganglion coordinates gland activity via neural and chemical signals [75]. Dopamine is a key activator, triggering fluid secretion through two pathways: a cAMP-dependent pathway via the D1 dopamine receptor and a calcium-dependent pathway via the InvD1L receptor [76]. These receptors are differentially expressed within the SG, with the D1 receptor promoting fluid uptake and the InvD1L receptor facilitating fluid expulsion [76]. Additionally, chemical agents, including octopamine, norepinephrine, and neuropeptides like SIFamide and myoinhibitory peptide, further modulate SG activity, generating a complex neural network that controls the SG secretion in response to the tick's physiological needs during feeding [62].

1.2.4. The impact of saliva on host responses

Tick saliva is a complex mixture of proteins and other molecules that play a critical role in the tick's ability to feed on blood and it is produced by tick SGs [62]. Numerous key components of the saliva of ticks have been discovered and studied, including various enzymes, inhibitors, and vasodilators that help ticks overcome host immune and haemostatic responses and facilitate blood feeding [62]. Tick saliva includes molecules that inhibit primary and secondary haemostasis, such as Kunitz-type inhibitors, which target blood coagulation factors like thrombin and factor Xa [77,78]. These anticoagulants, along with other components that disrupt platelet aggregation and fibrinogen binding, enable the tick to feed without triggering excessive blood clotting [78].

Salivary proteins, such as the serpin IRS-2 and histamine release factors, block platelet aggregation and modulate vascular permeability, which help prevent clotting and promote continued blood flow at the tick feeding site [78,79]. Their saliva includes molecules that inhibit primary and secondary haemostasis, such as Kunitz-type inhibitors, which target blood coagulation factors like thrombin and factor Xa [77,78]. These anticoagulants, along with other components that disrupt platelet aggregation and fibrinogen binding, enable the tick to feed without triggering excessive blood clotting [78].

I. ricinus has the capability to suppress the host’s immune response as well, using salivary components that modulate both host innate and adaptive immunity. Irac I and Irac II, which modulate the complement system, help prevent immune detection [80]. Ir-LBP, a lipocalin, binds to leukotriene B4, an inflammatory mediator, reducing neutrophil recruitment and activation [81]. Proteins like IRIS and BIP further modulate the host’s inflammatory response and wound healing processes [82,83], while Salp15-like proteins from *I. ricinus*

assist in evading immune responses by interfering with antigen presentation [84].

While many proteins from the saliva of *I. ricinus* and other ticks have been identified, their full functional roles are still being unraveled. In most cases the complex host evasion mechanisms cannot be attributed to a single tick salivary protein.

1.2.4.1. Extracellular vesicles in saliva

Recent studies have identified extracellular vesicles (EVs) as a critical component of tick saliva, with potential implications for vector-host interactions, even suggesting a direct effect of tick salivary EVs on host skin keratinocytes [85,86]. EVs are nanoscale vesicles known for their roles in intercellular communication, cargo trafficking, and influencing various biological processes [87]. These vesicles typically carry lipids, nucleic acids as RNAi or miRNA, and proteins, and their cargo composition varies depending on the source organism, cell type, and environmental conditions [87].

Recently, researchers identified several tick salivary effectors within EVs that may impact the host response, indicating their role in modulating host immune responses and facilitating blood feeding [88]. Specifically, the SNARE proteins Vamp33 and Synaptobrevin 2 have been identified to enable the blood feeding of *I. scapularis* and to support *Anaplasma phagocytophilum* infection through the modulation of dendritic and epidermal T cells function [89]. While primarily studied in mammalian contexts, EVs have garnered attention for their potential to influence the tripartite interactions between ticks, their microbial symbionts, and mammalian hosts [90].

One crucial aspect of tick salivary EVs is their potential to transfer miRNAs to the host. As further discussed in the Section 1.3, miRNAs are small non-coding

RNAs that regulate gene expression post-transcriptionally and are known to influence host-pathogen interactions in parasitic systems [91]. Preliminary evidence from related tick species, such as *Haemaphysalis longicornis*, has demonstrated the presence of miRNAs within EV-like structures in tick saliva [18].

Although this field remains poorly explored, this thesis will focus on demonstrating the presence of miRNAs in *I. ricinus* saliva and salivary EVs and their potential to cooperate with other salivary effectors in mediating the complex evasion strategies ticks use to counter host defense mechanisms, thereby facilitating blood feeding and ensuring tick survival.

1.3. Non-coding RNA in tick-host interactions: The key role of microRNAs and long non-coding RNAs

Traditionally, genetic research has centered on messenger RNAs (mRNAs) for their role in translating genetic information into proteins. However, RNAs that do not code for proteins, also known as non-coding RNAs (ncRNAs), have emerged as key regulators of gene expression and other cellular processes [92]. Advances in RNA sequencing technologies and bioinformatics have significantly expanded our understanding of ncRNAs, revealing them as a substantial portion of the transcriptome, with key roles in transcription, translation, and RNA modification [93,94]. ncRNAs are broadly categorized into two main groups: housekeeping ncRNAs and regulatory ncRNAs [92].

Housekeeping ncRNAs are typically constitutively expressed and necessary for basic cellular processes [95]. This group includes ribosomal RNA (rRNA), transfer RNA (tRNA), tRNA-derived small RNA (tsRNA), small nuclear RNA

(snRNA), small nucleolar RNA (snoRNA), and telomerase RNA (TERC), each with critical roles in supporting distinct cellular functions [92].

Regulatory ncRNAs, on the other hand, modulate gene expression and are further divided based on their size into small non-coding RNAs (sncRNAs) and long non-coding RNAs (lncRNAs). Key types of regulatory sncRNAs include microRNAs (miRNAs), small interfering RNAs (siRNAs), piwi-interacting RNAs (piRNAs), and enhancer RNAs (eRNAs), while lncRNAs and circular RNAs (circRNAs) represent the larger regulatory ncRNAs [92]. Each of these ncRNA classes plays a pivotal role in cellular homeostasis, by contributing to the complexity of gene expression control [92].

This thesis will focus on miRNAs and lncRNAs as key modulators at the tick-host interface. These two classes of ncRNAs are particularly intriguing due to their versatile roles in gene regulation and their potential involvement in host-parasite interactions. MiRNAs are well-known for their ability to fine-tune gene expression post-transcriptionally and, therefore, may play a crucial role in the modulation of host immune responses during tick blood feeding [96]. Beyond modulating chromatin states, transcription, and RNA stability in the host, lncRNAs are known to act as competing endogenous RNAs (ceRNAs) or "sponges" by sequestering host miRNAs [96]. The potential inhibition of host miRNA function by tick lncRNAs is particularly intriguing in the context of the tick-host interaction.

The decision to focus on miRNAs and lncRNAs in this thesis stems from growing evidence that these molecules are secreted in tick saliva and may directly impact host cellular pathways [17,97]. Understanding how miRNAs and lncRNAs are leveraged by ticks to evade host defenses could reveal novel insights into tick biology and the molecular mechanisms underlying tick lifecycle completion and the transmission of diseases.

1.3.1. MicroRNAs in tick-host interactions

miRNAs are endogenous small regulatory ncRNA molecules, approximately 22 nucleotides in length, which mediate the translational repression and transcript stability of target mRNAs through antisense base pairing [98]. They have been identified in all bilaterian animal species, with many miRNAs being evolutionarily conserved [99]. Their widespread presence across animal, plant and virus genomes, along with their high evolutionary conservation, suggests a significant regulatory role in various physiological processes. A large number of studies have demonstrated that miRNAs are essential in regulating development, differentiation, proliferation, apoptosis, and immune response [100].

The target regions of miRNAs in mRNAs typically involve perfect base pairing with the miRNA seed region (positions 2 to 7 of the miRNA) [101]. These target sites are usually located in the 3' untranslated region (3' UTR) of the mRNA [102]. The crucial roles miRNAs play in gene regulation underscore the importance of these target regions, which are often highly conserved. In humans, more than 60% of mRNAs contain at least one conserved target site , and on average, each mRNA target contains four to five preferentially conserved miRNA binding sites [102]. Previous research suggest that when a predicted target sequence is conserved across multiple species, it is more likely to have a functional role, potentially due to regulation by miRNAs [103].

In this section, we will explore essential aspects of miRNAs regarding their potential implication in the blood-feeding process of *I. ricinus*. Specifically, we will cover their biogenesis, their function in mRNA repression and pathway modulation, the emerging potential function of miRNAs in tick-host interface and the recent findings on the cooperative interactions between miRNAs.

1.3.1.1. Biogenesis and translocation to extracellular vesicles

The biogenesis of miRNAs begins with the processing of RNA polymerase II or III transcripts, occurring either post-transcriptionally or co-transcriptionally [104]. Approximately half of the identified miRNAs are intragenic, primarily derived from introns, with a smaller proportion originating from exons of protein-coding genes, while the remaining miRNAs are intergenic, transcribed independently [105,106]. In some cases, miRNAs are transcribed as a single long transcript, forming clusters that often share similar seed regions [107]. Each of these clusters are known as a miRNA family. The process of miRNA biogenesis can be categorized into two main pathways: canonical and non-canonical [108]. Figure 5 illustrates the canonical and non-canonical miRNA biogenesis pathways, which will be discussed more extensively in the following sections.

1.3.1.1.1. The canonical pathway of microRNA biogenesis

The canonical pathway is the primary route for miRNA biogenesis, involving several precise processing steps. Initially, primary miRNAs (pri-miRNAs) are transcribed from miRNA genes. These pri-miRNAs are then processed into precursor miRNAs (pre-miRNAs) by the Microprocessor complex, which includes two copies of the RNA-binding protein DiGeorge Syndrome Critical Region 8 (DGCR8) and the ribonuclease III enzyme Drosha [109]. DGCR8 recognizes specific motifs within the pri-miRNA, such as N6-methyladenylated GGAC, while Drosha cleaves the RNA duplex at the base of its characteristic hairpin structure, generating a pre-miRNA with a two-nucleotide 3' overhang [110,111]. Additionally, auxiliary proteins like SRSF3 may help the Microprocessor complex in its task to bind pri-miRNAs [112].

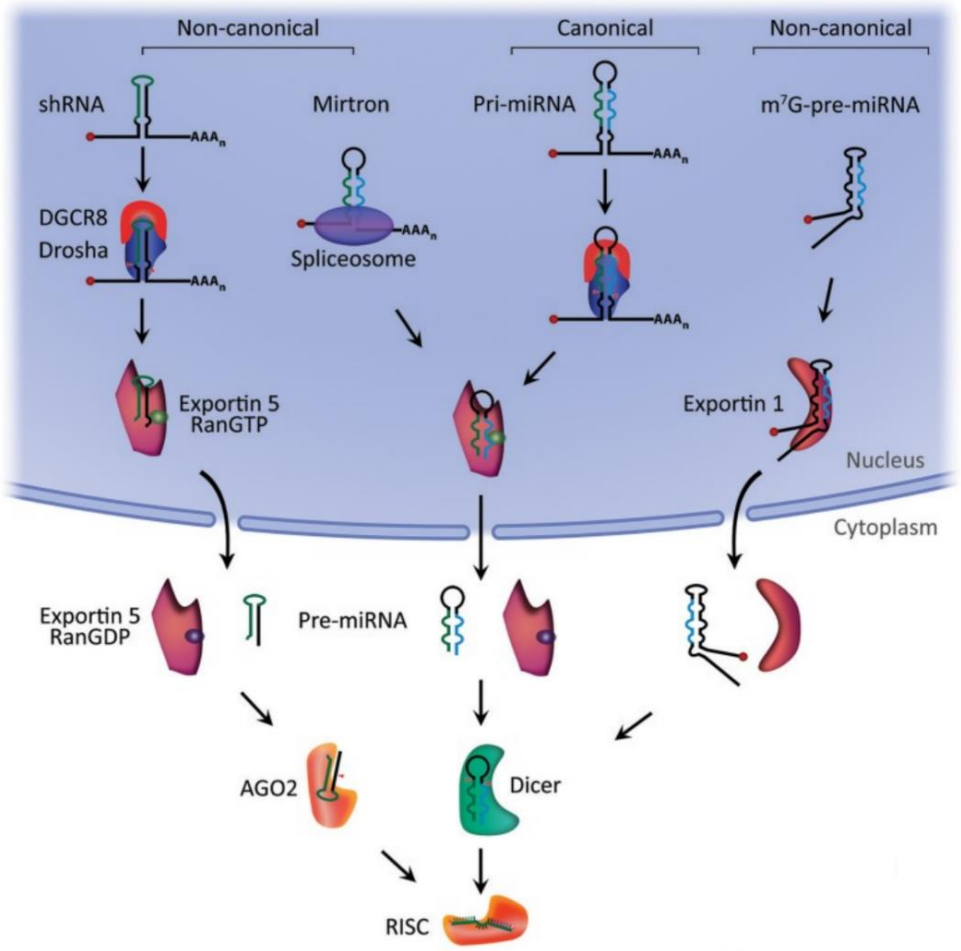

Figure 5. Canonical and non-canonical pathways involved in the biogenesis and maturation of microRNAs. *Adapted from [108].*

The pre-miRNAs are subsequently transported to the cytoplasm by the exportin 5 (XPO5)/RanGTP complex, where they are further processed by the RNase III enzyme Dicer [109,113]. This step removes the terminal loop of the hairpin, which generates a double stranded RNA structure known as the mature miRNA duplex [114]. The strands of this duplex are denoted as 5p and 3p, corresponding to their origin from the 5' and 3' ends of the hairpin, respectively. Both strands can be loaded into Argonaute (AGO) proteins (AGO1-4 in humans) in an ATP-

dependent process [115]. When the strands are loaded in Argonaute, a strand selection process occurs. Here, a strand is selected as the functional strand (guide strand), while the remaining strand, known as the passenger strand, is ejected to allow the recruitment of the rest of the RNA-induced silencing complex (RISC) [116]. This complex will be responsible for recognition and inhibition of miRNA targets [116].

1.3.1.1.2. Non-canonical microRNA biogenesis pathways

Several non-canonical miRNA biogenesis pathways have been identified, which utilize different combinations of proteins typically involved in the canonical pathway, such as Drosha, Dicer, XPO5, and AGO2 [108]. These non-canonical pathways can be broadly classified into two categories: Drosha/DGCR8-independent and Dicer-independent pathways [108].

In the Drosha/DGCR8-independent pathway, pre-miRNAs resemble Dicer substrates but bypass Drosha processing. This is the case of mirtrons, which are derived from introns during mRNA splicing [117,118]. Another example involves 7-methylguanosine (m7G)-capped pre-miRNAs, which are exported directly to the cytoplasm via XPO1, without Drosha cleavage [119]. These m7G-capped pre-miRNAs exhibit a strong bias towards the 3p strand, likely because the m7G cap prevents the loading of the 5p strand into Argonaute proteins [119].

On the other hand, Dicer-independent pathways are characterized by the processing of miRNAs by Drosha from endogenous short hairpin RNA (shRNA) transcripts [120]. These pre-miRNAs are too short to be substrates for Dicer and require AGO2 to complete their maturation in the cytoplasm [120]. The entire pre-miRNA is loaded into AGO2, which slices the 3p strand. The maturation is finalized by the trimming of the 5p strand, completing the miRNA biogenesis in a Dicer-independent manner [121].

1.3.1.1.3. MicroRNA sorting into extracellular vesicles

The process of miRNA trafficking and sorting into EVs is complex and not yet fully understood by the scientific community. Current research highlights the involvement of various binding proteins and mechanisms, suggesting multiple pathways rather than a single, uniform sorting process [122]. In this section, we will explore the various methods of miRNA sorting and trafficking.

Once exported from the nucleus to the cytosol, miRNAs can bind to various RNA-binding proteins (RBPs). When this occurs, both the RBPs and miRNAs are incorporated in the EV to be secreted. Several RBPs have been described to be involved in this miRNA sorting process. The knock-out of the major vault protein (MVP) resulted in the accumulation of miR-193a in the cytoplasm of donor cells, instead of being released in exosomes, suggesting a potential role of this RBP in the trafficking of miRNAs [123]. AGO2, the already mentioned crucial component of the RISC complex, has been found to mediate the sorting of miRNAs into EVs in a KRAS-dependent manner [124]. Human ELAV protein HuR has been reported to have a role modulating extracellular export of miR-122, potentially controlling stress response in starved human hepatic cells [125]. Recent studies have shown that sequence-specific interactions between miRNAs and fragile X mental retardation protein (FMRP), play a significant role in exosome cargo loading and enhance secretion during cellular inflammatory responses, leading to the activation of the inflammasome [126]. It is remarkable that post-translational modifications of RBPs such as SUMOylation, uridylation, and ubiquitination have a significant impact on the selection of miRNA cargo for secretion in EVs [127,128].

The presence of specific sequences within miRNAs, known as EXOmotifs, has been reported to be critical for their sorting into EVs. Specifically, studies have shown that EXOmotifs such as the GGAG motif, interact with SUMOylated

heterogeneous nuclear ribonucleoprotein A2B1 (hnRNPA2B1) to facilitate miRNA packaging into exosomes [129]. Synaptotagmin-binding cytoplasmic RNA-interaction protein (SYNCRIP), another hnRNP family member, similarly targets miRNAs with the EXOmotif GGCU for selective EV-sorting [130,131]. Interestingly, SYNCRIP is highly conserved between humans and arthropods, such as *D. melanogaster*, with domains important for RNA binding showing a high degree of similarity in these homologs [131]. Thus, SYNCRIP and its conservation may serve as a valuable starting point for research into how miRNAs are selectively sorted into EVs in ticks.

Biomolecular condensates, formed through liquid-liquid phase separation, provide an alternative mechanism for miRNA loading into EVs [132]. These condensates, which include stress granules and processing bodies, can preferentially concentrate specific proteins and RNAs, aiding in their targeting and incorporation for exosomal release [132]. Studies on miR-223 sorting into exosomes by YBX1 suggest that the local enrichment of cytosolic RBPs and their corresponding RNAs through phase separation facilitates their targeting and packaging into EVs.

In general, the processes mentioned above are largely unknown and represent an interesting research field that should be explored to clarify how miRNAs are selectively sorted into EVs. A schematic overview of the specific processes is provided in Figure 6.

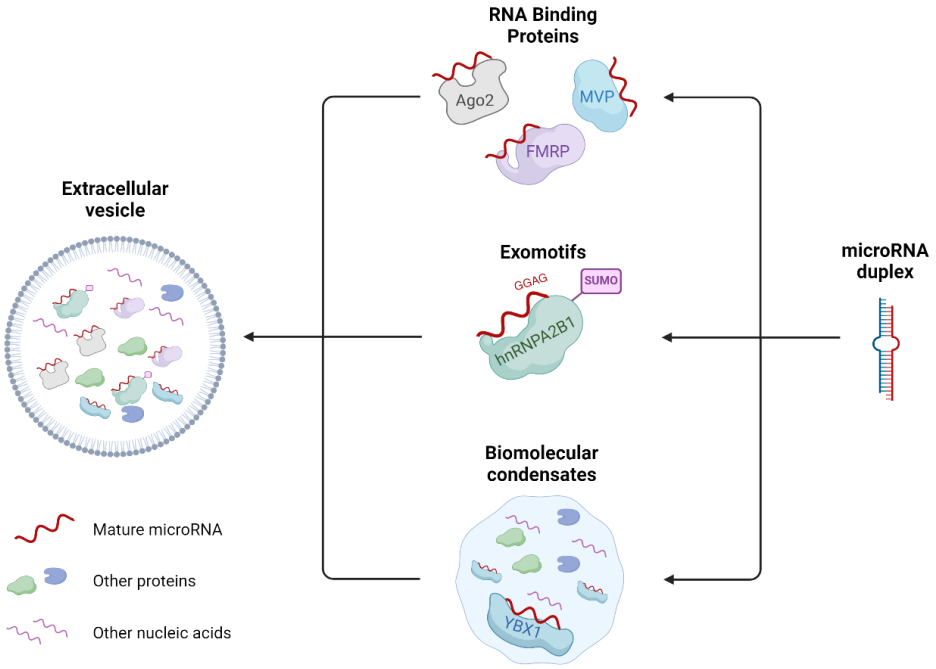

Figure 6. Mechanisms involved in the selective sorting of microRNAs into extracellular vesicles.

1.3.1.2. Target binding and gene silencing

The main function of miRNAs is to repress a target mRNA through antisense base pairing. However, most miRNAs exhibit only partial complementarity to their target sequences, as full or extensive complementarity is not typically required for effective binding[99,130]. The recognition of targets is predominantly dictated by the 'seed' region, which includes nucleotides 2–7 or 8 of the mature miRNA [133]. Thus, because miRNAs with identical seed sequences tend to regulate overlapping targets and have a similar effect in the cell, they are grouped into families by their seed sequence [134].

The binding between miRNA and their target mRNA is known to happen most frequently in the 3' UTR of the mRNA. This causes repression of the target mRNA

that can occur through destabilization of target transcripts or inhibition of gene translation [135–137]. Nevertheless, evidence also indicates non-canonical binding outside the 3'-UTR and beyond the seed region, adding complexity to the rules of target recognition [138–142]. Figure 7 illustrates the pathway of miRNA-mediated target mRNA repression.

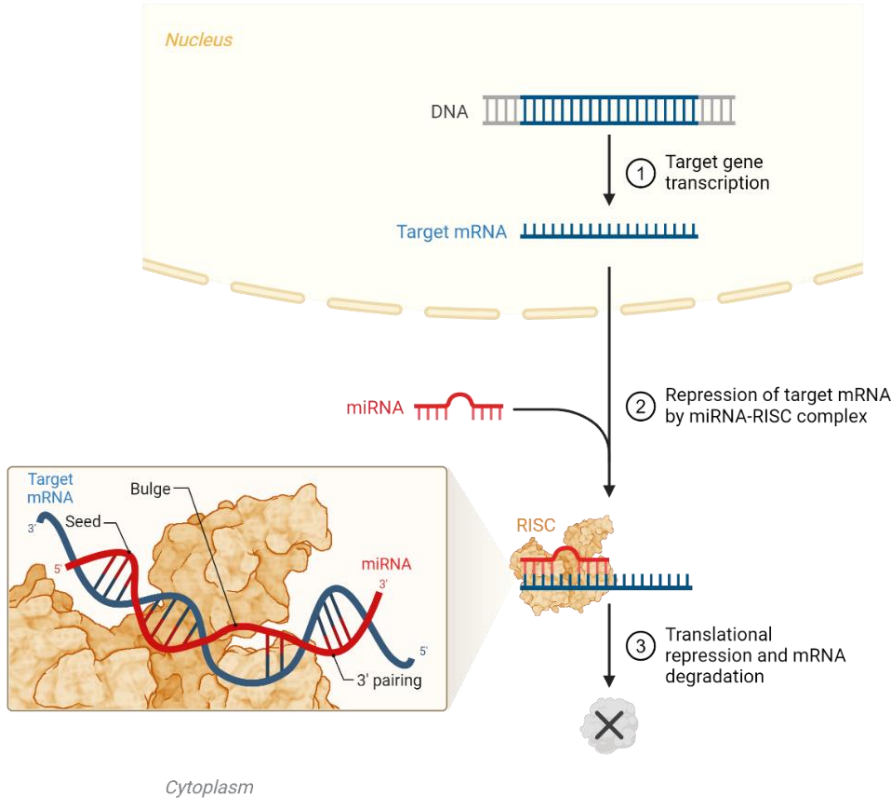

Figure 7. Pathway of microRNA-mediated target mRNA repression: pairing and gene silencing.

An important point to consider when discussing miRNA function is that the repression they exert on target mRNAs is partial, often referred to as a knock-down, and is influenced by the stoichiometry between the miRNA and its target mRNA [143]. Therefore, a highly expressed mRNA will require a greater

concentration of miRNA to achieve the desired level of repression [133,144,145]. This is particularly relevant to this thesis, as the concentration of miRNA that a tick can deliver to host cells is currently unknown. Consequently, it is more likely that ticks regulate mRNAs with lower abundance in host cells, where miRNA-mediated repression would be more effective.

1.3.1.3. The synergistic roles of microRNAs in gene regulation: The cooperative effect

In recent years, increasing attention has been given to the cooperative effects of multiple miRNAs targeting the same mRNA, a regulatory layer that adds complexity beyond the extensively studied individual miRNA–target interactions. Analyses of the global impact of miRNAs on mRNA levels suggest that when an mRNA contains multiple binding sites for the same miRNA, the resulting repression is greater than expected, indicating that miRNAs can function synergistically [138]. This cooperative interaction is a crucial aspect of the regulatory complexity that governs cellular processes, including those taking place at the tick-host interface. The mechanisms by which microRNAs can cooperate in target mRNA silencing are shown in Figure 8.

The cooperative action of miRNAs is governed by several factors, including the distance between their target sites on the mRNA [146]. When miRNAs bind close to each other on the same mRNA, they can mutually enhance each other's binding stability and silencing efficiency. This spatial arrangement facilitates a more robust repression of the target gene [146].

Recent analyses have provided further insights into the biochemical mechanisms underlying miRNA cooperativity [147]. The trinucleotide repeat containing 6 protein family (TNRC6), consists of a family of proteins that feature an N-terminal AGO-binding domain, containing Glycine/Tryptophan-repeats

with the capacity to recognize up to three AGO proteins simultaneously [148]. This ability of TNRC6 proteins to interact with multiple AGO proteins facilitate cooperative miRNA binding to adjacent sequences. As a result of the AGO:TNRC6 interaction, a single miRNA may bind weakly, but when two or more miRNAs bind to adjacent sites, multi-valent interactions can form and the affinity is increased, with TNRC6 bridging the connections [143,149] (Figure 8C).

Despite the above-presented explanation, and contrary to the traditional view that miRNAs must bind in close proximity to exhibit cooperative effects, researchers have recently explored scenarios where effective miRNA cooperation occurred despite greater distances between their target sites [150]. Their findings challenge the notion of strict spatial constraints, suggesting that miRNA cooperativity can also depend on other factors such as RNA secondary structure and the dynamic interactions between the RNA-binding proteins and the miRNA machinery [150]. This gives the cooperative effect of miRNAs another layer of complexity and remarks on the need for further research in this field.

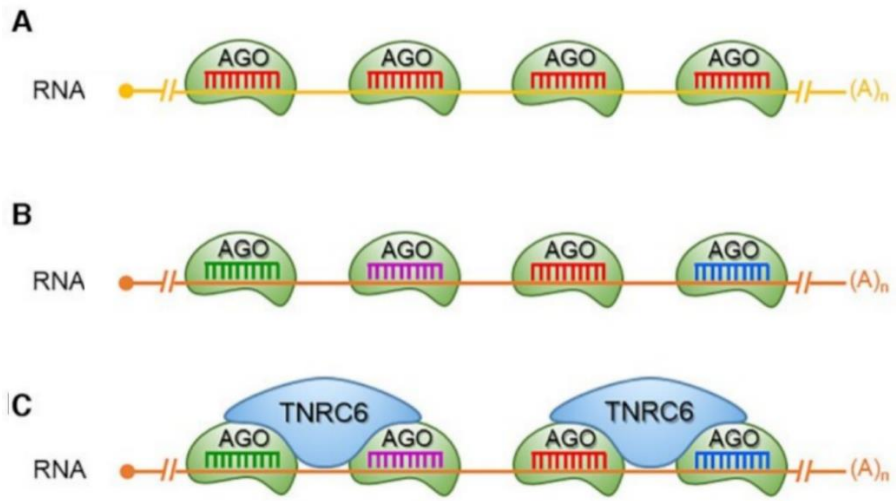

Figure 8. Mechanisms of microRNA cooperation in target mRNA silencing. *This figure shows how multiple miRNAs, either (A) from the same family or (B) from different miRNA families, are cooperating to silence a shared mRNA target. C) Cooperative effect mediated by trinucleotide repeat containing 6 protein. Adapted from [143].*

The role of the cooperation of miRNAs in modulating processes taking place at the tick-host interface is particularly intriguing. An *in silico* target network analysis of tick saliva-specific miRNAs revealed that miRNAs can exert significant combinatorial effects on the host's physiological pathways [17]. The specific study highlighted how multiple miRNAs in tick saliva can cooperatively target host genes involved in immune response, wound healing, and other critical processes [17]. This cooperative action likely enhances tick's ability to evade host defenses and to sustain prolonged blood feeding, underlining the importance of miRNA synergy in parasitic interactions.

The cooperative effects of tick miRNAs enhance the complexity of how they regulate host gene expression. Understanding these interactions, from the biochemical mechanisms behind miRNA cooperation to their strategic use at the tick-host interface, is crucial for fully understanding the complexity underlying miRNA function.

1.3.1.4. Role of microRNAs as modulators of cellular processes involved in tick-host interactions

In recent years, miRNAs have emerged as key regulatory players at the tick-host interface, with growing research uncovering their influence on host physiological processes which play an essential tole in host homeostatic response against blood feeding [151]. In ticks, miRNAs are sorted into extracellular vesicles (EVs), such as exosomes, and are secreted into the host during feeding [151]. An important question that requires further investigation is whether miRNAs, despite being protected within EVs, retain their functionality once they reach their new location in the host cell. It has been reported that the internalization of EV-derived miRNAs, such as miR-125b and bantam, by host monocytes led to increased monocyte proliferation and TNF-α production by

downregulating Pros1, Fam212b, and Clmp [152]. These findings suggest that miRNAs transferred by EVs remain functional in the host cell. Thus, this delivery system allows tick-derived miRNAs to interact directly with host immune cells, potentially modulating immune responses, wound healing, angiogenesis and other host defence mechanisms to facilitate prolonged tick feeding and to enhance pathogen transmission, as a side effect [17–19].

Delving deeper into the molecular components involved in the modulation of the host homeostatic response against blood feeding, recent studies identified key miRNAs in tick saliva that regulate host physiological pathways. For example, four miRNAs found to be overexpressed in *I. ricinus* saliva, miR-8-3p, miR-279a-3p, miR-bantam-3, and miR-317-3p, were predicted to regulate mitogen-activated protein kinases (MAPKs), such as MAPK10, which is involved in the JNK pathway and known to influence wound healing in mice [17,153]. Additionally, these miRNAs may also target components of the mTOR signaling pathway [17].

Similar regulatory effects have been proposed in other hematophagous arthropods. For example, miRNAs in the saliva of *Anopheles coluzzi* are believed to mimic human endogenous miRNAs to manipulate host physiology, potentially targeting key proteins involved in the mTOR pathway, T cell regulation, and inflammation. In *A. coluzzi*, the most abundant salivary miRNAs are predicted to target mammalian genes, including mTOR, PIK3CD, and FCGR3B, along with transcriptional factors like NF-κB, NFAT1, and IRF4, and immune-related genes such as CCL2, CCL8, and MyD88 [154]. Interestingly, several miRNAs identified in mosquito saliva, such as miR-276-3p and miR-100-5p, are also present in the saliva of *I. ricinus [154]*. This suggests that while different arthropod species differ in their blood-feeding behaviour, they may target similar pathways in their hosts, with specific miRNAs employed to alter host homeostatic response to be the same or varying between arthropod species [154].

The specific research field is still under development, and much more effort is needed to fully understand the role of miRNAs in tick-host interaction. In this thesis, we will continue to explore and analyze the potential functions of miRNAs in the saliva and EVs of *I. ricinus*, aiming to gain a deeper understanding of how the tick evades the host homeostatic response and defense mechanisms to secure successful blood feeding. This knowledge will facilitate the design of effective anti-tick strategies, which will be discussed in this thesis as well.

1.3.1.5. Applications of microRNAs and anti-microRNAs in clinic and pest management: Potential and challenges

The primary goal of miRNA therapeutics is to adjust and, ideally, reverse pathological changes in miRNA expression. This involves enhancing or restoring the expression of endogenous miRNAs that function as disease suppressors, as well as reducing or inhibiting the activity of miRNAs that drive pathological processes [155].

An approach to restore the miRNA activity involves the use of synthetic RNA duplexes, known as mimic miRNAs, which are usually chemically modified to enhance stability and cellular uptake [156–158]. In these double-stranded miRNA mimics, the guide strand, which is identical to the miRNA of interest, is the active (antisense) strand, while the complementary (passenger or sense) strand is designed to be less stable. The passenger strand can also be conjugated to molecules such as cholesterol to further improve cellular uptake efficiency [159].

Repression of the function of pathological miRNAs, can be achieved through antisense oligonucleotides, known as antimiRs [159]. For effective silencing of dysregulated miRNAs in vivo, antimiR oligonucleotides must undergo chemical modifications to enhance their binding affinity, stability, and pharmacokinetic

properties [160]. As was mentioned before in this thesis, the repression exerted by a miRNA on its target mRNA, and consequently its pathological effect, is driven by the stoichiometry between them. Given this, and the fact that miRNAs abundance can vary significantly across different cell types, tissues, and disease states, extensive preclinical studies in animal models are essential to determine the optimal level of inhibition for a specific miRNA target.

One of the main challenges for this therapeutic application is how to deliver mimics miRNAs and antimiRs to the individual so they can exert their functions [161]. Various strategies have been explored to enhance the efficacy of miRNAs and to direct them to specific cells of interest. These methods include both molecular vectors and non-vector approaches, ranging from lipid-based nanoparticles, polymeric vectors, dendrimer-based vectors, cell-derived membrane vesicles as EVs, 3D scaffold-based delivery systems, to various biodegradable and biocompatible nanoparticles derived from polymers and metals [155].

In the context of this thesis, tick miRNAs, tick-derived mimic miRNAs and tick salivary compounds are emerging as potential therapeutic agents. As described in the Section 1.2.4, tick saliva includes a variety of compounds that modulate the host's response to blood feeding. These same compounds may also have applications in treating host illnesses [162]. miRNAs, due to their conservation in blood-feeding arthropods [154] and their ability to modulate host immune, inflammatory, and wound healing responses [17–19], present significant potential for the development of novel therapeutics for tick-borne and other human diseases. Remarkably, the delivery of miRNAs via EVs has already been explored to accelerate wound healing [153] , to enhance the sensitivity of cancer cells to treatment [163], and to reduce aortic inflammation to improve survival during aneurysms [164]. Therefore, understanding tick miRNAs and their potential to influence the host processes mentioned above is essential for

developing new therapeutic strategies. This thesis will explore recent insights into the role of miRNAs in this context, along with their newly discovered cooperative effects, offering the research community fresh perspectives on how tick miRNAs could potentially be our friends instead of enemies as regulators of host homeostasis.

Another field that may see significant advancements through the application of miRNAs is pest management. Here, the use of miRNAs presents a fascinating opportunity to improve tick control strategies. This has been broadly studied in insects, where it has been reported that their feeding and development can be disrupted by delivering miRNAs that interfere with critical biological processes, a strategy known as trans-kingdom RNA interference [165]. This can be achieved through various delivery methods, such as viral vectors, nanoparticles, or exosomes [166,167]. Additionally, studies in insects have described that target pests can receive miRNAs by consuming bacteria that have been genetically modified to express miRNAs or antimiRs [167].

During feeding, ticks ingest bacteria from the skin microbiome of animals, such as livestock [168]. As in the case of insects, these bacteria could be genetically engineered to express precursors of tick miRNAs or antimiRs that disrupt essential biological processes in ticks, like oviposition or molting. These genetically modified bacteria could be introduced into the skin of these animals, thereby reducing tick populations by decreasing egg production or hindering the tick's ability to molt to its next life stage when the bacteria will be consumed with tick bloodmeal [151].

While the potential therapeutic or pest management application of tick miRNAs is highly promising, significant practical challenges must still be addressed. These include gaining a deeper knowledge of the roles played by tick miRNAs, determining the optimal routes of administration to individuals, ensuring in vivo

stability, targeting specific tissues and cell types, and achieving the desired intracellular effects [161].

1.3.2. Long non-coding RNA in tick-host interactions

Long non-coding RNAs are RNA molecules longer than 200 nucleotides and, structurally, similar to mRNAs but not translated into proteins. They play a critical role in gene regulation by influencing gene expression through various mechanisms, including activation or repression of transcription factors, chromatin remodeling, imprinting, and enhancer regulation [169]. lncRNAs are involved in multiple regulatory processes such as post-transcriptional modulation, mRNA processing, and protein trafficking [169]. For instance, chromatin remodeling is mediated by lncRNA-induced histone methylation, which alters chromatin structure to regulate DNA accessibility for transcription machinery. Acting as scaffolds with multiple binding domains, lncRNAs facilitate methylation and demethylation of histones, thereby modulating gene expression [170,171].

1.3.2.1. Role of long-non-coding RNAs as modulators of microRNA functions

In addition to the known roles in transcriptional regulation, lncRNAs may also function as ceRNAs or "miRNA sponges", sequestering miRNAs and preventing them from binding to their target mRNAs, effectively silencing miRNA activity [96]. These miRNA sponges are widespread regulators of miRNA function in eukaryotic cells and play a crucial role in ectoparasite-host interactions, such as the vector-host crosstalk [97]. A schematic representation of the role of lncRNAs as miRNA sponges is provided in Figure 9.

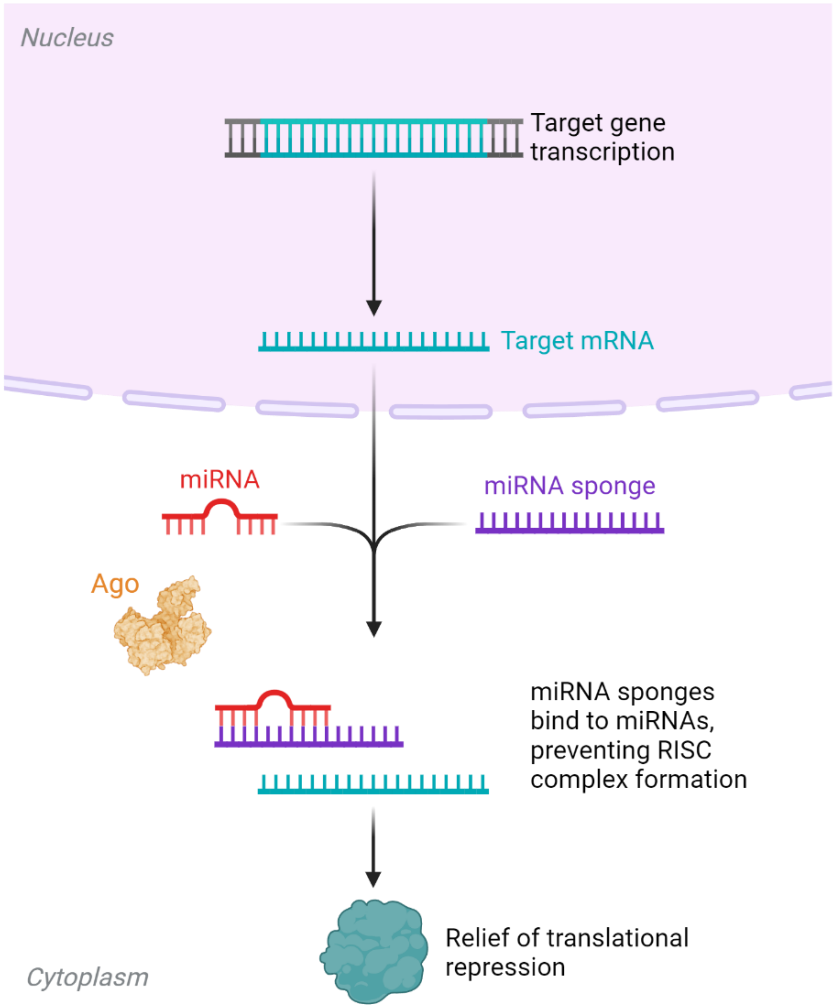

Figure 9. Disruption of microRNA-mediated target silencing by long non-coding RNAs acting as microRNA sponges.

While lncRNAs have been extensively studied in humans and model animals used in medical research [172], there is limited research on their role in host-parasite interactions in arthropods. In vector-host-pathogen interactions, small

ncRNAs have been identified as important mediators of trans-kingdom and inter-species communication [173,174]. However, the functions of lncRNAs in arthropods remain largely unexplored. It has been hypothesized that vectors express lncRNAs to counter host defenses, potentially transporting them in salivary exosomes to the host, where they may act as miRNA sponges to disrupt host immune responses. This intriguing possibility, however, still awaits empirical validation [175]. In this thesis, we will further analyze the potential role lncRNAs as miRNA sponges and their potential implications in the tick-host interaction.

Chapter 2.

Objectives

This thesis aims to characterize the regulatory role of *Ixodes ricinus* miRNAs and their synergistic interactions with non-coding RNAs in the tick-host interface. The ultimate goal is to establish a foundation for novel clinical and pest control strategies that leverage miRNA-based mechanisms.

The specific objectives are:

1. Enhance the *I. ricinus* miRNA reference catalog using the latest genome assembly.
2. Develop a bioinformatics workflow for *I. ricinus* miRNA target identification in *Homo sapiens*, including per-position conservation profiles and cooperative effects mediated by TNRC6.
3. Characterize the potential role of tick miRNAs and their synergistic interactions in the modulation of host pathways.
4. Determine the abundance of non-coding RNA molecules, including miRNAs and long non-coding RNAs, in tick saliva and extracellular vesicles.
5. Generate a high-confidence *I. ricinus* transcriptome from RNA-seq data covering coding and long non-coding RNAs.
6. Analyze transcriptional dynamics in *I. ricinus* salivary glands and midgut across feeding conditions, comparing unfed ticks to those that have fed on naïve or previously exposed hosts with an activated anti-tick response.

7. Assess the capacity of tick-derived long non-coding RNAs to regulate immune responses via host miRNA inhibition.

Chapter 3.

Materials and methods

In this section, we discuss the data, experimental procedures, computational methodologies, and data analysis techniques used to investigate the mechanisms by which *I. ricinus* evades host defenses to successfully feed and complete its lifecycle. This includes an exploration of tick miRNAs and their cooperative effects, transcriptomic dynamics of vital tick organs such as the midgut and salivary glands, and the potential role of lncRNAs in inhibiting host miRNAs and disrupting critical pathways of host homeostatic response to tick feeding.

First, a detailed description of the datasets used in this thesis is provided, covering the reference genomic and transcriptomic data, miRNA catalogs, and sequencing data. A summary of the datasets employed in this thesis can be found in Table 1.

Next, we offer an overview of the experimental procedures employed to obtain samples from *I. ricinus* and their corresponding sequenced RNA. This includes the methods used for tick rearing, blood feeding, tissue collection, and RNA extraction and sequencing.

Finally, we outline the computational methodologies and data analysis techniques used to process and interpret the biological data collected in this study. This includes data preprocessing, quality control, alignment, target

prediction, differential expression analysis, and functional enrichment assessments, all of which are crucial for understanding the biological implications of the results. The bioinformatics strategies and tools applied in this research are also discussed in this section.

3.1. Overview of datasets used in this thesis

3.1.1. Reference genomic data

3.1.1.1. The novel reference genome of Ixodes ricinus

To identify and annotate the non-coding RNAs in *I. ricinus*, including miRNAs and lncRNAs, a recently published reference genome was used [176]. This genome was assembled using Hi-C and 10X linked-read libraries, which greatly improved the assembly's quality. Hi-C data allowed for better chromosome-level organization, while 10X linked-reads helped resolve repetitive regions and connect distant genomic fragments. The final genome was well-structured, with 14 major scaffolds representing the autosomes and the X chromosome, covering 95.2% of the total genome size. This high-quality genome provided a solid basis for ncRNA annotation and analysis.

3.1.1.2. Reference genome of hosts

To ensure the accuracy of our contig set in transcript analysis and eliminate any potential host contamination, contigs from RNA-seq data were aligned to the reference genomes of *Oryctolagus cuniculus*, version 2.0 (OryCun2.0; accession AAGW02000000) and *Cavia porcellus*, version 3.0 (CavPor3.0; accession AAKN00000000.2) [177].

3.1.1.3. The Vertebrate Multiz Alignment & Conservation dataset

To assess the conservation of miRNA target sequences in *H. sapiens* mRNAs, we utilized the Vertebrate Multiz Alignment & Conservation dataset, provided by UCSC [178], which includes a multi-species multiple alignment of 100 vertebrate species. This alignment was generated using high-quality genome sequences from diverse vertebrate species to provide a comprehensive framework for studying evolutionary conservation across vertebrates. The data includes conserved genomic regions across species, enabling the identification of functionally important sequences that are likely under selective pressure. The dataset also provides a rich resource for comparative genomics and can be utilized to study conserved non-coding regions, regulatory elements, and other genomic features across vertebrates.

3.1.2. Reference transcriptomic data

3.1.2.1. Reference transcriptome of Ixodes ricinus

In this thesis, a comprehensive and high-quality reference transcriptome consisting of abundant and well-annotated transcripts was assembled and curated. This transcriptome was generated de novo from poly(A)-enriched RNA samples extracted from the midgut and salivary glands of *I. ricinus*, utilizing sequencing data from the corresponding datasets. This reference transcriptome was used as the foundation for various analyses conducted throughout this thesis.

3.1.2.2. 3' Untranslated regions of canonical mRNAs from Homo sapiens

As mentioned earlier, we selected *H. sapiens* as the model host to analyze. Therefore, to obtain the 3' UTR regions for canonical transcripts of *Homo sapiens*, we used the reference transcriptomic annotation (version 112) of the *H. sapiens* genome (GRCh38.p14) from Ensembl, with data retrieval carried out through Biomart [179,180].

3.1.3. MicroRNA datasets

3.1.3.1. MicroRNAs from Ixodes ricinus

To investigate the potential role of *I. ricinus* miRNAs in modulating the tick-host interface, a comprehensive and reliable reference miRNA catalog was essential. In this thesis, the previously available *I. ricinus* miRNA catalog (GenBank accession numbers MF061606-MF061678), constructed using the earlier *I. ricinus* reference genome [181], the *I. scapularis* genome [14], and transcriptomic data from previous studies [17], was expanded and refined. This expansion, along with the assessment of completeness and reliability of this updated dataset, was performed by identifying miRNAs in the newly sequenced *I. ricinus* genome [176], ensuring a more accurate and robust resource for this thesis and future research.

3.1.3.2. MicroRNAs from Homo sapiens

To sustain clinical relevance and support therapeutic applications, we selected *H. sapiens* as the model host to conduct *in silico* studies on how *I. ricinus* evades the host's homeostatic response against feeding. Thus, to explore the inhibitory

potential of *I. ricinus* lncRNAs on host miRNAs, we utilized the *H. sapiens* miRNA dataset from MirGeneDB 2.1. [182].

3.1.4. Sequencing datasets

3.1.4.1. Small RNA dataset: Saliva, midgut and salivary glands

A small RNA-seq dataset was obtained from previous research that analyzed the potential combinatorial effects of *I. ricinus* miRNAs [17]. The dataset consists of 10 small RNA samples derived from pooled tissue dissected from female adult ticks and nymphal ticks during various feeding periods. The samples include four samples from nymphal SG and MG at 0–12 h and 12–24 h and six samples from adult SG and MG at 0–12 h, 12–24 h, and 24–36 h. Additionally, a sample from tick saliva was collected as described in previous studies [183], with ticks fed on rabbits for a 6-day period.

3.1.4.2. Small RNA and RNA dataset: Extracellular vesicles

This dataset consisted of samples derived from the saliva of *I. ricinus*. Differential centrifugation was employed to isolate samples containing EVs of varying sizes and free molecules from the saliva, as discussed in Section 3.2.3. The dataset comprised a total of 16 samples, with 8 samples from each of two *I. ricinus* populations: one parasitizing a rabbit during its first exposure to ticks, and the other during the rabbit's second exposure. Each of these 8 samples included two biological replicates for the four different EV size categories. Both small RNA and poly(A)-enriched RNA were extracted and sequenced.

3.1.4.3. RNA dataset: Midgut and salivary glands

The dataset includes RNA samples from ticks exposed to rabbits for two separate feeding periods. Two rabbits were exposed to 25 female and 25 male ticks each. Ticks were collected at multiple time points (12, 24, 48, 72, and 96 hours post-exposure), and the following samples were retrieved:

- Five salivary gland (SG) biological-replicate samples from ticks feeding at five different time points (12, 24, 48, 72, 96 hours) per prior host exposure status. This sums a total of fifty samples. Additionally, five SG biological-replicate samples of ticks unfed were collected.
- The same sample collection was done for midgut (MG) tissue although obtaining three biological-replicate samples instead of five. Thus, three MG biological-replicate samples were retrieved from unfed ticks and ticks fed at each corresponding time point and host exposure status.

In total, 55 SG samples and 33 MG samples were collected for RNA extraction and subsequent sequencing analysis.

3.1.4.4. RNA dataset: Salivary glands only

To strengthen the reliability of the *I. ricinus* lncRNA set for identifying miRNA sponge candidates, we incorporated an additional *I. ricinus* RNA dataset previously published (BioProject accession PRJNA312361) [184]. The dataset includes RNA samples from tick salivary glands, collected at three different time points (24 h, 48 h, and 72 h) following either natural feeding on a rabbit or artificial feeding on reconstituted rabbit blood. At each time point and feeding mode, SGs were dissected from three individual ticks, each representing a separate library and biological-replicate sample. In total, the dataset is comprised of 18 single-tick salivary gland libraries.

3.1.4.5. RNA dataset: Whole body

An additional *I. ricinus* RNA-seq dataset, previously published (BioProject accession PRJNA395009) [185], was included to further increase the reliability of the *I. ricinus* lncRNA set. The dataset consists of RNA samples from ticks in five different biological states:

1. Unfed nymphs (n = 60)
2. Partially fed nymphs (n = 12)
3. Unfed adult females (n = 8)
4. Partially fed adult females (n = 4)
5. Unfed adult males (n = 12)

The sample sizes for cDNA sequencing varied among biological states due to differences in the mRNA yield per individual, which were influenced by developmental stage (nymphs vs. adults) and feeding condition (unfed vs. partially fed). Nymphs were fed on mice (*Mus musculus*) for 24 hours, while adult females were fed on *O. cuniculus* for 48 hours. These feeding durations correspond to phase 1 (the slow phase of engorgement) of tick feeding. Each biological condition had three replicates, resulting in a total of 15 samples for sequencing.

Table 1. Summary of the datasets employed in this thesis.

Dataset	Source	Type of data	Species	Purpose in this thesis
Reference genome of *I. ricinus*	Publication [176]	Genomic	*I. ricinus*	Annotation of RNA elements
Reference genome of hosts	GenBank [177]	Genomic	*O. cuniculus* and *C. porcellus*	Removing host contamination
The Vertebrate Multiz Alignment & Conservation dataset	UCSC [178]	Genomic alignment of 100 species	100 Vertebrate species	Conservation assessment of target sequences
Reference transcriptome of *I. ricinus*	Assembled in this thesis	Transcriptomic	*I. ricinus*	Obtention of coding RNA and lncRNA
3' UTR regions of canonical mRNAs from *H. sapiens*	Ensembl [179]	Transcriptomic	*H. sapiens*	Target prediction of *I. ricinus* miRNAs
MicroRNAs from *I. ricinus*	Produced in this thesis	MicroRNA	*I. ricinus*	miRNA and cooperative effect analysis
MicroRNAs from *H. sapiens*	MirGeneDB [182]	MicroRNA	*H. sapiens*	lncRNA as miRNA sponge analysis
Dataset from saliva, MG, and SG	Publication [17]	SmallRNA-seq	*I. ricinus*	miRNA abundance in saliva
Dataset from EVs	Produced in this thesis	SmallRNA-seq and RNA-seq	*I. ricinus*	EV dynamics of miRNAs and lncRNAs
Dataset from MG and SG	Produced in this thesis	RNA-seq	*I. ricinus*	Transcriptome assembly and dynamics
Dataset from SG only	Publication [184]	RNA-seq	*I. ricinus*	Generation of the consensus set of lncRNA
Dataset from whole body	Publication [185]	RNA-seq	*I. ricinus*	Generation of the consensus set of lncRNA

3.2. Experimental procedures: animal manipulation, sample collection and sequencing

3.2.1. Tick rearing, mating and repeated exposure to hosts

To investigate differentially expressed transcripts in *I. ricinus* ticks fed on either naïve or previously exposed to ticks rabbits, we established a generation of specific pathogen-free sibling ticks. Eggs were hatched, and the ticks were allowed to develop into adult females. These females were fed on an SPF guinea pig until fully engorged and then left to lay eggs.

The resulting larvae were fed on SPF guinea pigs (approximately 100 larvae per host). Once molted into adult females, these ticks, originating from the same maternal lineage, were pre-mated with sibling males and subsequently used for feeding experiments and tissue isolation. Using ticks from a single female helped minimize genetic variability between samples, ensuring more consistent results in downstream analyses.

Then, two rabbits were each exposed to female and male ticks. Females were collected at time points 12, 24, 48, 72, and 96 hours post-exposure. Ticks were dissected, and their salivary glands and midguts were stored in 200 µL of RNA later at 4°C overnight before long-term storage at -80°C. Two weeks after the end of the first rabbit exposure to ticks; a second exposure was carried out following the same protocol. SG samples from unfed ticks and from ticks fed till each feeding time point and samples of MG from unfed ticks and from ticks fed till each time point were collected.

3.2.2. Saliva collection from fully fed ticks

Fully fed ticks were washed with 15% ethanol, dried, and secured onto a glass slide using sticky tape. A small amount of plasticine was placed in the center of the slide to support a microcapillary tube. The hypostome, along with one palp, was carefully inserted into the microcapillary tube, ensuring a proper fit.

To stimulate saliva production, 2 µl of pilocarpine was applied to the tick's body, taking care to avoid contact with the microcapillary tube. The prepared slides with fixed ticks were then placed on a wet filter paper and incubated at 37°C in a CO_2-enriched environment. The correct positioning of the hypostome inside the microcapillary tube was monitored every 30 minutes.

After a 2.5-hour incubation period, saliva was collected from the microcapillary tubes and stored at -70°C until further use.

3.2.3. Isolation of extracellular vesicle fractions from *Ixodes ricinus* saliva

The different EV fractions were isolated from 7 mL or 2.5 mL of freshly frozen (<2 months) *I. ricinus* saliva for the first and second tick exposures, respectively, using differential ultracentrifugation following established protocols [186]. The isolation process is represented in Figure 10, and involved sequential centrifugation steps:

1. Removal of larger particles and cell debris by centrifugation at 300 g for 5 minutes.
2. Pelleting of large EVs (lEVs) at 2,000 g for 10 minutes at 4°C.
3. Isolation of medium EVs (mEVs) by centrifugation at 10,000 g for 40 minutes at 4°C.

4. Collection of small EVs (sEVs) by ultracentrifugation at 150,000 g for 90 minutes at 4ºC.

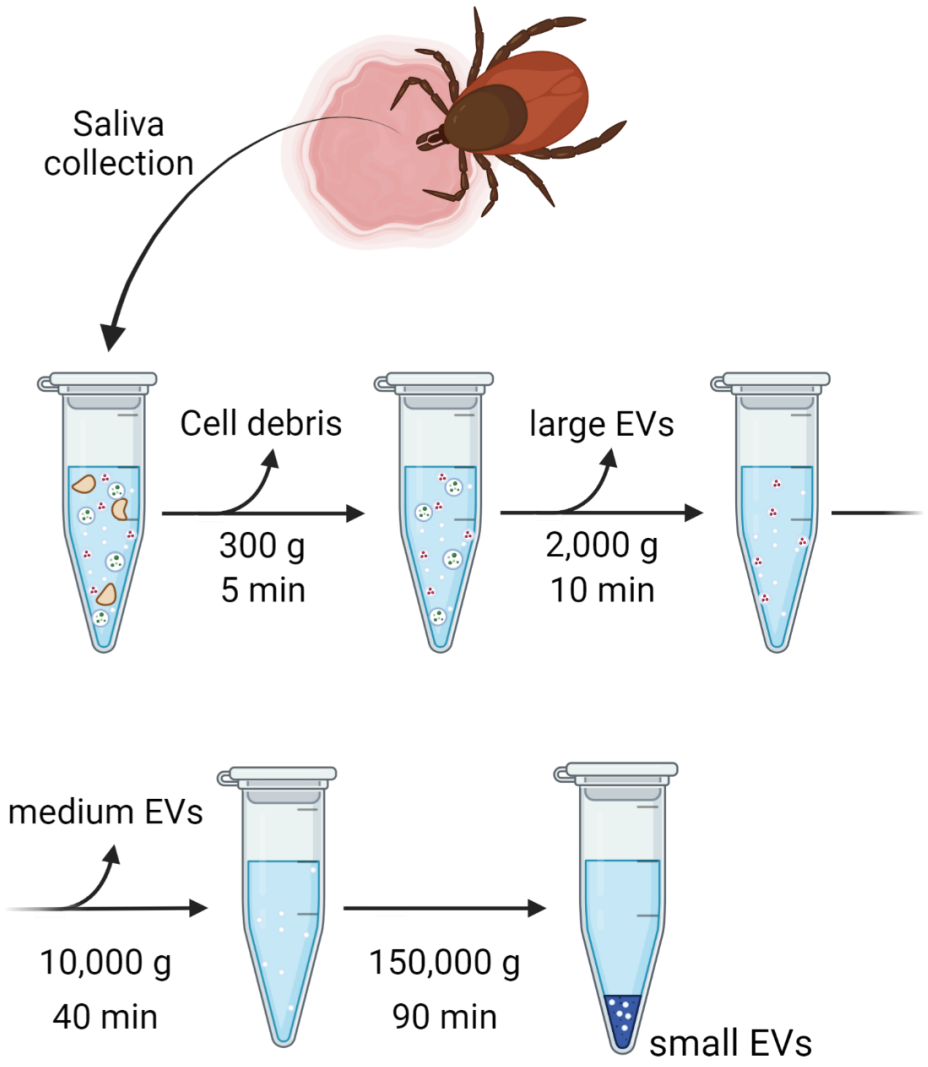

***Figure 10. Schematic representation of the differential ultracentrifugation protocol to isolate specific fractions of extracellular vesicles from* Ixodes ricinus *saliva*.**

The 10,000 g and 150,000 g centrifugations were performed using polycarbonate tubes (355645, Beckman-Coulter) in an MLA-50 rotor (Beckman-Coulter). Each EV pellet was resuspended in 400 µL of PBS. Additionally, the remaining saliva

supernatant (SN) after the final 150,000 g centrifugation was collected and analyzed as a separate fraction.

3.2.4. Sample preparation and RNA extraction

RNA extraction from *I. ricinus* samples was performed using the Qiagen TissueLyser and the Qiagen RNA Micro Plus Kit (#74034). Library preparation was carried out using the New England Biolabs (NEB) Poly(A) mRNA Magnetic Isolation Module (#E7490L) and the NEBNext Ultra Directional RNA Library Prep Kit (#E7420L).

Total RNA samples were submitted to the North Carolina State Genomic Sciences Laboratory (Raleigh, NC, USA) for Illumina RNA library construction and sequencing. Prior to library preparation, RNA integrity, purity, and concentration were assessed using an Agilent 2100 Bioanalyzer with an RNA 6000 Nano Chip (Agilent Technologies, USA). mRNA was purified using oligo-dT beads from the NEBNext Poly(A) mRNA Magnetic Isolation Module (New England Biolabs, USA).

cDNA libraries for Illumina sequencing were generated using the NEBNext Ultra Directional RNA Library Prep Kit and NEBNext Multiplex Oligos for Illumina, following the manufacturer's protocol. Briefly, mRNA was chemically fragmented and primed with random oligos for first-strand cDNA synthesis. Second-strand synthesis was performed using dUTPs to preserve strand orientation. The resulting double-stranded cDNA was purified, end-repaired, and A-tailed for adapter ligation. Size selection was carried out using AMPure XP beads (Beckman Coulter, USA) to obtain a final library size (including adapters) of 300–450 bp.

Library enrichment and indexing were performed through PCR amplification, followed by purification. The final library size and concentration were assessed

using an Agilent 2200 TapeStation (Agilent Technologies, USA) before sequencing.

3.2.5. RNA sequencing

The libraries derived from small RNA extracted from extracellular vesicles were prepared and sequenced using the QIAseq miRNA Library Kit (QIAGEN) following the manufacturer's protocol. This protocol includes adapter ligation, reverse transcription, and amplification steps optimized for small RNA sequencing. Unique molecular identifiers were incorporated to enhance quantification accuracy and minimize PCR bias. The final libraries were quality-checked for size distribution and concentration before sequencing on the QIAGEN NGS platform, ensuring high-fidelity small RNA profiling.

The final quantified poly(A)-enriched RNA libraries were pooled in equimolar amounts and loaded onto a NovaSeq 6000 DNA sequencer (Illumina, USA) using an S4 150×2 paired-end sequencing reagent kit. Raw base call files were generated using the Real-Time Analysis software package and subsequently de-multiplexed by sample into FASTQ files for data delivery.

3.3. Computational methodology and data analysis

3.3.1. Identification and *a*nnotation of *r*egulatory and *c*oding RNAs in *Ixodes ricinus*

3.3.1.1. Annotation of non-coding RNA and cis-regulatory elements in the novel genome of Ixodes ricinus

To ensure the reliable and accurate annotation of structural and regulatory non-coding elements in the novel reference genome of *I. ricinus* [176], we employed multiple approaches, software tools, and databases. Initially, we used Infernal and the latest version of the Rfam database to identify ncRNAs and cis-regulatory elements in the *I. ricinus* genome [187,188]. We then used tRNAscan-SE to annotate transfer RNAs [189].

For the annotation of lncRNAs, we relied on the dataset compiled and analyzed by the analysis of the transcriptome detailed in the next section. This dataset provided a consensus set of high-confidence lncRNAs. First, we verified the absence of coding properties in these lncRNAs using CPC2 [190]. Next, we aligned the lncRNAs to the *I. ricinus* genome using BLAT and retained only alignments with a score above 90 [191]. Finally, to eliminate potential assembly artifacts and prevent interference with the coding RNA set, we used gffcompare to remove any lncRNAs that overlapped with coding RNAs [192].

3.3.1.1.1. Annotation and assessment of the taxonomic conservation of *Ixodes ricinus* microRNAs

The software sRNAbench was used to identify the most accurate set of miRNAs along with their genomic positions [193]. Thus, based on our analysis of this novel high-quality *I. ricinus* genome, we enlarged the actual catalog of *I. ricinus*

miRNAs, compared to the one based on short-read sequencing data from midgut and salivary gland tissues [17] and on the information provided by the previously available genomes of *I. ricinus* and *I. scapularis* [181,194]. Novel miRNAs were annotated with two "X"s in their IDs. This catalog, containing 162 unique mature miRNAs, is used for the analyses presented in this thesis.

In our phylogenetic analysis, in order to determine the origin node of the mature *I. ricinus* microRNA sequences we analyzed comparatively their seed sequence to classify miRNA families. We used MirGeneDB 3.0, which includes data from 114 species representing all major metazoan groups, serving as our reference set [195]. First, we identified the seed sequences for all guide and passenger strand sequences. These seed sequences were then clustered, recording all species that contain a microRNA with the same seed. Using information from the NCBI taxonomy file [196], we were able to determine the origin node, i.e., the taxonomic level that includes all species possessing that particular seed sequence. For example, if a seed sequence is found in *Homo sapiens*, *Pan troglodytes*, and *Gorilla gorilla*, the node of origin would be classified as Hominidae. Thus, we determined the node of origin for all *I. ricinus* microRNA seed sequences, allowing us to classify their taxonomic level of conservation as "Bilateria", "Protostomia", or "Arthropoda". If a seed sequence was not present in the database, it was designated as "*I. ricinus*-specific", indicating its uniqueness to this species.

3.3.1.2. Assembly of a reference transcriptome for Ixodes ricinus *and annotation of coding and long non-coding RNAs*

3.3.1.2.1. Reference transcriptome assembly

Reads obtained from salivary glands and midgut from *I. ricinus* were preprocessed, as discussed in Section 3.3.3.1, and used to generate de novo

assemblies for SG and MG separately by means of Trinity version 2.8.6 [197], using default parameters. To generate a consensus transcriptome, the SG and MG contigs were clustered together by applying CD-HIT version 4.8.1 [198]. We considered two contigs as belonging to the same cluster if they share sequence similarity above 98% and a sequence coverage higher than 80%. Only the longest sequence within each cluster is used for further analysis. Please note that in this way, not only MG and SG assemblies become merged together, but also highly similar contigs within the individual assemblies are removed.

We analyzed several metrics of the transcriptome to ensure its good quality and completeness. The script TrinityStats.pl was used to calculate the N50 statistic and the median contig length [197]. The completeness of the final transcriptome was assessed using BUSCO version 4.0.6 [199], using the Arachnida lineage dataset as reference (arachnida_odb10).

To quantify and remove the presence of contigs that presumably belong to the host, we aligned the final set of contigs to the reference genomes of *O. cuniculus*, version 2.0 (OryCun2.0; accession AAGW02000000) and *C. porcellus,* version 3.0 (CavPor3.0; accession GCA_000151735.1). To do so, we used STAR and STARlong, version 2.7.6a, for sequences shorter than 650 pb and for sequences equal or longer than 650 pb, respectively [200]. For the alignment to be successful, the ratio of mismatches to contig length must be 5% or lower. Additionally, sporadic and low-expressed transcripts were removed. Specifically, we discarded transcripts that did not meet a minimum expression threshold of 5 fragments per kilobase of transcript per million mapped reads (FPKM) in all samples of at least one feeding condition.

Thus, we obtained the final set of reliable and abundant transcripts constituting the reference transcriptome of *I. ricinus*.

3.3.1.2.2. Annotation of RNA

To annotate the transcriptome, we first classified the transcripts into coding and non-coding categories. Candidate coding regions were identified using TransDecoder, version 5.5.0 [201], through a four-step process:

1. Open reading frames (ORFs) longer than 50 amino acids were identified using TransDecoder.LongOrfs.
2. The identified ORFs were then aligned against a custom local database consisting of proteomes from six *Arachnida* species: *I. scapularis, Dinothrombium tinctorium, Tetranychus urticae, Tropilaelaps mercedesae, Leptotrombidium deliense*, and *Stegodyphus mimosarum*. These proteomes were retrieved from the UniProt database [202]. The alignment was performed using BLASTp (version 2.10.1+) with an E-value cutoff of 10^{-5} [203].
3. Candidate coding regions were refined using TransDecoder.Predict.
4. Finally, CD-HIT (version 4.8.1) was used to eliminate redundancy and generate a final set of unique coding regions [198].

To gain a deeper understanding of the proteins encoded by these contigs, we performed an extensive annotation of those that contained a coding region. We used BLASTp (version 2.10.1+) to map the unique coding regions to four databases: the local *Arachnida* database, Swiss-Prot, UniRef90, and TickSialoFam [203–206]. Following Ribeiro et al. criteria, we applied an E-value threshold of 10^{-4} for the alignments [206]. The Bit-score, a similarity score independent of database size, was used to select the best alignment.

Once the best alignment was determined, we used UniProtKB to retrieve Gene Ontology (GO) annotations based on the protein ID of the best match [204]. For coding regions that did not receive an annotation through UniProtKB, we

followed the Gene Ontology Annotation workflow of Blast2GO (version 5.2.5) [207].

To identify conserved protein domains within the unique coding regions, we used InterProScan (version 5.48-83.0) [208]. Signal peptides were predicted using Phobius and SignalP (version 4.1) with sensitive parameters (-U 0.34 -u 0.34) to identify putative mature peptides [209,210]. Additionally, TMHMM (version 2.0c) was employed to predict transmembrane helices in both the unique coding regions and the mature peptides [211].

Thus, the transcriptome was partitioned into distinct sets of coding and non-coding RNAs.

3.3.1.2.3. Generation of a consensus and reliable set of long non-coding RNAs

To minimize potential assembly artifacts and ensure the reliability of the predicted lncRNAs, we isolated ncRNAs ranging from 200 bp to 1800 bp and generated a consensus set of lncRNAs. Using CD-HIT, we clustered distinct sets of lncRNAs [198]. First, lncRNAs from the reference transcriptome assembled using midgut and salivary gland samples (MG-SG lncRNAs). Second, lncRNAs from the additional datasets described in Section 3.1.4, which were classified as coming from salivary glands only (SG lncRNAs) or from whole tick bodies (WB lncRNAs) [184,185].

To accomplish this, transcriptomes were generated for the two additional datasets following the same criteria outlined above, with the exception of the final clustering step, since it was done before due to the inclusion of two different tissues, which is not the case for SG and WB transcriptomes. Additionally, the transcriptomes were annotated and partitioned into distinct sets of coding and non-coding RNAs, using the same criteria described above.

Then, a clustering step was made for the three set of lncRNAs obtained from the three transcriptomes as described above. Only clusters with at least one lncRNA belonging to MG-SG lncRNA remained for the rest of the analyses. This was done because MG-SG lncRNAs were the most reliable lncRNAs, because of the high number of samples used for the assembly of their sequences and the additional expression filter applied to it, as described in Section 3.3.1.2.1. Next, we selected the longest lncRNA from a cluster as its best representative. Through this approach, we obtained the final consensus set of lncRNAs.

For comparison purposes, we also generated a consensus set of coding RNAs by following the same methodology described above. All identified lncRNAs and coding RNAs from this study are available for download in the Downloads section of IxoriDB (Section 3.3.5).

3.3.2. Target prediction in microRNAs and microRNA sponges

Two distinct target prediction processes were carried out in this thesis. First, to investigate the role of miRNAs from *I. ricinus* in the tick-host interface, we performed target prediction on the 3' UTR regions of canonical mRNAs from *H. sapiens*. Secondly, we assessed the role of *I. ricinus* lncRNAs as miRNA sponges by predicting the targets of *H. sapiens* miRNAs, obtained from MirGeneDB 2.1 [182], within the tick lncRNA sequences.

Target prediction was performed by means of sRNAtoolbox [193]. The algorithms PITA, Seed, Miranda, and TargetSpy were applied [212–214]. A target was considered consensual if at least three of the four algorithms predicted it. Only consensual target regions were retained for further analysis.

3.3.2.1. Improving the target prediction: Conservation and cooperative effect

3.3.2.1.1. Prediction of conserved target regions

When analyzing the targets of *I. ricinus* miRNAs in the 3' UTR regions of canonical *H. sapiens* mRNAs, we assessed the conservation of consensual target regions. This step was motivated by two key factors: First, it has been shown that considering the conservation of target sequences enhances the reliability of the predicted targets [215]. Second, the targeted sequences must be conserved for *I. ricinus* miRNAs to effectively function across the broad range of host species it can parasitize.

Thus, a conservation analysis was conducted for consensual target regions using the Vertebrate Multiz Alignment & Conservation (100 Species) provided by UCSC [178]. The set of species was curated to include only evidenced and potential hosts for *I. ricinus,* resulting in the following 29 species: *H. sapiens, Pan troglodytes, Gorilla gorilla gorilla, Nomascus leucogenys, Macaca mulatta, Macaca fascicularis, Chlorocebus sabaeus, Callithrix jacchus, Spermophilus tridecemlineatus, Mus musculus, Rattus norvegicus, C. porcellus, O. cuniculus, Bos taurus, Ovis aries, Capra hircus, Equus caballus, Felis catus, Canis lupus familiaris, Mustela putorius furo, Myotis lucifugus, Erinaceus europaeus, Sorex araneus, Monodelphis domestica, Falco cherrug, Falco peregrinus, Ficedula albicollis, Columba livia* and *Anolis carolinensis*.

A conservation score was calculated for each position of the pairings between each miRNA and each target region. The conservation score for a position was calculated as the number of coincident bases divided by the number of species with sequence available in the multiple alignment for the analyzed region. Additionally, for each position, the phylogenetically furthest species with available sequence in the multiple alignment for the analyzed region was

identified to assess the level of conservation across different taxonomic groups. Only target regions with a conservation score greater than 0.9 for all positions of the seed, and whose phylogenetically furthest species was not a member of the Hominidae family, were considered conserved and remained for further analysis.

3.3.2.1.2. Prediction of cooperative target regions

To identify potential cluster regions indicating cooperation between consensual and conserved target sites, we selected target regions based on their nucleotide spacing, considering the role of NTRC6 in facilitating this cooperation [147]. Specifically, we focused on regions where target sites were spaced between 12 and 40 nucleotides apart.

Target regions meeting these criteria were categorized as cooperative and were analyzed in detail in this thesis.

3.3.2.1.3. Statistical significance of the number of conserved and cooperative target regions associated with a microRNA

In order to obtain miRNAs with a higher number of conserved or cooperative target regions than what is expected by chance, we compared miRNAs from *I. ricinus* with a negative control set of miRNAs. To obtain negative control miRNAs, we used shuffleseq to randomize the sequence of the miRNAs from *I. ricinus [216]*, making sure that the new sequence's seed didn't exist in MirGeneDB database [182].

Then, a ranked comparison was made between *I. ricinus* miRNAs and randomized miRNAs. First, we ranked both sets of miRNAs based on the total number of target regions and created a contingency table per comparison using total number of target regions and conserved target regions. We applied the Fisher's test and corrected the p-values for multiple comparisons. Thus, we

obtained the False Discovery Rate (FDR) and Odds Ratio for the conserved number of target regions of each *I. ricinus* miRNA.

In the case of the cooperative target regions, we ranked both sets by the number of conserved target regions and made the contingency tables using conserved and cooperative target regions. As before, Fisher's test and correction for multiple comparisons were applied to obtain miRNAs with a higher number of cooperative target regions than expected by chance.

3.3.3. Analysis of the sequencing data

3.3.3.1. Trimming and quality controls

We employed sRNAbench, a specialized tool designed for small RNA datasets, to perform adapter trimming, filter out low-quality reads, and evaluate data quality [193].

In the case of raw RNA-seq reads, to ensure high-quality sequencing data, the raw sequences underwent adapter trimming and quality filtering using Trim Galore [217]. This process removes sequencing adapters, trims low-quality bases via Cutadapt [218]. It also discards very short reads, which can otherwise introduce errors in downstream analyses. The quality of both raw and trimmed reads was evaluated using FastQC, and results were compiled using MultiQC [219,220].

3.3.3.2. Expression abundance analysis

To determine the abundance of *I. ricinus* miRNAs in saliva and extracellular vesicles, we used sRNAbench [193]. The tool first aligned and assigned reads to known *I. ricinus* miRNAs. Then, miRNA abundance was calculated by

normalizing read counts to the total number of reads assigned to miRNAs within the library, expressed as reads per million (RPM).

We obtained the expression profile of poly(A) enriched RNA sequences from the final reference transcriptome of *I. ricinus* in salivary glands, midgut, saliva and extracellular vesicles, by means of RSEM version 1.3.3 [221]. This tool applies Bowtie2 to align the preprocessed to the consensus transcriptome generating, among other statistics, the fragments per kilobase of transcript per million mapped reads (FPKM) expression values for each transcript [222].

3.3.3.3. Exploration of abundance data and its variability

A crucial step in ensuring the accuracy of sequencing data analysis is to explore the expression patterns across samples, which helps to identify outliers. Additionally, a global overview of expression variation enables a clearer understanding of how samples group together, revealing patterns of similarity and difference within the dataset.

This exploration was performed by realizing a principal component analysis (PCA), a hierarchical clustering analysis (HCA) and a correlation analysis of the expression profiles. These analyses were made using the libraries Scikit-learn and SciPy from Python, and stats and pheatmap from R [223–226]. The Ward method was employed for hierarchical clustering, a technique that minimizes the total within-cluster variance by iteratively merging the two clusters that result in the smallest increase in the sum of squared differences within all clusters [227].

At the individual transcript level, analyzing variation in transcript expression across biological or technical replicates is essential for assessing the consistency, reliability, and reproducibility of downstream analyses. The study conducted on the salivary glands and midgut of *I. ricinus* had a high number of

biological replicates and uniquely used genetic material from individual sibling ticks, rather than pooled samples, allowing for the detection of individual tick responses to feeding events.

To identify genes with significant individual variability, which may suggest either less reliable data or a strong individual response, we calculated the coefficient of variation (CV) for each unique coding transcript across different conditions and tissues. The CV normalizes variance by the mean expression value, making it independent of overall expression levels. To minimize potential artifacts from low-expression transcripts, only those with a minimum expression of 5 FPKM in at least one sample within a given condition were included. Additionally, we computed the mean CV and ranked the transcripts based on their variation.

3.3.3.4. Identification of differentially expressed transcripts

Two types of differential expression analyses were performed in this thesis: (1) pairwise differential expression analysis, which directly compares gene expression between two experimental conditions, and (2) global time-course analysis, which identifies genes exhibiting significant expression changes over time between two experimental conditions.

To perform pairwise differential expression analysis, we used EBSeq, which is integrated into RSEM version 1.3.3 [221]. Differential expression was determined using the "expected counts" calculated by RSEM, following these steps:

1. Expression levels for each sample were estimated using rsem-calculate-expression with the parameters –bowtie2 and –paired-end.
2. A data matrix was generated for each comparison using rsem-generate-data-matrix.
3. Differential expression analysis was performed using rsem-run-ebseq.

4. Transcripts were filtered using rsem-control-fdr with an FDR threshold of 0.05, retaining only those with an FDR < 0.05.
5. To ensure robust results, only transcripts with a mean coverage of at least 200 expected counts across the conditions compared were considered for further analyses.

For time-course analysis, we employed maSigPro version 1.68.0 [228]. An expression matrix was generated using the expected counts from RSEM. Since maSigPro lacks an internal normalization method, we applied TMM normalization by means of EdgeR prior to analysis [229]. The design matrix was constructed to assess expression differences between first and second host exposures over time. A maximum FDR of 0.05 was set as the threshold for a gene to be considered differentially expressed. The polynomial regression degree for the second step of the maSigPro pipeline was set to 4. Stepwise regression was performed using the forward elimination algorithm, with a minimum R-squared value of 0.6. Finally, hierarchical clustering with correlation distance and Ward's agglomeration method was used to classify transcripts into nine clusters per tissue [227].

To further investigate differences between ticks feeding on naïve versus previously exposed to tick hosts, we identified the most differentially expressed gene products between these two experimental conditions using a pipeline based on cumulative effect calculation [230]. Specifically, we calculated the cumulative absolute log-fold change between first and second host exposures to ticks as a metric to select the most differentially expressed transcripts over time. This analysis was conducted separately for midgut and salivary glands. The top 50 differentially expressed genes (DEGs) with the highest cumulative absolute log-fold change in each tissue were then subjected to functional *in silico* analysis.

Due to the large number of conditions and comparisons made in this study, we obtained numerous groups of interesting transcripts. To further analyze these groups, their intersections and their complex relationships, we applied SuperExactTest [231]. This tool allows the user to calculate and represent intersections among multiple sets.

3.3.4. Functional *in silico* analysis of *Ixodes ricinus* RNA elements: enrichment and network-based approaches

3.3.4.1. Functional role analysis of Ixodes ricinus *microRNAs and their cooperative effect*

To investigate the role of microRNAs in the tick-host interface, we identified sets of H. sapiens genes that were consistently targeted by *I. ricinus* miRNAs. Specifically, this thesis focuses on two gene sets for analysis:

1. A set of 526 genes that contained more than three conserved target sites in their 3' UTRs for the complete set of *I. ricinus* miRNAs.
2. A second set of the top 526 genes with the highest number of conserved targets for a subset of key *I. ricinus* miRNAs. To ensure consistency and allow for meaningful comparisons, if multiple genes shared the same number of conserved targets at the cutoff point, they were randomly selected to complete the set.

Key *I. ricinus* miRNAs were defined as the 12 miRNAs that exhibited the most promising characteristics based on: a) their abundance in tick saliva [17], b) their high ratio and statistical significance regarding the number of conserved target regions, c) targeting neighboring sites of the same target mRNA in the vertebrate host.

Using the previously defined gene sets, functional enrichment analysis was performed using ClusterProfiler [232], leveraging pathway and ontology annotations from MSigDB [233]. The analysis incorporated pathway databases, including KEGG, Reactome, and WikiPathways [234–236], while ontology terms were considered for the Biological Process, Molecular Function, and Cellular Component categories [237].

To further analyze the role of *I. ricinus* miRNAs and their potential cooperative effects, we identified genes with cooperative targets for the 12 key *I. ricinus* miRNAs. A crucial factor for the functionality of this gene silencing is the presence of these genes in skin cell types, enabling localized miRNA-gene interactions. Therefore, the abundance of genes across single-cell types from skin tissue and the ratio of single cells expressing these genes were calculated using the single-cell dataset from GTEx [238]. We calculated the proportion of cells with expression of a given gene, defined as the median fraction of single cells within each cell type that showed detectable expression for each of the genes in the set. The median expression was computed as the median expression level of all genes in the analyzed gene set for each cell type.

To assess the statistical significance of gene expression patterns, Z-scores and p-values were computed by randomly sampling 1,000 gene sets, with the same size as the set analyzed, from a background of genes that contained at least one conserved target for the full set of *I. ricinus* miRNAs (negative control). The observed expression metrics were then compared to the distribution of metrics expected by chance. P-values and Z-scores were estimated using a Monte Carlo approach, where random sampling was used to generate an empirical null distribution, and the probability of obtaining the observed values under this null model was calculated.

3.3.4.2. Functional enrichment analysis of coding RNA

Once the sets of differentially expressed transcripts, from both pairwise comparisons and time-course analyses, were defined, we proceeded with their functional enrichment analysis. This was performed using StringDB, version 11.0b [239], by mapping the identified transcripts to the model organism *Drosophila melanogaster,* as proper annotation and protein interactions for *I. ricinus* are not yet well-defined. This approach enabled us to gain a deeper understanding of the relationships between the proteins encoded by the transcripts. Additionally, it allowed us to determine whether these relationships were associated with significantly enriched Gene Ontology (GO) terms, providing insights into their potential biological roles and pathways [237].

3.3.4.3. Functional analysis of Ixodes long non-coding RNAs as microRNA sponges: Identification of candidates and their roles in the tick-host interface

The main objective of the analysis of *I. ricinus* lncRNAs was to predict which lncRNAs from the consensus set had the highest potential to function as miRNA sponges. We employed three distinct approaches to identify the best sponge candidates. The first approach focused on determining which lncRNAs had the greatest number of miRNA targets. The second approach aimed to normalize the number of targets by considering the length of the lncRNA, identifying those with the highest number of targets per kilobase. Finally, instead of concentrating on lncRNAs with a high number of targets for a single miRNA, we explored lncRNAs consistently targeted by multiple miRNAs. To do so, we applied the Apriori algorithm, which identifies statistically significant combinations of miRNAs that jointly target a specific set of lncRNAs [240]. This allowed us to identify groups of miRNAs that consistently targeted lncRNAs together. In the end, we

considered the best sponge candidates to be the consensus lncRNAs that met the following criteria: 1) the greatest number of targets for a specific miRNA, 2) the highest number of targets per kilobase for a given miRNA, and 3) three distinct groups of consensus lncRNAs with no overlap, each significantly and consistently targeted by a group of miRNAs.

The functional analysis of *I. ricinus* lncRNA candidates to serve as miRNA sponges is based on the miRNAs that target them. We assigned functions to the combinations of miRNAs and sponge candidates using miTALOS v2.0 and DIANA-miRPath v3.0 [241,242]. Through these web tools, we obtained information about the pathways in which the miRNAs are involved and the locations of the genes they target within those pathways.

3.3.4.4. Protein-protein interaction network

Protein-protein interaction (PPI) networks in this thesis were made using StringDB directly or StringDB module in Cytoscape [243,244]. To gain a broader understanding of the functions of the proteins of interest, interactors were included with a high-confidence threshold of 0.7. Eigenvector centrality of the network was calculated using CentiScaPe [245].

3.3.5. Webtools: IxoriDB

IxoriDB was developed using the high-level Python web framework Django, version 3.1.5 [246]. This framework facilitated the integration of Python, HTML, CSS, and JavaScript to create a fully functional web application. The database-driven webpage provides users with an intuitive interface for exploring the transcriptome and the features of its unique coding regions. Additionally, users can retrieve information on other sequences through the use of Blast, version 2.10.1+ [203]. A customized version of BlasterJS was employed to display the

Blast results [247]. The webpage is publicly accessible at https://arn.ugr.es/IxoriDB.

3.3.6. Custom scripts and tools for data processing

Throughout this thesis, various custom scripts were written using Python, R, HTML, JavaScript, and CSS. These scripts helped carry out the data analysis, generate visualizations, and create interactive tools for exploring the results. All the scripts used in this thesis are available for access and download in the GitHub repository: https://github.com/Chemamm.

Chapter 4.

Annotation of non-coding RNA in the novel genome of *Ixodes ricinus*

The primary requirement for conducting a thorough analysis in this thesis is to have a well-annotated and reliable set of *I. ricinus* miRNAs to work with. Thus, in this chapter we will set the basis for the analyses shown in this thesis regarding the miRNAs, their cooperative effect and their potential key role as modulator of the tick-host interaction.

Historically, researchers on the specific field of *I. ricinus* miRNAs relied on a sequence-based predicted miRNA catalog generated using sRNAbench and miRanalyzer [193], based on short-read sequencing data from midgut and salivary gland tissues [17] and on the information provided by the available genomes of *I. ricinus* and *I. scapularis* [14,181]. This catalog included 67 unique guide strand miRNAs, of which 35 were reported as novel since they were not found in miRBase at that time and notated with an "X" in their ID [17].

However, the available genome for *I. ricinus* was highly fragmented due to the limitations of previous assembly techniques. It contained 204,516 scaffolds, meaning that many genes and miRNAs were likely either split across multiple contigs or entirely absent from the assembly [181]. This fact highlights the need for a more continuous and comprehensive genome assembly.

New efforts to assemble the *I. ricinus* genome with higher quality emerged [176]. A novel genome was assembled using reads generated from Hi-C and 10X linked-read libraries, which provided significant advantages in terms of assembly quality. The Hi-C data enabled chromosome-scale scaffolding by leveraging long-range chromatin contact information, ensuring proper ordering and orientation of the genomic fragments. Complementarily, the 10X linked-read libraries facilitated the resolution of repetitive regions and improved the contiguity of the assembly by bridging gaps between distant contigs. Together, these technologies resulted in a highly continuous and well-scaffolded genome, with 14 major scaffolds corresponding to 13 autosomes and the X sex chromosome, and accounting for the 95.2% of the assembly size. This provided a robust foundation for downstream annotation and analysis of ncRNA.

4.1. Non-coding RNA and cis-regulatory elements

We made extensive analysis to identify and annotate putative structural and regulatory non-coding elements in the aforementioned new *I. ricinus* genome [176]. This analysis revealed a total of 21,792 ncRNAs and cis-regulatory elements. These included small nuclear RNAs, small nucleolar RNAs, ribosomal RNAs, lncRNAs, transfer RNAs, microRNAs, ribozymes, and riboswitches, among others. Table 2.

The annotation and characterization of ncRNAs and cis-regulatory elements in the *I. ricinus* genome provide a foundation not only for this thesis, which focuses on miRNAs and lncRNAs, but also for future studies investigating the often-overlooked non-coding RNAs in this tick species. Specifically, for the purposes of this thesis, the annotation of the genome has yielded an improved catalog of miRNAs and lncRNAs while also provided confidence about their existence due to their presence within the genome.

***Table 2. Regions containing non-coding RNA and cis-regulatory elements identified in the genome of* Ixodes ricinus.**

Non-coding element	Class	Number
Transfer RNA	Non-coding RNA	9815
Ribosomal RNA	Non-coding RNA	267
Small nuclear RNA	Non-coding RNA	192
Small nucleolar RNA	Non-coding RNA	21
Binding small RNA	Non-coding RNA	1
microRNA	Non-coding RNA	226
Long non-coding RNA	Non-coding RNA	10696
Signal recognition particle	Non-coding RNA	16
Ribozyme	Non-coding RNA	3
Riboswitch	Cis-regulatory element	35
UTR stem-loop	Cis-regulatory element	662
Iron response element	Cis-regulatory element	5
Potassium channel RNA editing signal	Cis-regulatory element	5

4.1.1. MicroRNAs

Using this new high-quality genome, we enlarged the catalog of *I. ricinus* miRNAs. Specifically, 14 new unique guide miRNAs were added, of which 8 were catalogued as novel, since their seed sequence was not found in miRGeneDB or miRBase [134,195]. They were noted with two "X" in their IDs to differentiate them from the miRNAs with only one "X" in their IDs, whose seed sequence was not present in miRBase at the time of the production of the old catalog. Thus, the final miRNA catalog included 162 mature miRNAs, including guide and passenger strands. Based on sequence similarity, we categorized these miRNAs into 69 families.

From the complete catalog, 111 mature miRNAs (68.5%) belonging to 56 different families were found in the genome and were noted as high confidence for the rest of the analyses in this thesis. Some of these miRNAs were identified several times in the genome, having multiple copies that may serve as a reservoir for the development of new miRNAs in this species or to regulate and augment the expression of these miRNAs [248]. Specifically, hairpin sequences of the family iri-miR-X1 were found 121 times in the genome, while sequences for iri-miR-X5 were identified 20 times, iri-miR-X7 19 times and iri-miR-XX5 5 times. Other families were detected a couple of times in the genome: iri-miR-X17, iri-miR-3931, iri-miR-9a and iri-miR-X18.

Regarding the location of the miRNAs in the genome, as expected, most miRNAs are identified in the 14 larger scaffolds of the genome, which correspond to the majority of the 14 chromosomes of *I. ricinus*. Scaffolds 1 and 2 were the ones with the highest number of miRNAs annotated, with 40 and 31 identified miRNA hairpin sequences, respectively. A total of 8 hairpin sequences were found in other smaller scaffolds (Figure 11).

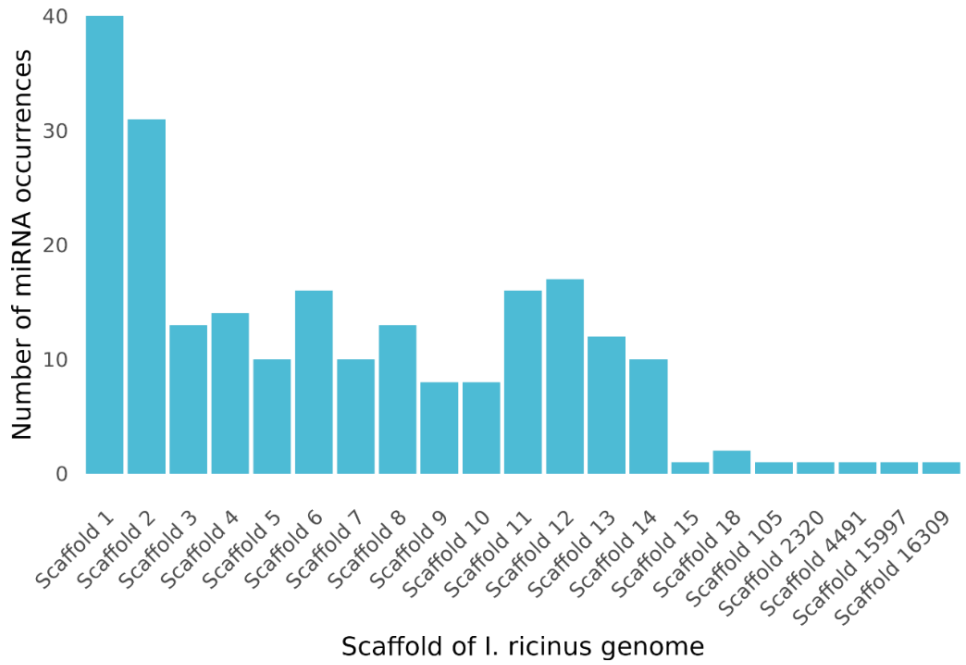

Figure 11. Distribution of microRNA hairpin sequences in the scaffolds of* the Ixodes ricinus *genome. *The X-axis represents the 14 largest scaffolds from the* I. ricinus *genome, corresponding to the 14 chromosomes, along with 7 complementary scaffolds. The Y-axis represents the number of times a hairpin miRNA sequence is found in a specific scaffold.*

Our analysis revealed that miRNA genes in *I. ricinus* do not tend to form close-distance clusters, unlike in many other organisms [249,250]. Applying the well-established criterion that sequences within 10 kb of each other form a cluster [249,250], only four clusters of miRNA hairpin sequences were identified. One of these clusters contained three miRNAs, while the remaining clusters were composed of miRNA pairs. The scaffold, genomic location, and composition of these clusters can be found in Table 3.

***Table 3. Scaffold, genomic location, and composition of microRNA clusters identified in the genome of* Ixodes ricinus.**

miRNAs	Scaffold	Genomic start	Genomic end
iri-mir-XX7; iri-let-7	1	80442251	80446982
iri-mir-12; iri-mir-5307	9	79371221	79371858
iri-mir-750; iri-mir-1175	10	33460377	33461655
iri-mir-2b; iri-mir-2b2; iri-mir-71	12	104673137	104673737

4.1.1.1. Assessment of the taxonomic level of conservation of microRNAs

Conservation provides a framework for understanding the functional relevance of miRNAs across different species, particularly in evolutionary contexts. It will also help in exploring key concepts such as the potential for *I. ricinus* to employ novel miRNAs that may contribute to its evolutionary adaptation and successful blood-feeding behavior.

For the classification of miRNAs, we analyzed the sequence similarity of mature miRNA sequences against all other species in miRGeneDB [182], using their comprehensive database of miRNA sequences and annotations from different species. This analysis allowed us to determine the taxonomic level of conservation for each mature miRNA in our catalog, from highly conserved miRNAs present across all bilaterian animals to those unique to *I. ricinus*. This conservation analysis not only helps in validating the predicted miRNAs but also

provides insights into their evolutionary significance and roles. Accordingly, we report that 52 mature *I. ricinus* miRNAs are conserved at the taxon level of bilaterian species (32.1%), 18 belong to Protostomia (11.1%), 4 are only conserved in Arthropods (2.5%), and 88 are specific of *I. ricinus* (54.3%).

The percentage of mature miRNAs identified in the genome, categorized by conservation, is shown in Figure 12. It can be observed that all miRNAs conserved at the Arthropoda taxonomic level, along with the majority of those conserved at the Bilateria and Protostomia levels, have been identified in the genome. However, approximately half of the *I. ricinus*-specific miRNAs have not been identified in the reference genome.

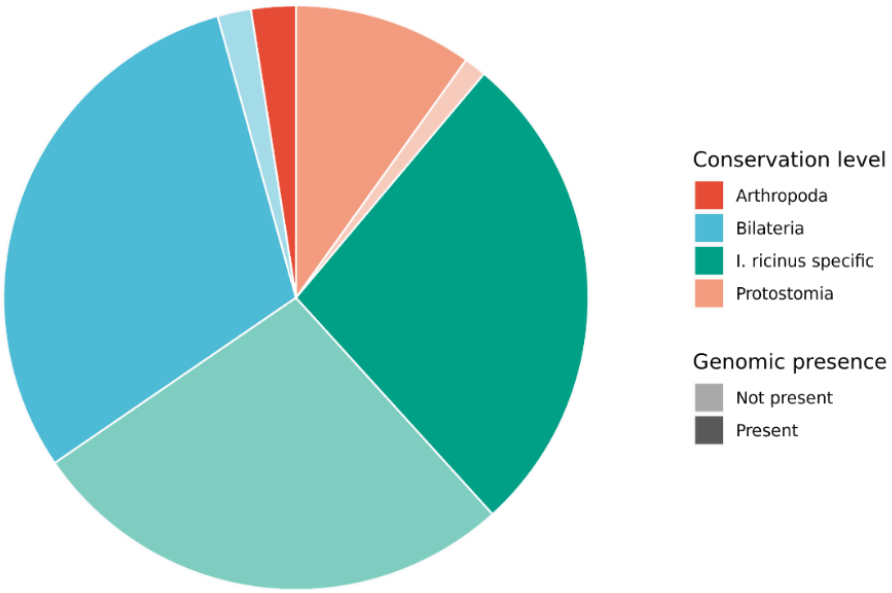

Figure 12. Pie chart illustrating the proportion of mature microRNAs conserved at various taxonomic levels and their presence in the reference genome. *Different colors represent different taxonomic levels. Opaque colors denote mature miRNAs that are present in the reference genome, while translucent shades indicate mature miRNAs not identified in the reference genome.*

Thus, as expected, miRNAs with a certain level of sequence conservation are more reliably supported by the reference genome, while a significant number of miRNAs annotated as *I. ricinus*-specific will be considered low-confidence for the subsequent analyses. Additionally, this highlights the need for continued efforts to refine the miRNA catalog in order to determine whether miRNAs not found in this genome were missed by the assembly process, or whether they originate from modifications not detectable at the genomic level, or to test the hypothesis that sequence changes due to poor conservation results in differences between tick populations. Of course, it is still possible that the sequences not identified in the reference genome correspond to artifacts resulting from RNA-seq and older methods employed for bioinformatics analysis.

4.1.2. Long non-coding RNAs

Annotating the lncRNAs was challenging due to the limited information available about them in *I. ricinus* and the absence of a previously complete annotation for this tick species. To address this, we utilized a lncRNA dataset containing both putative and consensus lncRNAs for *I. ricinus* which will be further described in *Chapter 7*. Consensus lncRNAs from this dataset were considered high-confidence annotations. Prior to aligning the putative lncRNAs to the *I. ricinus* genome, their non-coding properties were verified. This analysis identified 13,287 lncRNAs with alignment scores above 90, indicating significant matches to the genome. To ensure result reliability, 2,591 lncRNAs overlapping with coding RNAs were removed. Ultimately, we annotated a total of 10,696 lncRNAs, of which 2,433 were classified as high-confidence lncRNAs.

This provides a foundation for the analysis in Chapter 7, where these lncRNAs will be tested for their potential to inhibit the function of endogenous host

miRNAs. By doing so, they may alter critical pathways in the host's response to blood feeding, ultimately facilitating the successful blood feeding of *I. ricinus*.

Chapter 5.

Evaluation of the functional and synergistic roles of *Ixodes ricinus* microRNAs in host response modulation

The main focus of this thesis is to explore one of the most novel mechanisms by which *I. ricinus* can modulate the host response to blood feeding: the mediation of tick miRNAs in host homeostasis modulation. This was accomplished by combining recent progress in miRNA target prediction [193,251], discoveries regarding miRNA cooperative interactions [143,147], and knowledge of key host defense pathways against blood-feeding parasites, which appear to be targeted and modified in this scenario [62]. These insights, along with the results presented in the following chapters, will help us understand how ticks evade host defenses and provide a holistic view of the intricate network of interactions between tick-derived molecules and host cells.

In this chapter, we analyze the potential of miRNAs to target and cooperatively regulate host genes involved in key processes, including wound healing, angiogenesis, immune response, and sensory functions such as mechanosensation and nociception.

5.1. Prediction of conserved target regions

In this study, we conducted an *in silico* target prediction analysis to investigate the potential interactions between miRNAs from *I. ricinus* and their predicted mRNA target regions in *H. sapiens*. A total of 380,696 regions in the UTRs of *H. sapiens* were predicted to be targeted by 162 unique *I. ricinus* mature miRNAs.

As a negative control, we generated a set of miRNAs with randomized sequences and non-existent seed regions, following criteria from mirGeneDB [182]. These randomized miRNAs targeted a total of 353,239 regions in the UTRs of *H. sapiens*.

To refine the analysis, we examined the conservation of predicted target regions. *I. ricinus* has a wide range of evolutionarily diverse potential hosts, including humans, large and small mammals, birds, and reptiles [46] and thus, *for I. ricinus* miRNAs to mediate tick lifecycle and feeding success, they would likely need to target conserved mRNA regions across these different hosts. Moreover, it is known that target prediction tools are prone to generating false positives [252], and conservation of target regions has been previously validated as an effective filter to reduce these false positives [215].

Of the 380,696 predicted target regions, 11,746 (3.08%) were identified as conserved. In contrast, only 7,454 conserved target regions (2.11%) were identified from the 353,239 predicted target regions for the randomized miRNAs. The proportion of conserved target regions for *I. ricinus* miRNAs was significantly higher than that for the randomized set ($p < 10^{-5}$).

This significant difference, along with the substantial reduction in the total number of predicted target regions after conservation filtering, remarks the critical importance of conservation analysis in this study.

The difference between the predicted target regions of *I. ricinus* miRNAs and the randomized set of miRNAs is illustrated more clearly in Figure 13. Overall, *I. ricinus* miRNAs tend to have a higher number of predicted target regions compared to the randomized miRNAs, especially in the middle range of the distribution. However, it is remarkable that randomized miRNAs can occasionally achieve an exceptionally high number of predicted target regions purely by chance, even exceeding those observed in *I. ricinus* miRNAs.

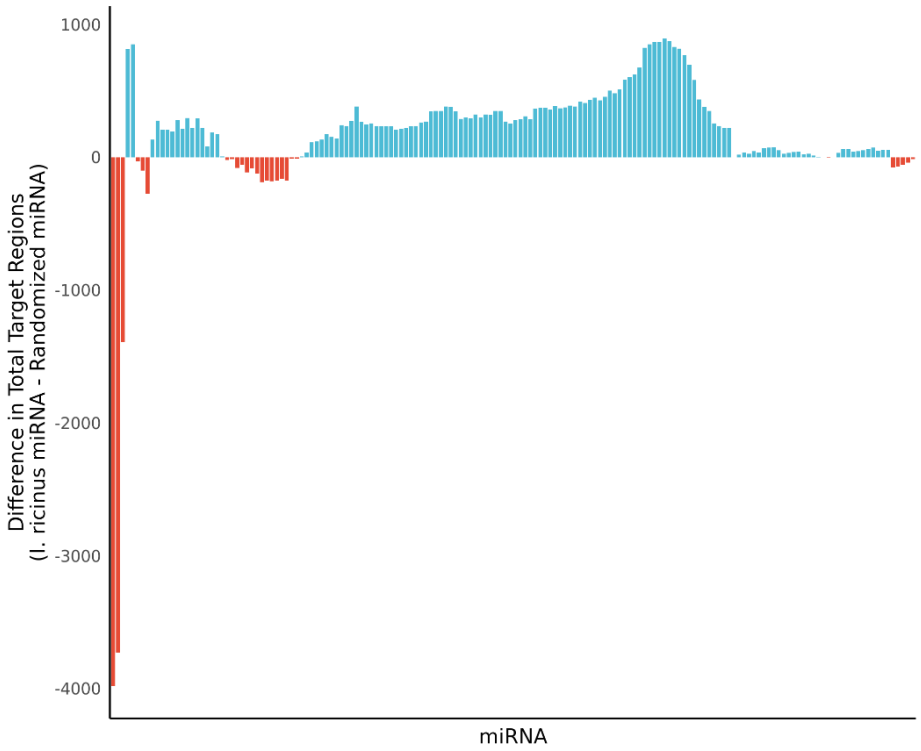

Figure 13. Comparison of predicted target regions between* Ixodes ricinus *microRNAs and randomized microRNAs. *The X-axis represents pairs of miRNAs, each consisting of one* I. ricinus *miRNA and one randomized miRNA, ordered by their number of predicted target regions. The Y-axis shows the difference in predicted target counts, with positive values (blue bars) indicating more targets for* I. ricinus *miRNAs and negative values (red bars) indicating more targets for randomized miRNAs.*

Figure 14 illustrates that miRNAs with the highest number of target regions do not necessarily exhibit the highest number of conserved target regions. This indicates that a biologically meaningful bias influences this correlation, which might otherwise be expected in a random distribution of target regions. This observation is supported by the randomized set shown in the same figure, where miRNAs with more target regions tend to have a proportional increase in conserved target regions. These findings highlight the biological significance of target region conservation in the *I. ricinus* tick-host relationship.

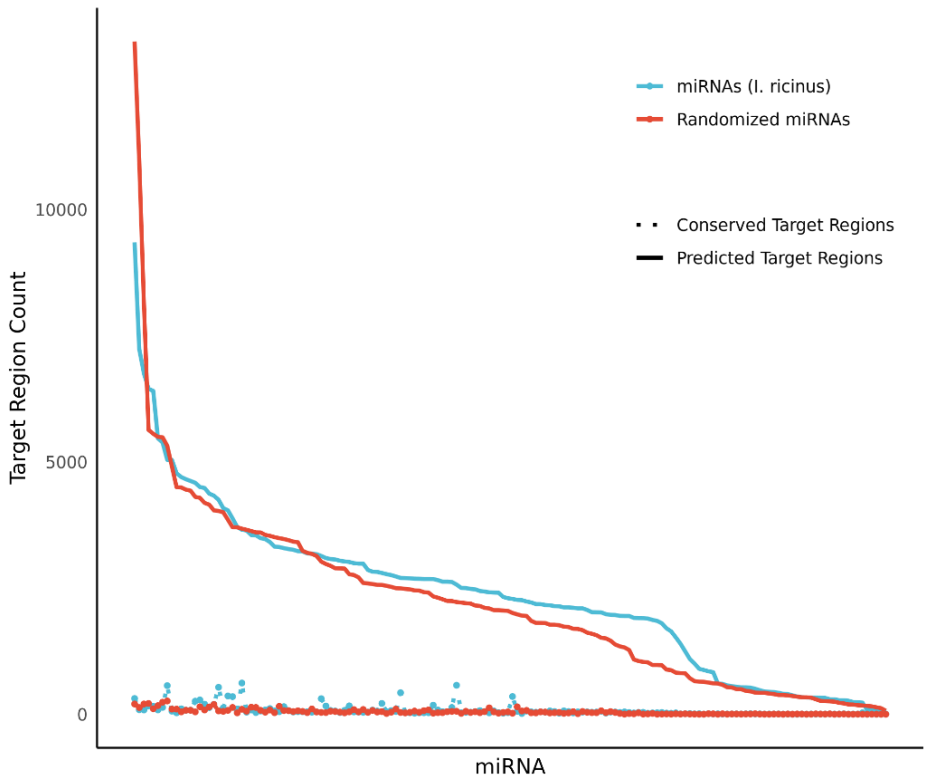

Figure 14. Relationship between predicted and conserved microRNA target regions in* Ixodes ricinus *and randomized microRNAs. *The X-axis represents pairs of miRNAs, each consisting of one* I. ricinus *miRNA and one randomized miRNA, ordered by their number of predicted target regions. The Y-axis shows the count of predicted and conserved target regions. The blue line represents* I. ricinus *miRNAs, while the red line corresponds to the randomized miRNAs.*

Ratios of conserved target regions to predicted target regions were calculated, and their distribution is shown in Figure 15. These results support the findings from Figure 14 and collectively reinforce the idea that the hypothesis about conservation of *I. ricinus* miRNAs concerning their targets in host genes has not only biological relevance, but also bioinformatics support. Notably, high ratio values were observed in *I. ricinus* miRNAs that cannot be achieved by chance, as they do not appear in the distribution of the randomized set of miRNAs.

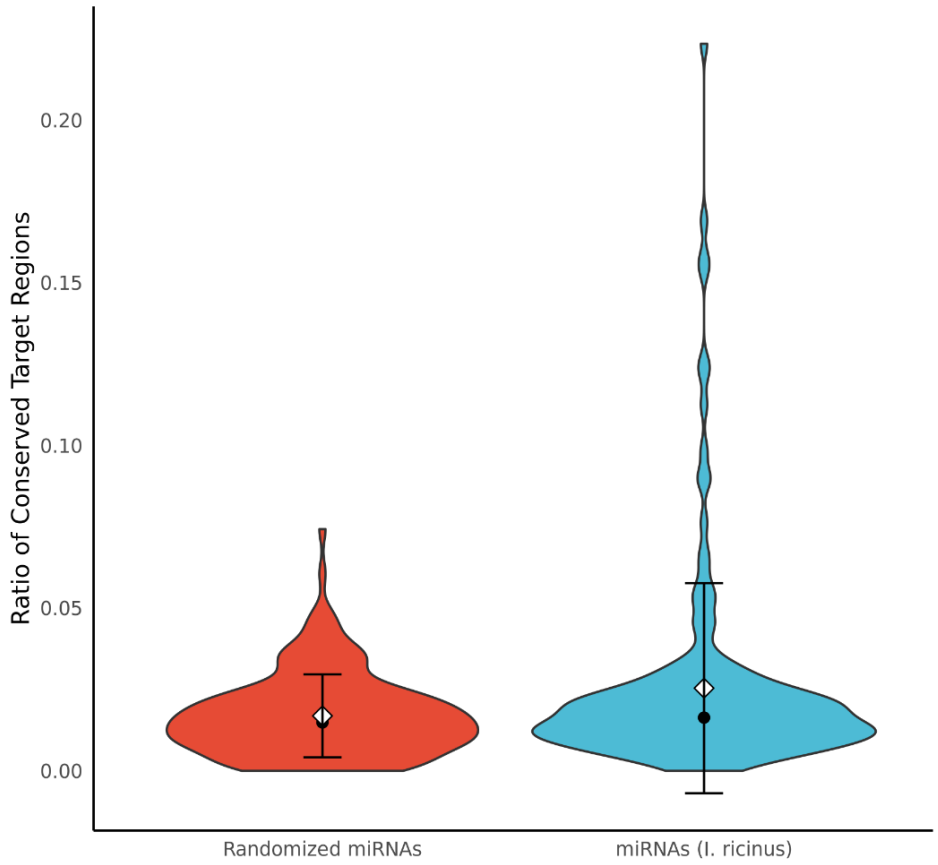

Figure 15. Distribution of conserved-to-predicted target ratios in* Ixodes ricinus *and randomized miRNAs. *The violin plot highlights a broader and more variable distribution of conserved-to-predicted target ratios (Y-axis) for* I. ricinus *miRNAs, with higher ratio values that are absent in the randomized set.*

5.2. *In silico* functional annotation of host genes 'conservedly' targeted by *Ixodes ricinus* microRNAs across different hosts

Based on the analyzed target regions, we made a computational analysis to identify which host genes and functions are targeted by the *I. ricinus* miRNAs in a conserved way among different hosts. A total of 20061 genes had a target region identified for at least one of the 162 *I. ricinus* miRNAs. From this number, a great reduction was achieved using the analysis of conservation of the target regions, since only 4938 had at least one of these target regions identified as conserved. Additionally, to focus on those genes with the highest potential to be modulated by the specific miRNA we analyzed a set of 526 genes which had 5 identified conserved target regions or more. These genes were functionally characterized, and their pathway and ontology enrichment were analyzed by pathway enrichment analysis using the KEGG, Reactome, and WikiPathways databases [234–236]. The analysis revealed that this set of genes was significantly enriched in 16 KEGG pathways, 45 Reactome pathways, and 35 WikiPathways pathways. The high number of pathways with statistically significant enrichment underscores the biological significance of the host genes that *I. ricinus* miRNAs potentially modulate as presented in Figure 16, Figure 17 and Figure 18.

Notably, the pathway enrichment analysis showed that genes consistently targeted in conserved regions by *I. ricinus* miRNAs play important roles in several signaling pathways and biological processes, whose modulation could enhance the efficiency of the tick's blood feeding. Pathways such as the Wnt

signaling pathway and those involved in mesodermal differentiation stood out due to their significant enrichment, indicating a potential role for *I. ricinus* in modulating host wound healing processes [253,254]. Additionally, enrichment in pathways like TGF-beta signaling, T-cell receptor signaling, SUMOylation, and heme signaling highlights mechanisms by which ticks might suppress the host's innate immune defenses [255–258], reducing the likelihood of rejection. Furthermore, pathways related to neural and nerve signaling, including axon guidance, MECP2-associated pathways, and calcium channel-associated pathways [259–261], suggest that *I. ricinus* may interfere with the host's ability to detect pain or their presence, further aiding in the success of their parasitism.

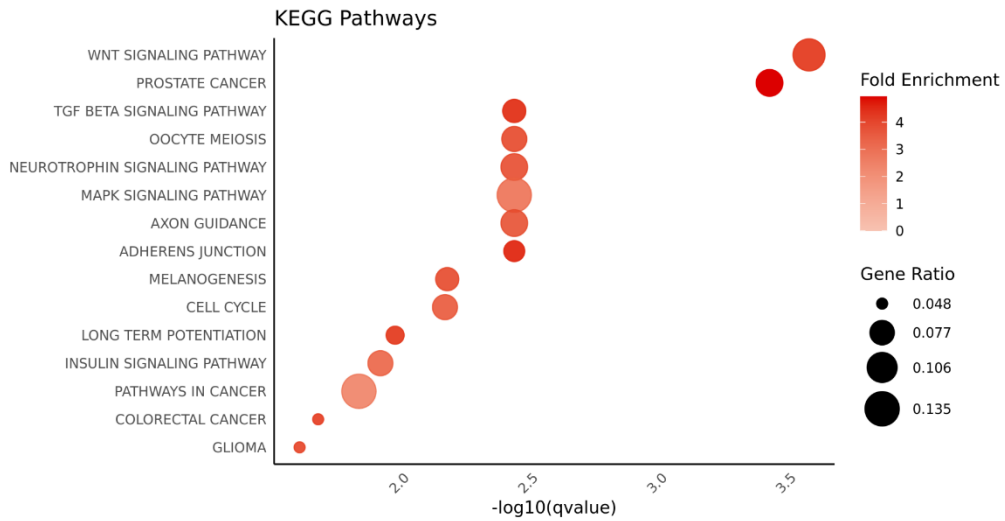

Figure 16. Pathway enrichment analysis, using KEGG database, of genes with more than five conserved target regions for* Ixodes ricinus *microRNAs. *The X-axis represents the statistical significance (-log10(qvalue)). The dots in the plot represent individual pathways, and their size is proportional to the Gene Ratio, which is the proportion of genes in the given pathway that have more than five conserved target regions for* I. ricinus *miRNAs, relative to the total number of genes in the pathway. The intensity of color of each dot corresponds to the fold enrichment value, which reflects the percentage of genes with more than five conserved target regions belonging to a pathway, divided by the corresponding percentage of genes with conserved target regions (background) for the specific pathway.*

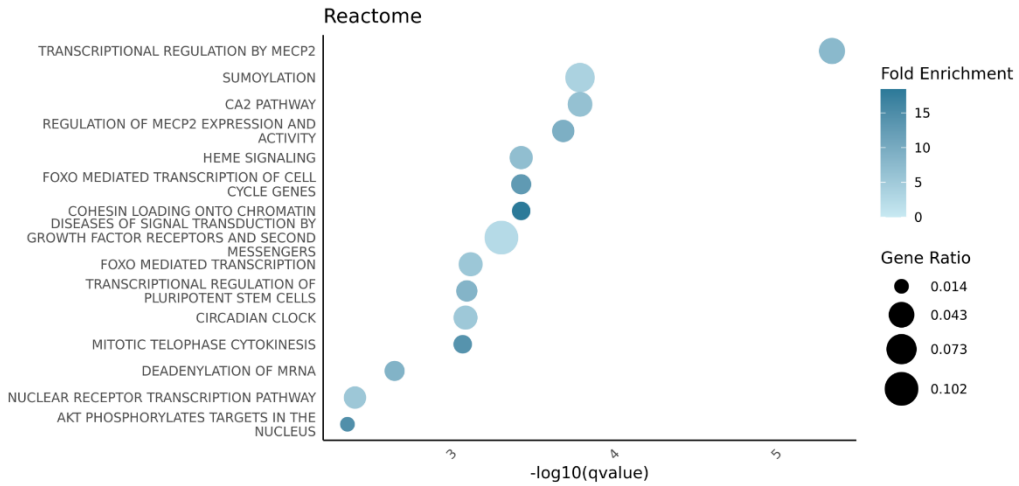

Figure 17. Pathway enrichment analysis, using Reactome database, of genes with more than five conserved target regions for* Ixodes ricinus *microRNAs. *For a detailed explanation of the statistics shown in this figure, please refer to Figure 16.*

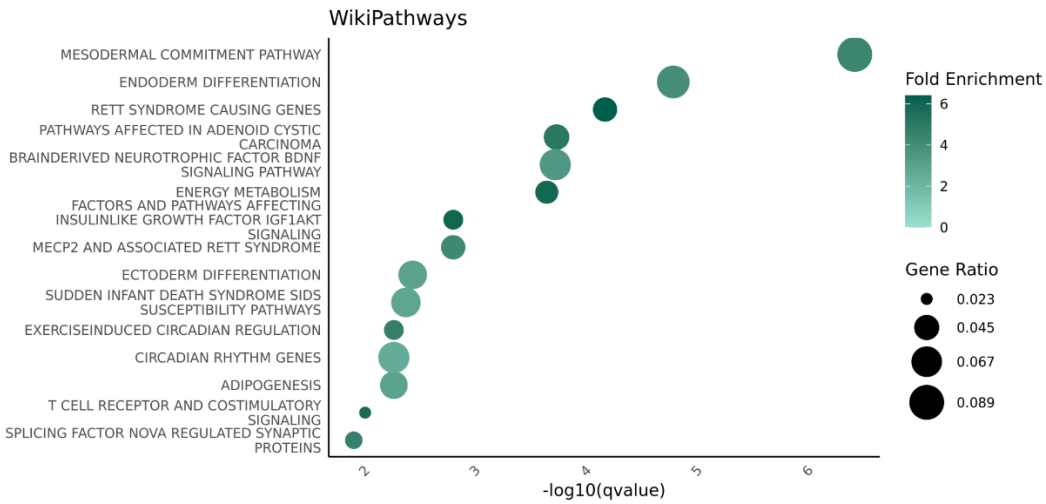

Figure 18. Pathway enrichment analysis, using Wikipathways database, of genes with more than five conserved target regions for* Ixodes ricinus *microRNAs. *For a detailed explanation of the statistics shown in this figure, please refer to Figure 16.*

In consonance with the results obtained in the pathway enrichment analysis, the finding of several ontology terms as significantly enriched in the genes analyzed remarks the biological relevance of the genes potentially targeted by *I. ricinus* miRNAs. Specifically, 351 GO terms from the category Biological Process were enriched, 41 from the category Molecular Function and 112 from the category Cellular Component. The most significant ontology terms are depicted in Figure 19, Figure 20 and Figure 21. The modulation of signaling pathways such as nerve growth factor signaling pathway, neuron axon guidance, insulin receptor binding and steroid hormone receptor signaling can delay local repair processes in the tick infestation site, alter the immune response or the ability to detect the tick [262–267], allowing prolonged access to the blood meal. Additionally, we observed enrichment in pathways such as stress granule dynamics, which could potentially be mediating a reduced host innate immune response [268].

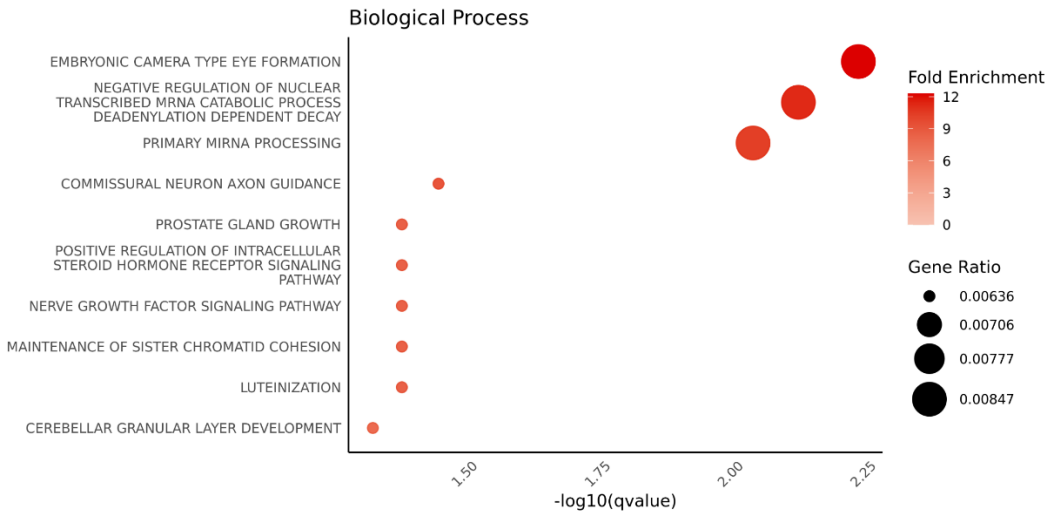

Figure 19. Ontology enrichment analysis of genes with more than five conserved target regions for* Ixodes ricinus *microRNAs in the Biological Process category. *For a detailed explanation of the statistics shown in this figure, please refer to Figure 16.*

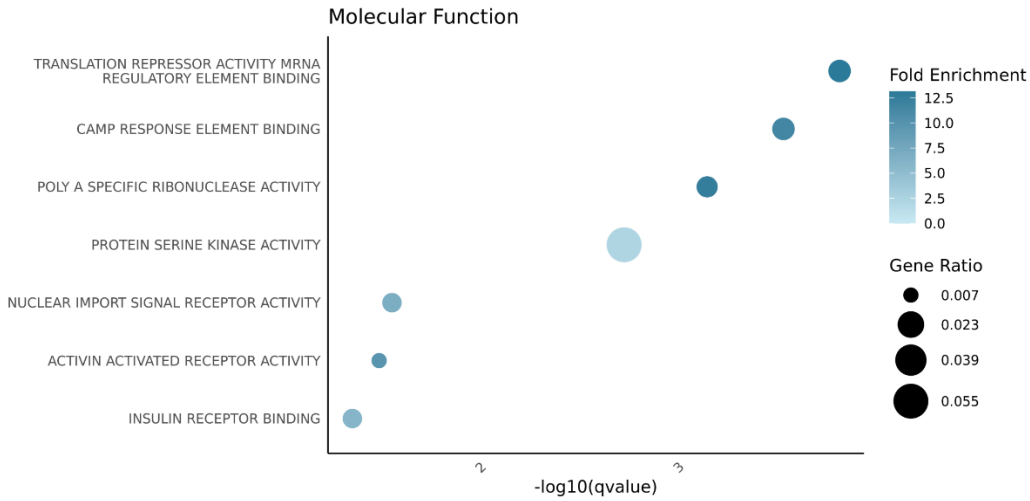

Figure 20. Ontology enrichment analysis of genes with more than five conserved target regions for* Ixodes ricinus *microRNAs in the Molecular Function category. *For a detailed explanation of the statistics shown in this figure, please refer to Figure 16.*

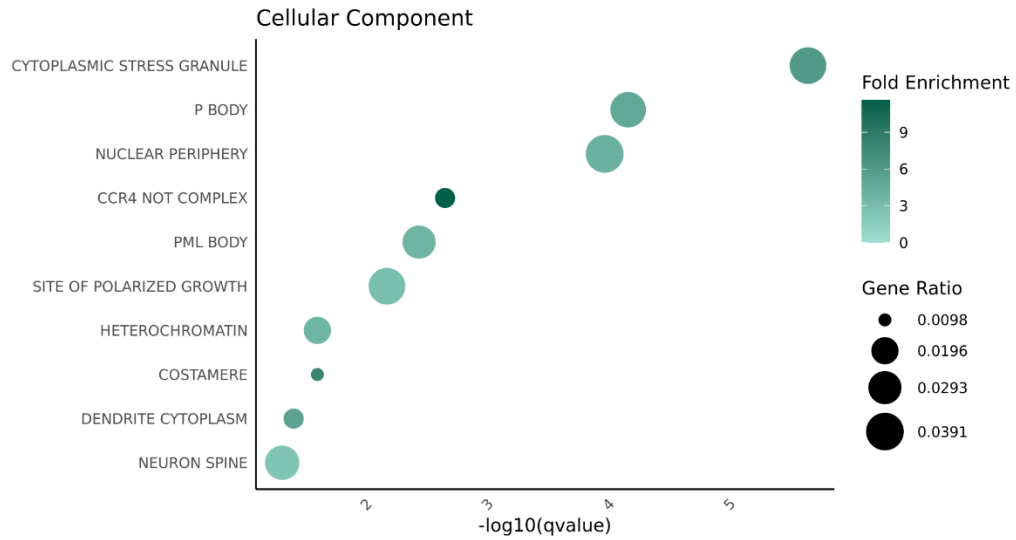

Figure 21. Ontology enrichment analysis of genes with more than five conserved target regions for* Ixodes ricinus *microRNAs in the Cellular Component category. *For a detailed explanation of the statistics shown in this figure, please refer to Figure 16.*

5.3. Assessing the evolutionary conservation *of Ixodes ricinus* microRNAs and their mRNA targets: Potential implications for molecular mimicry

To understand the evolutionary origins and potential functional roles of *I. ricinus* miRNAs, their seed sequences were classified based on their presence in Metazoan Taxa. The results revealed that the miRNAs with the highest number of conserved target regions were predominantly conserved up to the Bilateria taxon (Figure 22). This indicates that many of these miRNAs originated early in animal evolution and have been maintained across diverse species, including vertebrate hosts.

The high level of conservation suggests that these miRNAs play fundamental biological roles, likely involved in core cellular processes such as immune regulation and tissue homeostasis. Their evolutionary persistence implies strong selective pressure to retain their functions, which could be advantageous for *I. ricinus* in its interactions with the host. Notably, several tick miRNAs share seed sequences with vertebrate miRNAs, raising the possibility that they mimic host miRNAs to manipulate gene expression.

This finding aligns with the hypothesis that miRNA mimicry plays a critical role in enabling the tick to modulate the host's biological processes, as previously demonstrated in other blood-feeding arthropods [154]. miRNA mimicry refers to the ability of a miRNA to resemble or functionally substitute for another miRNA, often by sharing similar target sites within target genes. The concept of miRNA mimicry is well known in clinical research [156–158] and is further discussed in Section 1.3.1.5. Thus, our findings support the idea that *I. ricinus* employs miRNA mimicry as a molecular strategy to influence host biology, potentially modulating immune responses, inflammatory pathways, or other processes

crucial for successful parasitism. The presence of highly conserved miRNAs in the tick further reinforces their relevance in host-pathogen interactions and highlights their potential as targets for future studies on tick-host molecular crosstalk.

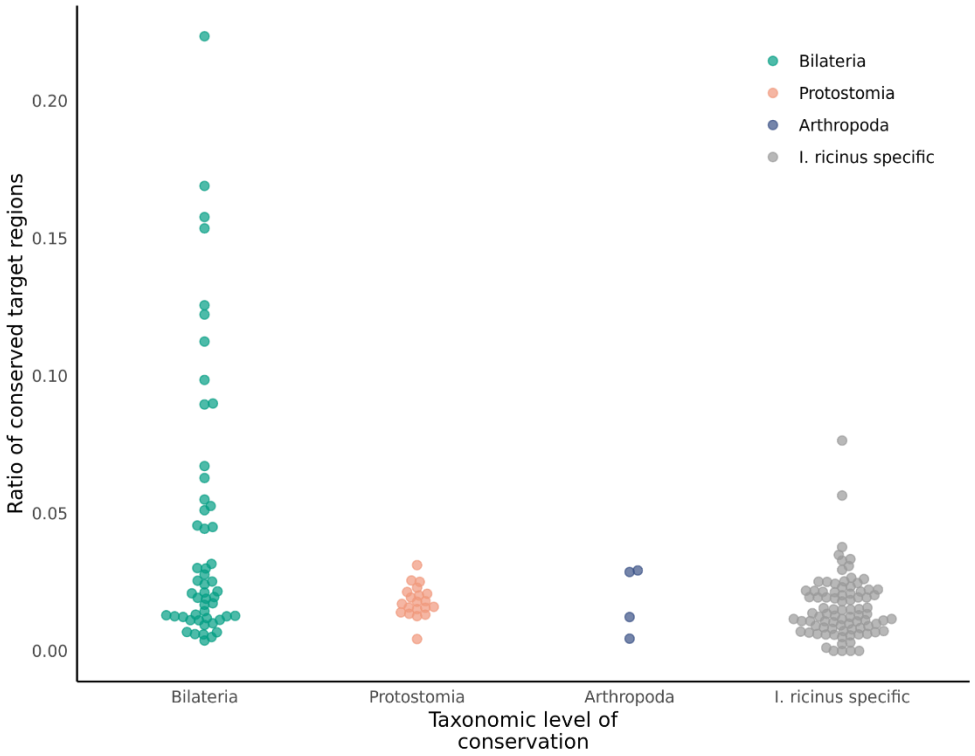

Figure 22. Evolutionary conservation of* Ixodes ricinus *microRNAs and their conserved-to-predicted target ratios. *The Y-axis represents the ratio of conserved mRNA target regions to the total predicted target regions. The X-axis represents the taxonomic level of seed sequence conservation, with higher-level taxa, and consequently greater sequence conservation, positioned on the left.*

Interestingly, a ranked comparison to determine which miRNAs had more conserved target regions than expected by chance identified two statistically significant groups, as shown in Figure 23. The first group comprises of miRNAs whose sequences are conserved to the bilaterian taxonomic level, as discussed earlier. The second group consists of specific miRNAs unique to *I. ricinus*. These

miRNAs appear to have emerged more recently in *I. ricinus*, which suggests that they may have emerged as a rapid adaptation mechanism to meet the tick's needs for host homeostasis modulation.

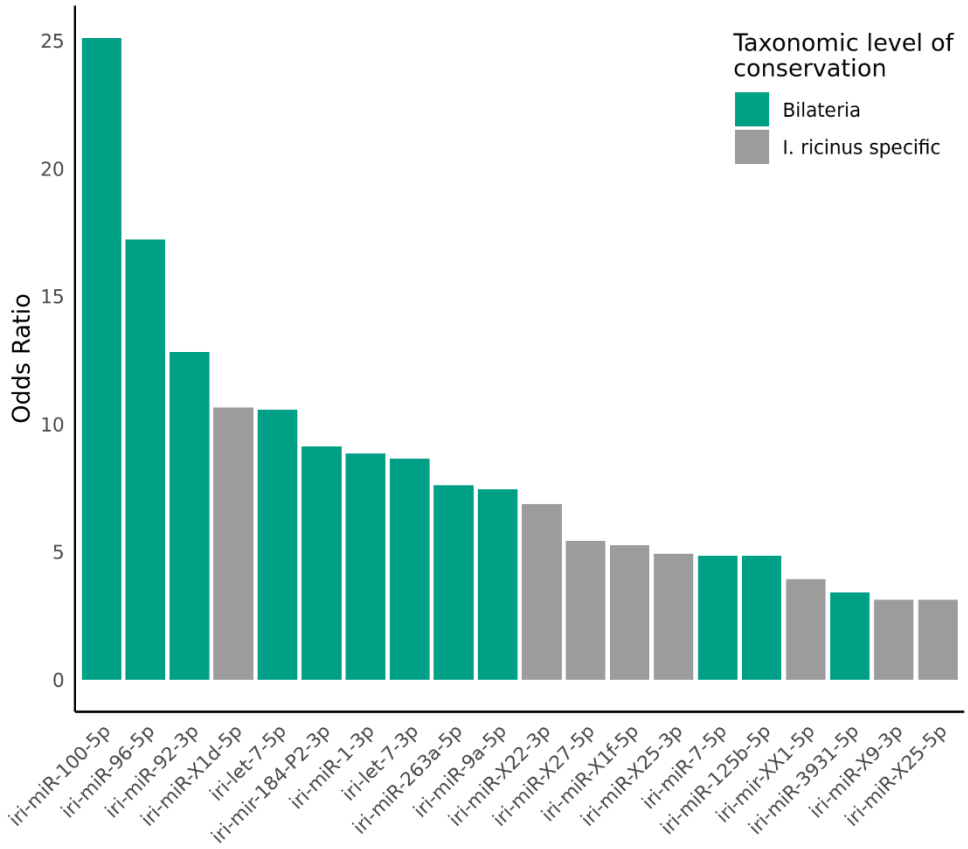

Figure 23. Top 20 microRNAs showing greater target conservation than randomized expectation. *The Y-axis represents the odds ratio obtained from Fisher's exact test, comparing* Ixodes ricinus *miRNAs with randomized miRNAs after ranking both by the number of predicted target regions. The taxonomic level of miRNA conservation is indicated by different colors.*

5.4. Relationship between microRNA abundance in *Ixodes ricinus* saliva and target region conservation

To further investigate how *I. ricinus* miRNAs modulate host homeostasis, we analyzed the relationship between the ratio of conserved target regions and miRNA abundance in *I. ricinus* saliva. A comparison between the 50 most abundant miRNAs in saliva and the 50 least abundant miRNAs, as shown in Figure 24, revealed that several miRNAs highly present in tick saliva exhibit a significantly higher ratio of conserved target regions compared to lesser abundant in tick saliva. Additionally, those miRNAs with the highest ratio of conserved target regions were found to be conserved up to the bilaterian taxon, which suggests evolutionary pressure to maintain their sequence and function, potentially due to their involvement in fundamental biological pathways. This finding further supports the hypothesis that *I. ricinus* miRNAs would mimic host endogenous miRNAs that are crucial for the host's homeostasis.

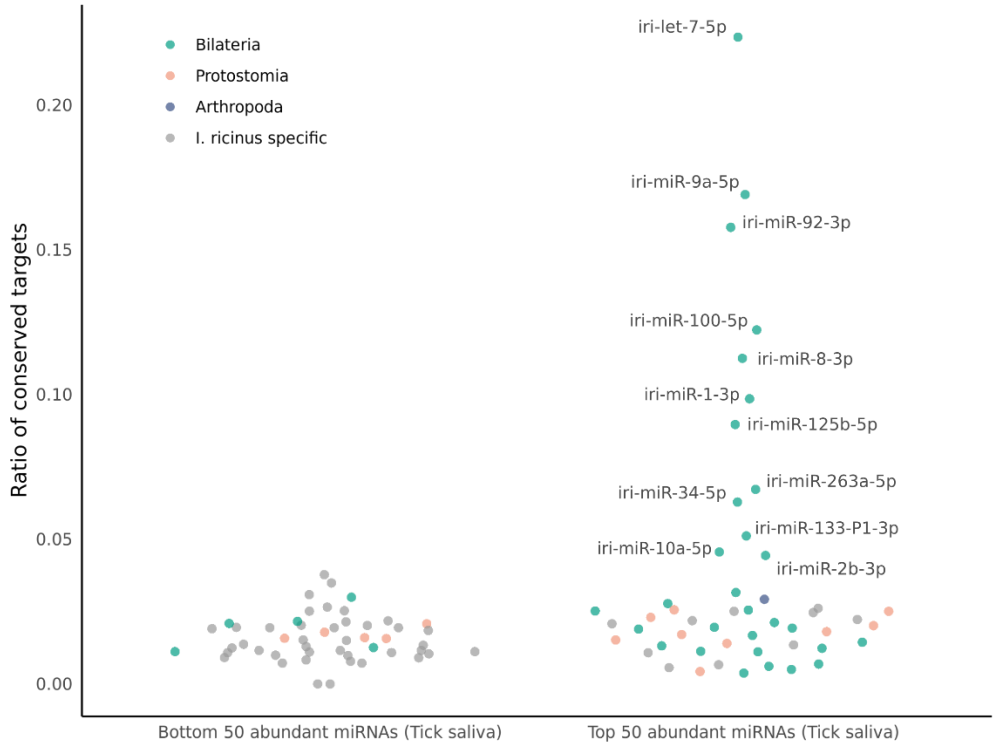

Figure 24. Ratio of conserved target regions between the least and most abundant microRNAs in* Ixodes ricinus *saliva. *The top 50 most abundant and the bottom 50 least abundant miRNAs in tick saliva are represented in this plot. The Y-axis shows the ratio of conserved mRNA target regions to the total predicted target regions. Different taxonomic levels of conservation are indicated by different colors.*

5.5. Cooperative effect analysis

It has been demonstrated that miRNAs may act synergistically in gene expression regulation leading to a cooperative effect. This synergy enables even a limited number of miRNAs to exert significant influence over their target mRNAs. We next examined the potential cooperative effects of the complete set of *I. ricinus* miRNAs, focusing on their ability to target neighboring conserved (to different hosts) regions within the same mRNA. Such a close arrangement of conserved targets facilitates the simultaneous attachment of AGO-miRNA

complexes to the TNRC6 protein. A total of 11746 conserved target regions were tested for their ability to cooperate with each other. As a result, 755 target regions (6.43%) were identified as capable of forming 451 distinct synergistic interactions. In comparison, a randomized set of miRNAs revealed that 394 out of 7,454 conserved target regions (5.29%) could cooperate, forming 218 unique interactions.

We examined the distribution of cooperative target regions relative to conserved target regions across *I. ricinus* miRNAs and the randomized miRNAs, as presented in Figure 25. Unlike the patterns observed between conserved and total target regions, the distribution of cooperative target regions appeared more stochastic. Specifically, miRNAs with more conserved target regions tended to also have more cooperative target regions. This pattern held true for the randomized miRNA set as well. Regarding the ratio of cooperative to conserved target regions per miRNA, no significant differences were observed between the *I. ricinus* and randomized miRNA sets. Notably, miRNAs with the highest ratios of cooperative target regions were *I. ricinus*-specific, with only one miRNA, iri-miR-2b2-3p, showing more cooperative target regions than expected by chance.

These findings indicate that if miRNA cooperations are biologically relevant in this context, their potential may be masked by their low number and high level of noise in the data. Furthermore, the analysis was limited by small sample sizes in some ratios and statistical tests, which may have impacted on the robustness of the results.

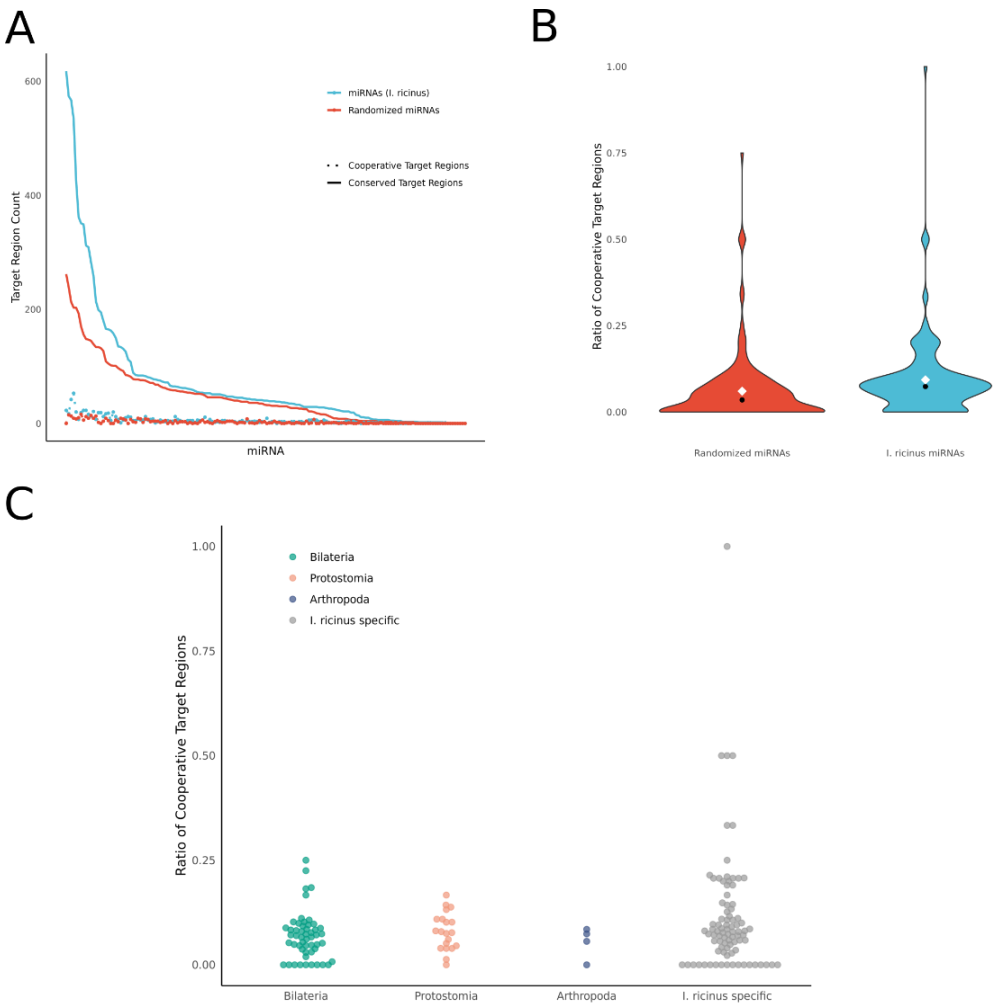

***Figure 25. Analysis of cooperation between microRNAs of* Ixodes ricinus.** *A) Relationship between conserved and cooperative miRNA target regions in* I. ricinus *and randomized miRNAs. The X-axis represents pairs of miRNAs, each consisting of one* I. ricinus *miRNA and one randomized miRNA, ordered by their number of conserved target regions. The Y-axis shows the count of conserved and cooperative target regions. The blue line represents* I. ricinus *miRNAs, while the red line corresponds to the randomized miRNAs. B) Distribution of cooperative-to-conserved target ratios in* I. ricinus *and randomized miRNAs. C) Evolutionary conservation of* I. ricinus *miRNAs and their cooperative-to-conserved target ratios. The Y-axis represents the ratio of cooperative mRNA target regions to the conserved target regions. The X-axis represents the taxonomic level of seed sequence conservation, with higher-level taxa, and consequently greater sequence conservation, positioned on the left.*

5.6. Identification of key microRNAs: Saliva abundance and ratio of conserved target regions.

Due to the limitations found analyzing the cooperative effect of *I. ricinus* miRNAs globally, we focused on revealing the most potential and biologically relevant cooperative effects in regulating conserved host gene target regions. Thus, we selected 12 *I. ricinus* miRNAs that excelled a) in their abundance in tick saliva [17], b) in their high ratio and statistical significance regarding the number of conserved target regions, c) in targeting neighboring sites of the same target mRNA in the vertebrate host as presented in Figure 24. These miRNAs, iri-miR-8-3p, iri-miR-9a-5p, iri-miR-92-3p, iri-miR-2b-3p, iri-let-7-5p, iri-miR-1-3p, iri-miR-34-5p, iri-miR-10a-5p, iri-miR-263a-5p, iri-miR-125b-5p, iri-miR-100-5p, and iri-miR-133-P1-3p, were all conserved at the bilaterian taxonomic level and thus able to mimic host miRNAs. They were also confirmed to be present in the most recent *I. ricinus* genome assembly [176]. The genomic coordinates of the specific miRNAs in the *I. ricinus* reference genome are shown in Table 4.

In total, these twelve miRNAs had 38952 predicted target regions, from whom a total of 3830 were identified as conserved (9.8%). These conserved target regions were distributed among 2662 different host genes. Of these genes, 233 had at least 3 conserved target regions, and 771 had at least 2 conserved target regions. To maintain consistency and to obtain comparable results with the prior functional analysis of target genes shown in Figure 16 and Figure 19, we functionally characterized the 233 genes with at least 3 conserved targets and 293 genes (out of 771) randomly selected from those with 2 conserved target regions, resulting in the desired total of 526 genes for functional characterization so that the results are comparable with our previous analysis.

***Table 4. Location of key microRNAs in the novel genome of* Ixodes ricinus.** *Please note that if a miRNA is found multiple times in the genome, it will appear in the table that same number of times.*

miRNA	Scaffold	Strand	Start	End
iri-mir-8	2	-	75491833	75491901
iri-mir-9a	11	-	50558401	50558469
iri-mir-9a	11	-	50585880	50585948
iri-mir-92	1	-	101747924	101747992
iri-mir-2b	12	-	104673137	104673206
iri-let-7	1	-	80446901	80446982
iri-mir-1	8	-	50544961	50545034
iri-mir-34	1	-	51076146	51076214
iri-mir-10a	1	+	54376231	54376300
iri-mir-263a	8	+	38398838	38398908
iri-mir-125b	1	-	80428613	80428685
iri-mir-100	1	-	80461353	80461424
iri-mir-133-P1	8	+	50800705	50800806

Pathway enrichment analysis revealed that these genes were associated with 10 KEGG pathways, 17 Reactome pathways, and 16 pathways from the WikiPathways database. Several pathways that were functionally enriched for the set of genes with more than 5 conserved targets for the full set of miRNAs are observed as functionally enriched in this analysis too. Key pathways regarding signaling like Wnt, neurotrophin, TGF- β, heme, activin, growth-factor and Mapk signaling pathways, as well as MECP2-related pathways can be potentially modulated by the specific miRNAs. The most relevant functionally enriched pathways are shown in Figure 26, Figure 27 and Figure 28.

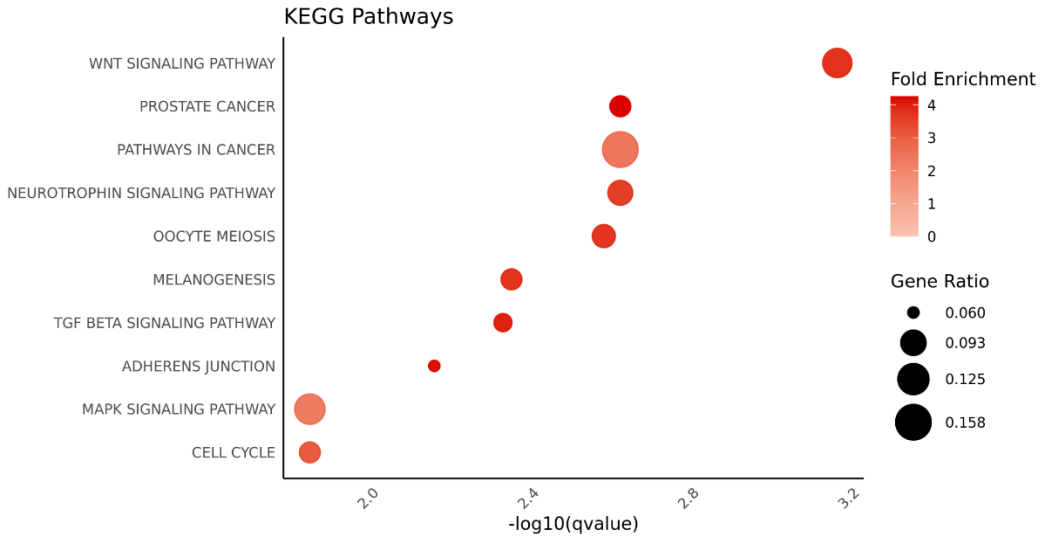

Figure 26. Pathway enrichment analysis, using KEGG database, of the 526 genes with more conserved target regions for* Ixodes ricinus *key microRNAs. *The X-axis represents the -log10(p-value), which reflects the statistical significance of the pathway enrichment. The dots in the plot represent individual pathways, and their size is proportional to the Gene Ratio, which is the proportion of genes in the given pathway targeted by* I. ricinus *key miRNAs, relative to the total number of genes in the pathway. The intensity of color of each dot corresponds to the fold enrichment value, which reflects the percentage of genes with conserved target regions for the key miRNAs belonging to a pathway, divided by the corresponding percentage of genes with conserved target regions for all* I. ricinus *miRNAs (background) for the specific pathway.*

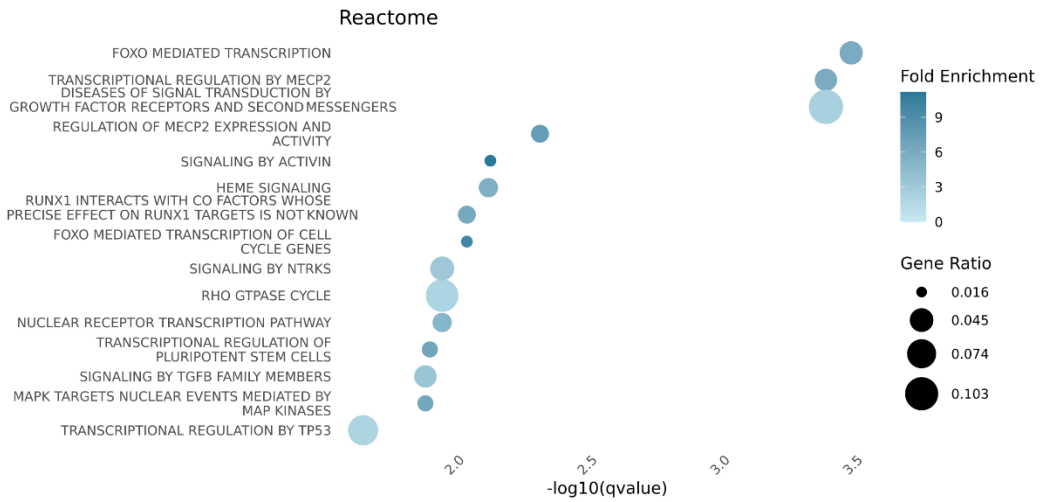

Figure 27. Pathway enrichment analysis, using Reactome database, of the 526 genes with more conserved target regions for* Ixodes ricinus *key microRNAs. *For a detailed explanation of the statistics shown in this figure, please refer to Figure 26.*

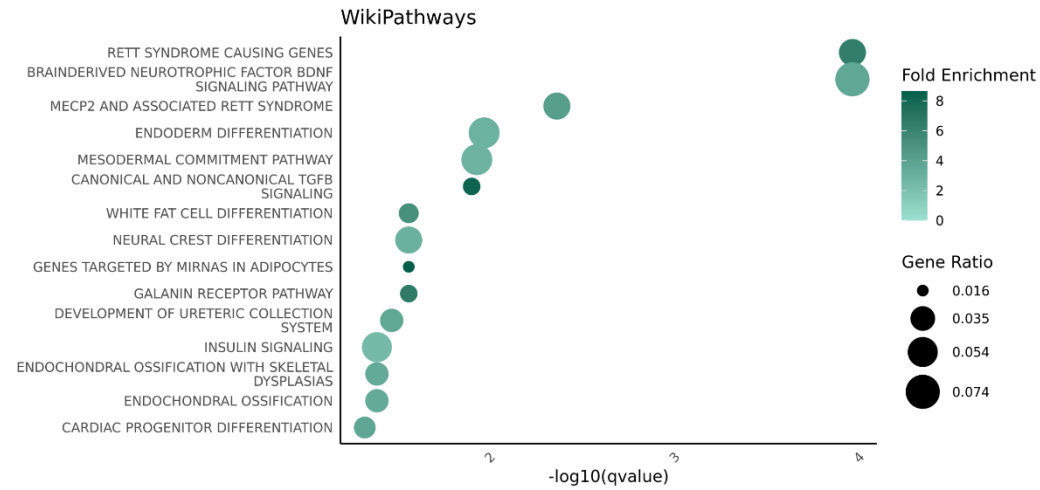

Figure 28. Pathway enrichment analysis, using Wikipathways database, of the 526 genes with more conserved target regions for* Ixodes ricinus *key microRNAs. *For a detailed explanation of the statistics shown in this figure, please refer to Figure 26.*

Ontology enrichment analysis identified 307 enriched GO terms in the Biological Process category, 32 in the Molecular Function category, and 8 in the Cellular Component category. Most significant functionally enriched ontology terms are shown in Figure 29, Figure 30 and Figure 31.

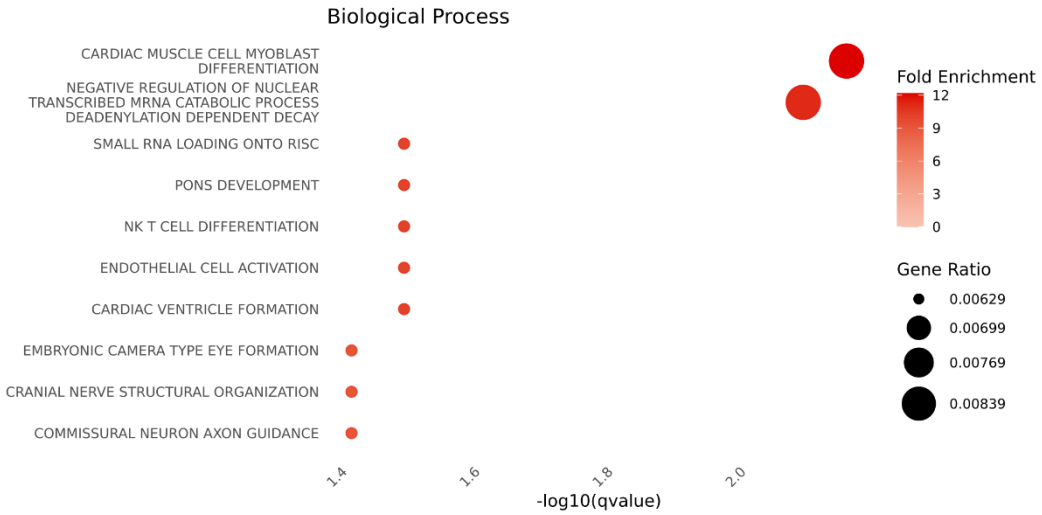

Figure 29. Ontology enrichment analysis of the 526 genes with more conserved target regions for* Ixodes ricinus *key microRNAs in the Biological Process category. *For a detailed explanation of the statistics shown in this figure, please refer to Figure 26.*

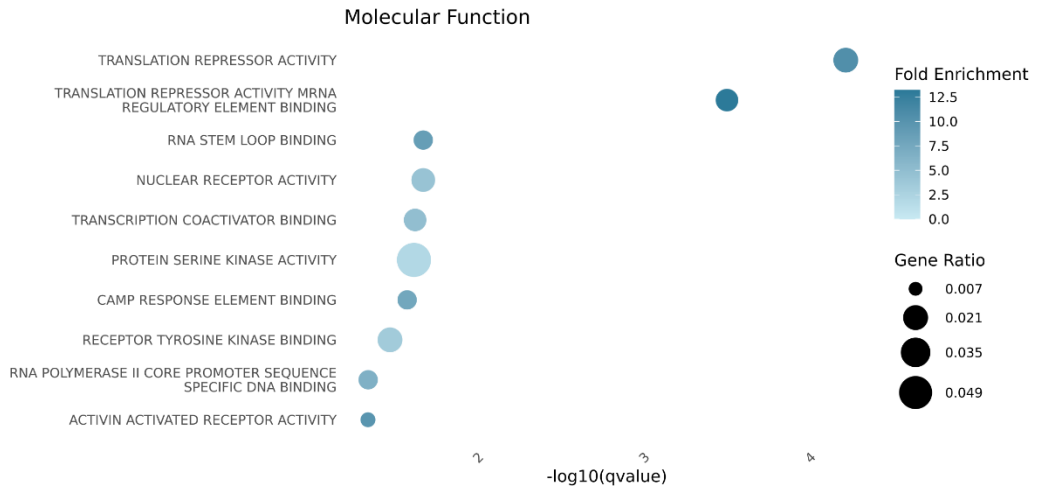

Figure 30. Ontology enrichment analysis of the 526 genes with more conserved target regions for* Ixodes ricinus *key microRNAs in the Molecular Function category. *For a detailed explanation of the statistics shown in this figure, please refer to Figure 26.*

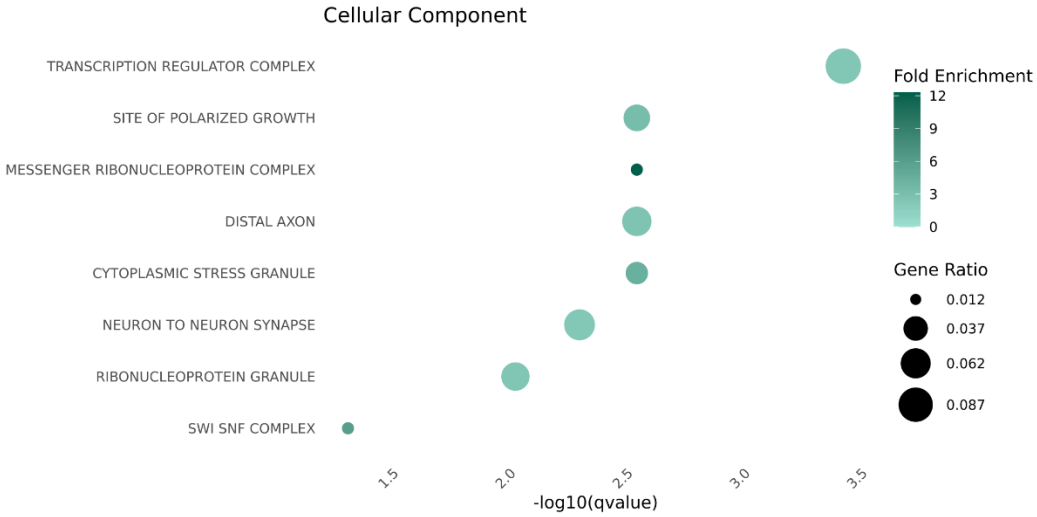

Figure 31. Ontology enrichment analysis of the 526 genes with more conserved target regions for* Ixodes ricinus *key microRNAs in the Cellular Component category. *For a detailed explanation of the statistics shown in this figure, please refer to Figure 26.*

We compared the results of the pathway and ontology enrichment analyses of genes with conserved target regions for the 12 miRNAs to those obtained using the full set of *I. ricinus* miRNAs. For pathway enrichment, the mean Jaccard index and overlap index were 0.35 and 0.73, respectively. For ontology enrichment, the mean Jaccard index was 0.38, and the mean overlap index was 0.68 (Figure 32).

Although some differences were observed between the results, the functional enrichment analysis of genes with conserved target regions for these 12 miRNAs produced conclusions largely consistent with those derived from the full set of miRNAs. A clear pattern emerged, indicating modulation of the host response and identifying several signaling pathways with the potential to be affected. These findings indicate that these 12 miRNAs can independently account for a substantial portion of the functional effects observed in the full *I. ricinus* miRNA set and may also possess additional functional roles. Notably, pathways and ontologies related to Natural Killer (NK) cells have emerged, highlighting their significance. NK cells are pivotal components of the innate immune system, known for their rapid response, signaling functions, and cytotoxic properties, acting even faster than T cells [269].

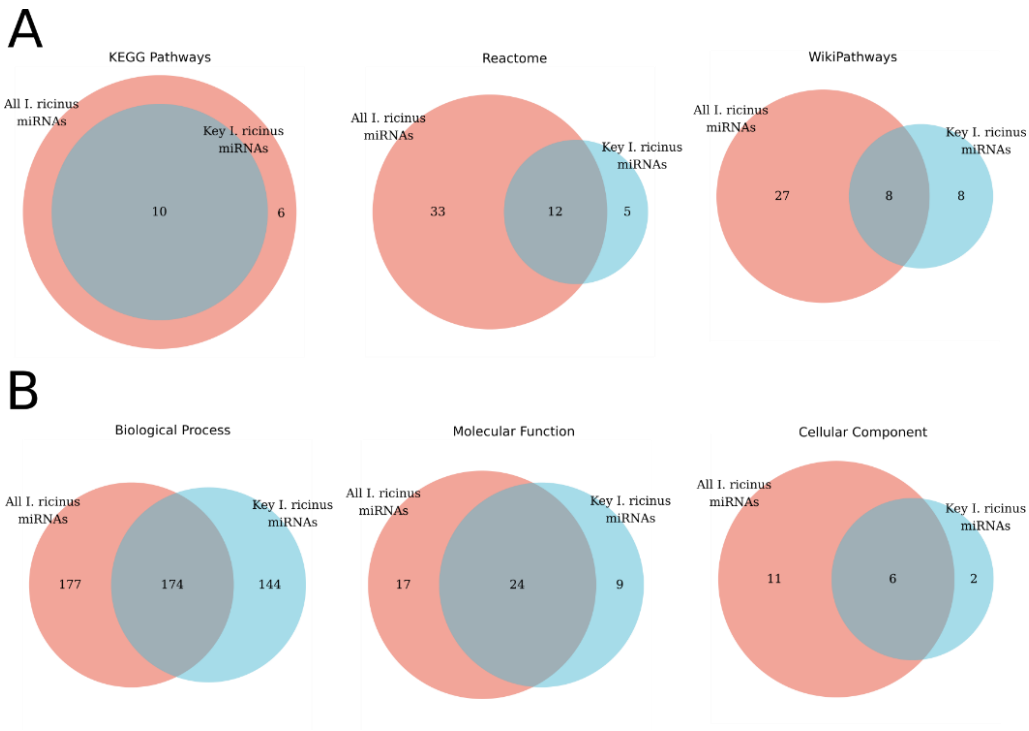

Figure 32. Overlap of enriched pathways and ontologies between the full set and key* Ixodes ricinus *microRNAs. *A) Comparison of pathway enrichment analysis for genes with conserved target regions between the full set and key* I. ricinus *miRNAs. The analysis was performed for the three different pathway databases: A) KEGG pathways, Reactome pathways and Wikipathways. B) Comparison of ontology enrichment analysis for genes with conserved target regions between the full set and key* I. ricinus *miRNAs. The analysis was performed for the three ontology categories: Biological Process, Molecular Function, and Cellular Component.*

5.7. Cooperative effect analysis of key microRNAs

We made a refined cooperative effect analysis using the key miRNAs depicted before. This analysis identified 45 cooperative target regions forming 23 distinct interactions among the 12 miRNAs. These cooperative target regions were associated with 22 genes, which were functionally characterized and further analyzed.

This gene set was broadly expressed in skin tissue cells, as depicted in Figure 33. Specifically, genes such as SRSF10, CELF1, RIC1, GPC6, and NFIA were abundant across all skin cell types, except mast cells. Certain cell types, such as fibroblasts, key players in wound healing and pro-inflammatory response [270,271], expressed nearly all these genes, with only one gene absent. Analysis of GTEx single-cell dataset [238] revealed that 12 out of 16 skin cell types, including adipocytes, lymphatic and vascular endothelial cells, basal and suprabasal keratinocytes, fibroblasts, dendritic cells, macrophages, Langerhans cells, melanocytes, pericytes, and sebaceous and sweat gland cells, exhibited a significantly higher proportion of single cells expressing these genes. Additionally, lymphatic endothelial cells and sebaceous and sweat gland cells showed significantly high expression levels of these genes. These findings highlight the potential importance of genes with cooperative target regions in the host's skin homeostasis, the primary interface upon the encounter with a tick.

A PPI network analysis revealed connections between half of the genes in this set (Figure 34). PDGFRA, NRG1, and PIKFYVE exhibited the highest eigenvector centrality, remarking on their central roles in the network and their potential significance in modulating the host's response.

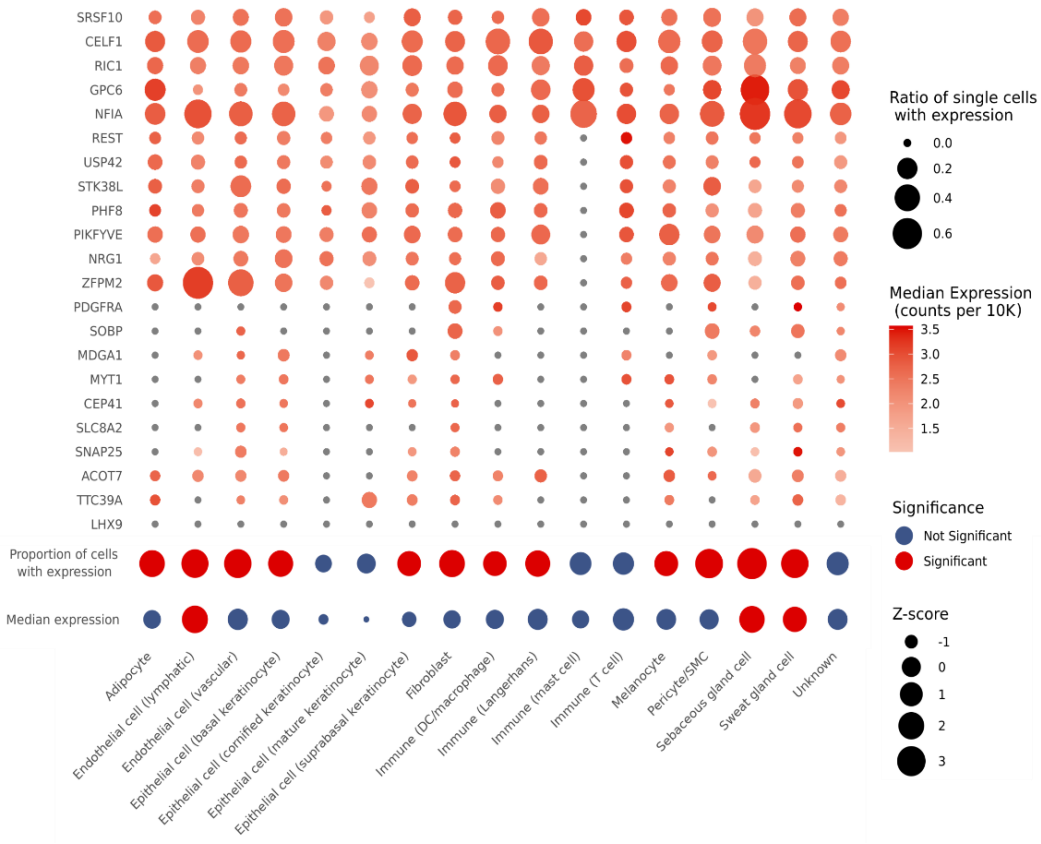

Figure 33. Abundance patterns and statistical significance in single cell types from skin tissue of the 'conservedly' and cooperatively targeted mRNAs by key* Ixodes ricinus *microRNAs. *The analysis was performed using the GTEx single-cell dataset. The top part of the figure shows the abundance of genes (rows) across single-cell types (columns), where bubble size represents the proportion of single cells within each cell type expressing a given gene, and color intensity indicates median expression (counts per 10K). The bottom part illustrates the statistical significance of the median expression and the median proportion of cells expressing the genes, with red circles indicating statistically significant enrichment. Z-scores are represented by bubble size.*

We further investigated the roles of these 22 genes in processes that may benefit the host in response to *I. ricinus* parasitism. Several genes, including GPC6, NRG1, ZFPM2, PDGFRA, and CEP41, were implicated in wound healing or angiogenesis processes, potentially aiding in wound closure and limiting tick feeding [272–276]. Additionally, genes such as CELF1, NFIA, STK38L, also known as NDR2, PHF8, PIKFYVE, and ACOT7 were associated with innate immunity,

promoting either inflammation or immune cell activity (e.g., macrophages, T cells, and NK cells) [277–283]. USP42 regulates inflammatory response through the deubiquitylation of histone H2B [284,285]. Pain and mechanosensation, critical for host responses to prolonged tick bites, involved genes such as REST, MDGA1, and SNAP25 [286–289]. Although, to our current knowledge SRSF10, RIC1, SOBP, SLC8A2, and TTC39A have not been directly linked to the mentioned functions, their expression characteristics suggest potential roles in host defense mechanisms, but additional experimental analysis is essential for such a statement to be supported. Moreover, the functions of this set of genes will be further discussed in *Chapter 8*.

In summary, while the interaction network did not encompass all genes, functional analyses and abundance in cells from the skin tissue indicate that most genes with cooperative target regions for the most relevant and abundant miRNAs in *I. ricinus* saliva could benefit the host and impede tick parasitism. Simultaneous targeting of these genes may significantly impact the effectiveness of tick feeding and parasitism, granting *I. ricinus* the ability to successfully feed on the host's blood.

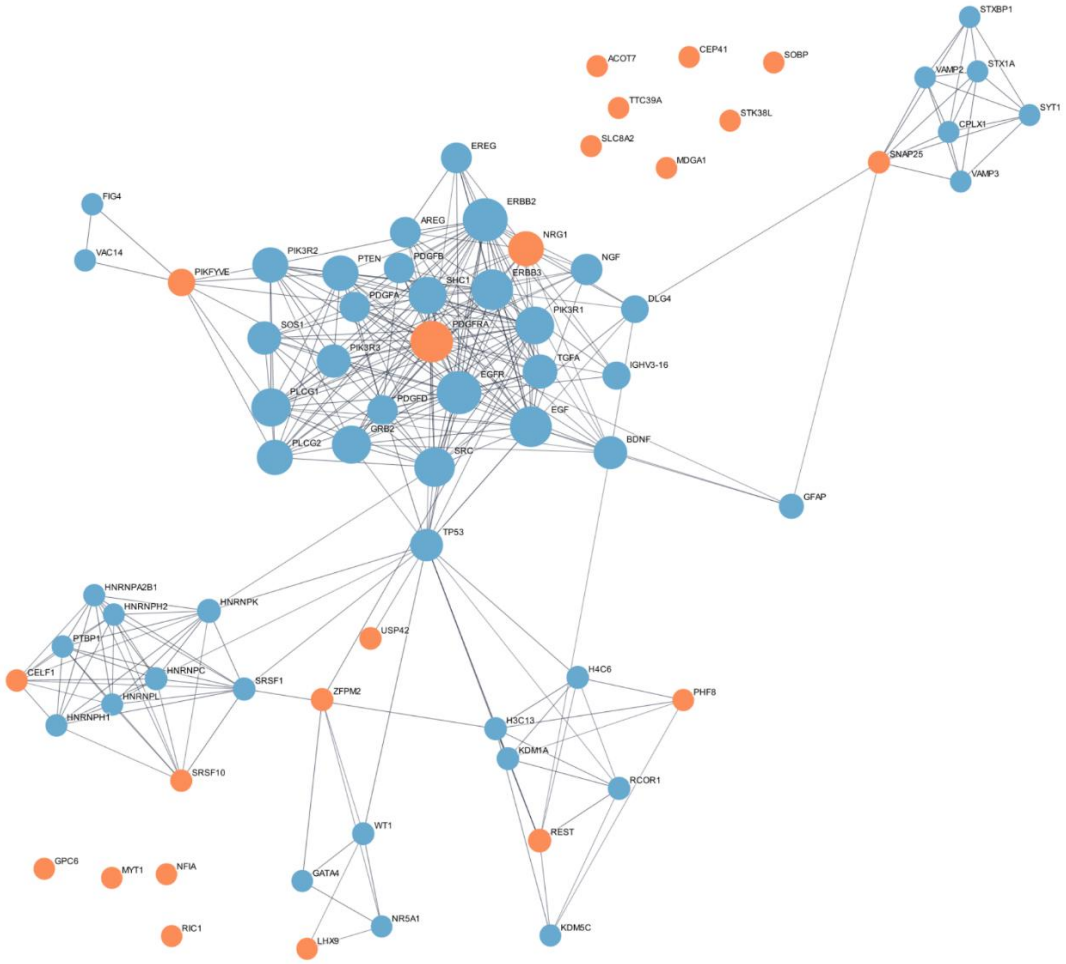

Figure 34. Protein-protein interaction network of gene products 'conservedly' and cooperatively targeted by key* Ixodes ricinus *microRNAs. *The set of genes 'conservedly' and cooperatively targeted by key* I. ricinus *miRNAs are represented by color orange. Fifty interacting proteins were added using StringDB with a high-confidence threshold of 0.7 and are shown in blue.*

5.8. microRNA abundance in extracellular vesicles

Building on our findings regarding the role of miRNAs in modulating the tick-host interface and their potential cooperative effects on host responses, a key question remains: Do these miRNAs associate with EVs, and is their incorporation into these vesicles a selective process?

To investigate this, we isolated and analyzed EV samples from *I. ricinus* saliva, assessing the abundance of miRNAs within these extracellular compartments.

5.8.1. Sequencing data: Read preprocessing and analysis

We obtained saliva samples from *I. ricinus* parasitizing a naïve host and samples from *I. ricinus* feeding on the same host for a second time and thus the host was sensitized to ticks. It is known that ticks feeding for the second time in the same host meet resistance from the host and this resistance has negative impact on tick's feeing ability. Next, a process of differential centrifugation and EV isolation allowed us to classify and separate four phases of EVs, sorted by size and the centrifugation speed required for sedimentation. These phases, ordered from larger EVs to smaller ones, were as follows: 1) large EVs that sedimented at 2,000 g, 2) medium EVs in the pellet after centrifugation at 10,000 g, 3) small EVs obtained after centrifugation at 150,000 g, and 4) the supernatant after this last centrifugation, containing the saliva content outside the EVs and the smallest EVs.

Next, we isolated and sequenced small RNAs from these samples, obtaining a total of 256,812,923 single-end reads. After trimming and quality filtering, 99.82% of the reads were of high quality, resulting in 256,364,683 reads

available for further analysis. The distribution of reads per sample is shown in Figure 35.

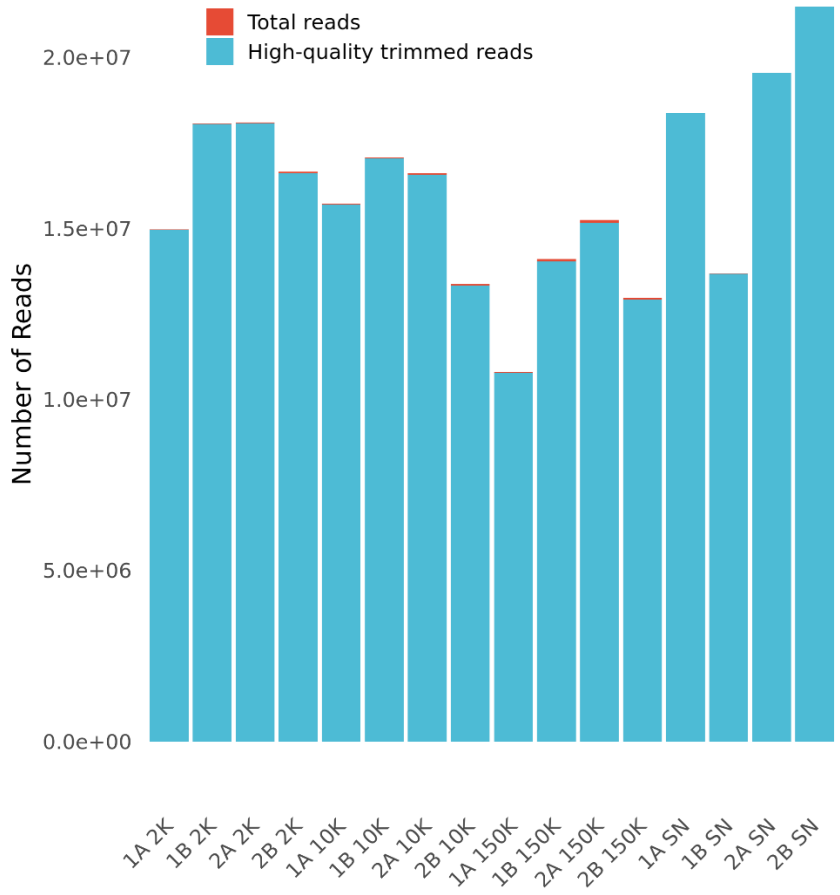

Figure 35. Distribution of total and high-quality trimmed reads in small RNA-seq data from* Ixodes ricinus *extracellular-vesicle samples. *Total and high-quality trimmed reads are represented by different colors. The Y-axis shows the number of reads and X-axis the different samples analyzed in this study. The sample IDs are displayed in the figure. The first number in these IDs indicates whether the host is being exposed to ticks for the first or second time during blood feeding. The subsequent letter represents the biological replicate, followed by the EV fraction.*

Next, we aimed to further assess the quality of the data and gain an initial overview of small RNA expression patterns across the different samples. To

achieve this, we performed PCA, correlation analysis, and HCA using Ward's method.

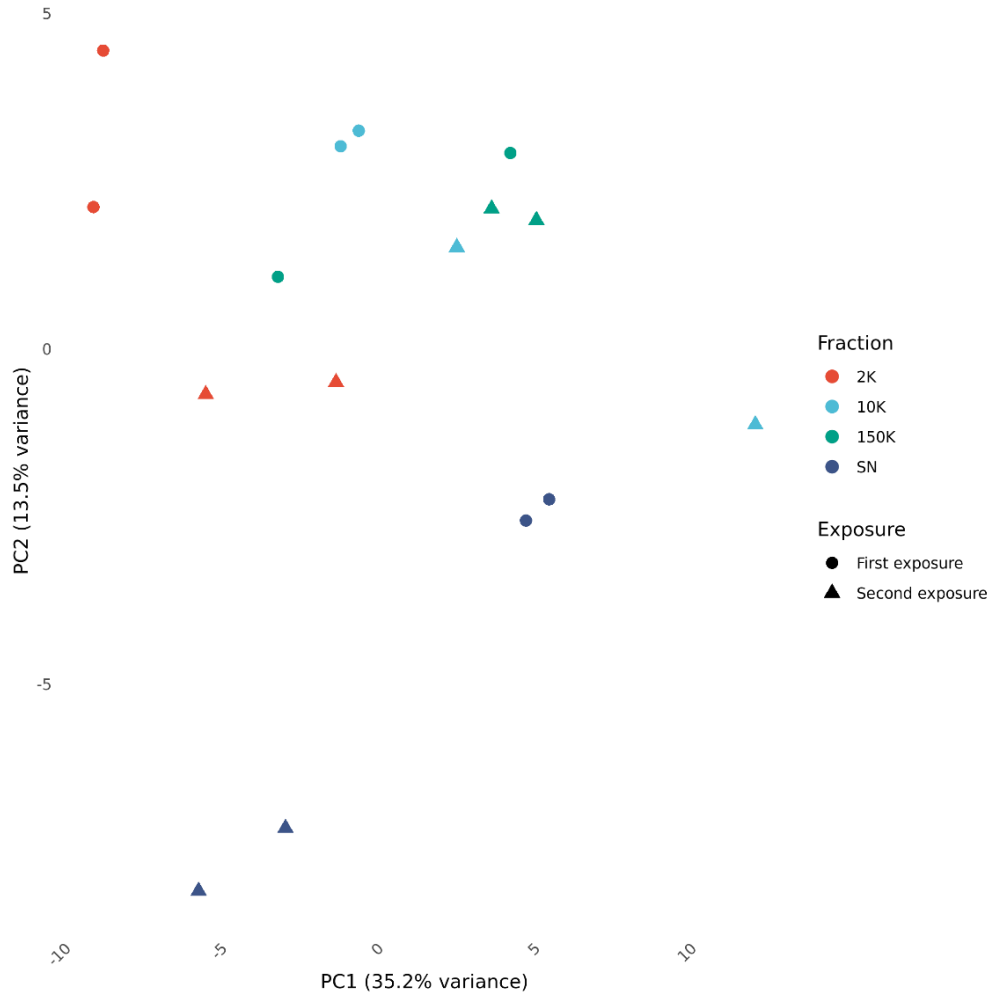

***Figure 36. Principal component analysis of small RNA expression variance in sequencing data from extracellular vesicles of* Ixodes ricinus.** *Colors represent different EV fractions, while shapes distinguish between samples from ticks parasitizing a naïve host and those from ticks parasitizing a host previously exposed to ticks.*

PCA results indicated that the first principal component did not effectively separate samples based on fraction type or prior exposure status. However, the second principal component distinctly segregated supernatant samples from

the sedimented fraction, with the most pronounced separation observed in supernatant samples from ticks feeding on previously exposed hosts. Furthermore, the combined effect of both components delineated large EVs from medium and small EVs, which exhibited a higher degree of similarity in their miRNA expression profiles. Figure 36 illustrates PCA results.

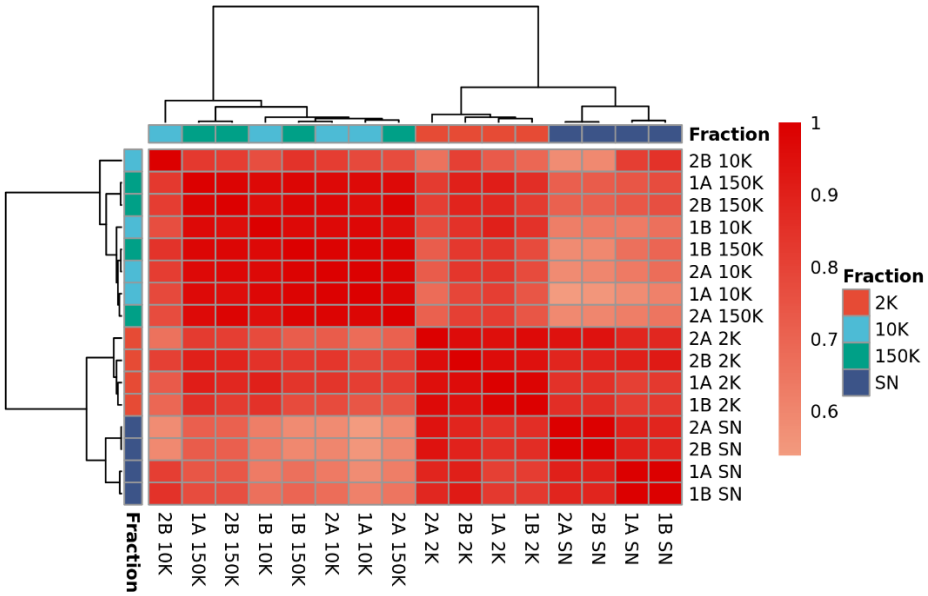

***Figure 37. Correlation and hierarchical clustering of transcript expression patterns in small RNA-seq data from extracellular vesicles of* Ixodes ricinus.** *Different fractions are represented by distinct colors in the margins of the correlation matrix. The gradient of the color (red) in the inside the matrix indicates the correlation level between the expression pattern of a pair of samples. The sample IDs are displayed in the figure. The first number in these IDs indicates whether the host is being exposed to ticks for the first or second time during blood feeding. The subsequent letter represents the biological replicate, followed by the EV fraction.*

Consistently, hierarchical clustering and the correlation matrix reinforced the emergence of three distinct sample clusters: 1) supernatant samples, 2) large EVs, 3) and small and medium EVs (Figure 37). Notably, despite forming separate clusters, the supernatant and large EV samples exhibited a high degree of correlation, suggesting similarities in their molecular composition. This

observation can be attributed to the presence of biological material within the large EV fraction which is released into the supernatant. As these vesicles break down over time, their contents may disperse into the surrounding supernatant, contributing to the observed correlation between these two fractions. This distinction further sets them apart from medium and small EVs, which primarily originate from active cellular processes such as exocytosis.

5.8.2. Abundance in extracellular vesicles of key microRNAs

In the previous sections, we identified a set of 12 miRNAs with the highest potential to facilitate tick parasitism. This selection was based on a) *t*heir abundance in tick saliva [16], b) *t*heir high conservation and statistically significant enrichment in target regions across vertebrate hosts, c) *t*heir ability to co-target adjacent sites within the same mRNA in the vertebrate host, suggesting cooperative regulation. Furthermore, *t*hese miRNAs appear to disrupt host homeostasis and synergistically target essential skin-related genes, potentially enhancing tick feeding success. In this section, we analyze their presence and dynamics within EVs in *I. ricinus* saliva, further exploring their potential role in host modulation (Figure 38).

Here, no global patterns were observed in terms of a specific fraction containing the majority of miRNAs or showing large expression differences between ticks parasitizing hosts with different prior exposure statuses. Overall, miRNA expression remained relatively stable across large, medium, and small EVs. However, in the supernatant fraction, which consists of the smallest EVs and non-packaged small RNAs from saliva, certain miRNAs exhibited expression divergence depending on the host's prior exposure to ticks.

Nevertheless, the most significant conclusion from this analysis is that these 12 key miRNAs are consistently present in tick saliva and are actively packaged and protected within EVs, enhancing their potential to interact with and modulate host cells. All the information presented in this thesis regarding this set of key *I. ricinus* miRNAs positions them as promising candidates for future clinical applications and pest control strategies.

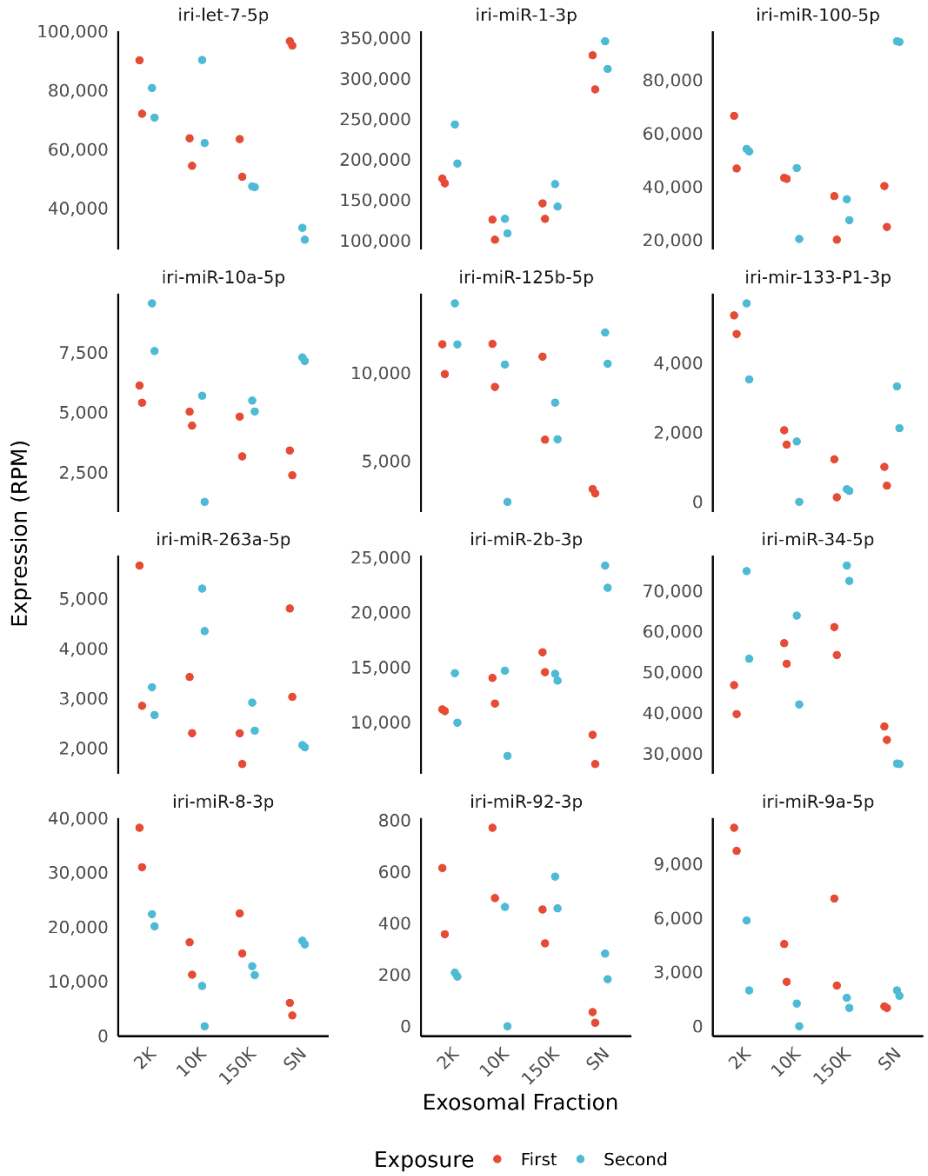

***Figure 38. Expression dynamics of key microRNAs in the extracellular vesicles of* Ixodes ricinus.** *The Y-axis represents expression levels in RPM, while the X-axis corresponds to the EV fraction to which a sample belongs. Each dot represents a sample from an EV fraction, with different colors indicating whether the host is being exposed to ticks for the first or second time during blood feeding.*

Chapter 6.

Transcriptomic analysis of *Ixodes ricinus* midgut and salivary gland responses to repeated blood feeding on a vertebrate host

Till this point, this thesis has focused on how *I. ricinus* miRNAs from saliva can modulate the host's response. To fully comprehend the intricate interplay between the tick and its host, we will shift the focus to the dynamics of gene expression in the salivary glands and midgut of *I. ricinus* at the transcription level, aiming to better understand molecules expressed during blood feeding. An schematic representation of the analysis is provided in Figure 39. Both coding RNA, in this chapter, and long non-coding RNA, discussed in *Chapter 7*, will be analyzed and tested to determine their roles in *I. ricinus* blood feeding. By exploring these elements and interconnecting them, we aim to present a broader and more integrated view of the molecular interactions at the tick-host interface.

Building on our integrated view of *I. ricinus* lifecycle and its ability to bypass host immune defenses, we analyzed the transcriptomic dynamics of 1) unfed *I. ricinus* ticks, 2) ticks parasitizing hosts for the first time, and 3) ticks blood

feeding on sensitized hosts to tick feeding (the host is exposed to ticks for a second time and raises resistance to tick feeding). Blood-feeding ticks were detached at different time points to allow for the analysis of temporal dynamics. The hypothesis is that blood-feeding *I. ricinus* ticks will over-express molecules that facilitate feeding and help them evade host defense mechanisms. This effect is expected to be more pronounced in ticks feeding on hosts that have already been parasitized by ticks for one time, as these hosts have a more active immune response [290]. Single salivary glands and midguts from individual, pathogen-free female *I. ricinus* ticks, all derived from the same "mother", have been used to minimize genetic variability between tick individuals. This study was the first to analyze expression dynamics of ticks at the individual tick level.

Thus, RNA was extracted and sequenced from a total of 88 individual *I. ricinus* tick samples with the objective of assembling a reference transcriptome containing both coding and non-coding transcripts. This transcriptome will serve as the foundation for identifying proteins and lncRNAs that may help the tick evade host defenses.

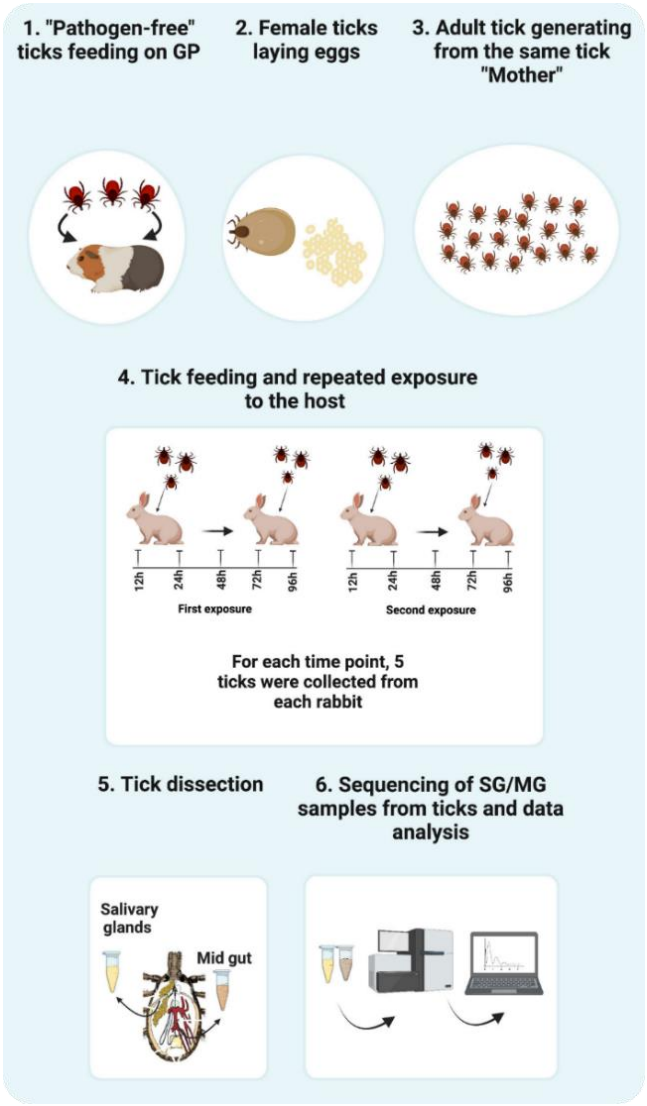

***Figure 39. Schematic illustration of the experimental design for the analysis of salivary glands and midgut from pathogen-free* Ixodes ricinus.** *1) Pathogen-free sibling ticks were hatched, fed on SPF (specific pathogen-free) guinea pigs, and allowed to develop into adult ticks. 2) Fully engorged female ticks, having fed on an SPF guinea pig, were allowed to lay eggs. 3) Molted larvae were fed on SPF guinea pigs to produce adult female ticks, which were pre-mated with sibling male ticks. These adult females were used for feeding and tissue isolation. 4) Two rabbits were each exposed to 25 female and 25 male sibling ticks. Female ticks were collected at 12, 24, 48, 72, and 96 hours post-exposure. Two weeks after the initial rabbit exposure to ticks, a second exposure was performed following the same protocol. 5) Ticks were dissected, and their salivary glands (SGs) and midguts (MGs) were stored in 200 µL of RNA later at 4°C overnight, then transferred to -80°C. 6) RNA was extracted from five SG and three MG samples at each time point and sequenced using Illumina technology.*

6.1. Assembly of a de novo transcriptome

Using high-throughput sequencing, we generated a total of 3.64 billion paired-end reads from the 88 aforementioned *I. ricinus* samples. Following adapter trimming and removal of low-quality reads, 3.51 billion clean reads remained. As mentioned in *Chapter 1,* although an *I. ricinus* genome assembly existed at the time this study was made [181], its 204,516 contigs presented challenges, such as genes being split across multiple contigs of this genome or being completely missed. To address this, we opted to construct a de novo transcriptome assembly.

Two approaches were considered: individual sample assemblies followed by clustering to create a consensus transcriptome or merging all samples first for a single de novo assembly. Preliminary analyses indicated that the first method yielded significantly more contigs (1,770,231 compared to 981,846 with the second method) and poorer quality metrics. Consequently, we adopted the second approach, generating separate transcriptomes for salivary glands and midgut tissues, which initially produced 816,408 and 495,556 contigs, respectively.

Clustering highly similar sequences reduced the total contigs to 981,846. By applying a minimum expression threshold of 5 FPKM across all samples for at least one condition, we further refined this into a final consensus transcriptome comprising 25,010 contigs with an average length of 1,489 and an N50 value of 2,763. In comparison, the unfiltered transcriptome (981,846 contigs) exhibited a median length of 329 and an N50 of 542, demonstrating significant improvements in assembly quality after filtering. Remarkably, 87.6% of paired-end reads could be mapped back to the assembly, more than generally expected.

Next, we partitioned the transcriptome into coding and non-coding transcripts in a two-step process. This identified 13,458 coding transcripts, which were further clustered to remove redundancy, resulting in 12,158 unique coding transcripts and 11,552 putatively non-coding transcripts. A workflow summary and primary results are depicted in Figure 40.

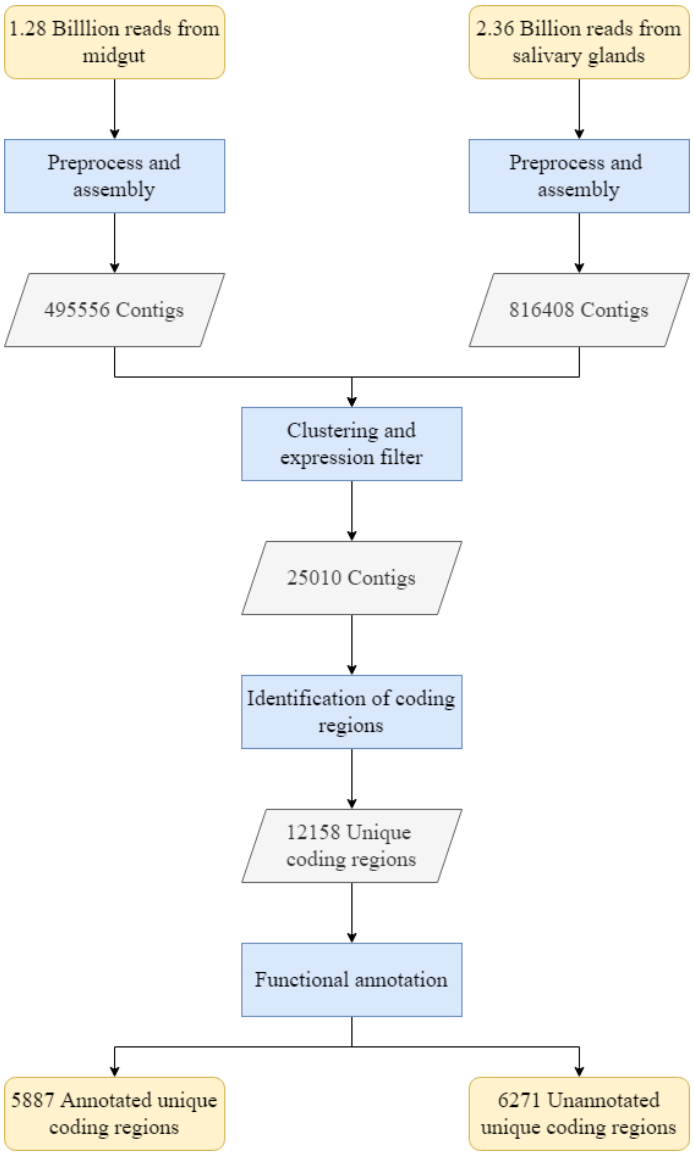

Figure 40. Step-by-step process and results of transcriptome assembly, including the identification of coding regions and their subsequent functional annotation.

To assess the completeness of the transcriptome, BUSCO [199] analysis with the Arachnida lineage dataset revealed that 83.1% of Benchmarked Universal Single-Copy Orthologs (BUSCOs) were complete, with 24.3% duplicated due to isoforms, 0.4% fragmented, and 16.5% missing (Figure 41).

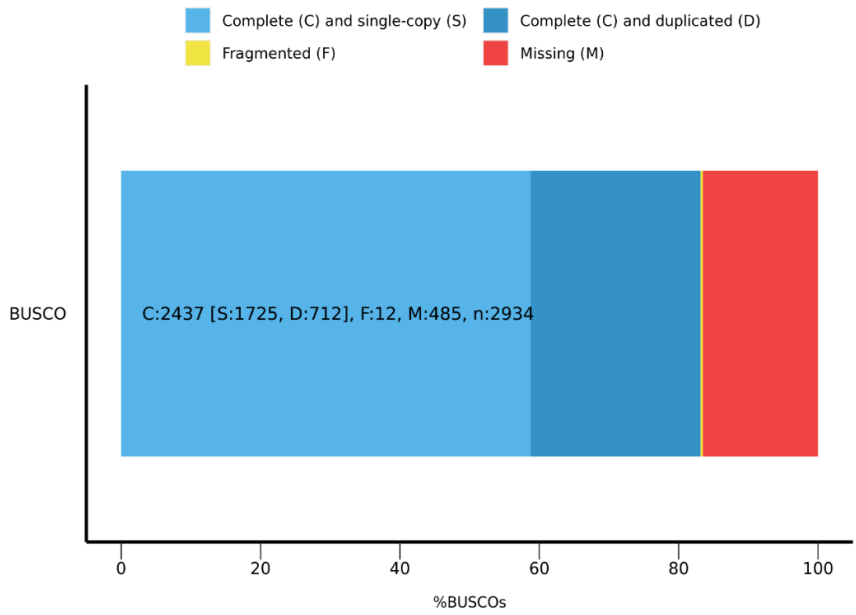

Figure 41. Results of the Benchmarked Universal Single-Copy Orthologs (BUSCO) analysis assessing the completeness of the transcriptome. *The analysis utilized the Arachnida lineage gene dataset. Different colors represent the percentages of complete single-copy, complete duplicated, fragmented, and missing BUSCOs. Exact numerical values are also displayed in the plot.*

A PCA was performed to identify potential outlier samples and to identify potential patterns in the RNA abundance of the samples from SG and MG (Figure 42). This analysis revealed no clear outliers. Instead, distinct clusters emerged, such as those formed by midgut samples from ticks fed for 48, 72, and 96 hours, as well as the grouping of unfed samples with early feeding time points. Notably, tissue was confirmed as the dominant factor in expression variation (component 1). Thus, no outlier samples were identified, validating their inclusion in downstream analyses.

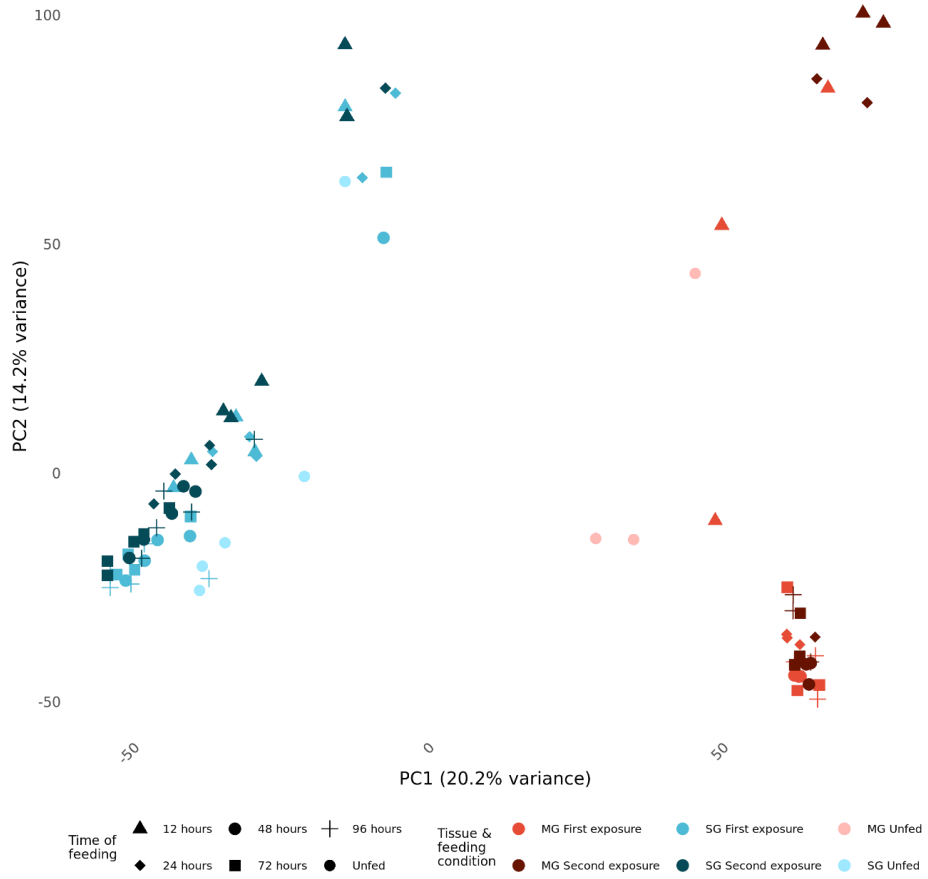

***Figure 42. Principal component analysis of RNA expression patterns in midgut and salivary glands samples of* Ixodes ricinus.** *This plot shows the two principal components that explain the largest proportion of variance in the expression data. RNA abundances were used for this analysis. Colors represent different tissues and distinguish between samples from ticks parasitizing a naïve host from those from ticks parasitizing a host previously exposed to ticks and from those coming from unfed ticks. Different shapes indicate the time-points in which the tick blood feeding has been stopped.*

6.2. Functional annotation of the transcriptome

Following assembly and quality evaluation, we proceeded to annotate the coding transcripts in detail. The 12,158 unique coding regions were mapped against four databases: the *Arachnidae* database, Swiss-Prot, UniRef90, and TickSialoFam [205,206,291] . Out of these, 7,225 coding regions were matched to at least one reference sequence in these databases. The optimal alignment for each coding region was determined using the Bit-score provided by Blastp. Where applicable, GO terms and keywords were assigned using the UniProtKB database [291], resulting in the annotation of 4,312 coding regions.

To further annotate regions not aligning with these databases or lacking GO annotations, we utilized Blast2GO [207], which contributed an additional 1,138 annotations. This brought the total number of annotated unique coding regions to 5,450, leaving 6,708 coding transcripts unannotated. We then employed identified conserved protein domains and associated GO terms, yielding a final set of 5,887 annotated unique coding regions with at least one functional annotation.

In summary, of the 12,158 unique coding regions, 5,456 were linked to at least one GO term under one or more categories: 3,190 (58.47%) under "Biological Process," 4,362 (79.95%) under "Molecular Function," and 3,335 (61.13%) under "Cellular Component." Within the "Biological Process" category, the most prominent subcategories included "organic substance metabolic process" (2,019, 63.29%), "nitrogen compound metabolic process" (1,692, 53.04%), and "cellular component metabolic process" (1,730, 54.23%). Under "Molecular Function," key subcategories were "binding" (2,648, 61.53%) and "catalytic activity" (2,349, 53.85%), with "hydrolase activity" being the most represented terminal node (880, 20.17%). For "Cellular Component," notable nodes included

"intracellular membrane-bound organelle" (1,328, 39.82%), "integral component of membrane" (1,277, 38.29%), and "cytoplasm" (1,378, 41.32%).

We also analyzed the presence of signal peptides and cleavage sites in unique coding regions starting with methionine, generating putative mature peptides for those with signal peptides. Additionally, we predicted transmembrane helices in the unique coding regions, enabling their classification into four categories:

1. **Putatively secreted and annotated**: Regions with both functional annotations and a predicted signal peptide, but no transmembrane domains, as per Ribeiro et al. [206].

2. **Putatively secreted but not annotated**: Secreted coding regions without GO or InterPro annotations.

3. **Non-secreted and annotated**: Regions with functional annotations that lack signal peptides or contain both signal peptides and transmembrane domains in the mature peptide.

4. **Non-secreted and non-annotated**: Regions without GO or InterPro annotations that are non-secreted.

Finally, coding regions were deemed tissue-specific if they exhibited a fold-change of 2 or higher between midgut and salivary gland samples. Thus, we achieved a comprehensive annotation of the transcriptome, providing a solid foundation for investigating the dynamics of transcripts in the salivary glands and midgut, as well as studying key processes such as immune modulation, nutrient acquisition, and the secretion of proteins essential for successful parasitism.

6.3. Analysis of the variance in expression data

Analyzing the variation in transcript expression across biological or technical replicates is crucial for assessing the consistency, reliability, and reproducibility of downstream analyses. This study uniquely utilized genetic material from individual ticks rather than pooled samples, allowing the detection of individual tick responses to feeding threads. These responses may manifest as significant fluctuations in the expression of certain genes, such as up- or downregulation within individuals under the same condition. To identify genes with a strong individual component, we calculated the CV for each unique coding transcript across conditions and tissues.

Figure 43 illustrates the CV distribution for each condition. A comparison with a randomized dataset (bottom of Figure 43), generated by calculating CVs from five randomly selected samples for each transcript, revealed that the observed variation was consistently lower than random expectations. This suggests that feeding time points and/or exposure influence gene expression patterns. Notably, later feeding time points exhibited lower variation in both tissues, indicating that gene expression variability decreases as feeding progresses. This trend suggests that individual variability in gene expression is more pronounced at the onset of feeding and diminishes as feeding progresses. Furthermore, the second exposure to the host resulted in reduced variation compared to the first exposure, particularly in salivary glands, corroborating observations from the PCA analysis, where early feeding time points showed some separation from the main clusters. Figure 44 plots CV as a function of expression, showing a general decrease in variation with higher expression levels. However, a subset of highly expressed transcripts exhibited substantial variability (peak on the right side of the plot).

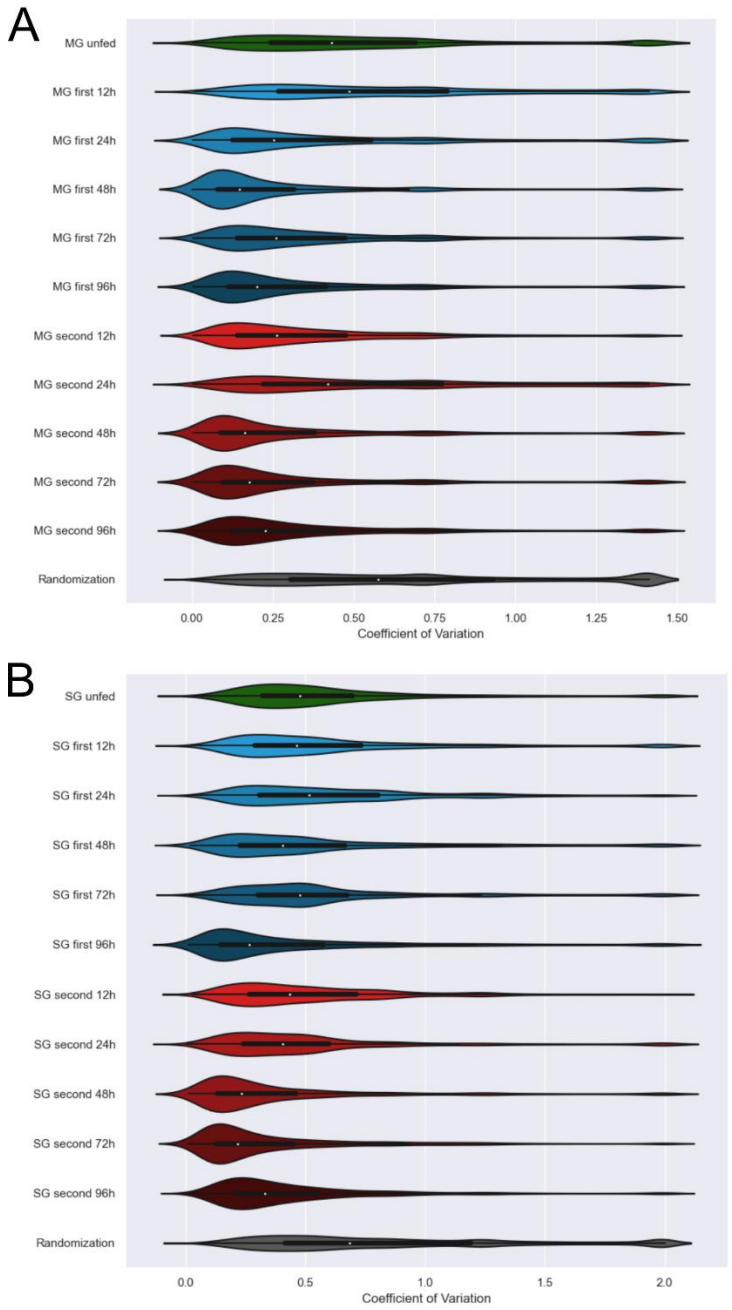

Figure 43. Analysis of expression variability in biological replicates of midgut and salivary glands across different feeding conditions. *Sample labels are coded as follows: tissue (MG (A) for midgut or SG (B) for salivary glands), exposure number (unfed, first, or second), and feeding time point in hours (12h, 24h, 48h, 72h, and 96h). Each plot also includes a negative control showing the distribution of coefficients of variation derived from random values for both tissues independently.*

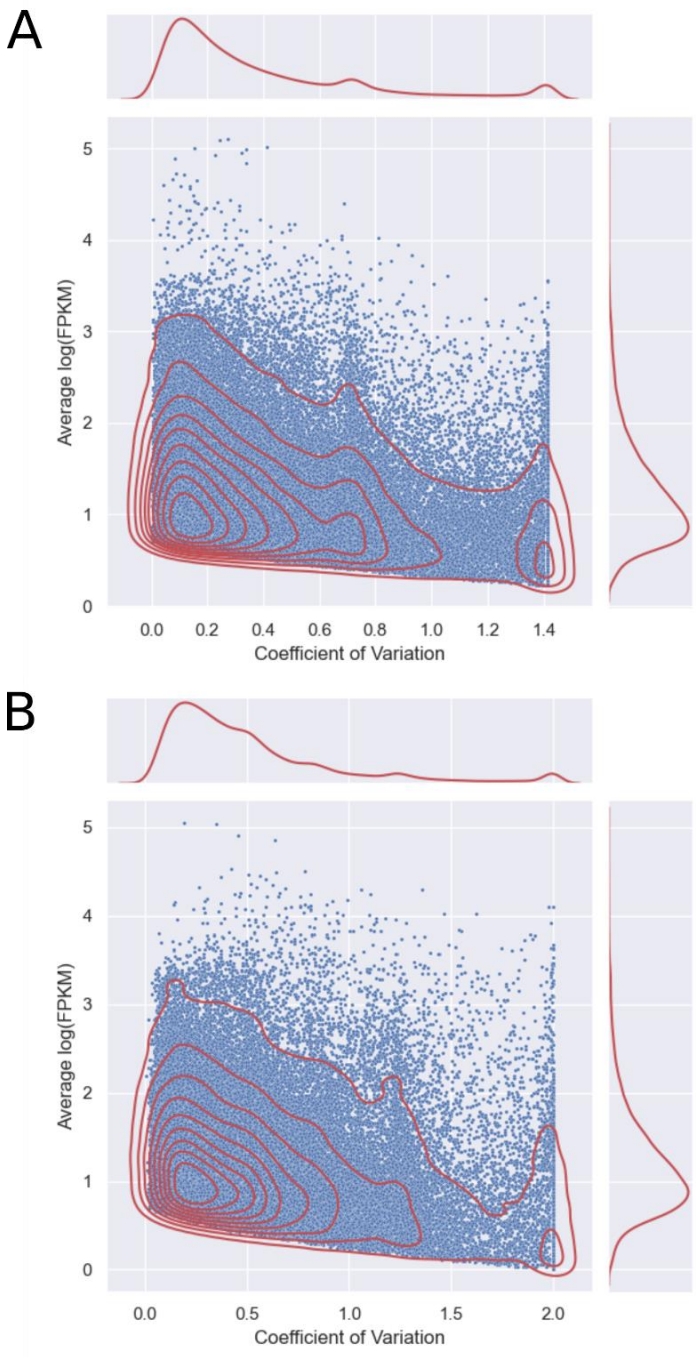

Figure 44. Distribution of coefficients of variation relative to the logarithm of the mean expression of unique coding regions for each condition in both midgut and salivary glands. *Distributions of CV for (A) midgut and (B) are shown in this figure.*

To test whether high CV transcripts consistently reflected individual variability and potential responses to feeding threads, we identified sets of 1,000 transcripts with the highest CV for each condition in salivary glands and analyzed their intersections across conditions. A total of 3,358 transcripts were identified as highly variable in at least 8 of 11 conditions. The overlap between conditions was greater than expected by chance, suggesting that certain transcripts consistently display high variability. Similarly, we identified 4,182 transcripts with low variance across conditions. These consistently low-variance transcripts also showed greater overlap between conditions than expected by chance, suggesting significance in both high- and low-variance transcript sets.

Functional characterization revealed insights into transcripts with high and low individual components. GO enrichment analysis showed that transcripts with high variability were associated with essential functions, including "translation," "structural constituent of ribosome," "protein folding," and "gene expression." Enrichment was also observed in biosynthetic processes such as "organonitrogen compound biosynthetic process" and "cellular macromolecule biosynthetic process" (Figure 45A). In contrast, transcripts with low variability were associated with metabolic processes, though overlaps with high-variance transcripts were noted for terms like "translation" and "gene expression" (Figure 45B).

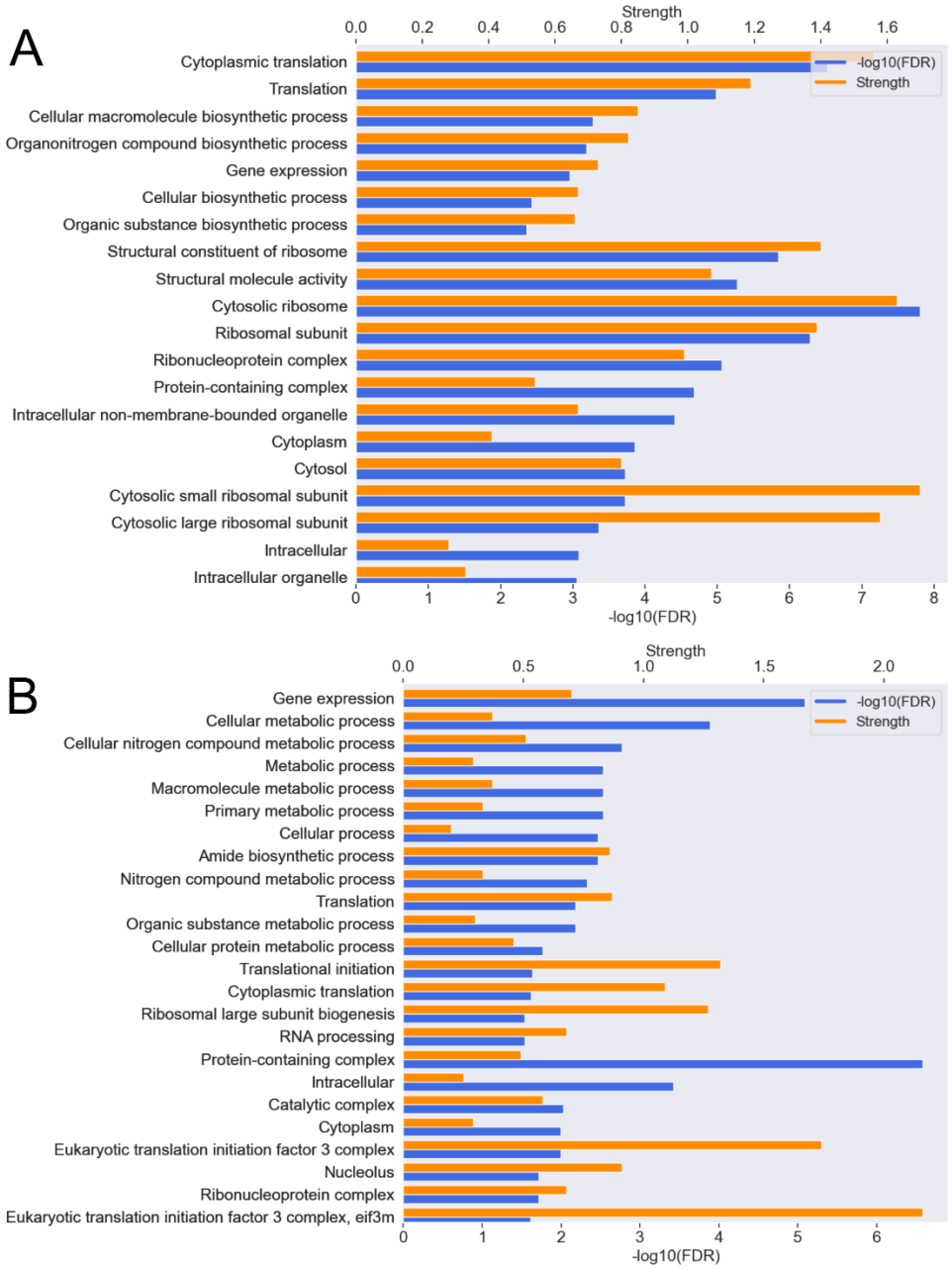

***Figure 45. Functional enrichment of unique coding regions with high and low expression variability in biological replicates in midgut and salivary glands of* Ixodes ricinus.** *This figure shows the most relevant significantly enriched GO terms in the set of unique coding regions with the highest or (B) lowest coefficients of variation across at least eight conditions. The significance and strength of enrichment, represented by the log10(observed/expected) ratio, are provided for each GO term.*

PPI networks gave more information about these findings. Transcripts with high variation formed networks with significant interactions, i098ncluding ribosomal proteins and factors involved in translation (Figure 46A). In contrast, networks for low-variance transcripts displayed fewer ribosomal proteins and elongation factors (Figure 46B).

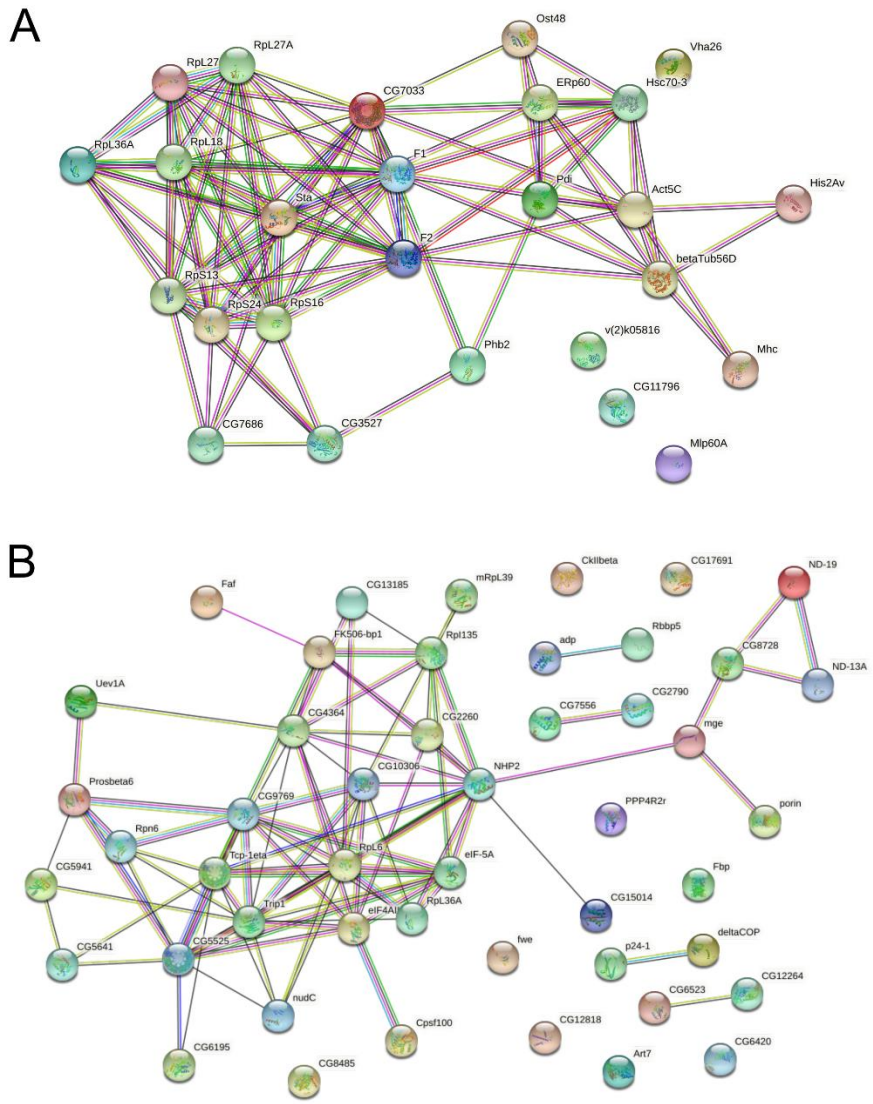

Figure 46. Interaction network of the unique coding regions exhibiting extreme coefficients of variation across at least eight conditions. *PPI networks are shown for unique coding regions with the highest (A) or lowest (B), highlighting key functional connections.*

A similar analysis was conducted for the midgut, but significant results were not observed. To determine whether this was due to lower statistical power, we simulated the analysis using three random salivary gland samples. While high-variance transcripts maintained their significance, low-variance transcripts did not, indicating both statistical power limitations and inherent differences between salivary glands and midgut tissues.

6.4. Differential expression analysis: Sialome switch and time-course dynamics

To elucidate the impact of tick feeding duration and the potential effect of previous host exposure to ticks on gene expression, we performed two types of analysis: (1) pairwise comparisons, which involve direct comparisons between two conditions (e.g., unfed ticks versus a specific feeding time point), and (2) global time-course analysis, which identifies genes with significant expression changes over feeding time in tick tissues coming from ticks either fed for the first time or for a second time to the same animal.

6.4.1. Pairwise analysis

The pairwise analysis provides detailed insights into the differences between specific conditions, offering a global perspective on the dynamics of gene expression. This approach allows us to examine differences between ticks feeding at various time points, ticks feeding from naive versus immunized hosts, and overall trends during the feeding time course by analyzing intersections of DEGs. The experimental design enabled numerous comparisons, summarized in Figure 47.

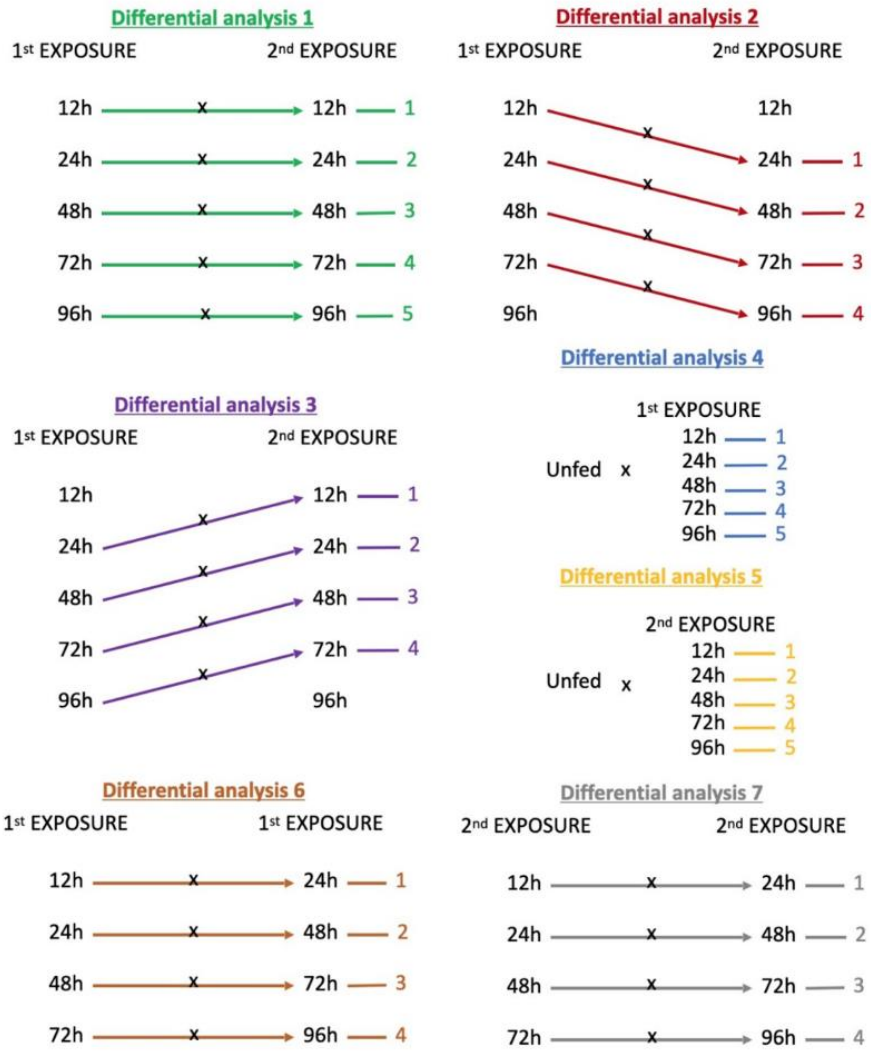

Figure 47. Overview of pairwise differential expression comparisons in midgut and salivary gland transcriptomes. *Comparisons include: (1) ticks feeding for the first versus second host exposure to ticks at five time points; (2) ticks feeding for the first versus second exposure at consecutive time points; (3) first versus second exposure at preceding time points; (4) unfed versus first exposure across five time points; (5) unfed versus second exposure across five time points; (6) first exposure at initial versus subsequent time points; and (7) second exposure at initial versus subsequent time points.*

The number of DEGs obtained for every comparison depicted in Figure 47 is shown in Figure 48. When comparing the first versus second exposures to ticks, one major problem is that tick feeding lasts lesser upon second exposure [292]. Therefore, we tested the comparisons between first and second feeding on the same animal either at identical time points (e.g., 12h first exposure versus 12h second exposure), delayed time points (e.g., 12h first exposure versus 24h second exposure), or advanced time points (e.g., 24h first exposure versus 12h second exposure). In these comparisons, the number of DEGs was generally lower than those observed in comparison to unfed ticks. An exception to this general trend was observed when testing the hypothesis that feeding is delayed in the second exposure. Nearly 3,000 DEGs were identified when comparing 24h first exposure to 12h second exposure, and approximately 1,900 DEGs were found between 48h first exposure and 24h second exposure. These findings suggest significant differences in gene regulation between the first and second exposures.

However, comparisons between adjacent feeding time points (Differential analysis 6 and 7) revealed significantly fewer DEGs. Interestingly, the largest number of DEGs was consistently identified in comparisons between 24h and 48h feeding time points, a critical period for gene expression changes, while differences between adjacent time points diminished at later feeding stages. This trend was consistent across midgut and salivary glands for both exposures.

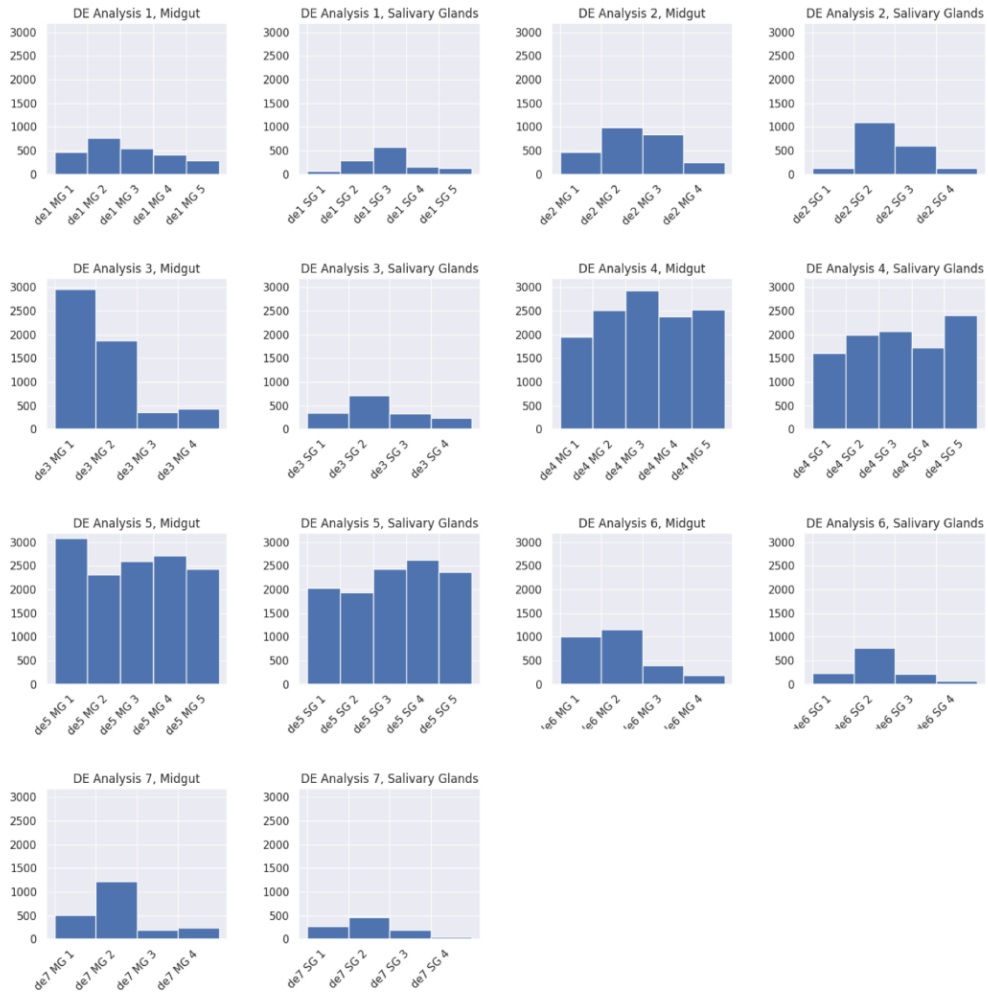

Figure 48. Comparative analysis of differentially expressed genes (DEGs) in* Ixodes ricinus *midgut and salivary glands during the first and second host exposures to ticks across feeding time points. *The histograms display the number of DEGs for each comparison, with coding corresponding to Figure 47.*

To explore similarities and differences between feeding times, we calculated the intersection of DEG sets across feeding time points by tissue. Figure 49 and Figure 50 illustrate that as feeding progresses, the overlap between DEGs increases, indicating less regulation of gene expression toward the end of the feeding process in both the midgut and salivary glands. Additionally, changes in differential expression between feeding time points were quantified. Figure 51 depicts the normalized overlap between adjacent time points, with 100% indicating identical DEG sets. Differences between the first and second exposures were most pronounced at early feeding stages but diminished toward the end of the feeding process. In salivary glands, gene expression dynamics were generally less pronounced during the second exposure, with higher overlap between adjacent time points compared to the first exposure. This is opposite of what we initially expected, since we hypothesized that ticks feeding on a previously exposed host should have significantly more changes in the salivary glands when compared to ticks feeding on a naive host. Nevertheless, this may explain the lower feeding success that has been observed for ticks feeding for the second time on the same host; the lack of different response in their SGs (to counteract the changed host response) lead to their feeding failure.

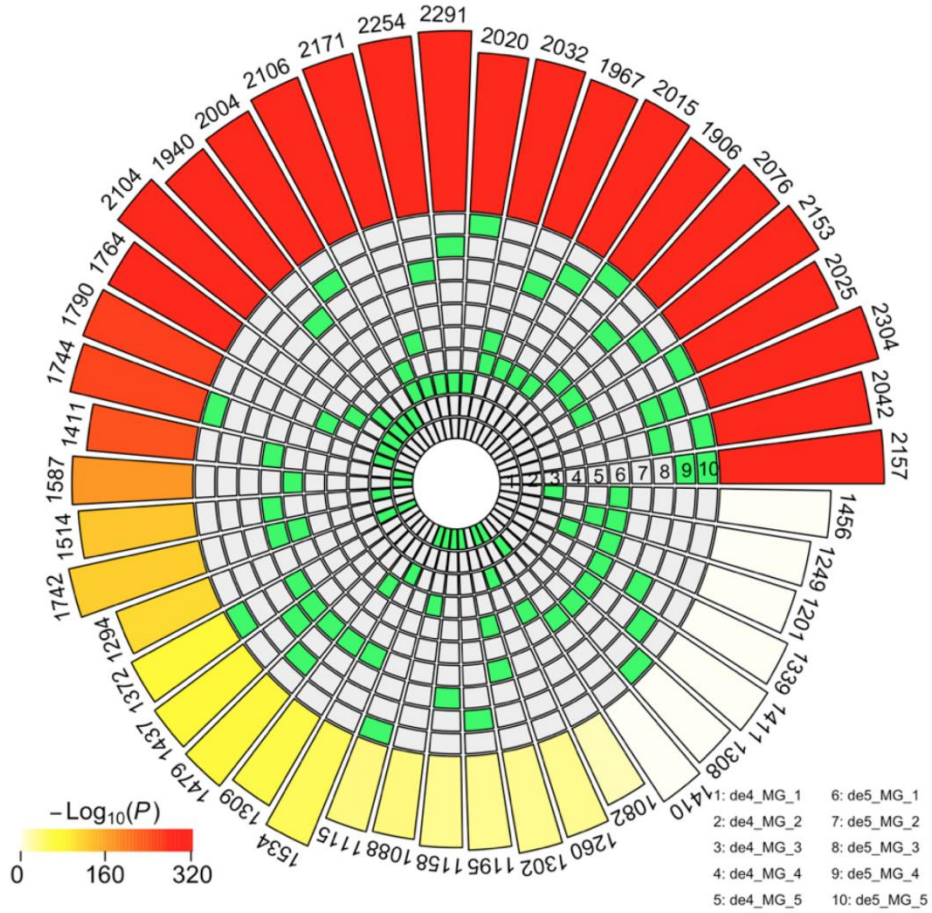

Figure 49. Intersection analysis of differentially expressed genes compared to the unfed condition across first and second host exposure scenarios in tick midgut. *The snail plot illustrates the intersecting numbers of DEGs for all possible pairwise comparisons among the analyzed sets of* I. ricinus *MG. The ten blocks in the middle part of the snail represent the ten DEG sets, with the corresponding code provided in the bottom-right corner of the figure. Individual blocks show "presence" (green) or "absence" (grey) of the DEG sets in each intersection. For each intersection, the statistical significance of having more DEGs than expected by chance is represented by the intensity of red shading, with higher significance indicated by deeper red. Additionally, the exact number of intersecting DEGs is displayed directly within the plot for clarity.*

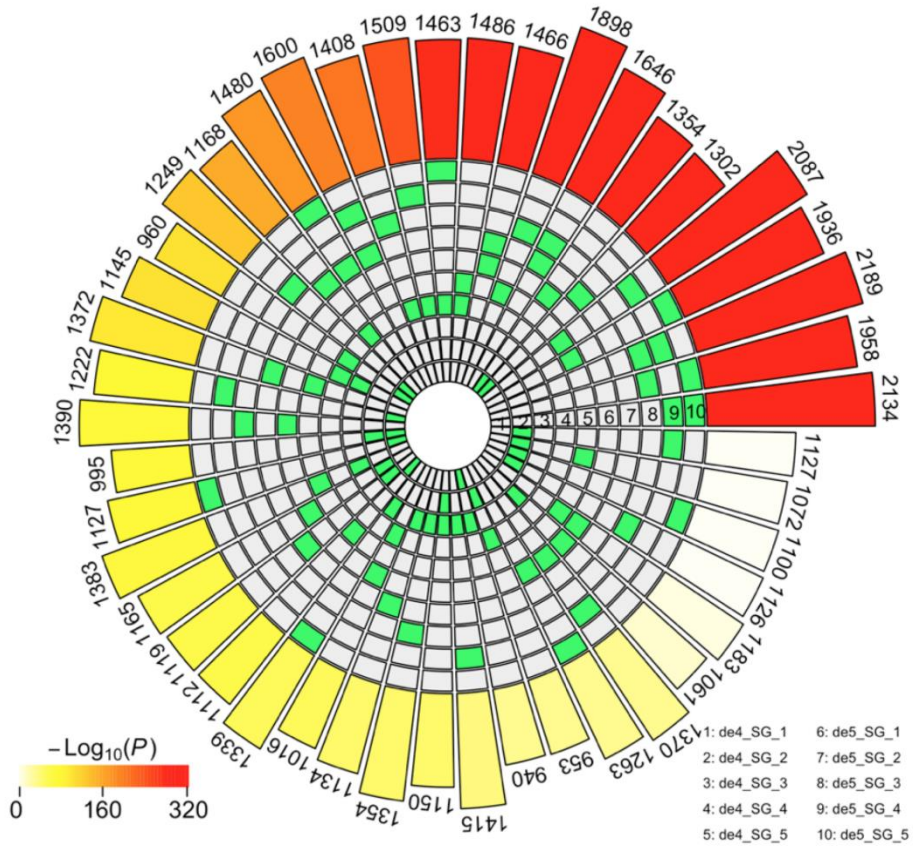

Figure 50. Intersection analysis of differentially expressed genes compared to the unfed condition across first and second host exposure scenarios in tick salivary glands. *The snail plot illustrates the intersecting numbers of DEGs for all possible pairwise comparisons among the analyzed sets of* I. ricinus *SGs. The ten blocks in the middle part of the snail represent the ten DEG sets, with the corresponding code provided in the bottom-right corner of the figure. Individual blocks show "presence" (green) or "absence" (grey) of the DEG sets in each intersection. For each intersection, the statistical significance of having more DEGs than expected by chance is represented by the intensity of red shading, with higher significance indicated by deeper red. Additionally, the exact number of intersecting DEGs is displayed directly within the plot for clarity.*

The gene expression dynamics observed in this study and the acute changes that tick suffers in salivary glands between 24 and 48 hours of feeding, all together support the idea of the sialome switch. The sialome switch was recently introduced by the research community, and it is a modulation of the

biochemical behavior of tick salivary glands that enables ticks to evade host hemostasis and the immune system, and to complete their life cycles [293]. During the sialome switch, the tick transcriptome changes either in preparation or due to tick feeding. These changes likely occur through epigenetic modifications [294] or signal transduction pathways that alter the activity of specific transcription factors [293]. Thus, molecules such as proteases and protease inhibitors are expressed during this process, disrupting host hemostasis and immunosuppressing the host [293]. Our findings captured these changes in gene expression, particularly during the transition from the attachment phase to the slow feeding phase.

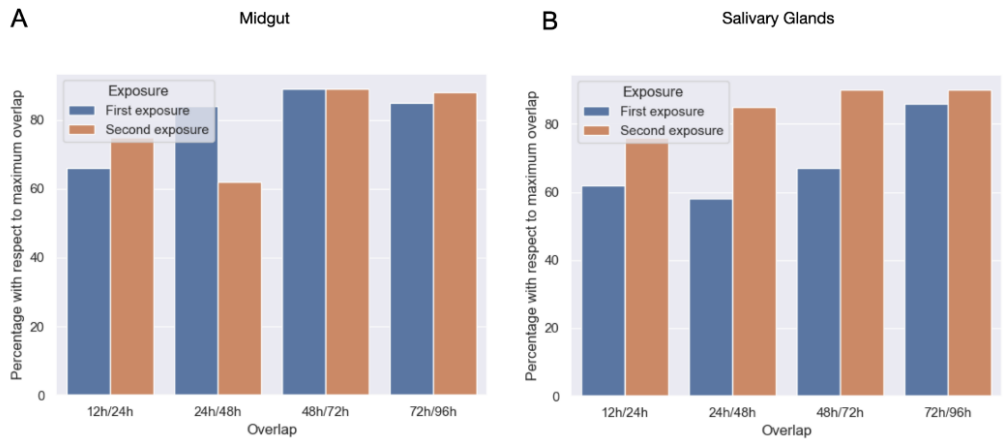

Figure 51. Differences in the sets of differentially expressed genes against unfed Across the timeline for first and second host exposure scenarios in* Ixodes ricinus *midgut and salivary glands. *The Y-axis represents percentages relative to the maximum possible overlap of shared genes in* I. ricinus *A) midgut and B) salivary glands. The maximum possible overlap corresponds to the size of the smallest set of DEGs against unfed in each comparison.*

In the midgut, the most significant expression changes in ticks feeding on a host during the first exposure occurred between 12 and 24 hours. In contrast, in ticks feeding on a host during the second exposure, we observed that on the 12 hours' time point the tick has experienced a high response to blood feeding, having the highest number of DEGs against the unfed ticks (Differential analysis 5).

Nevertheless, the midgut of these ticks then changes with the highest pronunciation between 24 and 48 hours, as depicted in Figure 51.

6.4.2. Time-course analysis

A key objective of this study was to assess the molecular response of *I. ricinus* salivary glands and midgut during the second exposure to an immunized host. A global time-course analysis identified 1,402 DEGs in the midgut and 647 DEGs in the salivary glands between the first and second exposures. Of these, 123 DEGs were shared between the two tissues. The DEGs from the time-course analysis were subjected to hierarchical clustering based on their expression profiles during the first and second exposures, resulting in nine clusters for both tissues.

In the midgut, clusters 1, 3, and 4 contained 808 DEGs with higher expression during early feeding stages of the second exposure. Cluster 2 included 106 DEGs with higher expression at later feeding stages of the second exposure, while cluster 5 comprised 126 DEGs with increased expression in late feeding stages of the first exposure. Cluster 8 represented 49 DEGs exclusively expressed during the first exposure. These clusters are shown in Figure 52.

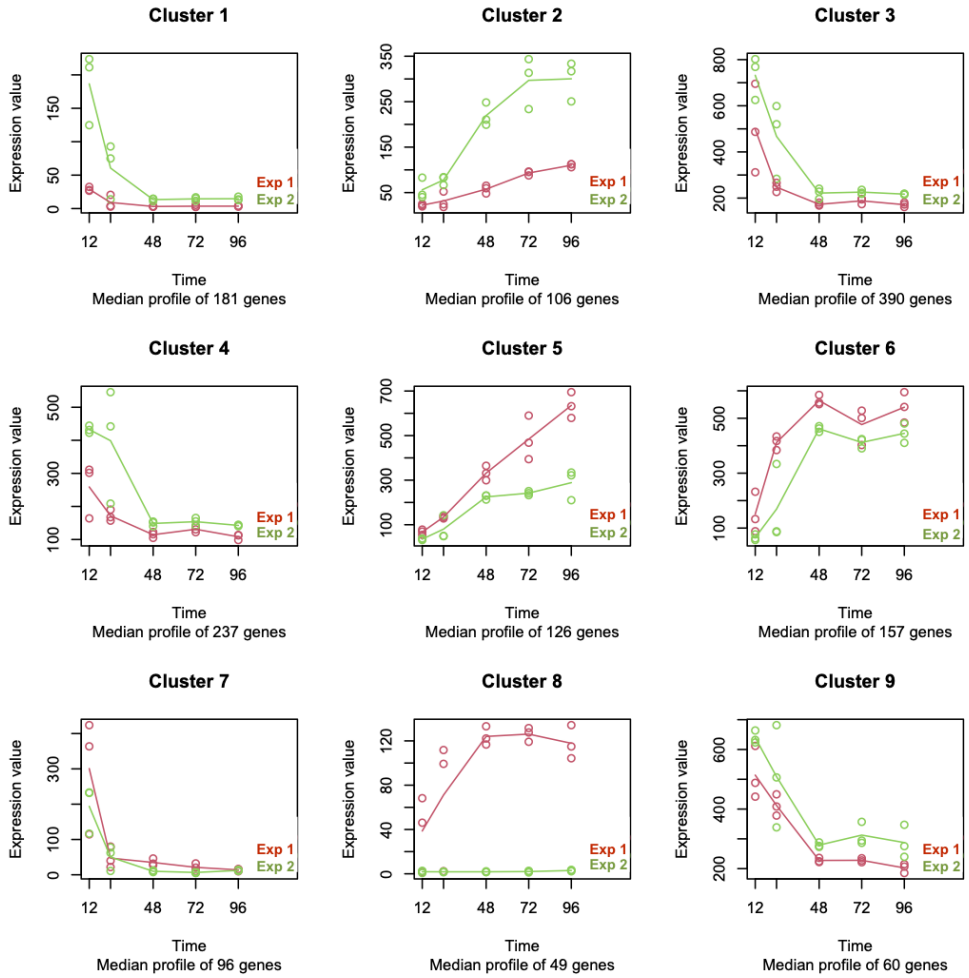

Figure 52. Hierarchical clustering of differentially expressed gene expression patterns in* Ixodes ricinus *midgut across the time course. *Abundance values are presented in FPKM, with distinct colored lines representing the first and second host exposures to ticks.*

In the salivary glands, cluster 1 included 38 DEGs with higher expression during the first exposure, peaking at 72 hours of feeding. Clusters 2 and 3 contained 153 and 78 DEGs, respectively, with increased expression at late and early feeding stages of the second exposure. Cluster 4 comprised 47 DEGs with higher expression at 48 hours during the first exposure, while cluster 6, like midgut cluster 8, represented 64 DEGs uniquely expressed during the first exposure.

Figure 53 provides the expression patterns over time and distribution of these clusters.

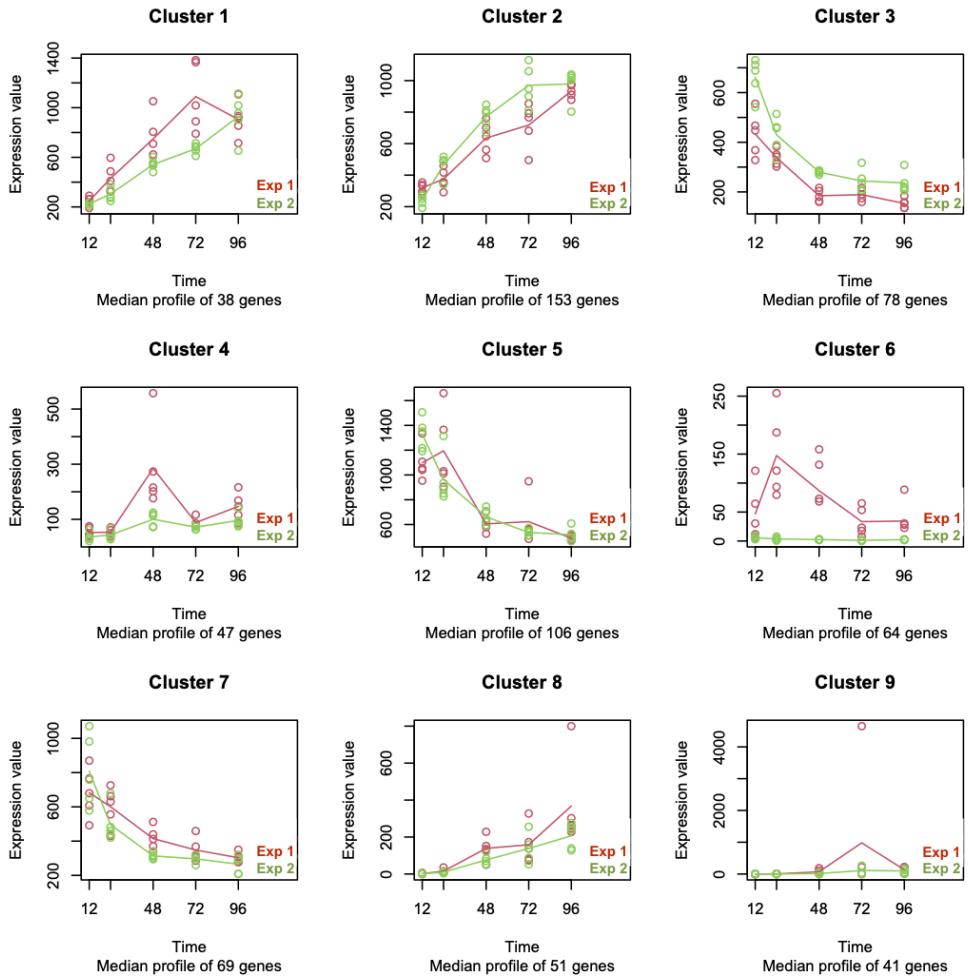

Figure 53. Hierarchical clustering of differentially expressed gene expression patterns in* Ixodes ricinus *salivary glands across the time course. *Abundance values are presented in FPKM, with distinct colored lines representing the first and second host exposures to ticks.*

This analysis showed that a greater number of DEGs in the time course with similar expression patterns can be found in the midgut rather than in salivary glands. This agrees with the dynamics observed in the pairwise analysis, in

which midgut showed a delay in the response to feeding in ticks parasitizing a previously exposed to ticks host. Relatively few DEGs were shared between both tissues, suggesting that the response to the second exposure of the host is tissue specific.

To gain further insight into these changes, the clusters were functionally characterized. In the midgut, 57.6% of the time-course DEGs were overexpressed in early feeding stages of the second exposure, with clusters 1, 3, and 4 formed by DEG enriched in processes such as gene expression, translation, and metabolism (Figure 54A). The PPI network highlighted ribosomal proteins, elongation factors, and metabolic enzymes as key components, as depicted in Figure 55A. For other clusters, no significant interaction networks or enriched GO terms were identified. This suggests that, during the early stages of feeding, the midgut of ticks parasitizing previously exposed hosts experiences stress that activates a general response not observed to the same extent in ticks feeding on naïve hosts. This stress likely engages the expression machinery in ticks feeding on immunized hosts to overcome the challenge and metabolize the ingested blood.

Regarding tick SGs, clusters 1, 2, and 3 showed significant GO term enrichment and PPI networks with a significant number of interactions, as illustrated in Figure 54B and Figure 55B, respectively.

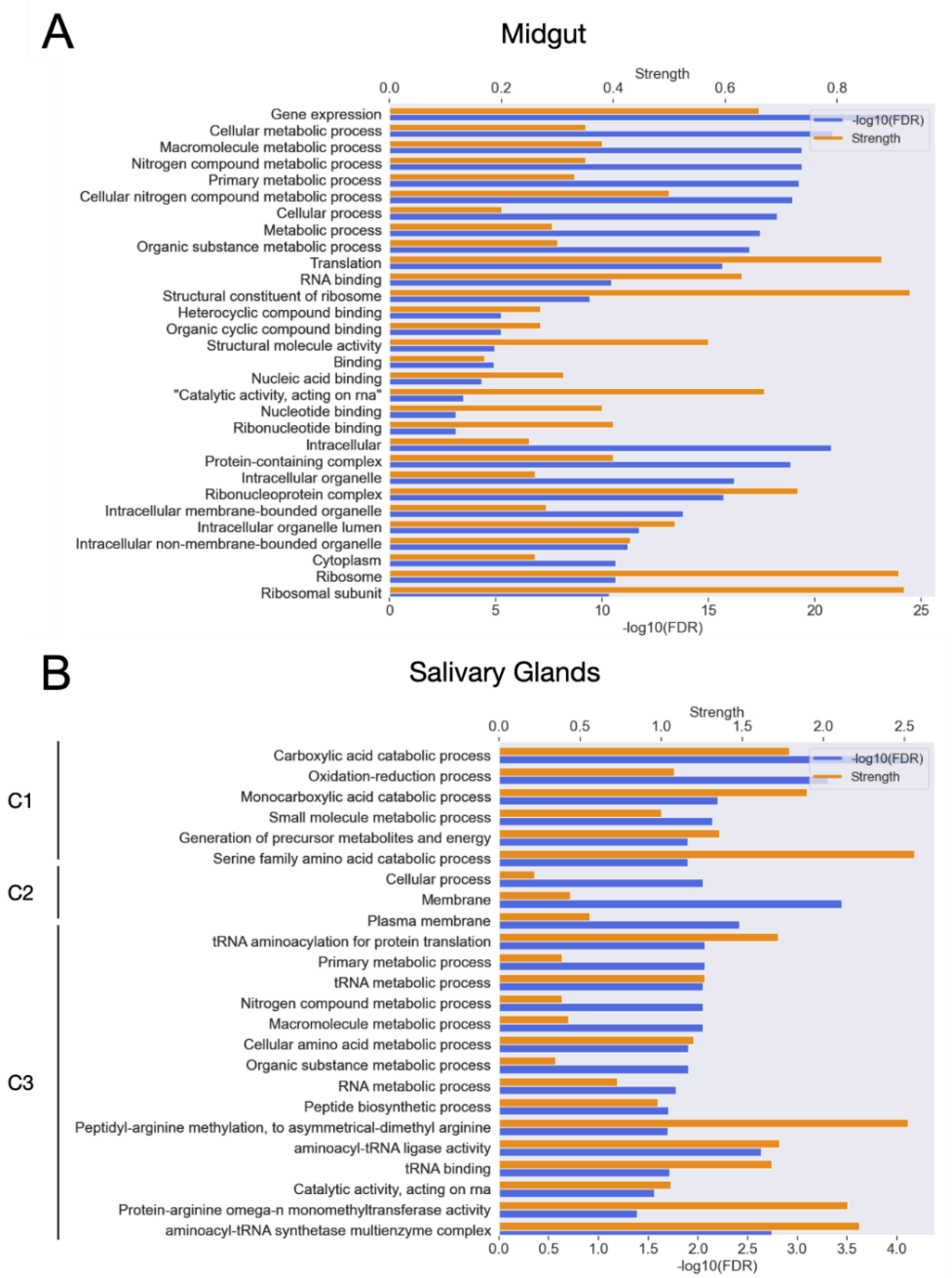

Figure 54. Ontology enrichment analysis for selected clusters of DEGs in midgut and salivary glands. *Significance (-log10(FDR)) and strength (log10(observed/expected)) for each GO term are displayed. A) Analysis for the merged cluster combining clusters 1, 3, and 4 in the midgut. B) Analysis for clusters 1, 2, and 3 in tick SGs.*

Cluster 1 included proteins involved in metabolic processes that were overexpressed in SGs during the first exposure. In this cluster, we found proteins involved in fatty acids oxidation and energy production. This suggests that, for reasons that need to be further analyzed, ticks which parasite naïve hosts obtain energy from fat to feed, which may explain the slower weight gain that we observed in these ticks.

Cluster 2, which contained the highest number of DEGs, comprised overexpressed genes in SGs of ticks parasitizing a host on its second exposure to ticks at late feeding time points. Notably, ticks in the second exposure began to overexpress proteins associated with neuronal activity, circadian rhythm and responses to starvation during feeding. While the exact mechanisms underlying this overexpression remain to be uncovered, starvation responses have been linked to more aggressive behaviors toward infection and feeding on hosts [295]. Other notable proteins were associated with redox homeostasis, ATP synthesis, and N-linked glycosylation, further highlighting the complex molecular adaptations occurring during the second exposure of ticks on the same host. Cluster 3 exhibited expression patterns similar to midgut clusters 1, 3, and 4, involving proteins in translation and metabolism.

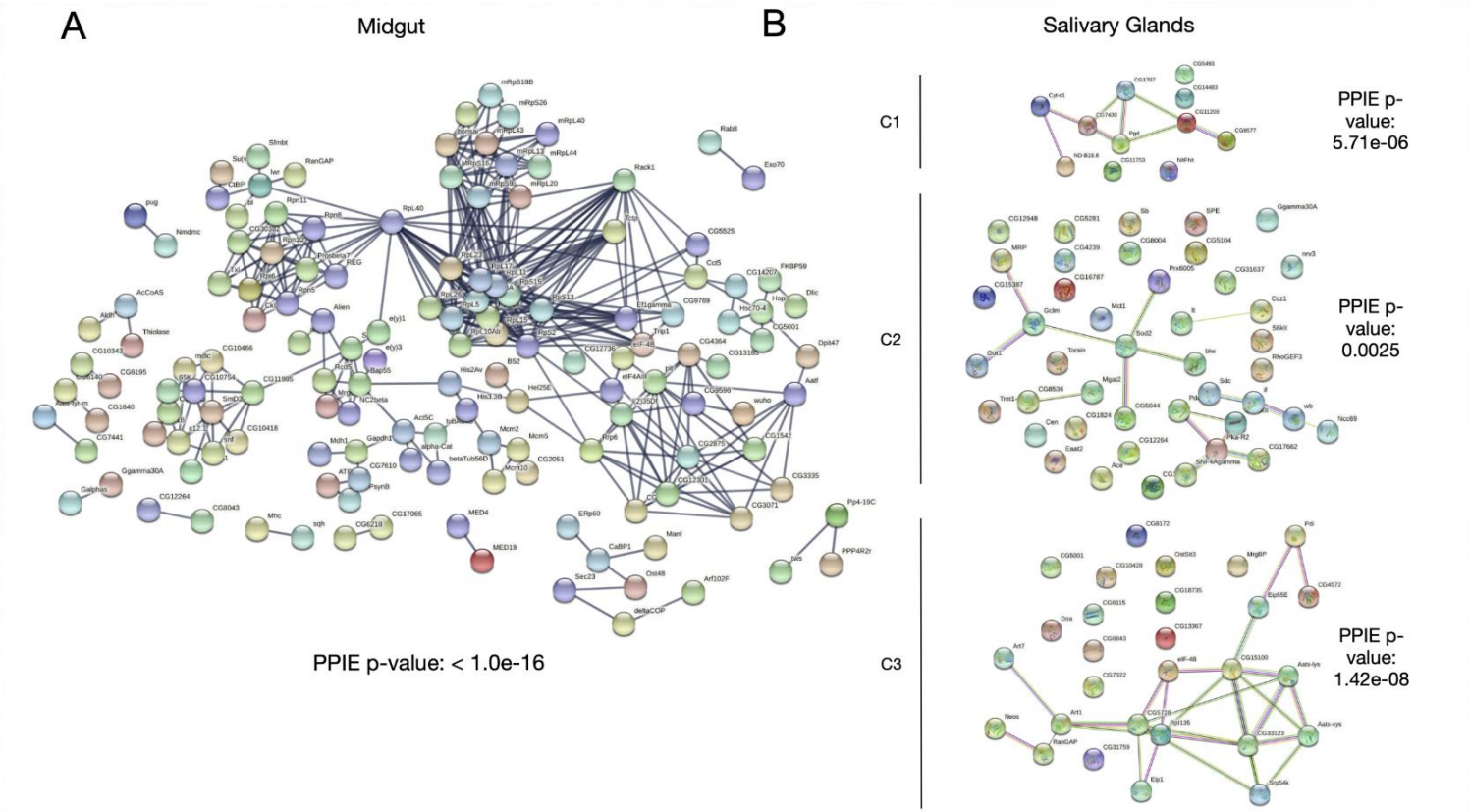

Figure 55. Protein-protein interaction networks for selected DEG clusters in* Ixodes ricinus *midgut and salivary glands. *(E) Network for the merged cluster of 1, 3, and 4 in the midgut. (F) Network for clusters 1, 2, and 3 in the salivary glands. Nodes represent proteins, and edges indicate predicted interactions based on functional and physical association.*

Finally, the top 50 DEGs with the largest cumulative differences between the first and second exposures were functionally characterized (Figure 56). Enrichment analysis revealed differences in hydrolase activity and translation processes in the midgut, while ribosomal proteins and N-linked glycosylation pathways were enriched in the salivary glands. Key proteins identified in the interaction network included dolichyldiphosphooligosaccharide–protein glycotransferase and protein disulfide isomerase, which play critical roles in the tick-host interface and protein folding. Since ribosomal components are essential for synthesizing all proteins and glycosylation ensures their proper function and activity [296,297], the results from the time course analysis suggest that ticks do not rely exclusively on genes specifically tailored to counter immune hosts. Instead, ticks may respond to sensitized hosts by global and more rapidly increasing transcription.

Rather than developing a highly host-specific strategy to counter the diverse repertoire of host countermeasures, ticks appear to employ an accelerated, amplified, but somewhat imperfect transcriptional program as a generalized strategy to feed on sensitized hosts. Consequently, this suggests that the coding portion of the transcriptome is only partially responsible for host-specific evasion.

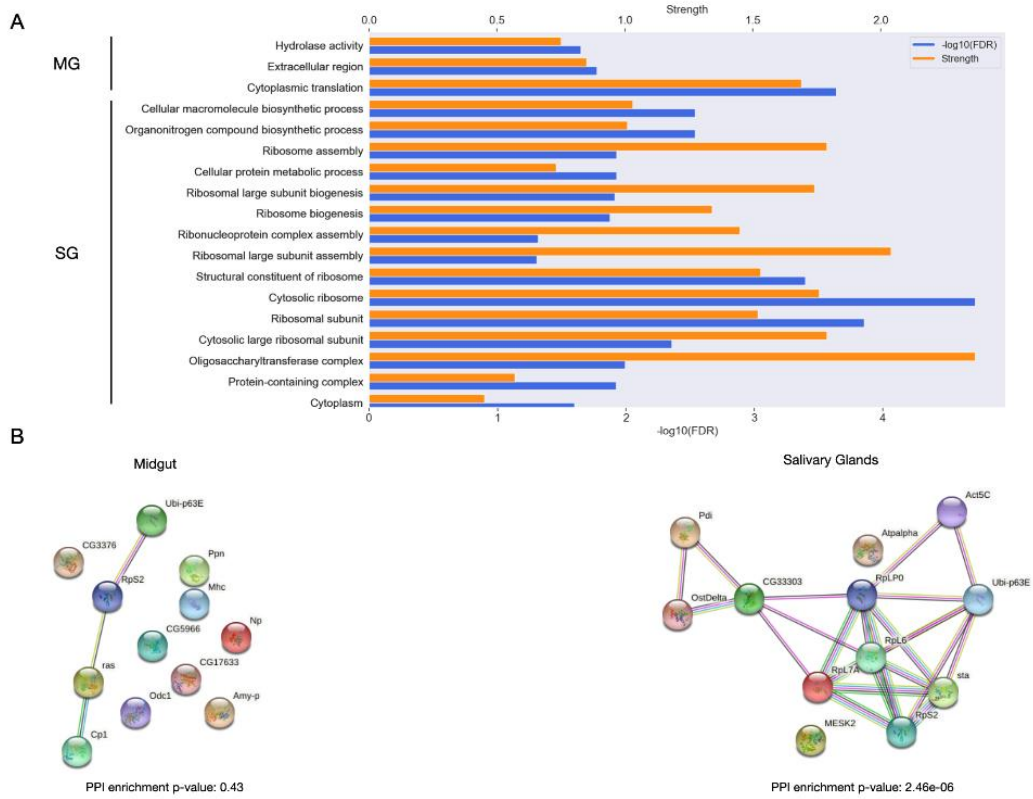

Figure 56. Functional* in silico *analysis of differentially expressed genes exhibiting the most cumulative expression differences between the first and second exposure to the host during feeding. *A) Significantly enriched GO terms for genes with the most pronounced differential expression over the time course between the first and second exposures in both the midgut and salivary glands. Significance and strength, represented by the log10(observed/expected), for each GO term are shown. B) PPI network for the differentially expressed genes with the greatest cumulative effect in* I. ricinus *for both midgut and salivary glands.*

6.5. Database-associated webpage: IxoriDB

To provide comprehensive access to the data on the unique coding transcripts, we developed a 'queryable' and browsable database (https://arn.ugr.es/IxoriDB). Users can easily access and download key features such as sequence, CDS, expression values, homologous proteins, functional annotations (including family, GO terms, and InterPro domains), putative secretion (SignalP), transmembrane domains, classification based on annotations, and tissue specificity (Figure 57). The database allows browsing by transcript name, protein name, or by selecting various options based on the available features. Additionally, the platform enables users to BLAST their own sequences against the transcriptome to identify the best matches and associated features (Figure 58). Finally, the complete transcriptome, CDS sequences, and an Excel file containing all the features of each unique coding region are available for download in the "Downloads" section of the website.

Thus, IxoriDB database provides a user-friendly platform for accessing detailed data on unique coding transcripts of *I. ricinus*. It offers searchable features, including sequence information, functional annotations, expression values, and tissue specificity. BLAST functionality, the downloadable resources, such as the complete transcriptome and associated features, further enhance its utility. Together with the transcriptomic analysis of midgut and salivary glands in *I. ricinus* discussed in this chapter, IxoriDB serves as a valuable tool for advancing the understanding of tick biology and molecular interactions during blood feeding.

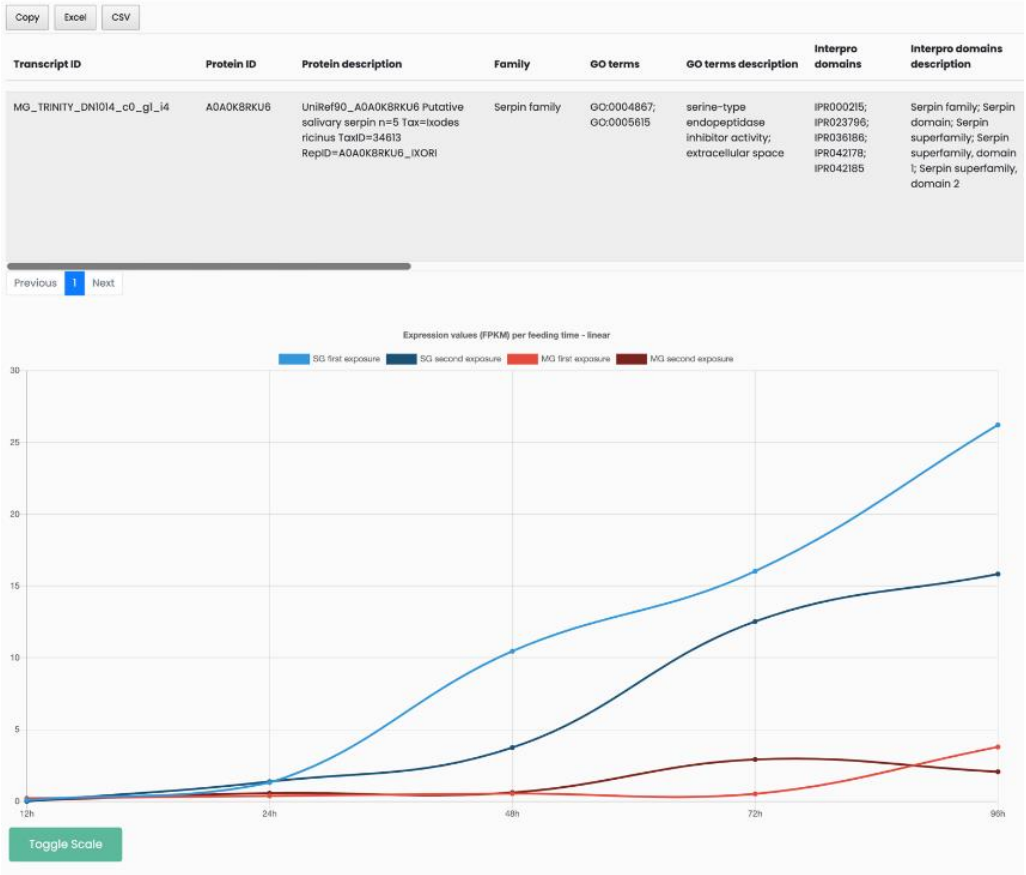

Figure 57. Overview of results from IxoriDB when browsing a protein or unique coding region. *Key features displayed include sequence, CDS, best-matching known protein, functional annotations (family, GO terms, InterPro domains), putative secretion (SignalP), transmembrane domains, classification, and tissue specificity. Expression data across feeding time points for both midgut and salivary glands can be visualized, with an adjustable logarithmic scale*

Figure 58. Results from aligning user-provided sequences to the IxoriDB transcriptome. *This query results in alignment details and the best matching representatives for each input sequence.*

Chapter 7.

Bioinformatic insights into the role of *Ixodes ricinus* long non-coding RNAs in host microRNA regulation

In this chapter, we will explore another intriguing mechanism by which *I. ricinus* may modulate the host's response to tick infestation. While this thesis has primarily focused on how *I. ricinus* miRNAs assist the tick in evading host defense mechanisms, this chapter will shift attention to how *I. ricinus* may inhibit host miRNAs using long non-coding RNAs (lncRNAs). These lncRNAs can compete with the host's miRNA targets, potentially diminishing the efficacy of the host's miRNAs and defense response.

Even though the molecular mechanisms and physiological impacts of lncRNAs are an intense focus of applied human and animal research [172], there is currently very limited literature on the identification and functional analysis of lncRNAs in tick–host interactions. This gap in knowledge significantly hinders our understanding of the role of lncRNAs in ectoparasite–host dynamics. To address this, we *in silico* investigated the potential regulatory roles of lncRNAs in *I. ricinus*–host interactions by analyzing their differential expression in the midguts and salivary glands of unfed and fed *I. ricinus* ticks.

7.1. Summary of transcriptome assembly and long non-coding RNA isolation

One of the main problems when working with lncRNAs is the poor capability to bioinformatically validate assembled lncRNA in species with rather unknown or with poor reference genome, which was the case for *I. ricinus* until high quality genomes for this tick were became public available during the last year [176]. With coding RNA, someone can gather evidence by analyzing the existence of coding regions, their domains, other similar proteins from other organisms found in the database, etc. This is not possible with lncRNAs which also tend to have less overall base conservation than coding RNAs. For this reason, for the analysis of lncRNA, we resorted on three sources to isolate lncRNAs and to generate a consensus set of lncRNAs for the specific tick species. Thus, using transcriptome assembly and lncRNA isolation, we identified a total of 14,079 lncRNAs from the midgut and salivary gland transcriptome (MG-SG lncRNAs, *Chapter 1*), 677,278 from a salivary gland-only transcriptome (SG lncRNAs) [298], and 358,278 from whole-body samples (WB lncRNAs) [185]. The relatively lower number of lncRNAs identified in the MG-SG dataset reflects the additional and more stringent steps applied during its transcriptome assembly.

To create the consensus set, we clustered the three lncRNA datasets. A consensus lncRNA was defined as the longest transcript from a given cluster that could be detected in the MG-SG dataset (the most reliable set due to its stringent selection process) and at least one of the other two transcriptomes. This approach yielded a final set of 3,118 consensus lncRNAs.

Similarly, for comparison purposes, we identified 12,158 coding RNA sequences from the MG-SG transcriptome (MG-SG coding RNAs), 55,825 from the SG transcriptome (SG coding RNAs), and 47,472 from the WB transcriptome (WB

coding RNAs). Applying the same clustering protocol used for lncRNAs, we generated a final consensus set of 5,659 coding RNAs.

7.2. Expression patterns of long non-coding RNAs in the midgut and salivary glands under different tick feeding conditions

Initially, four *I. ricinus* lncRNA datasets were analyzed: consensus lncRNAs, MG-SG lncRNAs, SG lncRNAs, and WB lncRNAs. To evaluate the quality of these datasets, we assessed and visualized their length distributions, which are shown in Figure 59. LncRNAs obtained from the individual projects displayed a strikingly different distribution compared to the consensus sequences. In the individual sets, short lncRNAs were clearly overrepresented, with a peak around 250 nucleotides, while the consensus dataset exhibited a more homogeneous distribution. This suggests that the consensus approach successfully recovered longer sequences, particularly those that were adequately represented in only one of the individual datasets. Based on these findings, this study was focused on the consensus set of lncRNAs.

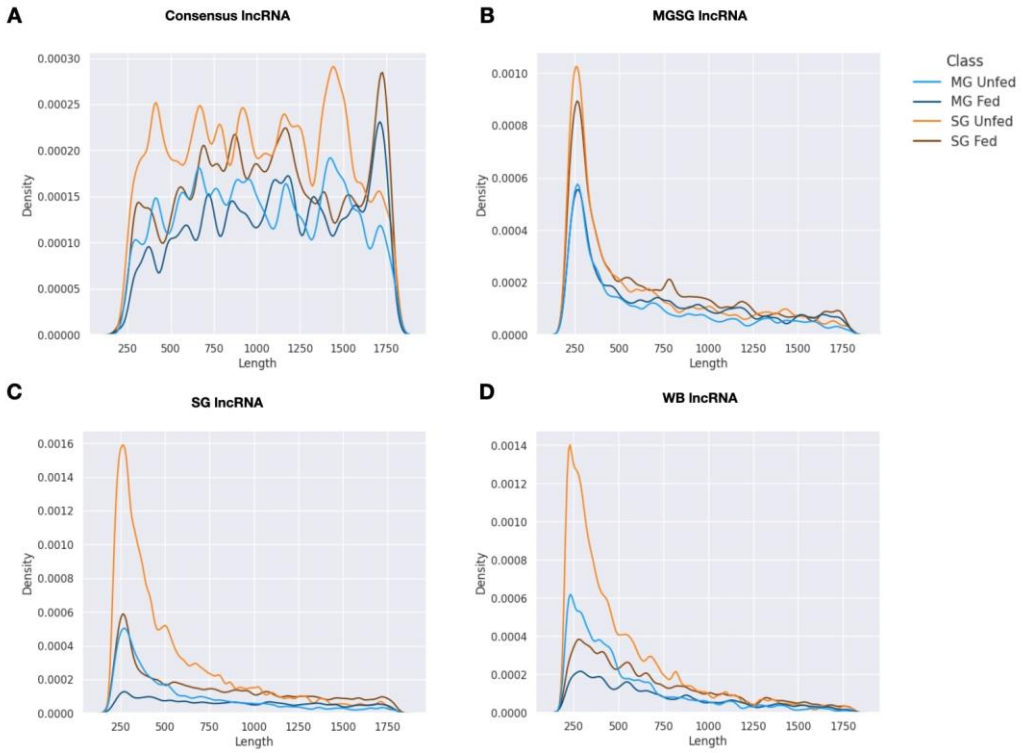

***Figure 59. Length distribution of differentially expressed long non-coding RNAs in the midgut and salivary glands of unfed and fed* Ixodes ricinus.** *A) Length distribution of significantly differentially expressed consensus lncRNAs, (B) MG-SG lncRNAs, (C) SG lncRNAs, and (D) WB lncRNAs, upregulated in the midgut and salivary glands of unfed and fed ticks. Different lines represent lncRNAs that are either upregulated or downregulated upon feeding in the midgut (MG fed, MG unfed) and salivary glands (SG fed, SG unfed).*

As a preliminary step, we characterized the overall expression levels of lncRNAs relative to coding sequences. Figure 60 displays the mean normalized expression values for lncRNAs and coding sequences across different tissues and feeding states. The mean expression value of consensus lncRNAs was consistent across conditions, representing approximately 30% of total expression. Interestingly, some samples, particularly those from unfed or early feeding ticks, exhibited significantly increased lncRNA expression levels.

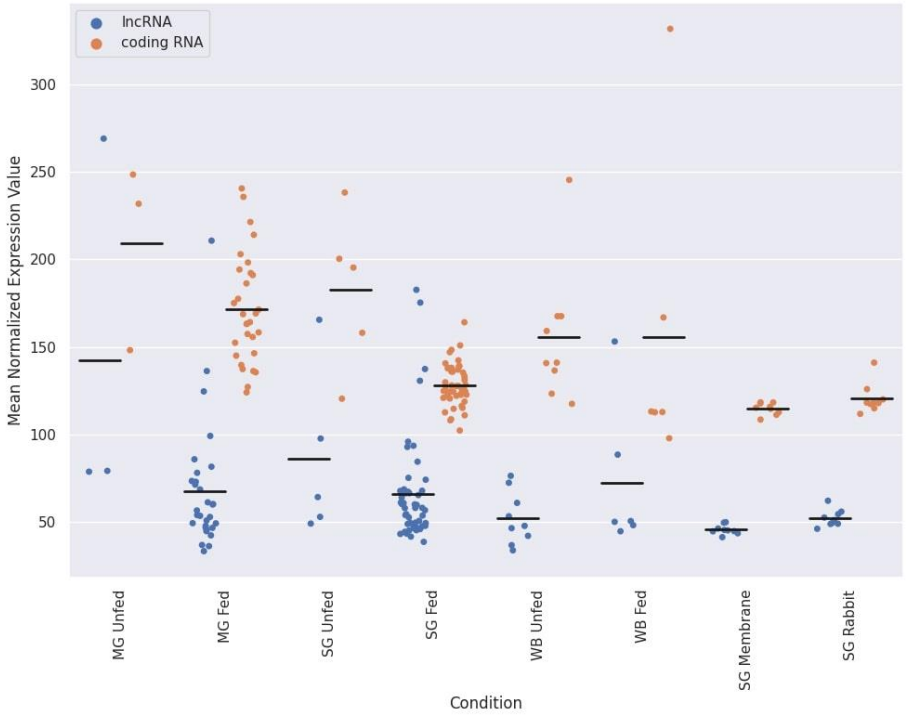

Figure 60. Expression analysis of long non-coding RNAs and coding RNAs across different sets and conditions. *The expression levels of lncRNAs and coding RNAs were analyzed under various feeding treatments: MG unfed and MG fed correspond to samples from the midgut of ticks that were either unfed or in the slow feeding phase, respectively; SG unfed and SG fed represent samples from the salivary glands of ticks in these same conditions. WB unfed and WB fed denote whole-body samples from unfed ticks or those in the slow feeding phase, respectively. Lastly, SG Membrane and SG Rabbits indicate salivary gland samples from ticks fed on an artificial membrane or rabbits, respectively. Mean expression values for each condition are highlighted with a black line.*

To further investigate the role of lncRNAs in ticks during feeding and non-feeding states, we analyzed the differential expression of lncRNAs and coding RNAs between unfed and fed ticks in both midgut and salivary glands, using the samples depicted in *Chapter 1*. In the midgut, we identified 1,110 DE lncRNAs (35.6% of the total consensus lncRNAs) and 2,727 DE coding RNAs (48.2% of the total consensus coding RNAs). In the salivary glands, 1,311 lncRNAs (42% of the

consensus lncRNAs) and 2,965 coding RNAs (52.4% of the consensus coding RNAs) were differentially expressed between feeding states (Figure 61).

The DE lncRNAs and coding RNAs were categorized into two groups: (1) overexpressed when *I. ricinus* was not feeding and (2) overexpressed when *I. ricinus* was actively feeding. In both tissues, the majority of DE lncRNAs and DE coding RNAs were overexpressed during active feeding (Figure 61B-C). Specifically, in the midgut, 74.6% of lncRNAs and 63% of coding RNAs were overexpressed in fed ticks. Similarly, in the salivary glands, 59.9% of lncRNAs and 68.4% of coding RNAs were overexpressed during feeding.

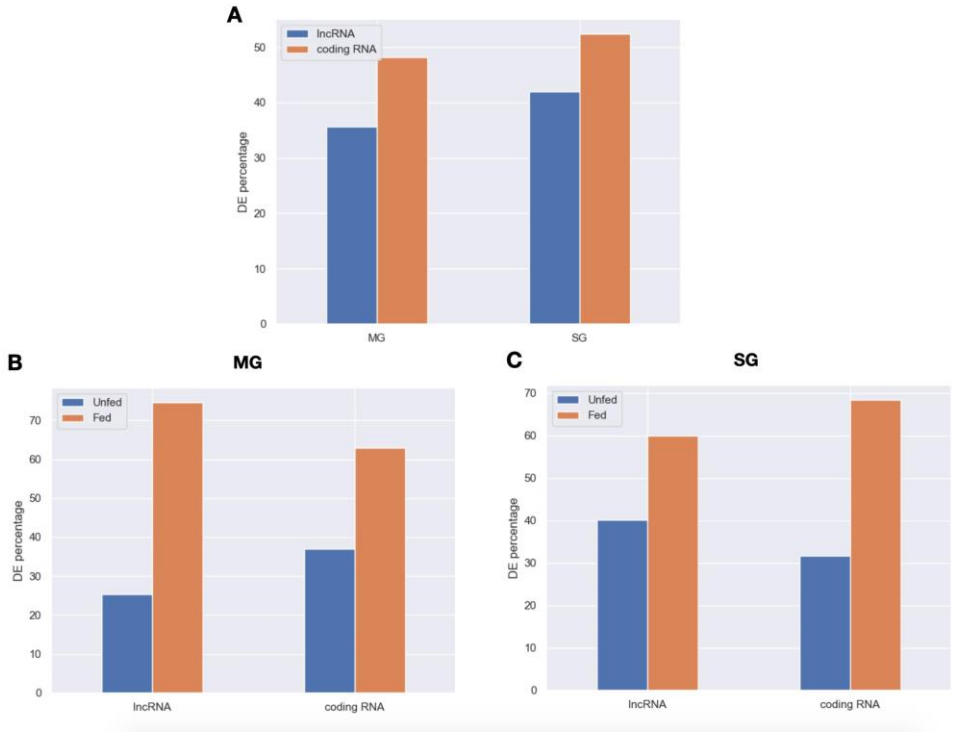

***Figure 61. Statistics on differentially expressed long non-coding RNAs and coding RNAs in the midgut and salivary glands of* Ixodes ricinus.** *(A) Percentage of differentially expressed lncRNAs and coding RNAs in the midgut and salivary glands. (B) Distribution of differentially expressed (DE) lncRNAs and coding RNAs across feeding treatments in the midgut. (C) Distribution of DE lncRNAs and coding RNAs across feeding treatments in the salivary glands.*

The results showed that although the percentage of consensus lncRNAs identified as differentially expressed (DE) was lower than that of coding RNAs in both the midgut and salivary glands, most DE lncRNAs were upregulated in fed ticks, particularly in the midgut. This finding suggests that the predicted consensus lncRNAs play a role in the feeding process of *I. ricinus* in both the midgut and salivary glands.

7.3. Analysis of the reproducibility of the differential expression of long non-coding RNAs

Reproducibility is a key concept for increasing the reliability of scientific results. To evaluate this, we utilized two independent studies with salivary gland samples from ticks fed on rabbits for 24 and 72 hours, identifying differentially expressed lncRNAs and coding sequences in both datasets.

Our analysis revealed that the percentage of differentially expressed sequences shared between the two studies was comparable for lncRNAs and coding RNAs, at 23.97% and 21.16%, respectively (Figure 62A-B). A detailed breakdown of these results into upregulated and downregulated sequences at 72 hours compared to 24 hours is shown in Figure 62C–F. Interestingly, the overlap between the two studies was notably higher for upregulated sequences (approximately 27%, depicted in Figure 62E, F) than for downregulated sequences (8% for lncRNAs) (Figure 62C-D).

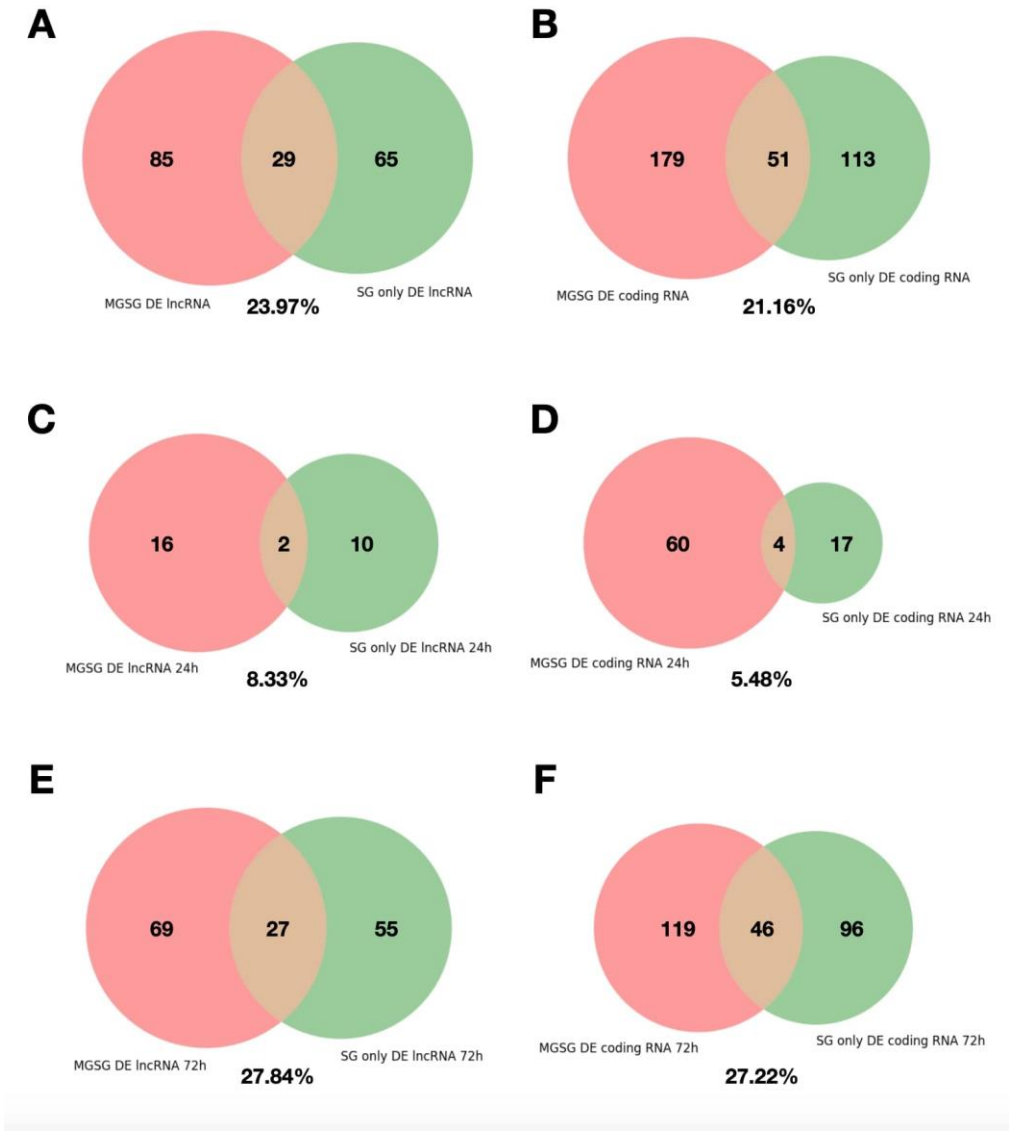

Figure 62. Reproducibility analysis of differential expression of consensus long non-coding RNAs and coding RNAs between MGSG and SG only studies in salivary glands. *Venn diagrams illustrate the overlap between: (A) Differentially expressed (DE) lncRNAs in MGSG samples and DE lncRNAs in SG-only samples, (B) DE coding RNAs in MGSG samples and DE coding RNAs in SG-only samples, (C) DE lncRNAs downregulated at 72 hours of feeding in MGSG and SG-only samples, (D) DE coding RNAs downregulated at 72 hours of feeding in MGSG and SG-only samples, (E) lncRNAs upregulated at 72 hours of feeding in MGSG and SG-only samples, and (F) coding RNAs upregulated at 72 hours of feeding in MGSG and SG-only samples.*

7.4. Prediction of Sponge candidates and functional analysis

The main focus of this chapter is to analyze if tick lncRNAs found in the host cytoplasm (for example when transported in the tick-host interface enclosed in exosomes and then endocytosed and released in the host cytoplasm) can act as "miRNA sponges", competing with host mRNA molecules for miRNA binding, which may result in the loss of miRNA function. To investigate whether tick lncRNAs play a role in the feeding process, we explored three sponge models: (i) high-frequency of target sequences, (ii) high-density of target sequences and (iii) recurrent host miRNA combinations. The first two models are based on the probability of a lncRNA being targeted by miRNAs. If a lncRNA has a high number or high density of target sequences, it is more likely that a miRNA will bind to it. The third approach is based on the hypothesis that tick lncRNAs may act cooperatively by binding the same miRNAs. If the specific miRNAs play important roles in the host's homeostatic response, their binding to tick lncRNAs would result in augmenting the probability of successful blood feeding.

First, we performed target prediction analysis for all consensus lncRNAs. As a negative control, we conducted target prediction for a sequence-randomized set of consensus lncRNAs. Most consensus lncRNAs in this set contain more targets than their randomized counterparts for a specific miRNA. Notably, we observed a median of 2.48 targets per kilobase for a specific miRNA in the consensus set of lncRNAs, with a standard deviation of 1.36 targets per kilobase and the maximum number of targets per kilobase for a specific miRNA being 10.34. In contrast, the randomized set of lncRNAs had a median of 1.93 targets per kilobase for a specific miRNA, a standard deviation of 0.63 targets per

kilobase and 5.22 as the maximum number of targets per kilobase for a specific miRNA.

Next, we identified the subset of lncRNAs with the highest likelihood of acting as sponge candidates by applying three different approaches: (i) identifying the lncRNAs with the highest number of targets for a given miRNA, (ii) identifying lncRNAs with the highest density of targets per kilobase, and (iii) analyzing combinations of miRNA target sites. For all approaches, negative controls were generated using shuffled sequences. Significant miRNA combinations were identified using the Apriori algorithm, resulting in sets of miRNAs that consistently target specific lncRNAs.

To explore the function of sponge candidates, we selected the top lncRNAs from each analysis: the consensus lncRNA with the greatest number of targets for a given miRNA, the lncRNA with the highest target density per kilobase, and three groups of consensus lncRNAs (with no overlap) significantly targeted by specific host miRNA combinations. A heatmap was constructed to analyze the expression variability of potential sponge candidates in unfed and fed midguts and salivary glands. Notably, the expression of many DE lncRNAs was significantly higher in the salivary glands of fed ticks compared to the midgut (Figure 63).

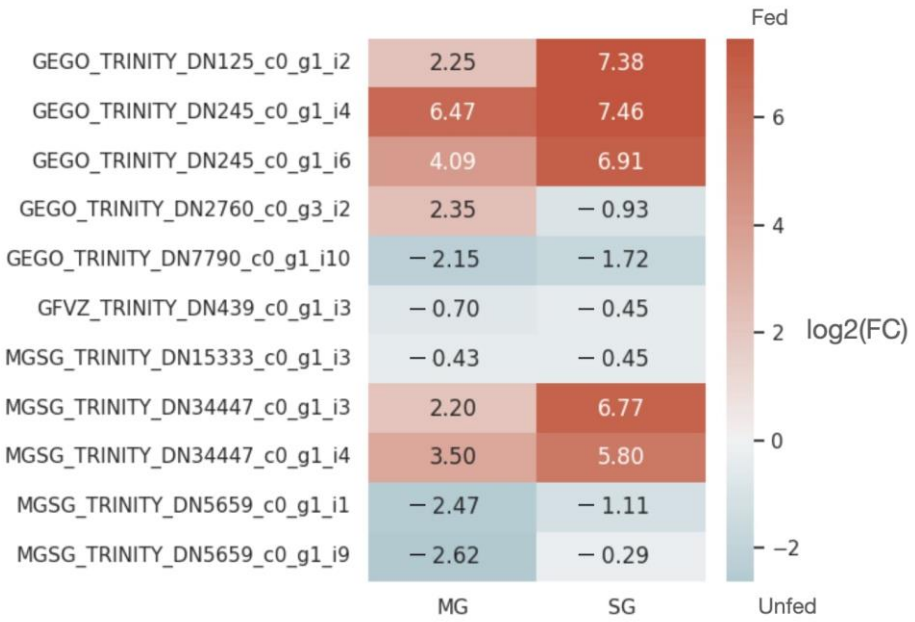

***Figure 63. Differential expression of microRNA sponge candidates in the midgut and salivary glands of unfed and fed* Ixodes ricinus.** *The heatmap illustrates the log2 fold change in expression between unfed and fed* I. ricinus *for each sponge candidate in the midgut and salivary glands. A log2 fold change greater than 0 indicates that the sponge candidate is upregulated in fed ticks, while a log2 fold change less than 0 indicates upregulation in unfed ticks.*

To further understand the potential function of these sponge candidates, we characterized human miRNAs or human miRNA combinations that may be targeted by tick lncRNAs. These host miRNAs or host miRNA combinations were found to regulate critical pathways mediating defense mechanisms of the host against tick feeding. Additionally, miRNAs or miRNA combinations targeted a variable number of genes within these pathways, suggesting that tick lncRNAs may play a role in tick feeding and ectoparasite–host interactions.

We observed that the targeted host miRNAs significantly impacted the hemostasis-associated pathway named as glycosaminoglycan biosynthesis–heparan sulfate/heparin. Heparin is essential for catalyzing antithrombin III, a

plasma enzyme that enhances its activity in vertebrates. Antithrombin III inactivates several activated serine proteases of the coagulation cascade, most notably thrombin and activated factor X, which gives it an important role in wound healing [299].

Additionally, several immune pathways were influenced by these miRNAs. For example, the TGF-β signaling pathway, a potent cytokine regulator, exerts diverse effects on hematopoietic cells. TGF-β plays a critical role in maintaining immune tolerance by regulating lymphocyte proliferation, differentiation, and survival [300,301]. Another immune signaling pathway potentially regulated by tick sponge candidates is the WNT signaling pathway. WNT ligands bind to Frizzled and lipoprotein receptor-related proteins, triggering the canonical WNT signaling cascade. This process inactivates the destruction complex, stabilizes β-catenin, promotes its nuclear translocation, and subsequently activates T-cell factor/lymphoid enhancer factor-dependent transcription [302,303].

Thus, ticks are likely to deliver lncRNAs into the host body (via saliva or salivary EVs), which, in turn, may act as sponges for host miRNAs or host miRNA combinations critical to host hemostasis and innate and adaptive immune responses, thereby facilitating tick feeding on the host.

7.5. Target prediction and KEGG analysis of the consensus differentially expressed long non-coding RNAs

To investigate the potential roles of lncRNAs in tick feeding, we analyzed the putative functions of host miRNAs that tick lncRNAs target. We performed a target prediction analysis with human microRNAs from MirGeneDB [182] and DE lncRNA sequences serving as their sponges. We selected and functionally

analyzed miRNAs with the highest overall target ratio. The results revealed that hsa-miR-5683, hsa-miR-29b-3p, and hsa-miR-154-3p exhibited the highest target ratios in feeding-regulated lncRNAs. According to MirPath [242], the target genes of these three miRNAs are involved in focal adhesion and the PI3K-Akt signaling pathway. This is really interesting since focal adhesion has been related to epithelial motility and mucosal healing of gut due to its involvement in cell motility, proliferation, and survival [304]. Additionally, PI3K-Akt signaling pathway has been reported to control the proliferation of gut cells [305]. Furthermore, specific human miRNAs target genes with roles in ECM-receptor interaction, fatty acid metabolism, and biosynthesis, among other processes.

When looking specifically at the SGs, the miRNAs with the highest target ratios for lncRNAs upregulated in SGs from fed ticks were hsa-miR-4664-3p, hsa-miR-431-5p, and hsa-miR-28-3p. KEGG pathway enrichment analysis for the genes targeted by these miRNAs revealed pathways that their deregulation may be beneficial for the tick. We identified interesting KEGG pathways as Hippo signaling pathway, which has been reported to maintain the immune homeostasis in immune cells [306]; adherens junction, which is involved in the innate immune response to endotoxins [307]; and biosynthesis of mucin type O-Glycans, which are involved in the inflammatory response [308]. Here, we found that these miRNAs are involved in the immune response of the host, so disrupting their function may be beneficial for the tick interaction with the vertebrate host and facilitate pathogen transmission. Thus, our results may establish future lines of research in the field of tick–host interactions aiming to address the detrimental effect of ticks in veterinary and human health.

7.6. Analysis of the presence of microRNA sponge candidates in the novel *Ixodes ricinus* reference genome

A crucial step in assessing the role of *I. ricinus* lncRNAs as miRNA sponges was their presence verification in the newly assembled reference genome of this tick. Our results strongly support their authenticity, as all sponge candidates were detected with an identity score, representing the ratio of matching bases, above 0.9 and alignment coverage exceeding 90% of their sequence. The specific results of the alignment with the reference genome are provided in Table 5.

These findings confirm the existence of these lncRNAs in the tick genome, reinforcing the reliability of their annotation and providing a solid foundation for further analyses of their role in the tick-host interface. The high sequence identity and coverage suggest that these lncRNAs are bona fide genomic elements, increasing confidence in their functional relevance as miRNA sponges in *I. ricinus* biology.

***Table 5. Alignment of microRNA sponge candidates with the novel genome of* Ixodes ricinus.** *The table includes the miRNA sponge candidate ID, the corresponding genome scaffold, the identity and percentage of miRNA sponge sequence covered by the alignment, the number of exons and the start and end positions of the alignment within both the sponge and the genome.*

miRNA sponge candidate	Scaffold	Identity	Coverage	Exons	QStart	QEnd	GStart	GEnd
GEGO_TRINITY_DN125_c0_g1_i2	3	0.93	100.00	3	0	1206	115845458	115991768
GEGO_TRINITY_DN245_c0_g1_i4	6	0.93	99.26	3	1	1757	92550934	167247118
GEGO_TRINITY_DN245_c0_g1_i6	6	0.94	99.26	3	1	1757	92550934	167247118
GEGO_TRINITY_DN2760_c0_g3_i2	13	0.97	99.66	1	0	289	49325864	49326152
GEGO_TRINITY_DN7790_c0_g1_i10	4	0.92	97.34	1	1	1027	73435841	73497494
GFVZ_TRINITY_DN439_c0_g1_i3	8	1.00	99.93	1	1	1477	2994973	2996449
MGSG_TRINITY_DN15333_c0_g1_i3	4	0.98	99.78	1	3	1390	74663672	74665038
MGSG_TRINITY_DN34447_c0_g1_i3	3	0.96	89.81	2	0	596	115845458	115964063
MGSG_TRINITY_DN34447_c0_g1_i4	3	0.92	91.10	2	0	693	115845458	115964063
MGSG_TRINITY_DN5659_c0_g1_i1	6	0.99	95.04	1	0	1285	91508892	91516537
MGSG_TRINITY_DN5659_c0_g1_i9	6	0.96	95.62	1	0	1461	91508689	91516537

7.7. Analysis of long non-coding RNAs from extracellular vesicles in the saliva of *Ixodes ricinus*

Up to this point, our investigation about lncRNAs focused on the salivary glands and midgut of *I. ricinus* and bioinformatic predictions regarding how these may act as miRNA sponges to disrupt key pathways involved in host response against tick feeding. Nevertheless, based on the promising aforementioned results, we decided to further investigate the existence and function of lncRNAs in the saliva of *I. ricinus*. To achieve this, we obtained and analyzed RNA samples from extracellular vesicles (EVs) and saliva of *I. ricinus*.

7.7.1. Sequencing data: Read preprocessing and analysis

A process of differential centrifugation and EV isolation allowed us to classify and separate from pure tick saliva the four phases of EVs, containing large EVs, medium EVs, small EVs and saliva with the smallest EVs, as detailed in the Section 5.8.1. Additionally, in parallel to Chapter 6, saliva samples from *I. ricinus* parasitizing a naïve host and samples from *I. ricinus* feeding on the same host for a second time were obtained.

We sequenced RNAs from these samples and obtained a total of 1,437,353,460 paired-end reads. After trimming and quality filtering, 98,26% of the reads were of good quality. Thus, 1,412,365,266 reads remained for further analyses. The distribution of reads by sample is shown in Figure 64.

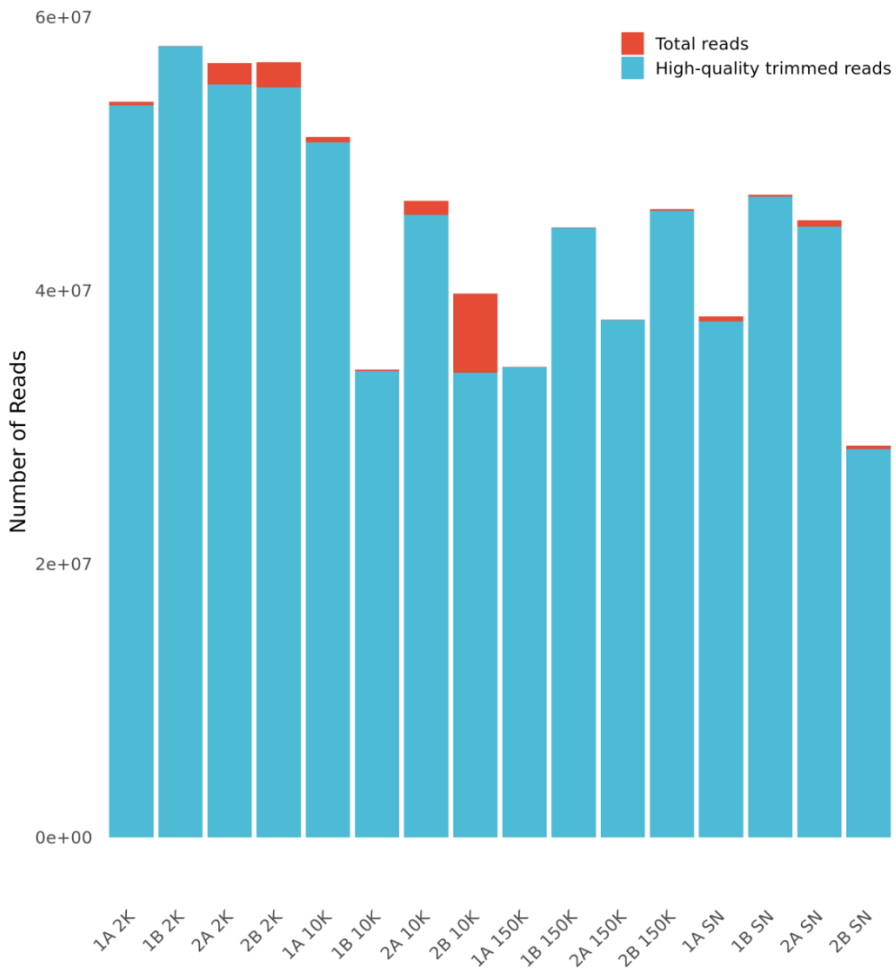

Figure 64. Distribution of total and high-quality trimmed reads in RNA-seq data from* Ixodes ricinus *extracellular-vesicle samples. *Total and high-quality trimmed reads are represented by different colors. The Y-axis shows the number of reads and X-axis the different samples analyzed in this study. The sample IDs are displayed in the figure. The first number in these IDs indicates whether the host is being exposed to ticks for the first or second time during blood feeding. The subsequent letter represents the biological replicate, followed by the EV fraction.*

Next, the objective was to keep assessing the quality of the data and to get a first glance at the expression patterns of coding RNAs and non-coding RNAs in the different samples. Thus, we obtained the abundance of the different transcripts, either coding RNAs or non-coding RNAs, of the transcriptome assembled in

Chapter 6. To keep consistent with the analyses made before, and in order to eliminate spurious and non-reliable RNA in EVs, an abundance filter was applied. Only transcripts with a minimum of 1 FPKM in all the replicates of one condition remained for the rest of the analyses. This filter left us with 5738 transcripts out of 25011. Then, a PCA analysis, a correlation analysis and a hierarchical clustering using ward method were made.

The PCA shows that both depicted components indicate that the small EVs have the most diversified expression patterns, as they are clearly separated from the other samples. Additionally, samples coming from EVs of the same size either from ticks feeding on a host for the first time or from ticks feeding on a host for a second time tend to match (Figure 65). In the correlation matrix, provided in Figure 66, it can be observed that the level of correlation between samples of different EVs fractions tend to be quite high (>0.9). Nevertheless, as pointed out in the PCA, the small EVs and large EVs produced in ticks parasitizing an already exposed host, are those with more differences to other samples. Even so, no clear clustering between samples coming from ticks parasitizing a naïve host and ticks parasitizing a host in its second exposure to ticks could be observed in hierarchical clustering analysis.

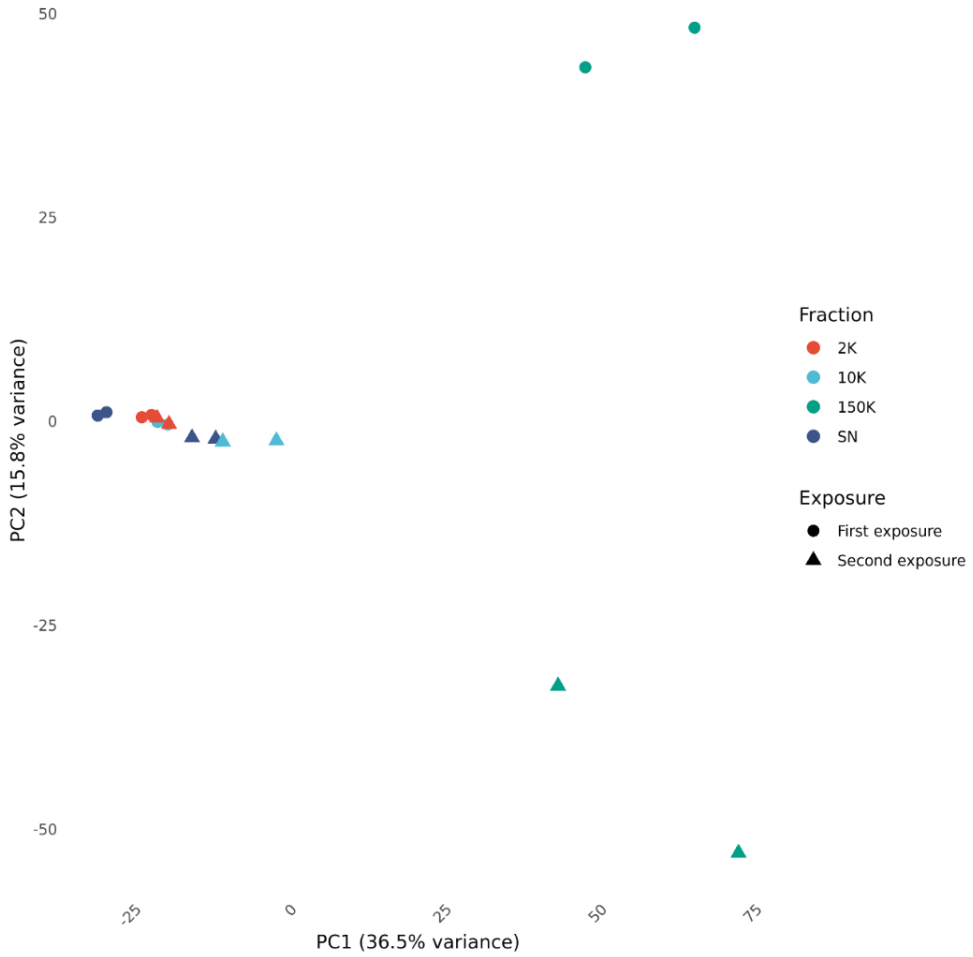

***Figure 65. Principal component analysis of transcript expression variance in RNA-seq data from extracellular vesicles of* Ixodes ricinus.** *Both coding and non-coding RNA abundances were used for this analysis. Colors represent different EV fractions, while shapes distinguish between samples from ticks parasitizing a naïve host and those from ticks parasitizing a host previously exposed to ticks.*

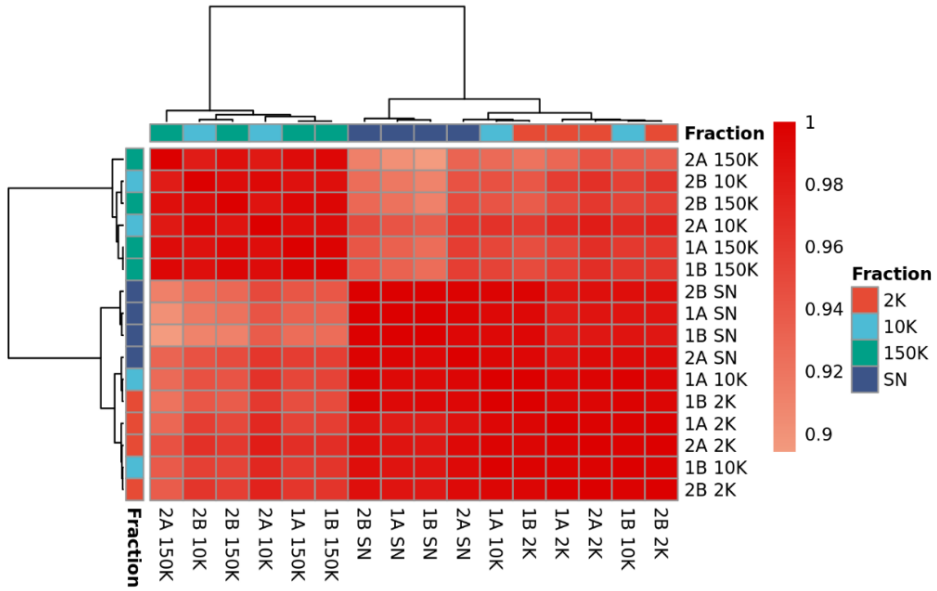

***Figure 66. Correlation and hierarchical clustering of transcript expression patterns in extracellular vesicles of* Ixodes ricinus.** *Different fractions are represented by distinct colors in the margins of the correlation matrix. The gradient of the color (red) in the inside the matrix indicates the correlation level between the expression pattern of a pair of samples. The sample IDs are displayed in the figure. The first number in these IDs indicates whether the host is being exposed to ticks for the first or second time during blood feeding. The subsequent letter represents the biological replicate, followed by the EV fraction.*

7.7.2. The long non-coding RNA content in saliva and extracellular vesicles

One of the most straightforward comparisons with this dataset is the proportion of ncRNAs and coding RNAs in EVs and saliva compared to what is typically expected in internal tick cells. Leveraging the extensive salivary gland data analyzed in Chapter 6, we calculated the percentage of ncRNAs in these samples and compared it to the proportions obtained in this study.

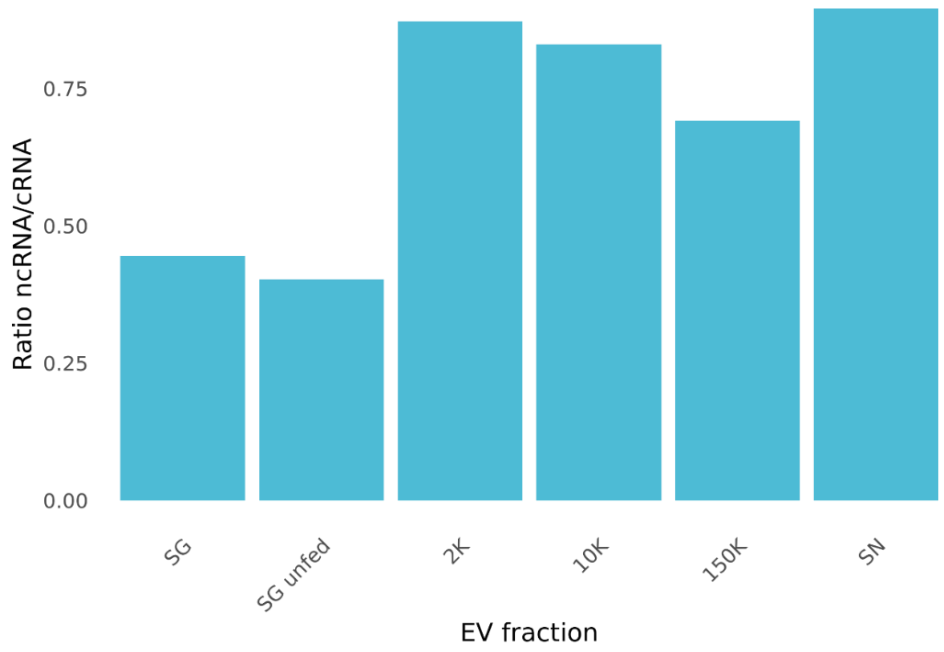

***Figure 67. Ratio of non-coding RNAs to coding RNAs in extracellular-vesicle fractions and salivary glands of* Ixodes ricinus.**

The proportion of ncRNA and coding RNA is displayed in Figure 67. Notably, we observed a crucial feature of the EVs: they contain an exceptionally high proportion of ncRNA compared to salivary glands, with the fraction of EVs precipitated at 2,000 g and the supernatant having more than 85% of reads assigned to ncRNA. This finding suggests the existence of a directed mechanism or regulatory process that selectively delivers ncRNA into EVs. Furthermore, it implies that this ncRNA may serve a specific purpose for the tick, potentially facilitating blood feeding.

Previously, we demonstrated that lncRNAs have the potential to act as sponges to modulate host miRNAs, thereby altering critical pathways involved in host defense, such as wound healing and immune responses. The directed delivery

of lncRNAs into EVs to transfer them to the host could be advantageous for the tick, aligning with what we may be observing in this study. Additionally, and even though we previously selected certain candidates based on their potential to inhibit host miRNAs, this data and analysis will offer us, and the research community, the opportunity to identify novel lncRNAs that may act as miRNA sponges and modulate the tick-host interface, providing a valuable new starting point for further exploration in this field.

7.7.3. Extracellular vesicle dynamics of potential long non-coding RNA sponges

In this thesis, we identified several lncRNAs from salivary glands with the potential to act as sponges, targeting crucial regions of host miRNAs. To further investigate their role, we conducted an expression dynamics analysis to determine the abundance of these lncRNAs in the saliva of *I. ricinus* (Figure 68).

Contrary to expectations, most of the miRNA sponge candidates exhibited a sporadic or null presence in the EVs of *I. ricinus*. However, despite their sporadic occurrence, 6 out of the 11 candidates were detected in the saliva of *I. ricinus*, encapsulated within EVs. Notably, the candidate GFVZ_TRINITY_DN439_c0_g1_i3 stands out, as it was consistently present in all samples of small EVs precipitated at 150,000 g. This fraction, enriched in small EVs such as exosomes, is particularly intriguing regarding the potential functionality of this miRNA sponge candidate. A total of 16 mature miRNAs from *H. sapiens* have targets in this miRNA sponge candidate: hsa-miR-203b-3p, hsa-miR-10b-5p, hsa-miR-101-3p, hsa-miR-103a-3p, hsa-miR-134-5p, hsa-miR-154-3p, hsa-miR-194-5p, hsa-miR-224-5p, hsa-miR-30a-5p, hsa-miR-3136-5p, hsa-miR-320c, hsa-miR-302b-5p, hsa-miR-302b-3p, hsa-miR-506-3p, hsa-miR-675-3p, hsa-miR-95-3p.

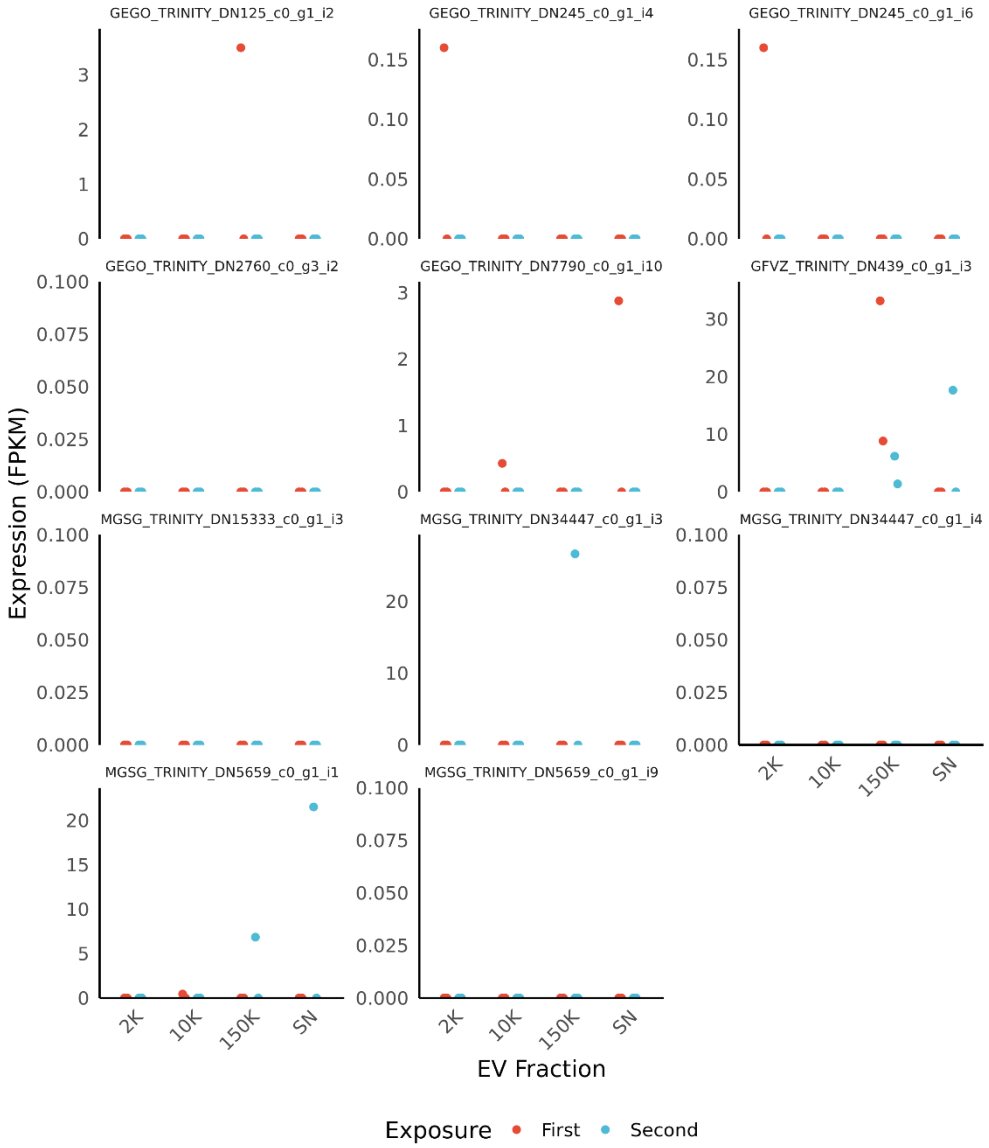

***Figure 68. Expression dynamics of potential microRNA sponges in the extracellular vesicles of* Ixodes ricinus.** *This figure presents the expression dynamics of 11 miRNA sponge candidates. The Y-axis represents expression levels in FPKM, while the X-axis corresponds to the EV fraction to which a sample belongs. Each dot represents a sample from an EV fraction, with different colors indicating whether the host is being exposed to ticks for the first or second time during blood feeding.*

An analysis to identify pathways significantly associated with genes targeted by these miRNAs revealed that GFVZ_TRINITY_DN439_c0_g1_i3 may disrupt pathways such as Mucin type O-Glycan biosynthesis, N-Glycan biosynthesis, ECM-receptor interaction and Phosphatidylinositol signaling system. Protein glycosylation pathways have been identified as critical components of homeostatic mechanisms, serving as key regulators of immune responses and offering potential molecular targets for modulating immune tolerance and activation [309,310]. The ability to disrupt the functionality of ECM-receptors would be a great advantage for ticks, since they are implicated in key roles for the defense against its blood feeding such as the immune system and the wound healing [311]. Lastly, the inhibition of the phosphatidylinositol signaling pathway has been reported to cause alterations and deficiencies in the immune system [312]. Therefore, this miRNA sponge may have the potential to simultaneously modulate immune responses and wound repair processes, facilitating successful blood feeding by the tick.

Thus, we demonstrated that lncRNAs predicted through bioinformatic analysis to modulate critical host pathways can be present in the saliva of *I. ricinus* but are also protected within the tick's EVs. This finding strengthens the evidence for the potential role of non-coding RNAs as modulators of the host response. It adds another layer to the intricate network by which female *I. ricinus* successfully evades host defenses, completes its blood meal, and ultimately sacrifices herself to produce offspring and ensure the perpetuation of the species.

Chapter 8.

General discussion

This thesis presents a comprehensive analysis of how *I. ricinus* may utilize its molecular arsenal to modulate host homeostatic response to tick feeding, enabling successful blood feeding and, ultimately, ensuring its own fitness. Specifically, this study explores the role of miRNAs, gene products expressed in the salivary glands and midgut, and lncRNAs, in this context. Through bioinformatics approaches, these molecular components have been tested *in silico* for their potential contributions to host homeostasis modulation for the benefit of the tick. Thus, this thesis enhances our knowledge of tick-host molecular interactions, paving the way for potential clinical applications and pest management strategies to control *I. ricinus* populations and minimize their impact on public and veterinary health.

The first objective of this thesis was to establish reliable reference datasets as a foundation for further analyses. This was particularly crucial given the significant gaps in the field of *I. ricinus* research, especially regarding lncRNAs and miRNAs. Without well-annotated reference data, meaningful investigations into tick-host interactions would have been severely limited.

Beyond the need for solid reference data, this thesis confronted a significant challenge related to its main focus, the analysis of miRNAs and their cooperative effects. One of the well-known limitations in miRNA research is the reliability of target prediction algorithms [313]. The available computational tools tend to

generate a high number of false positives, making it difficult to distinguish true biological interactions from background noise [252,313]. This issue became particularly evident when analyzing *I. ricinus* miRNAs in this thesis and comparing the achieved results with randomized miRNAs mapped to *H. sapiens* 3' UTRs, both of which yielded a high volume of predicted target regions.

Sequence conservation indicates function at a sequence level, i.e., the precise sequence is needed to fulfill the function. Therefore, when looking at predicted endogenous miRNA/mRNA interactions it is generally accepted that predictions improve if conservation is considered [103]. In the case of cross-species target site prediction, the usefulness of a conservation-based target site filter is less obvious. Our reasoning is that if miRNAs contribute to the tick's ability to successfully blood-feed on a broad range of hosts, this could be achieved by targeting conserved sites in the 3' UTR regions of the host species.

With this in mind, we analyzed the conservation of predicted target sequences across 30 potential hosts of *I. ricinus*. This approach significantly reduced the number of predicted targets while also revealing distinct patterns in the distribution of miRNA targets, particularly when compared to randomized sequences. These patterns, which were previously obscured by the noise of false positives, provided new insights into miRNA target selection and helped us to select the most interesting miRNAs in the context of tick-host interaction. Thus, this thesis reinforces the idea that sequence conservation serves as an effective filtering criterion in miRNA target prediction and should be systematically considered in future studies to enhance the biological relevance of predicted interactions.

Another important contribution of this thesis was the development of a workflow capable of identifying conserved target regions for miRNA binding and assessing their potential for cooperative interactions, based on the latest findings on miRNA cooperativity [149]. The cooperative action of miRNAs in this context is

particularly intriguing for several reasons. One key aspect of this interaction is that it enhances the silencing potential of miRNAs [149]. It is well established that miRNA-mediated silencing is a stochastic process, largely dependent on the stoichiometric balance between the miRNAs and their target mRNA [143]. Given that the exact quantity of *I. ricinus* miRNAs that can invade host cells remains unknown, but it is reasonable to assume that their concentration may be low, the cooperative effect among miRNAs might be crucial. In such a scenario, the cooperative effect can enable gene silencing in the host even at low concentrations of individual miRNAs, as it amplifies their inhibition potential.

Although no global cooperative properties were observed when analyzing the full set of *I. ricinus* miRNAs, a clearer pattern emerged when data noise was reduced. By selecting the top 12 miRNA candidates most likely to modulate host responses, we identified a compelling set of genes that were cooperatively affected by these miRNAs. Notably, the majority of these genes were expressed in *H. sapiens* skin cells and played key roles in the host's response to tick infestation. These findings suggest that cooperative miRNA interactions may facilitate the success of ticks in their parasitic lifestyle by modulating host gene expression. This opens new avenues for further investigation, including experimental validation of these effects and their potential implications for tick-host interactions.

A future perspective of this thesis is to extend the analysis of miRNA cooperative effects to a broader range of biological contexts and to develop a web tool capable of efficiently assessing these interactions. Additionally, our future research should focus on refining target prediction methodologies by incorporating key determinants of miRNA binding that have not yet been fully implemented. These include RNA modifications in both the miRNA and target regions, as well as the influence of RNA-binding proteins in modulating target

site accessibility, among others [315]. Other factors, such as target site accessibility and the binding energy between miRNAs and their mRNA targets, have already been integrated into various prediction tools, such as TargetScan [251]. However, these tools often support only a limited number of organisms [251], leaving room for significant improvement. In this regard, deep learning holds great potential [315]. Advances in deep learning could improve the reliability of miRNA target prediction by identifying complex patterns in large-scale datasets, accounting for multiple determinants simultaneously, allowing for the integration of experimentally validated data, and thus reducing false positives.

As previously discussed in this thesis, there is still significant work to be done in establishing a reliable reference for the genomic and transcriptomic data of *I. ricinus*. The recent publication of the *I. ricinus* genome represents a crucial step forward [176], and the exhaustive annotation of miRNAs and lncRNAs provided in this thesis further contributes to enhancing the accuracy and reliability of future analyses. However, despite these advancements, additional efforts are needed to refine genome assembly, improve transcript annotation, and integrate functional data.

The immune system presents one of the most significant challenges for ticks during parasitism, as host defenses can detect tick-derived molecules and mount innate immune responses, such as inflammation, which can disrupt successful blood feeding. Numerous salivary proteins, such as lipocalins, protease inhibitors, Salp15-like proteins and complement system modulators (Irac I and II), have already been identified as key players in suppressing immune activation, as previously discussed in *Section 1.2.4*. However, these proteins alone cannot fully explain the complex immune evasion exerted by *I. ricinus*.

Notably, we identified tick-derived miRNAs predicted to target critical immune signaling pathways, including TGF-beta signaling, T-cell receptor signaling,

SUMOylation, pathways related to NK cells and heme metabolism, which could suppress both innate and adaptive immune responses [255–258]. Furthermore, our analysis of miRNA cooperativity, focusing on the most promising *I. ricinus* miRNAs in terms of host modulation, highlighted several key genes as potential targets for cooperative silencing by tick miRNAs. These include CELF1, NFIA, STK38L (NDR2), PHF8, PIKFYVE, USP42, and ACOT7. All these genes were expressed in *H. sapiens* skin cell types, and they are associated with innate immunity, either by promoting inflammation or by regulating immune cell activity (e.g., macrophages, T cells, and NK cells) [277–285]. Additionally, lncRNAs from *I. ricinus* were found to act as miRNA sponges, binding to and neutralizing host miRNAs that regulate immune-related genes. These lncRNAs could disrupt Hippo signaling pathway, adherens junction, ECM-receptors and phosphatidylinositol signaling pathway, all involved in immune responses of the host [306,307,311,312].

Along with immune evasion, to successfully feed on its host, *I. ricinus* must overcome a series of physiological barriers, including wound healing, blood coagulation, and angiogenesis. A rapid and effective hemostatic response is triggered at the bite site, involving platelet aggregation, vasoconstriction, and clot formation, which could impair the tick's ability to maintain a steady blood meal. This thesis contributes to the understanding of how *I. ricinus* counteracts these processes using a combination of salivary proteins, and ncRNAs, including miRNAs and lncRNAs. Furthermore, this thesis explores how ncRNAs, particularly miRNAs and lncRNAs, complement salivary proteins in evading host immunity while also inhibiting wound healing, angiogenesis, and blood coagulation, processes that could otherwise hinder prolonged tick feeding. Additionally, it examines the role of ncRNAs in avoiding tick detection by interfering with host mechanosensation and pain receptors, preventing the host from recognizing and removing the tick. For successful blood feeding, *I. ricinus* must remain undetected by the host to avoid defensive behaviors such as

grooming or scratching, which could lead to premature detachment or even death. This necessitates the suppression of pain perception and mechanosensation at the tick bite site. In this context, tick saliva contains a variety of bioactive molecules that interfere with the host's nervous system and sensory signaling pathways [62]. In a parallel way, genes targeted cooperatively by *I. ricinus* miRNAs, such as REST, MDGA1, and SNAP25 have been found to be involved in these processes [286–289].

In this thesis, we have demonstrated that extracellular vesicles present in the saliva of *I. ricinus* are enriched in ncRNAs, including miRNAs and lncRNAs with the potential to modulate the host physiology upon tick feeding. Importantly, these ncRNAs are not only present but also protected within these vesicles, enhancing their probability to interact with the cells of the host during parasitism. This finding reinforces the hypothesis that both miRNAs and lncRNAs are missing parts of the puzzling regulatory network that together with the activity of other already known salivary molecules in *I. ricinus* synergistically or cooperatively suppress host homeostatic responses to secure prolonged feeding. Beyond the proteins discussed in Section 1.2.4, miRNAs secreted in tick saliva and EVs play a crucial role in modulating wound healing in *I. ricinus*. Specifically, these miRNAs have the potential to disrupt key pathways such as the Wnt signaling pathway and mesodermal differentiation pathways, both of which are closely associated with wound healing and angiogenesis [253,254]. Several specific genes have been identified as potential cooperative targets of *I. ricinus* miRNAs. Among them, GPC6, NRG1, ZFPM2, PDGFRA, and CEP41 have been linked to wound healing and angiogenesis, processes that may contribute to wound closure and restrict tick feeding [272–276]. Additionally, *I. ricinus* miRNA sponges have the capability to disrupt ECM-receptor interactions, which are also known to play a critical role in wound healing [311].

Thus, this thesis has provided key insights into the molecular strategies that *I. ricinus* employs for prolonged blood feeding, identifying specific miRNAs, miRNA sponges, and gene targets involved in the strategies that a feeding tick employs to achieve immune evasion, coagulation suppression, wound healing modification, and sensory modulation. This offers a strong foundation for future research, paving the way for in-depth functional studies and potential applications in tick control strategies.

An intriguing finding of this thesis is that glycosylation-related pathways in both *I. ricinus* and its host may be modulated during parasitism, suggesting a critical role for glycosylation in tick-host interactions. Specifically, during active feeding, genes differentially expressed in ticks feeding on naïve hosts compared to ticks feeding on previously exposed hosts were significantly enriched in N-linked glycosylation pathways. Among these, dolichyldiphosphooligosaccharide–protein glycotransferase, a key enzyme in protein glycosylation, emerged as one of the most differentially expressed genes over time, based on cumulative differences in expression levels. Additionally, *I. ricinus* appears to influence host glycosylation pathways through the action of lncRNAs. Tick-derived lncRNAs were found to have the potential to inhibit host miRNAs involved in the regulation of glycosaminoglycan biosynthesis, mucin-type O-glycan biosynthesis, and N-linked glycosylation.

Glycosylation generates a diverse and abundant repertoire of glycans, collectively known as the glycome [316]. Glycans play a crucial role in both adaptive and innate immune responses, influencing key processes such as immune cell development and differentiation, production of immunoglobulins or attachment of N-glycans to T-cell and B-cell receptors, which modulates their signaling pathways [316,317].

In recent years, glycosylation has gained increasing relevance in the context of parasite-host interactions [297]. Growing evidence underscores the importance

of carbohydrate-based interactions in the complex relationship between ticks and their hosts, as well as in the transmission of tick-borne pathogens [297]. Given that glycoconjugates, are major structural components of the outer surface of animal cells, including EVs [318,319], they likely play a significant role in tick-host interactions. The findings presented in this thesis support this idea, highlighting glycosylation as a key factor in tick parasitism. Our results reinforce the notion that glycosylation-related mechanisms warrant further investigation in both *I. ricinus* and their hosts, positioning it as an important area for future research on tick-host interactions and potential control strategies.

By both establishing a foundational reference for future analyses of miRNAs and lncRNAs and providing new insights into molecules that may act as cornerstone mediators of tick-host molecular interactions, this thesis opens new research avenues and contributes to the development of potential clinical and pest management strategies. <Ticks gaining resistances. One promising approach involves the targeting of *I. ricinus* miRNAs using antimiRs, a technique that has been gaining relevance in recent years and has demonstrated effectiveness in various biological contexts [159,320,321]. By inhibiting key tick miRNAs involved in host immune suppression and coagulation, antimiR-based strategies could impair the tick's ability to feed successfully, offering a novel method for tick control. Additionally, further research into the glycosylation of *I. ricinus* and the surface composition of EVs could pave the way for the development of anti-tick vaccines, something that has been previously proposed [322].

Beyond pest control, *I. ricinus* miRNAs and lncRNAs may also have therapeutic potential in human medicine. Given their ability to inhibit innate immune responses and modulate inflammatory pathways, these molecules could be explored for their application in autoimmune and chronic inflammatory diseases, where excessive immune activation plays a detrimental role.

Even though miRNA therapies hold great potential, significant work is still needed to bring them to market, including improving delivery methods and minimizing unintended off-target effects [323]. Despite these challenges, exploiting tick-derived regulatory RNAs and antimiRs (including tick miRNA sponges) as immunomodulatory agents, represents an exciting avenue for future biomedical research.

Overall, this thesis aims to provide the foundation for multiple new research directions and potential clinical applications. Further efforts, including biological validation and a more in-depth investigation of the host's response to tick bites, could significantly enhance our understanding of tick-host interactions and build upon the analyses conducted in this thesis. Such knowledge and advancements could help prevent the spread of tick-borne diseases, protect livestock and agricultural industries from economic losses, and ultimately improve public health and well-being.

Chapter 9.

Conclusions

1. By means of the novel genome of *I. ricinus*, we expanded and assessed the reliability of its miRNA catalog. Additionally, we annotated several non-coding RNA molecules, including lncRNAs. Thus, we provided a robust foundation for the study of non-coding RNA in this thesis and for future research.

2. We assembled a *de novo* transcriptome using an extensive set of samples from salivary glands and midgut of *I. ricinus* sibling ticks. The fact that they were siblings reduced genetic variance and allowed us to perform the assembly with greater accuracy. This reference also laid the foundation for transcriptomic (and proteomic by collaborative groups) studies in this tick species.

3. Target prediction tools are prone to many false positives, and phylogenetic footprinting (target site conservation) can be applied to mitigate this issue. In this context, the use of target sequence conservation can be justified given the capacity of *I. ricinus* to modulate a broad range of hosts. We implemented a workflow which generates conservation profiles for each target site at a base pair level. By applying a conservation filter, we were able to reveal clear differences between target sites of tick miRNAs and the negative control. Without this filter,

tick target sites are much closer to a randomized negative control, showing clearly the noisy nature of primary target site predictions.

4. Based on saliva abundance, ratio of conserved targets, and comparison with the negative control, we selected 12 candidate miRNAs that are all conserved across species within the Bilateria clade. Furthermore, all 12 are detectable in extracellular vesicles extracted from tick saliva, thus enhancing the probability that they indeed interact with host cells. The *H. sapiens* target genes of these 12 candidates are involved in crucial processes such as wound healing, immune response, and tick detection.

5. We implemented a workflow to analyze the potential synergistic cooperation between *I. ricinus* miRNAs based on recent advances in the understanding of the mechanistic action of negative regulation by miRNAs. Our results suggest that a subset of tick miRNAs cooperate in the repression of certain host genes. Interestingly, these target genes are abundant in human skin cells with known functions in key pathways of the tick-host interaction. The fact that this synergistic action increases the efficiency of gene silencing by miRNAs could reduce the need for high concentrations of *I. ricinus* miRNAs in host cells. This enhances their effectiveness and makes this effect an interesting area for further exploration, especially in the topic of therapeutics development.

6. The analysis of transcriptomic dynamics revealed that ticks parasitizing sensitized hosts (previously exposed to tick infestations) exhibit distinct gene expression patterns over time compared to those ticks feeding on naïve hosts, to counteract this host sensitization. Differentially expressed genes are associated with key biological processes, including

glycosylation and protein folding, which play crucial roles in tick adaptation to parasitism and immune evasion. Further investigation into these gene expression changes could provide valuable insights into host sensitization and tick response to this adversity, an essential first step to develop novel tick control strategies such as anti-tick vaccines.

7. We reported here that lncRNAs have the potential to act as miRNA sponges, potentially inhibiting important host miRNAs. Specifically, one lncRNA present in small extracellular vesicles and capable of impairing glycosylation and cell-to-cell signaling processes, appears as a promising candidate for further studies.

8. This thesis presents numerous tick candidate molecules for biological validation and further research to clarify their precise role in manipulating host responses. These candidates could contribute to clinical advancements and may be utilized as therapeutic tick-derived molecules.

Publications during the PhD

Publications as first author:

- Medina, J. M., Abbas, M. N., Bensaoud, C., Hackenberg, M., & Kotsyfakis, M. (2022). Bioinformatic **Analysis of Ixodes ricinus Long Non-Coding RNAs Predicts Their Binding Ability of Host miRNAs.** *International Journal of Molecular Sciences*, *23*(17), 9761. https://doi.org/10.3390/ijms23179761

- Medina, J. M., Jmel, M. A., Cuveele, B., Gómez-Martín, C., Aparicio-Puerta, E., Mekki, I., Kotál, J., Martins, L. A., Hackenberg, M., Bensaoud, C., & Kotsyfakis, M. (2022). **Transcriptomic analysis of the tick midgut and salivary gland responses upon repeated blood-feeding on a vertebrate host.** *Frontiers in Cellular and Infection Microbiology*, *12*, 1125. https://doi.org/10.3389/fcimb.2022.919786

Publications as coauthor:

- Cerqueira de Araujo, A., Noel, B., Bretaudeau, A., Labadie, K., Boudet, M., Tadrent, N., Istace, B., Kritli, S., Cruaud, C., Olaso, R., Deleuze, J.-F., Voordouw, M. J., Hervet, C., Plantard, O., Zamoto-Niikura, A., Chertemps, T., Maïbèche, M., Hilliou, F., le Goff, G., Chmelař, J., Mazák, V., Jmel, M., Kotsyfakis, M., Medina, J. M.,... Rispe, C. (2025). **Genome sequences of four Ixodes species expands understanding of tick evolution.** *BMC Biology*, *23*(1), 17. https://doi.org/10.1186/s12915-025-02121-1

- Gómez-Martín, C., Aparicio-Puerta, E., van Eijndhoven, M. A. J., Medina, J. M., Hackenberg, M., & Pegtel, D. M. (2023). **Reassessment of miRNA variant (isomiRs) composition by small RNA sequencing.** *Cell Reports Methods*, 3(5), 100480. https://doi.org/10.1016/j.crmeth.2023.100480

- Gómez-Martín, C., Zhou, H., Medina, J. M., Aparicio-Puerta, E., Shi, B., & Hackenberg, M. (2023). **Genome-Wide Analysis of microRNA Expression Profile in Roots and Leaves of Three Wheat Cultivars under Water and Drought Conditions.** *Biomolecules*, 13(3). https://doi.org/10.3390/BIOM13030440

- Aparicio-Puerta, E., Gómez-Martín, C., Giannoukakos, S., Medina, J. M., Scheepbouwer, C., García-Moreno, A., Carmona-Saez, P., Fromm, B., Pegtel, M., Keller, A., Marchal, J. A., & Hackenberg, M. (2022). **sRNAbench and sRNAtoolbox 2022 update: accurate miRNA and sncRNA profiling for model and non-model organisms.** *Nucleic Acids Research*, 50(W1), W710–W717.https://doi.org/10.1093/NAR/GKAC363

- Bensaoud, C., Tenzer, S., Poplawski, A., Medina, J. M., Jmel, M. A., Voet, H., Mekki, I., Aparicio-Puerta, E., Cuveele, B., Distler, U., Marini, F., Hackenberg, M., & Kotsyfakis, M. (2022). **Quantitative proteomics analysis reveals core and variable tick salivary proteins at the tick-vertebrate host interface.** *Molecular Ecology*, 31(15), 4162–4175. https://doi.org/10.1111/mec.16561

- Gómez-Martín, C., Zhou, H., Medina, J. M., Aparicio-Puerta, E., Hackenberg, M., & Shi, B. (2022). **Comprehensive, integrative genomic analysis of microRNA expression profiles in different tissues of two wheat cultivars with different traits.** *Functional & Integrative Genomics*, 23(1), 15. https://doi.org/10.1007/s10142-022-00920-1

- Eijndhoven, M. A. J. van, Aparicio-Puerta, E., Gómez-Martín, C., Medina, J. M., Drees, E. E. E., Bradley, E. J., Bosch, L., Scheepbouwer, C., Hackenberg, M., & Pegtel, D. M. (2021). **Unbiased and UMI-informed sequencing of cell-free miRNAs at single-nucleotide resolution.** *BioRxiv*, 2021.05.04.442244. https://doi.org/10.1101/2021.05.04.442244

- Gómez-Martín, C., Aparicio-Puerta, E., Medina, J. M., Barturen, G., Oliver, J. L., & Hackenberg, M. (2021). **geno5mC: A Database to Explore the Association between Genetic Variation (SNPs) and CpG Methylation in the Human Genome.** *Journal of Molecular Biology*, 433(11), 166709. https://doi.org/10.1016/j.jmb.2020.11.008

- Aparicio-Puerta, E., Gomez-Martin, C., Giannoukakos, S., Medina, J. M., Marchal, J. A., & Hackenberg, M. (2020**). mirnaQC: A webserver for comparative quality control of miRNA-seq data.** *Nucleic Acids Research*, 48(W1), W262–W267. https://doi.org/10.1093/NAR/GKAA452

Acknowledgements

Esta tesis es el resultado de un largo y arduo camino que no hubiera podido recorrer sin haber tenido caminando a mi lado a tan buenas personas. Se dice que cuando alguien te proporciona su tiempo, te proporciona una parte de su vida, y es por ello que estoy tan agradecido a todos aquellos que han aportado un pedacito de su alma para que esta tesis sea posible.

En primer lugar, me gustaría agradecer por innumerables razones a mi director de tesis y mentor. Muchas gracias, Michael. Todo lo que escriba será insuficiente para describir la suerte que he tenido de tener un director de tesis al que puedo llamar amigo y que me ha enseñado tanto en lo personal y en lo científico. Es un buen momento para confesar lo mucho que te admiro y mis deseos de llegar a ser alguien parecido a ti. Me llevo grandes recuerdos y enseñanzas de esta etapa gracias a ti. Me has enseñado como ser riguroso y directo, y cómo es necesario hacerse preguntas y seleccionar las preguntas correctas. Como bien sabes, siempre he dejado la vida fluir y ahora no sé qué me deparará el futuro, y aun así estoy seguro de que con la preparación que me has dado serán grandes cosas y sabré afrontarlas. Ojalá este camino me lleve a que sigas presente en mi vida, estaría profundamente agradecido.

I would like to express my deepest gratitude to a person that could be perfectly treated as co-director of this thesis and that now I can call a friend. Thanks, Michalis, for the time and effort you devoted to my journey and thesis. Your selfless dedication, even offering to review and correct my work, has been invaluable. Beyond that, I am profoundly grateful for the many things you have taught me, both academically and personally. I truly admire you and I feel fortunate to have had your guidance and support throughout this journey. As I

told Michael, life is uncertain yet promising, and even so, I would love to continue collaborating with you.

Es de recibo tener una mención especial con aquel que estuvo y participó en mi mentorización inicial, cuando comencé como alumno interno en el departamento de Genética. Pepe, que me enseñaste tanto y me diste una más que cálida bienvenida al grupo. Sin ti, nada de esto hubiera sucedido. Muchas gracias, me enseñaste lo elegante que puede ser una persona y cómo esto puede trasladarse a la investigación.

He de agradecer a todos aquellos que han sido compañeros y amigos durante esta etapa de mi vida.

En primer lugar, a mis compañeros de grupo con los que he pasado tanto tiempo y de los que he aprendido tanto. Cris, muchas gracias por ser tan amable, diligente y siempre tener una sonrisa para mí, desde lo profundo del corazón te digo que hiciste que todo en el grupo fuera más fácil. Ernesto, admiro mucho tu valentía y esa inteligencia pícara que tienes, ojalá algún día poder aplicarla. Muchas gracias por todo. Ricardo, gracias por enseñarme tanto, gran parte de mis habilidades programando se deben a ti, y muchas gracias por acogerme en el grupo sin pensártelo dos veces. Guillermo, en el relativamente poco tiempo que hemos pasado juntos, me has enseñado muchísimo. Gracias por recordarme que no debo dejar que la vida me coma. Ángel, siempre te lo digo, el profesor que mejor hacía los exámenes y que ahora ni los necesita. Muchas gracias por tu inmensa amabilidad y cariño, de corazón. And Stavros, I am truly lucky to have always been surrounded by people with warm smiles, thank you for being the kindest of all.

Quiero hacer mención especial a Esther Viseras, con la que he participado en varias asignaturas como docente y me ha tutorizado en el ámbito de la enseñanza. Muchas gracias por contagiarme tu inmensurable pasión por la

docencia y por ayudarme a ser mejor orador y profesor. En este ámbito también querría agradecer a Lara y David, grandes docentes e investigadores, pero casi mejor desarrolladores de *scape rooms*, de los cuales he aprendido muchísimo en estos años.

Me encantaría agradecer a mis compañeros de departamento. Con todos vosotros he compartido charlas en desayunos, siempre tratando de arreglar el mundo, alguna reunión en los pasillos, y en general, momentos de alegría. De cada uno de vosotros me llevo un pedacito en forma de recuerdos y enseñanzas.

I would gladly mention everyone who made my stay in Czech Republic one of the best experiences of my life. At first, I was hesitant to go on an international internship, and when I departed for Czech Republic the day after New Year's Eve, I felt a bit sad. But then, out of nowhere, I started meeting amazing people who made my return to Spain just as bittersweet. But enough sadness, I want to thank you all for giving me such a heartwarming welcome. Thanks, Markéta, Ouns, Dorsaf, Imen, Amine, Claudio, Ana María, Miri, Marcela, and Fernando.

Quiero agradecer a Isa Barbeito, que de forma totalmente desinteresada, y siempre con una sonrisa, se ofreció a ayudarme a hacer la obra de arte al estilo boceto de Leonardo da Vinci que es la portada de esta tesis.

En el ámbito familiar, quiero agradecer a mis abuelos, ellos saben que para mí han sido ejemplo de perseverancia y dedicación y que agradezco muchísimo su cariño. Quiero agradecer a mis primos y tíos y hacer mención especial a mi primo Nico, que además de primo es uno de mis mejores amigos. Hemos pasado incontables buenos momentos juntos y quiero que sepas que admiro muchísimo tu determinación y obsesión sana por cumplir tus objetivos. También agradecer a mis amigos, que entran en esta sección familiar por

descontado, ya que siempre me han apoyado en todo y que son gran parte del motivo de felicidad.

Muchas gracias a mi hermano Sergio. Gracias a que compartimos prácticamente todos los gustos, me has acompañado siempre en todas mis aventuras. Ahora estamos algo lejos y se te echa mucho de menos. Me alegro mucho de tu proceso de maduración, de haber sido parte de él y me enorgullece decirte que vas en un muy buen camino para alcanzar todos tus objetivos. Y, por último, ¿un besito?, pues un saludito, loquete.

Por supuesto, quiero agradecer a los mejores padres que alguien podría tener, Me habéis regalado una vida llena oportunidades, habéis estado ahí en mis momentos más duros, sin fallarme y demostrándome lo que es el amor incondicional. Habéis sido el mejor ejemplo y me habéis enseñado todos los valores necesarios para llegar a ser el tipo de padre que cualquiera querría, alguien como vosotros.

Y qué decir de aquella que felizmente puedo llamar mi compañera de vida. Hace doce años y nueve meses que te convertiste en mi refugio, en la hoguera en la cual descansar del duro camino que a veces es la vida. Toda una vida juntos nos espera, y a tu lado no parece tiempo suficiente. Por ser la luz que ilumina mis días y aquella a la que siempre querré y protegeré. Te amo, María.

References

[1] Cupp, E.W. Biology of Ticks. *Veterinary Clinics of North America: Small Animal Practice* **1991**, *21*, 1–26, doi:10.1016/S0195-5616(91)50001-2.

[2] De La Fuente, J.; Estrada-Pena, A.; Venzal, J.M.; Kocan, K.M.; Sonenshine, D.E. Overview: Ticks as Vectors of Pathogens That Cause Disease in Humans and Animals. *Front Biosci* **2008**, *13*, 6938–6946, doi:10.2741/3200.

[3] Beccaloni, Jan. *Arachnids*; Natural History Museum, 2009; ISBN 9780565092207.

[4] Walker, M.D. The Biology and Ecology of the Sheep Tick Ixodes Ricinus 2018.

[5] Brites-Neto, J.; Duarte, K.M.R.; Martins, T.F. Tick-Borne Infections in Human and Animal Population Worldwide. *Vet World* **2015**, *8*, 301, doi:10.14202/VETWORLD.2015.301-315.

[6] Gray, J.S.; Dautel, H.; Estrada-Peña, A.; Kahl, O.; Lindgren, E. Effects of Climate Change on Ticks and Tick-Borne Diseases in Europe. *Interdiscip Perspect Infect Dis* **2009**, *2009*, 1–12, doi:10.1155/2009/593232.

[7] Aounallah, H.; Bensaoud, C.; M'ghirbi, Y.; Faria, F.; Chmelař, J.; Kotsyfakis, M. Tick Salivary Compounds for Targeted Immunomodulatory Therapy. *Front Immunol* **2020**, *11*, 2440, doi:10.3389/FIMMU.2020.583845/BIBTEX.

[8] Pham, M.; Underwood, J.; Chávez, A.S.O. Changing the Recipe: Pathogen Directed Changes in Tick Saliva Components. *International Journal of*

Environmental Research and Public Health 2021, Vol. 18, Page 1806 **2021**, *18*, 1806, doi:10.3390/IJERPH18041806.

[9] Kazimírová, M.; Štibrániová, I. Tick Salivary Compounds: Their Role in Modulation of Host Defences and Pathogen Transmission. *Front Cell Infect Microbiol* **2013**, *4*, 43, doi:10.3389/FCIMB.2013.00043/BIBTEX.

[10] Barker, S.C.; Walker, A.R. Ticks of Australia. The Species That Infest Domestic Animals and Humans. *Zootaxa* **2014**, *3816*, 1–144–1–144, doi:10.11646/ZOOTAXA.3816.1.1.

[11] Jia, N.; Wang, J.; Shi, W.; Du, L.; Sun, Y.; Zhan, W.; Jiang, J.F.; Wang, Q.; Zhang, B.; Ji, P.; et al. Large-Scale Comparative Analyses of Tick Genomes Elucidate Their Genetic Diversity and Vector Capacities. *Cell* **2020**, *182*, 1328-1340.e13, doi:10.1016/J.CELL.2020.07.023.

[12] Janzén, T.; Choudhury, F.; Hammer, M.; Petersson, M.; Dinnétz, P. Ticks - Public Health Risks in Urban Green Spaces. *BMC Public Health* **2024**, *24*, 1031, doi:10.1186/s12889-024-18540-8.

[13] Beard, C. Ben; Occi, J.; Bonilla, D.L.; Egizi, A.M.; Fonseca, D.M.; Mertins, J.W.; Backenson, B.P.; Bajwa, W.I.; Barbarin, A.M.; Bertone, M.A.; et al. Multistate Infestation with the Exotic Disease–Vector Tick Haemaphysalis Longicornis — United States, August 2017–September 2018. *MMWR Morb Mortal Wkly Rep* **2019**, *67*, 1310–1313, doi:10.15585/MMWR.MM6747A3.

[14] Gulia-Nuss, M.; Nuss, A.B.; Meyer, J.M.; Sonenshine, D.E.; Roe, R.M.; Waterhouse, R.M.; Sattelle, D.B.; De La Fuente, J.; Ribeiro, J.M.; Megy, K.; et al. Genomic Insights into the Ixodes Scapularis Tick Vector of Lyme Disease. *Nature Communications 2016 7:1* **2016**, *7*, 1–13, doi:10.1038/ncomms10507.

[15] Chmelař, J.; Kotál, J.; Karim, S.; Kopacek, P.; Francischetti, I.M.B.; Pedra, J.H.F.; Kotsyfakis, M. Sialomes and Mialomes: A Systems-Biology View of Tick Tissues and Tick–Host Interactions. *Trends Parasitol* **2016**, *32*, 242–254, doi:10.1016/J.PT.2015.10.002.

[16] Schwarz, A.; Von Reumont, B.M.; Erhart, J.; Chagas, A.C.; Ribeiro, J.M.C.; Kotsyfakis, M. De Novo Ixodes Ricinus Salivary Gland Transcriptome Analysis Using Two Next-Generation Sequencing Methodologies. *The FASEB Journal* **2013**, *27*, 4745–4756, doi:10.1096/FJ.13-232140.

[17] Hackenberg, M.; Langenberger, D.; Schwarz, A.; Erhart, J.; Kotsyfakis, M. In Silico Target Network Analysis of de Novo-Discovered, Tick Saliva-Specific MicroRNAs Reveals Important Combinatorial Effects in Their Interference with Vertebrate Host Physiology. *RNA* **2017**, *23*, 1259–1269, doi:10.1261/rna.061168.117.

[18] Nawaz, M.; Malik, M.I.; Zhang, H.; Gebremedhin, M.B.; Cao, J.; Zhou, Y.; Zhou, J. MiRNA Profile of Extracellular Vesicles Isolated from Saliva of Haemaphysalis Longicornis Tick. *Acta Trop* **2020**, *212*, 105718, doi:10.1016/J.ACTATROPICA.2020.105718.

[19] Cano-Argüelles, A.L.; Pérez-Sánchez, R.; Oleaga, A. A MicroRNA Profile of the Saliva in the Argasid Ticks Ornithodoros Erraticus and Ornithodoros Moubata and Prediction of Specific Target Genes. *Ticks Tick Borne Dis* **2023**, *14*, 102249, doi:10.1016/j.ttbdis.2023.102249.

[20] Semenza, J.C.; Suk, J.E. Vector-Borne Diseases and Climate Change: A European Perspective. *FEMS Microbiol Lett* **2018**, *365*, doi:10.1093/femsle/fnx244.

[21] Zhioua, E.; Bouattour, A.; Hu, C.M.; Gharbi, M.; Aeschliman, A.; Ginsberg, H.S.; Gern, L. Infection of Ixodes Ricinus (Acari: Ixodidae) by Borrelia

Burgdorferi Sensu Lato in North Africa. *J Med Entomol* **1999**, *36*, 216–218, doi:10.1093/jmedent/36.2.216.

[22] Arthur, D.R. *Ticks and Disease*; Elsevier Science & Technology, 1962;

[23] Sprong, H.; Azagi, T.; Hoornstra, D.; Nijhof, A.M.; Knorr, S.; Baarsma, M.E.; Hovius, J.W. Control of Lyme Borreliosis and Other Ixodes Ricinus-Borne Diseases. *Parasit Vectors* **2018**, *11*, 145, doi:10.1186/s13071-018-2744-5.

[24] European Centre for Disease Prevention and Control and European Food Safety Authority Tick Maps. Available from: Https://Ecdc.Europa.Eu/En/Disease-Vectors/Surveillance-and-Disease-Data/Tick-Maps.

[25] Biswas, B.K. Effect of Climate Change on Vector-Borne Disease. *Emerging Issues in Climate Smart Livestock Production: Biological Tools and Techniques* **2022**, 263–316, doi:10.1016/B978-0-12-822265-2.00006-5.

[26] Hillyard, P.D.. Ticks of North-West Europe : Keys and Notes for Identification of the Species. **1996**, 178.

[27] Arthur, D.R. *British Ticks.*; Butterworths: London, U. K, 1963;

[28] Andersen, S.O.; Roepstorff, P. The Extensible Alloscutal Cuticle of the Tick, Ixodes Ricinus. *Insect Biochem Mol Biol* **2005**, *35*, 1181–1188, doi:10.1016/j.ibmb.2005.05.009.

[29] Sonenshine, D.E..; Roe, R.Michael. *Biology of Ticks*. *Volume 1*; Oxford University Press, 2014; ISBN 9780199379279.

[30] Simo, L.; Park, Y. Neuropeptidergic Control of the Hindgut in the Black-Legged Tick Ixodes Scapularis. *Int J Parasitol* **2014**, *44*, 819–826, doi:10.1016/j.ijpara.2014.06.007.

[31] Tidwell, J.P.; Treviño, D.E.; Thomas, D.B.; Mitchell, R.D.; Heerman, M.C.; Pérez de León, A.; Lohmeyer, K.H. Pictorial Dissection Guide and Internal Anatomy of the Cattle Tick, Rhipicephalus (Boophilus) Microplus (Canestrini). *Ticks Tick Borne Dis* **2021**, *12*, 101685, doi:10.1016/j.ttbdis.2021.101685.

[32] Starck, J.M.; Mehnert, L.; Biging, A.; Bjarsch, J.; Franz-Guess, S.; Kleeberger, D.; Hörnig, M. Morphological Responses to Feeding in Ticks (Ixodes Ricinus). *Zoological Lett* **2018**, *4*, 20, doi:10.1186/s40851-018-0104-0.

[33] Kiszewski, A.E.; Matuschka, F.R.; Spielman, A. Mating Strategies and Spermiogenesis in Ixodid Ticks. *Annu Rev Entomol* **2001**, *46*, 167–182, doi:10.1146/annurev.ento.46.1.167.

[34] Kahl, O.; Gray, J.S. The Biology of Ixodes Ricinus with Emphasis on Its Ecology. *Ticks Tick Borne Dis* **2023**, *14*, 102114, doi:10.1016/J.TTBDIS.2022.102114.

[35] Ehrmann, S.; Liira, J.; Gärtner, S.; Hansen, K.; Brunet, J.; Cousins, S.A.O.; Deconchat, M.; Decocq, G.; Frenne, P.; Smedt, P.; et al. Environmental Drivers of Ixodes Ricinus Abundance in Forest Fragments of Rural European Landscapes. *BMC Ecol* **2017**, *17*, 1–14, doi:10.1186/S12898-017-0141-0/FIGURES/4.

[36] Gaede, K.; Knülle, W. On the Mechanism of Water Vapour Sorption From Unsaturated Atmospheres by Ticks. *Journal of Experimental Biology* **1997**, *200*, 1491–1498, doi:10.1242/JEB.200.10.1491.

[37] Kahl, O. Investigations on the Water Balance of Ticks (Acari, Ixodoidea) in the Course of Their Postembryonic Development with Special Reference to Active Water Vapour Uptake in the Engorged Phases. PhD Thesis, Free University of Berlin, Germany, in German. **1989**.

[38] Carlson, R.W. Instar, Stadium, and Stage: Definitions to Fit Usage. *Ann Entomol Soc Am* **1983**, *76*, 319–319, doi:10.1093/AESA/76.3.319.

[39] Kahl, O.; Hoff, R.; Knülle, W. Gross Morphological Changes in the Salivary Glands of Ixodes Ricinus (Acari, Ixodidae) between Bloodmeals in Relation to Active Uptake of Atmospheric Water Vapour. *Exp Appl Acarol* **1990**, *9*, 239–258, doi:10.1007/BF01193431.

[40] (Ixodoidea), Y.B.-A.T. of'Bloodsucking T.; 1972, undefined Bloodsucking Ticks (Ixodoidea)—Vectors of Diseases of Man and Animals. *BioOneYS BalashovA Translation of'Bloodsucking Ticks (Ixodoidea)—Vectors of Diseases of Man and, 1972•BioOne*.

[41] Sonenshine, D.E. Biology of Ticks, Svazek 1. *Veterinary Clinics of North America: Small Animal Practice* **1991**, *21*, 1–26.

[42] Ticks, R.K.-B. of; Sonenshine, 2nd ed.; DE, undefined; Roe, undefined; 2013, undefined Integument and Ecdysis. *books.google.comRW KaufmanBiology of Ticks, 2nd ed.; Sonenshine, DE, Roe, RM, Eds, 2013•books.google.com*.

[43] Gray, J.; Kahl, O.; Lane, R.; Levin, M.; tick-borne, J.T.-T. and; 2016, undefined Diapause in Ticks of the Medically Important Ixodes Ricinus Species Complex. *Elsevier*.

[44] Gray, J.S. Mating and Behavioural Diapause in Ixodes Ricinus L. *Exp Appl Acarol* **1987**, *3*, 61–71, doi:10.1007/BF01200414.

[45] Hofmeester, T.R. The Wild Life of Tick-Borne Pathogens. **2016**, doi:10.18174/393112.

[46] Gern, L.; Humair, P. Ecology of Borrelia Burgdorferi Sensu Lato in Europe. **2002**.

[47] Jaenson, T.G.T.; Tälleklint, L. Lyme Borreliosis Spirochetes in Ixodes Ricinus (Acari: Ixodidae) and the Varying Hare on Isolated Islands in the Baltic Sea. *J Med Entomol* **1996**, *33*, 339–343, doi:10.1093/JMEDENT/33.3.339.

[48] Hrazdilová, K.; Lesiczka, P.M.; Bardoň, J.; Vyroubalová, Š.; Šimek, B.; Zurek, L.; Modrý, D. Wild Boar as a Potential Reservoir of Zoonotic Tick-Borne Pathogens. *Ticks Tick Borne Dis* **2021**, *12*, 101558, doi:10.1016/j.ttbdis.2020.101558.

[49] Gray, J.S. The Ecology of Lyme Borreliosis Vector Ticks. In *Ecology and Evolution of the Acari*; Springer Netherlands: Dordrecht, 1999; pp. 269–276 ISBN 978-94-017-1343-6.

[50] Rizzoli, A.; Hauffe, H.C.; Carpi, G.; Vourc'h, G.I.; Neteler, M.; Rosà, R. Lyme Borreliosis in Europe. *Eurosurveillance* **2011**, *16*, doi:10.2807/ESE.16.27.19906-EN.

[51] Rizzoli, A.; Silaghi, C.; Obiegala, A.; Rudolf, I.; Hubálek, Z.; Földvári, G.; Plantard, O.; Vayssier-Taussat, M.; Bonnet, S.; Špitalská, E.; et al. Ixodes Ricinus and Its Transmitted Pathogens in Urban and Peri-Urban Areas in Europe: New Hazards and Relevance for Public Health. *Front Public Health* **2014**, *2*, 251, doi:10.3389/FPUBH.2014.00251.

[52] Dobler, G.; Gniel, D.; Petermann, R.; Pfeffer, M. Epidemiology and Distribution of Tick-Borne Encephalitis. *Wiener Medizinische Wochenschrift* **2012**, *162*, 230–238, doi:10.1007/S10354-012-0100-5/TABLES/2.

[53] Stuen, S.; Granquist, E.G.; Silaghi, C. Anaplasma Phagocytophilum-a Widespread Multi-Host Pathogen with Highly Adaptive Strategies. *Front Cell Infect Microbiol* **2013**, *4*, 54479, doi:10.3389/FCIMB.2013.00031/BIBTEX.

[54] Azagi, T.; Jaarsma, R.I.; van Leeuwen, A.D.; Fonville, M.; Maas, M.; Franssen, F.F.J.; Kik, M.; Rijks, J.M.; Montizaan, M.G.; Groenevelt, M.; et al. Circulation of Babesia Species and Their Exposure to Humans through Ixodes Ricinus. *Pathogens* **2021**, *10*, 386, doi:10.3390/PATHOGENS10040386/S1.

[55] Oteo, J.A.; Portillo, A. Tick-Borne Rickettsioses in Europe. *Ticks Tick Borne Dis* **2012**, *3*, 271–278, doi:10.1016/J.TTBDIS.2012.10.035.

[56] Krause, P.J.; Fish, D.; Narasimhan, S.; Barbour, A.G. Borrelia Miyamotoi Infection in Nature and in Humans. *Clinical Microbiology and Infection* **2015**, *21*, 631–639, doi:10.1016/J.CMI.2015.02.006.

[57] Portillo, A.; Santibáñez, P.; Palomar, A.M.; Santibáñez, S.; Oteo, J.A. 'Candidatus Neoehrlichia Mikurensis' in Europe. *New Microbes New Infect* **2018**, *22*, 30, doi:10.1016/J.NMNI.2017.12.011.

[58] Kemp, D.H.; Stone, B.F.; Binnington, K.C. Tick Attachment and Feeding: Role of the Mouthparts, Feeding Apparatus, Salivary Gland Secretions and the Host Response. In *Physiology of Ticks*; Elsevier, 1982; pp. 119–168.

[59] Suppan, J.; Engel, B.; Marchetti-Deschmann, M.; Nürnberger, S. Tick Attachment Cement–Reviewing the Mysteries of a Biological Skin Plug System. *Wiley Online LibraryJ Suppan, B Engel, M Marchetti-Deschmann, S NürnbergerBiological Reviews, 2018•Wiley Online Library* **2018**, *93*, 1056–1076, doi:10.1111/brv.12384.

[60] Francischetti, I.M.B.; Sa-Nunes, A.; Mans, B.J.; Santos, I.M.; Ribeiro, J.M.C. The Role of Saliva in Tick Feeding. *Frontiers in Bioscience* **2009**, *14*, 2051–2088, doi:10.2741/3363/PDF.

[61] Glatz, M.; Means, T.; Haas, J.; Steere, A.C.; Müllegger, R.R. Characterization of the Early Local Immune Response to Ixodes Ricinus

Tick Bites in Human Skin. *Exp Dermatol* **2017**, *26*, 263–269, doi:10.1111/EXD.13207.

[62] Šimo, L.; Kazimirova, M.; Richardson, J.; Bonnet, S.I. The Essential Role of Tick Salivary Glands and Saliva in Tick Feeding and Pathogen Transmission. *Front Cell Infect Microbiol* **2017**, *7*, doi:10.3389/fcimb.2017.00281.

[63] Grandjean, O.; Aeschlimann, A. Contribution to the Study of Digestion in Ticks: Histology and Fine Structure of the Midgut Epithelium of Ornithodorus Moubata, Murray (Ixodoidea, Argasidae). **1973**.

[64] Harrison, F.W..; Foelix, R.F.. Chelicerate Arthropoda. **1999**, 1116.

[65] Sojka, D.; Franta, Z.; Horn, M.; Caffrey, C.R.; Mareš, M.; Kopáček, P. New Insights into the Machinery of Blood Digestion by Ticks. *Trends Parasitol* **2013**, *29*, 276–285, doi:10.1016/J.PT.2013.04.002.

[66] Lara, F.A.; Lins, U.; Bechara, G.H.; Oliveira, P.L. Tracing Heme in a Living Cell: Hemoglobin Degradation and Heme Traffic in Digest Cells of the Cattle Tick Boophilus Microplus. *J Exp Biol* **2005**, *208*, 3093–3101, doi:10.1242/JEB.01749.

[67] Vincent, S.H.; Grady, R.W.; Shaklai, N.; Snider, J.M.; Muller-Eberhard, U. The Influence of Heme-Binding Proteins in Heme-Catalyzed Oxidations. *Arch Biochem Biophys* **1988**, *265*, 539–550, doi:10.1016/0003-9861(88)90159-2.

[68] Lara, F.; Lins, U.; ... G.P.-S.-J. of; 2003, undefined A New Intracellular Pathway of Haem Detoxification in the Midgut of the Cattle Tick Boophilus Microplus: Aggregation inside a Specialized Organelle, the Hemosome. *journals.biologists.comFA Lara, U Lins, G Paiva-Silva, IC Almeida, CM*

Braga, FC Miguens, PL OliveiraJournal of Experimental Biology, 2003•journals.biologists.com **2003**, doi:10.1242/jeb.00334.

[69] Bowman, A.S.; Sauer, J.R. Tick Salivary Glands: Function, Physiology and Future. *Parasitology* **2004**, *129 Suppl*, doi:10.1017/S0031182004006468.

[70] Needham, G.R.; Rosell, R.; Greenwald, L. Ultrastructure of Type-I Salivary-Gland Acini in Four Species of Ticks and the Influence of Hydration States on the Type-I Acini of Amblyomma Americanum. *Exp Appl Acarol* **1990**, *10*, 83–104, doi:10.1007/BF01194085/METRICS.

[71] Tatchell, R.J. Salivary Secretion in the Cattle Tick as a Means of Water Elimination. *Nature 1967 213:5079* **1967**, *213*, 940–941, doi:10.1038/213940a0.

[72] Kim, D.; Urban, J.; Boyle, D.L.; Park, Y. Multiple Functions of Na/K-ATPase in Dopamine-Induced Salivation of the Blacklegged Tick, Ixodes Scapularis. *Sci Rep* **2016**, *6*, doi:10.1038/SREP21047.

[73] Kim, D.; Maldonado-Ruiz, P.; Zurek, L.; Park, Y. Water Absorption through Salivary Gland Type I Acini in the Blacklegged Tick, Ixodes Scapularis. *PeerJ* **2017**, *2017*, e3984, doi:10.7717/PEERJ.3984/SUPP-10.

[74] Gaede, K.; Knülle, W. On the Mechanism of Water Vapour Sorption from Unsaturated Atmospheres by Ticks. *J Exp Biol* **1997**, *200*, 1491–1498, doi:10.1242/JEB.200.10.1491.

[75] Lees, K.; Bowman, A.S. Tick Neurobiology: Recent Advances and the Post-Genomic Era. *Invertebrate Neuroscience* **2007**, *7*, 183–198, doi:10.1007/S10158-007-0060-4/FIGURES/7.

[76] Šimo, L.; Koči, J.; Žitňan, D.; Park, Y. Evidence for D1 Dopamine Receptor Activation by a Paracrine Signal of Dopamine in Tick Salivary Glands. *PLoS One* **2011**, *6*, e16158, doi:10.1371/JOURNAL.PONE.0016158.

[77] Decrem, Y.; Rath, G.; Blasioli, V.; Cauchie, P.; Robert, S.; Beaufays, J.; Frère, J.-M.; Feron, O.; Dogné, J.-M.; Dessy, C.; et al. Ir-CPI, a Coagulation Contact Phase Inhibitor from the Tick Ixodes Ricinus, Inhibits Thrombus Formation without Impairing Hemostasis. *J Exp Med* **2009**, *206*, 2381–2395, doi:10.1084/jem.20091007.

[78] Chmelar, J.; Calvo, E.; Pedra, J.H.F.; Francischetti, I.M.B.; Kotsyfakis, M. Tick Salivary Secretion as a Source of Antihemostatics. *J Proteomics* **2012**, *75*, 3842, doi:10.1016/J.JPROT.2012.04.026.

[79] Chmelar, J.; Oliveira, C.J.; Rezacova, P.; Francischetti, I.M.B.; Kovarova, Z.; Pejler, G.; Kopacek, P.; Ribeiro, J.M.C.; Mares, M.; Kopecky, J.; et al. A Tick Salivary Protein Targets Cathepsin G and Chymase and Inhibits Host Inflammation and Platelet Aggregation. *Blood* **2011**, *117*, 736–744, doi:10.1182/blood-2010-06-293241.

[80] Schroeder, H.; Daix, V.; Gillet, L.; Renauld, J.-C.; Vanderplasschen, A. The Paralogous Salivary Anti-Complement Proteins IRAC I and IRAC II Encoded by Ixodes Ricinus Ticks Have Broad and Complementary Inhibitory Activities against the Complement of Different Host Species. *Microbes Infect* **2007**, *9*, 247–250, doi:10.1016/j.micinf.2006.10.020.

[81] Beaufays, J.; Adam, B.; Menten-Dedoyart, C.; Fievez, L.; Grosjean, A.; Decrem, Y.; Prévôt, P.-P.; Santini, S.; Brasseur, R.; Brossard, M.; et al. Ir-LBP, an Ixodes Ricinus Tick Salivary LTB4-Binding Lipocalin, Interferes with Host Neutrophil Function. *PLoS One* **2008**, *3*, e3987, doi:10.1371/journal.pone.0003987.

[82] Leboulle, G.; Crippa, M.; Decrem, Y.; Mejri, N.; Brossard, M.; Bollen, A.; Godfroid, E. Characterization of a Novel Salivary Immunosuppressive Protein from Ixodes Ricinus Ticks. *J Biol Chem* **2002**, *277*, 10083–10089, doi:10.1074/jbc.M111391200.

[83] Hannier, S.; Liversidge, J.; Sternberg, J.M.; Bowman, A.S. Characterization of the B-Cell Inhibitory Protein Factor in Ixodes Ricinus Tick Saliva: A Potential Role in Enhanced Borrelia Burgdoferi Transmission. *Immunology* **2004**, *113*, 401–408, doi:10.1111/j.1365-2567.2004.01975.x.

[84] Liu, J.; Renneker, S.; Beyer, D.; Kullmann, B.; Seitzer, U.; Ahmed, J.; Bakheit, M.A. Identification and Partial Characterization of a Salp15 Homolog from Ixodes Ricinus. *Ticks Tick Borne Dis* **2014**, *5*, 318–322, doi:10.1016/j.ttbdis.2013.12.004.

[85] Zhou, W.; Woodson, M.; Neupane, B.; Bai, F.; Sherman, M.B.; Choi, K.H.; Neelakanta, G.; Sultana, H. Exosomes Serve as Novel Modes of Tick-Borne Flavivirus Transmission from Arthropod to Human Cells and Facilitates Dissemination of Viral RNA and Proteins to the Vertebrate Neuronal Cells. *PLoS Pathog* **2018**, *14*, e1006764, doi:10.1371/JOURNAL.PPAT.1006764.

[86] Zhou, W.; Tahir, F.; Wang, J.C.Y.; Woodson, M.; Sherman, M.B.; Karim, S.; Neelakanta, G.; Sultana, H. Discovery of Exosomes From Tick Saliva and Salivary Glands Reveals Therapeutic Roles for CXCL12 and IL-8 in Wound Healing at the Tick–Human Skin Interface. *Front Cell Dev Biol* **2020**, *8*, 511273, doi:10.3389/FCELL.2020.00554/BIBTEX.

[87] Van Niel, G.; D'Angelo, G.; Raposo, G. Shedding Light on the Cell Biology of Extracellular Vesicles. *Nature Reviews Molecular Cell Biology 2018 19:4* **2018**, *19*, 213–228, doi:10.1038/nrm.2017.125.

[88] Nawaz, M.; Malik, M.I.; Zhang, H.; Hassan, I.A.; Cao, J.; Zhou, Y.; Hameed, M.; Hussain Kuthu, Z.; Zhou, J. Proteomic Analysis of Exosome-Like Vesicles Isolated From Saliva of the Tick Haemaphysalis Longicornis. *Front Cell Infect Microbiol* **2020**, *10*, 542319, doi:10.3389/FCIMB.2020.542319/BIBTEX.

[89] Oliva Chávez, A.S.; Wang, X.; Marnin, L.; Archer, N.K.; Hammond, H.L.; Carroll, E.E.M.C.; Shaw, D.K.; Tully, B.G.; Buskirk, A.D.; Ford, S.L.; et al. Tick Extracellular Vesicles Enable Arthropod Feeding and Promote Distinct Outcomes of Bacterial Infection. *Nature Communications 2021 12:1* **2021**, *12*, 1–17, doi:10.1038/s41467-021-23900-8.

[90] Butler, L.R.; Gonzalez, J.; Pedra, J.H.F.; Oliva Chavez, A.S. Tick Extracellular Vesicles in Host Skin Immunity and Pathogen Transmission. *Trends Parasitol* **2023**, *39*, 873–885, doi:10.1016/J.PT.2023.07.009.

[91] Nawaz, M.; Malik, M.I.; Hameed, M.; Zhou, J. Research Progress on the Composition and Function of Parasite-Derived Exosomes. *Acta Trop* **2019**, *196*, 30–36, doi:10.1016/J.ACTATROPICA.2019.05.004.

[92] Zhang, P.; Wu, W.; Chen, Q.; Chen, M. Non-Coding RNAs and Their Integrated Networks. *J Integr Bioinform* **2019**, *16*, 20190027, doi:10.1515/JIB-2019-0027.

[93] Lander, E.S.; Linton, L.M.; Birren, B.; Nusbaum, C.; Zody, M.C.; Baldwin, J.; Devon, K.; Dewar, K.; Doyle, M.; Fitzhugh, W.; et al. Initial Sequencing and Analysis of the Human Genome. *Nature* **2001**, *409*, 860–921, doi:10.1038/35057062.

[94] Carninci, P.; Kasukawa, T.; Katayama, S.; Gough, J.; Frith, M.C.; Maeda, N.; Oyama, R.; Ravasi, T.; Lenhard, B.; Wells, C.; et al. Molecular Biology: The Transcriptional Landscape of the Mammalian Genome. *Science (1979)* **2005**, *309*, 1559–1563, doi:10.1126/SCIENCE.1112014.

[95] Chen, Q.; Meng, X.; Liao, Q.; Chen, M. Versatile Interactions and Bioinformatics Analysis of Noncoding RNAs. *Brief Bioinform* **2019**, *20*, 1781–1794, doi:10.1093/BIB/BBY050.

[96] Chen, L.L.; Kim, V.N. Small and Long Non-Coding RNAs: Past, Present, and Future. *Cell* **2024**, *187*, 6451–6485, doi:10.1016/J.CELL.2024.10.024.

[97] Ahmad, P.; Bensaoud, C.; Mekki, I.; Rehman, M.U.; Kotsyfakis, M. Long Non-Coding RNAs and Their Potential Roles in the Vector–Host–Pathogen Triad. *Life 2021, Vol. 11, Page 56* **2021**, *11*, 56, doi:10.3390/LIFE11010056.

[98] Bartel, D.P. Metazoan MicroRNAs. *Cell* **2018**, *173*, 20–51, doi:10.1016/j.cell.2018.03.006.

[99] Grimson, A.; Srivastava, M.; Fahey, B.; Woodcroft, B.J.; Chiang, H.R.; King, N.; Degnan, B.M.; Rokhsar, D.S.; Bartel, D.P. Early Origins and Evolution of MicroRNAs and Piwi-Interacting RNAs in Animals. *Nature* **2008**, *455*, 1193–1197, doi:10.1038/nature07415.

[100] Tüfekci, K.U.; Meuwissen, R.L.J.; Genç, Ş. The Role of MicroRNAs in Biological Processes. In; Humana Press, Totowa, NJ, 2014; pp. 15–31 ISBN 978-1-62703-748-8.

[101] Lewis, B.P.; Shih, I.; Jones-Rhoades, M.W.; Bartel, D.P.; Burge, C.B. Prediction of Mammalian MicroRNA Targets. *Cell* **2003**, *115*, 787–798, doi:10.1016/s0092-8674(03)01018-3.

[102] Friedman, R.C.; Farh, K.K.-H.; Burge, C.B.; Bartel, D.P. Most Mammalian MRNAs Are Conserved Targets of MicroRNAs. *Genome Res* **2009**, *19*, 92–105, doi:10.1101/gr.082701.108.

[103] BP, L.; CB, B.; DP, B. Conserved Seed Pairing, Often Flanked by Adenosines, Indicates That Thousands of Human Genes Are MicroRNA Targets. *Cell* **2005**, *120*, doi:10.1016/J.CELL.2004.12.035.

[104] Ha, M.; Kim, V.N. Regulation of MicroRNA Biogenesis. *Nat Rev Mol Cell Biol* **2014**, *15*, 509–524, doi:10.1038/nrm3838.

[105] Kim, Y.-K.; Kim, V.N. Processing of Intronic MicroRNAs. *EMBO J* **2007**, *26*, 775–783, doi:10.1038/sj.emboj.7601512.

[106] de Rie, D.; Abugessaisa, I.; Alam, T.; Arner, E.; Arner, P.; Ashoor, H.; Åström, G.; Babina, M.; Bertin, N.; Burroughs, A.M.; et al. An Integrated Expression Atlas of MiRNAs and Their Promoters in Human and Mouse. *Nat Biotechnol* **2017**, *35*, 872–878, doi:10.1038/nbt.3947.

[107] Tanzer, A.; Stadler, P.F. Molecular Evolution of a MicroRNA Cluster. *J Mol Biol* **2004**, *339*, 327–335, doi:10.1016/j.jmb.2004.03.065.

[108] O'Brien, J.; Hayder, H.; Zayed, Y.; Peng, C. Overview of MicroRNA Biogenesis, Mechanisms of Actions, and Circulation. *Front Endocrinol (Lausanne)* **2018**, *9*, 388354, doi:10.3389/fendo.2018.00402.

[109] Denli, A.M.; Tops, B.B.J.; Plasterk, R.H.A.; Ketting, R.F.; Hannon, G.J. Processing of Primary MicroRNAs by the Microprocessor Complex. *Nature* **2004**, *432*, 231–235, doi:10.1038/nature03049.

[110] Han, J.; Lee, Y.; Yeom, K.-H.; Kim, Y.-K.; Jin, H.; Kim, V.N. The Drosha-DGCR8 Complex in Primary MicroRNA Processing. *Genes Dev* **2004**, *18*, 3016–3027, doi:10.1101/gad.1262504.

[111] Alarcón, C.R.; Lee, H.; Goodarzi, H.; Halberg, N.; Tavazoie, S.F. N6-Methyladenosine Marks Primary MicroRNAs for Processing. *Nature* **2015**, *519*, 482–485, doi:10.1038/nature14281.

[112] Kim, K.; Baek, S.C.; Lee, Y.-Y.; Bastiaanssen, C.; Kim, J.; Kim, H.; Kim, V.N. A Quantitative Map of Human Primary MicroRNA Processing Sites. *Mol Cell* **2021**, *81*, 3422-3439.e11, doi:10.1016/j.molcel.2021.07.002.

[113] Okada, C.; Yamashita, E.; Lee, S.J.; Shibata, S.; Katahira, J.; Nakagawa, A.; Yoneda, Y.; Tsukihara, T. A High-Resolution Structure of the Pre-MicroRNA

Nuclear Export Machinery. *Science* **2009**, *326*, 1275–1279, doi:10.1126/science.1178705.

[114] Zhang, H.; Kolb, F.A.; Jaskiewicz, L.; Westhof, E.; Filipowicz, W. Single Processing Center Models for Human Dicer and Bacterial RNase III. *Cell* **2004**, *118*, 57–68, doi:10.1016/j.cell.2004.06.017.

[115] M, Y.; T, K.; Z, P.; X, Y.; S, I.; Q, L.; Y, T. ATP-Dependent Human RISC Assembly Pathways. *Nat Struct Mol Biol* **2010**, *17*, doi:10.1038/NSMB.1733.

[116] Kawamata, T.; Tomari, Y. Making RISC. *Trends Biochem Sci* **2010**, *35*, 368–376, doi:10.1016/j.tibs.2010.03.009.

[117] Ruby, J.G.; Jan, C.H.; Bartel, D.P. Intronic MicroRNA Precursors That Bypass Drosha Processing. *Nature* **2007**, *448*, 83–86, doi:10.1038/nature05983.

[118] Babiarz, J.E.; Ruby, J.G.; Wang, Y.; Bartel, D.P.; Blelloch, R. Mouse ES Cells Express Endogenous ShRNAs, SiRNAs, and Other Microprocessor-Independent, Dicer-Dependent Small RNAs. *Genes Dev* **2008**, *22*, 2773–2785, doi:10.1101/gad.1705308.

[119] Xie, M.; Li, M.; Vilborg, A.; Lee, N.; Shu, M.-D.; Yartseva, V.; Šestan, N.; Steitz, J.A. Mammalian 5'-Capped MicroRNA Precursors That Generate a Single MicroRNA. *Cell* **2013**, *155*, 1568–1580, doi:10.1016/j.cell.2013.11.027.

[120] Yang, J.-S.; Maurin, T.; Robine, N.; Rasmussen, K.D.; Jeffrey, K.L.; Chandwani, R.; Papapetrou, E.P.; Sadelain, M.; O'Carroll, D.; Lai, E.C. Conserved Vertebrate Mir-451 Provides a Platform for Dicer-Independent, Ago2-Mediated MicroRNA Biogenesis. *Proc Natl Acad Sci U S A* **2010**, *107*, 15163–15168, doi:10.1073/pnas.1006432107.

[121] Cheloufi, S.; Dos Santos, C.O.; Chong, M.M.W.; Hannon, G.J. A Dicer-Independent MiRNA Biogenesis Pathway That Requires Ago Catalysis. *Nature* **2010**, *465*, 584–589, doi:10.1038/nature09092.

[122] DaCunza, J.T.; Wickman, J.R.; Ajit, S.K. MiRNA Packaging into Small Extracellular Vesicles and Implications in Pain. *Pain Rep* **2024**, *9*, e1198, doi:10.1097/PR9.0000000000001198.

[123] Teng, Y.; Ren, Y.; Hu, X.; Mu, J.; Samykutty, A.; Zhuang, X.; Deng, Z.; Kumar, A.; Zhang, L.; Merchant, M.L.; et al. MVP-Mediated Exosomal Sorting of MiR-193a Promotes Colon Cancer Progression. *Nat Commun* **2017**, *8*, 14448, doi:10.1038/ncomms14448.

[124] McKenzie, A.J.; Hoshino, D.; Hong, N.H.; Cha, D.J.; Franklin, J.L.; Coffey, R.J.; Patton, J.G.; Weaver, A.M. KRAS-MEK Signaling Controls Ago2 Sorting into Exosomes. *Cell Rep* **2016**, *15*, 978–987, doi:10.1016/j.celrep.2016.03.085.

[125] Mukherjee, K.; Ghoshal, B.; Ghosh, S.; Chakrabarty, Y.; Shwetha, S.; Das, S.; Bhattacharyya, S.N. Reversible HuR-MicroRNA Binding Controls Extracellular Export of MiR-122 and Augments Stress Response. *EMBO Rep* **2016**, *17*, 1184–1203, doi:10.15252/embr.201541930.

[126] Wozniak, A.L.; Adams, A.; King, K.E.; Dunn, W.; Christenson, L.K.; Hung, W.-T.; Weinman, S.A. The RNA Binding Protein FMR1 Controls Selective Exosomal MiRNA Cargo Loading during Inflammation. *J Cell Biol* **2020**, *219*, e201912074, doi:10.1083/jcb.201912074.

[127] Villarroya-Beltri, C.; Gutiérrez-Vázquez, C.; Sánchez-Cabo, F.; Pérez-Hernández, D.; Vázquez, J.; Martin-Cofreces, N.; Martinez-Herrera, D.J.; Pascual-Montano, A.; Mittelbrunn, M.; Sánchez-Madrid, F. Sumoylated HnRNPA2B1 Controls the Sorting of MiRNAs into Exosomes through

Binding to Specific Motifs. *Nat Commun* **2013**, *4*, 2980, doi:10.1038/ncomms3980.

[128] D, K.-L.; M, H.; IV, B.; MAJ, van E.; P, S.; D, S.; N, Z.; JM, M.; B, Y.; RX, de M.; et al. Nontemplated Nucleotide Additions Distinguish the Small RNA Composition in Cells from Exosomes. *Cell Rep* **2014**, *8*, doi:10.1016/J.CELREP.2014.08.027.

[129] Villarroya-Beltri, C.; Gutiérrez-Vázquez, C.; Sánchez-Cabo, F.; Pérez-Hernández, D.; Vázquez, J.; Martin-Cofreces, N.; Martinez-Herrera, D.J.; Pascual-Montano, A.; Mittelbrunn, M.; Sánchez-Madrid, F. Sumoylated HnRNPA2B1 Controls the Sorting of MiRNAs into Exosomes through Binding to Specific Motifs. *Nat Commun* **2013**, *4*, 2980, doi:10.1038/ncomms3980.

[130] Santangelo, L.; Giurato, G.; Cicchini, C.; Montaldo, C.; Mancone, C.; Tarallo, R.; Battistelli, C.; Alonzi, T.; Weisz, A.; Tripodi, M. The RNA-Binding Protein SYNCRIP Is a Component of the Hepatocyte Exosomal Machinery Controlling MicroRNA Sorting. *Cell Rep* **2016**, *17*, 799–808, doi:10.1016/j.celrep.2016.09.031.

[131] Hobor, F.; Dallmann, A.; Ball, N.J.; Cicchini, C.; Battistelli, C.; Ogrodowicz, R.W.; Christodoulou, E.; Martin, S.R.; Castello, A.; Tripodi, M.; et al. A Cryptic RNA-Binding Domain Mediates Syncrip Recognition and Exosomal Partitioning of MiRNA Targets. *Nat Commun* **2018**, *9*, 831, doi:10.1038/s41467-018-03182-3.

[132] Alberti, S.; Gladfelter, A.; Mittag, T. Considerations and Challenges in Studying Liquid-Liquid Phase Separation and Biomolecular Condensates. *Cell* **2019**, *176*, 419–434, doi:10.1016/j.cell.2018.12.035.

[133] Bartel, D.P. MicroRNAs: Target Recognition and Regulatory Functions. *Cell* **2009**, *136*, 215–233, doi:10.1016/j.cell.2009.01.002.

[134] Kozomara, A.; Birgaoanu, M.; Griffiths-Jones, S. MiRBase: From MicroRNA Sequences to Function. *Nucleic Acids Res* **2019**, *47*, D155–D162, doi:10.1093/nar/gky1141.

[135] Behm-Ansmant, I.; Rehwinkel, J.; Izaurralde, E. MicroRNAs Silence Gene Expression by Repressing Protein Expression and/or by Promoting MRNA Decay. *Cold Spring Harb Symp Quant Biol* **2006**, *71*, 523–530, doi:10.1101/sqb.2006.71.013.

[136] AO, S.; SW, E.; GR, C.; H, S.; DP, B. Poly(A)-Tail Profiling Reveals an Embryonic Switch in Translational Control. *Nature* **2014**, *508*, doi:10.1038/NATURE13007.

[137] Eichhorn, S.W.; Guo, H.; McGeary, S.E.; Rodriguez-Mias, R.A.; Shin, C.; Baek, D.; Hsu, S.-H.; Ghoshal, K.; Villén, J.; Bartel, D.P. MRNA Destabilization Is the Dominant Effect of Mammalian MicroRNAs by the Time Substantial Repression Ensues. *Mol Cell* **2014**, *56*, 104–115, doi:10.1016/j.molcel.2014.08.028.

[138] Grimson, A.; Farh, K.K.H.; Johnston, W.K.; Garrett-Engele, P.; Lim, L.P.; Bartel, D.P. MicroRNA Targeting Specificity in Mammals: Determinants beyond Seed Pairing. *Mol Cell* **2007**, *27*, 91–105, doi:10.1016/J.MOLCEL.2007.06.017.

[139] Loeb, G.B.; Khan, A.A.; Canner, D.; Hiatt, J.B.; Shendure, J.; Darnell, R.B.; Leslie, C.S.; Rudensky, A.Y. Transcriptome-Wide MiR-155 Binding Map Reveals Widespread Noncanonical MicroRNA Targeting. *Mol Cell* **2012**, *48*, 760–770, doi:10.1016/j.molcel.2012.10.002.

[140] Helwak, A.; Kudla, G.; Dudnakova, T.; Tollervey, D. Mapping the Human MiRNA Interactome by CLASH Reveals Frequent Noncanonical Binding. *Cell* **2013**, *153*, 654–665, doi:10.1016/j.cell.2013.03.043.

[141] Moore, M.J.; Scheel, T.K.H.; Luna, J.M.; Park, C.Y.; Fak, J.J.; Nishiuchi, E.; Rice, C.M.; Darnell, R.B. MiRNA-Target Chimeras Reveal MiRNA 3'-End Pairing as a Major Determinant of Argonaute Target Specificity. *Nat Commun* **2015**, *6*, 8864, doi:10.1038/ncomms9864.

[142] McGeary, S.E.; Lin, K.S.; Shi, C.Y.; Pham, T.M.; Bisaria, N.; Kelley, G.M.; Bartel, D.P. The Biochemical Basis of MicroRNA Targeting Efficacy. *Science* **2019**, *366*, doi:10.1126/science.aav1741.

[143] Kilikevicius, A.; Meister, G.; Corey, D.R. Reexamining Assumptions about MiRNA-Guided Gene Silencing. *Nucleic Acids Res* **2021**, doi:10.1093/nar/gkab1256.

[144] Arvey, A.; Larsson, E.; Sander, C.; Leslie, C.S.; Marks, D.S. Target MRNA Abundance Dilutes MicroRNA and SiRNA Activity. *Mol Syst Biol* **2010**, *6*, 363, doi:10.1038/msb.2010.24.

[145] Garcia, D.M.; Baek, D.; Shin, C.; Bell, G.W.; Grimson, A.; Bartel, D.P. Weak Seed-Pairing Stability and High Target-Site Abundance Decrease the Proficiency of Lsy-6 and Other MicroRNAs. *Nat Struct Mol Biol* **2011**, *18*, 1139–1146, doi:10.1038/nsmb.2115.

[146] Sætrom, P.; Heale, B.S.E.; Snøve, O.; Aagaard, L.; Alluin, J.; Rossi, J.J. Distance Constraints between MicroRNA Target Sites Dictate Efficacy and Cooperativity. *Nucleic Acids Res* **2007**, *35*, 2333–2342, doi:10.1093/NAR/GKM133.

[147] Briskin, D.; Wang, P.Y.; Bartel, D.P. The Biochemical Basis for the Cooperative Action of MicroRNAs. *Proc Natl Acad Sci U S A* **2020**, *117*, 17764–17774, doi:10.1073/PNAS.1920404117/-/DCSUPPLEMENTAL.

[148] Sheu-Gruttadauria, J.; MacRae, I.J. Phase Transitions in the Assembly and Function of Human MiRISC. *Cell* **2018**, *173*, 946-957.e16,

doi:10.1016/J.CELL.2018.02.051/ATTACHMENT/1D1977E6-4FC8-41F0-9B8E-5637B0AE2312/MMC3.MP4.

[149] Briskin, D.; Wang, P.Y.; Bartel, D.P. The Biochemical Basis for the Cooperative Action of MicroRNAs. *Proc Natl Acad Sci U S A* **2020**, *117*, 17764–17774, doi:10.1073/PNAS.1920404117/SUPPL_FILE/PNAS.1920404117.SAPP.PDF.

[150] Diener, C.; Hart, M.; Fecher-Trost, C.; Knittel, J.; Rheinheimer, S.; Meyer, M.R.; Mayer, J.; Flockerzi, V.; Keller, A.; Meese, E. Outside the Limit: Questioning the Distance Restrictions for Cooperative MiRNA Binding Sites. *Cell Mol Biol Lett* **2023**, *28*, doi:10.1186/S11658-023-00421-4.

[151] Leal-Galvan, B.; Kumar, D.; Karim, S.; Saelao, P.; Thomas, D.B.; Oliva Chavez, A. A Glimpse into the World of MicroRNAs and Their Putative Roles in Hard Ticks. *Front Cell Dev Biol* **2024**, *12*, 1460705, doi:10.3389/fcell.2024.1460705.

[152] Liu, J.; Zhu, L.; Wang, J.; Qiu, L.; Chen, Y.; Davis, R.E.; Cheng, G. Schistosoma Japonicum Extracellular Vesicle MiRNA Cargo Regulates Host Macrophage Functions Facilitating Parasitism. *PLoS Pathog* **2019**, *15*, e1007817, doi:10.1371/journal.ppat.1007817.

[153] Liu, X.; Jin, S.; Liu, J.; Xu, X. MiR-223-3p Overexpressed Adipose Mesenchymal Stem Cell-Derived Exosomes Promote Wound Healing via Targeting MAPK10. *Acta Histochem* **2023**, *125*, 152102, doi:10.1016/j.acthis.2023.152102.

[154] Arcà, B.; Colantoni, A.; Fiorillo, C.; Severini, F.; Benes, V.; Di Luca, M.; Calogero, R.A.; Lombardo, F. MicroRNAs from Saliva of Anopheline Mosquitoes Mimic Human Endogenous MiRNAs and May Contribute to

Vector-Host-Pathogen Interactions. *Sci Rep* **2019**, *9*, 2955, doi:10.1038/s41598-019-39880-1.

[155] Diener, C.; Keller, A.; Meese, E. Emerging Concepts of MiRNA Therapeutics: From Cells to Clinic. *Trends Genet* **2022**, *38*, 613–626, doi:10.1016/j.tig.2022.02.006.

[156] R, G.; G, M.; CM, C. Targeting MicroRNAs in Cancer: Rationale, Strategies and Challenges. *Nat Rev Drug Discov* **2010**, *9*, doi:10.1038/NRD3179.

[157] Bader, A.G.; Brown, D.; Stoudemire, J.; Lammers, P. Developing Therapeutic MicroRNAs for Cancer. *Gene Ther* **2011**, *18*, 1121–1126, doi:10.1038/gt.2011.79.

[158] Thorsen, S.B.; Obad, S.; Jensen, N.F.; Stenvang, J.; Kauppinen, S. The Therapeutic Potential of MicroRNAs in Cancer. *Cancer J* **2012**, *18*, 275–284, doi:10.1097/PPO.0b013e318258b5d6.

[159] van Rooij, E.; Kauppinen, S. Development of MicroRNA Therapeutics Is Coming of Age. *EMBO Mol Med* **2014**, *6*, 851–864, doi:10.15252/emmm.201100899.

[160] Lennox, K.A.; Behlke, M.A. Chemical Modification and Design of Anti-MiRNA Oligonucleotides. *Gene Ther* **2011**, *18*, 1111–1120, doi:10.1038/gt.2011.100.

[161] Seyhan, A.A. Trials and Tribulations of MicroRNA Therapeutics. *Int J Mol Sci* **2024**, *25*, 1469, doi:10.3390/ijms25031469.

[162] Aounallah, H.; Bensaoud, C.; M'ghirbi, Y.; Faria, F.; Chmelar, J.I.; Kotsyfakis, M. Tick Salivary Compounds for Targeted Immunomodulatory Therapy. *Front Immunol* **2020**, *11*, 583845, doi:10.3389/fimmu.2020.583845.

[163] Lou, G.; Chen, L.; Xia, C.; Wang, W.; Qi, J.; Li, A.; Zhao, L.; Chen, Z.; Zheng, M.; Liu, Y. MiR-199a-Modified Exosomes from Adipose Tissue-Derived Mesenchymal Stem Cells Improve Hepatocellular Carcinoma Chemosensitivity through MTOR Pathway. *J Exp Clin Cancer Res* **2020**, *39*, 4, doi:10.1186/s13046-019-1512-5.

[164] Hu, J.; Jiang, Y.; Wu, X.; Wu, Z.; Qin, J.; Zhao, Z.; Li, B.; Xu, Z.; Lu, X.; Wang, X.; et al. Exosomal MiR-17-5p from Adipose-Derived Mesenchymal Stem Cells Inhibits Abdominal Aortic Aneurysm by Suppressing TXNIP-NLRP3 Inflammasome. *Stem Cell Res Ther* **2022**, *13*, 349, doi:10.1186/s13287-022-03037-1.

[165] JH, Z.; T, Z.; QY, L.; HS, G. Trans-Kingdom RNAs and Their Fates in Recipient Cells: Advances, Utilization, and Perspectives. *Plant Commun* **2021**, *2*, doi:10.1016/J.XPLC.2021.100167.

[166] Bordoloi, K.S.; Agarwala, N. MicroRNAs in Plant Insect Interaction and Insect Pest Control. *Plant Gene* **2021**, *26*, 100271, doi:10.1016/j.plgene.2021.100271.

[167] Zhang, Q.; Dou, W.; Taning, C.N.T.; Smagghe, G.; Wang, J.-J. Regulatory Roles of MicroRNAs in Insect Pests: Prospective Targets for Insect Pest Control. *Curr Opin Biotechnol* **2021**, *70*, 158–166, doi:10.1016/j.copbio.2021.05.002.

[168] Boulanger, N.; Insonere, J.-L.-M.; Van Blerk, S.; Barthel, C.; Serres, C.; Rais, O.; Roulet, A.; Servant, F.; Duron, O.; Lelouvier, B. Cross-Alteration of Murine Skin and Tick Microbiome Concomitant with Pathogen Transmission after Ixodes Ricinus Bite. *Microbiome* **2023**, *11*, 250, doi:10.1186/s40168-023-01696-7.

[169] Dempsey, J.L.; Cui, J.Y. Long Non-Coding RNAs: A Novel Paradigm for Toxicology. *Toxicological Sciences* **2017**, *155*, 3–21, doi:10.1093/TOXSCI/KFW203.

[170] Wang, K.C.; Chang, H.Y. Molecular Mechanisms of Long Noncoding RNAs. *Mol Cell* **2011**, *43*, 904–914, doi:10.1016/J.MOLCEL.2011.08.018.

[171] Mariner, P.D.; Walters, R.D.; Espinoza, C.A.; Drullinger, L.F.; Wagner, S.D.; Kugel, J.F.; Goodrich, J.A. Human Alu RNA Is a Modular Transacting Repressor of MRNA Transcription during Heat Shock. *Mol Cell* **2008**, *29*, 499–509, doi:10.1016/J.MOLCEL.2007.12.013.

[172] Kern, C.; Wang, Y.; Chitwood, J.; Korf, I.; Delany, M.; Cheng, H.; Medrano, J.F.; Van Eenennaam, A.L.; Ernst, C.; Ross, P.; et al. Genome-Wide Identification of Tissue-Specific Long Non-Coding RNA in Three Farm Animal Species 06 Biological Sciences 0604 Genetics. *BMC Genomics* **2018**, *19*, 1–14, doi:10.1186/S12864-018-5037-7/FIGURES/4.

[173] Bayer-Santos, E.; Marini, M.M.; da Silveira, J.F. Non-Coding RNAs in Host–Pathogen Interactions: Subversion of Mammalian Cell Functions by Protozoan Parasites. *Front Microbiol* **2017**, *8*, doi:10.3389/FMICB.2017.00474.

[174] Bensaoud, C.; Hackenberg, M.; Kotsyfakis, M. Noncoding RNAs in Parasite–Vector–Host Interactions. *Trends Parasitol* **2019**, *35*, 715–724, doi:10.1016/J.PT.2019.06.012.

[175] Ahmad, P.; Bensaoud, C.; Mekki, I.; Rehman, M.U.; Kotsyfakis, M. Long Non-Coding RNAs and Their Potential Roles in the Vector-Host-Pathogen Triad. *Life (Basel)* **2021**, *11*, 1–12, doi:10.3390/LIFE11010056.

[176] Cerqueira de Araujo, A.; Noel, B.; Bretaudeau, A.; Labadie, K.; Boudet, M.; Tadrent, N.; Istace, B.; Kritli, S.; Cruaud, C.; Olaso, R.; et al. Genome

Sequences of Four Ixodes Species Expands Understanding of Tick Evolution. *BMC Biol* **2025**, *23*, 17, doi:10.1186/s12915-025-02121-1.

[177] Benson, D.A.; Cavanaugh, M.; Clark, K.; Karsch-Mizrachi, I.; Lipman, D.J.; Ostell, J.; Sayers, E.W. GenBank. *Nucleic Acids Res* **2013**, *41*, D36-42, doi:10.1093/nar/gks1195.

[178] Nassar, L.R.; Barber, G.P.; Benet-Pagès, A.; Casper, J.; Clawson, H.; Diekhans, M.; Fischer, C.; Gonzalez, J.N.; Hinrichs, A.S.; Lee, B.T.; et al. The UCSC Genome Browser Database: 2023 Update. *Nucleic Acids Res* **2023**, *51*, D1188–D1195, doi:10.1093/nar/gkac1072.

[179] Harrison, P.W.; Amode, M.R.; Austine-Orimoloye, O.; Azov, A.G.; Barba, M.; Barnes, I.; Becker, A.; Bennett, R.; Berry, A.; Bhai, J.; et al. Ensembl 2024. *Nucleic Acids Res* **2024**, *52*, D891–D899, doi:10.1093/NAR/GKAD1049.

[180] Smedley, D.; Haider, S.; Ballester, B.; Holland, R.; London, D.; Thorisson, G.; Kasprzyk, A. BioMart – Biological Queries Made Easy. *BMC Genomics* **2009**, *10*, 22, doi:10.1186/1471-2164-10-22.

[181] Cramaro, W.J.; Revets, D.; Hunewald, O.E.; Sinner, R.; Reye, A.L.; Muller, C.P. Integration of Ixodes Ricinus Genome Sequencing with Transcriptome and Proteome Annotation of the Naïve Midgut. *BMC Genomics* **2015**, *16*, 871, doi:10.1186/s12864-015-1981-7.

[182] Fromm, B.; Høye, E.; Domanska, D.; Zhong, X.; Aparicio-Puerta, E.; Ovchinnikov, V.; Umu, S.U.; Chabot, P.J.; Kang, W.; Aslanzadeh, M.; et al. MirGeneDB 2.1: Toward a Complete Sampling of All Major Animal Phyla. *Nucleic Acids Res* **2021**, doi:10.1093/nar/gkab1101.

[183] Horká, H.; Černá-Kýčková, K.; Skallová, A.; Kopecký, J. Tick Saliva Affects Both Proliferation and Distribution of Borrelia Burgdorferi Spirochetes in

Mouse Organs and Increases Transmission of Spirochetes to Ticks. *International Journal of Medical Microbiology* **2009**, *299*, 373–380, doi:10.1016/J.IJMM.2008.10.009.

[184] Perner, J.; Kropáčková, S.; Kopáček, P.; Ribeiro, J.M.C. Sialome Diversity of Ticks Revealed by RNAseq of Single Tick Salivary Glands. *PLoS Negl Trop Dis* **2018**, *12*, e0006410, doi:10.1371/JOURNAL.PNTD.0006410.

[185] Charrier, N.P.; Couton, M.; Voordouw, M.J.; Rais, O.; Durand-Hermouet, A.; Hervet, C.; Plantard, O.; Rispe, C. Whole Body Transcriptomes and New Insights into the Biology of the Tick Ixodes Ricinus. *Parasit Vectors* **2018**, *11*, 364, doi:10.1186/s13071-018-2932-3.

[186] A, T.C.; F, F.; K, N.; T, W.; U, E.; M, K.; D, B.; S, E.-H.; C, T.; M, S.; et al. Inter-Laboratory Comparison of Extracellular Vesicle Isolation Based on Ultracentrifugation. *Transfus Med Hemother* **2021**, *48*, doi:10.1159/000508712.

[187] Nawrocki, E.P.; Eddy, S.R. Infernal 1.1: 100-Fold Faster RNA Homology Searches. *Bioinformatics* **2013**, *29*, 2933, doi:10.1093/BIOINFORMATICS/BTT509.

[188] Kalvari, I.; Nawrocki, E.P.; Ontiveros-Palacios, N.; Argasinska, J.; Lamkiewicz, K.; Marz, M.; Griffiths-Jones, S.; Toffano-Nioche, C.; Gautheret, D.; Weinberg, Z.; et al. Rfam 14: Expanded Coverage of Metagenomic, Viral and MicroRNA Families. *Nucleic Acids Res* **2021**, *49*, D192–D200, doi:10.1093/NAR/GKAA1047.

[189] Chan, P.P.; Lowe, T.M. TRNAscan-SE: Searching for TRNA Genes in Genomic Sequences. *Methods Mol Biol* **2019**, *1962*, 1, doi:10.1007/978-1-4939-9173-0_1.

[190] Kang, Y.J.; Yang, D.C.; Kong, L.; Hou, M.; Meng, Y.Q.; Wei, L.; Gao, G. CPC2: A Fast and Accurate Coding Potential Calculator Based on Sequence Intrinsic Features. *Nucleic Acids Res* **2017**, *45*, W12–W16, doi:10.1093/NAR/GKX428.

[191] Kent, W.J. BLAT--the BLAST-like Alignment Tool. *Genome Res* **2002**, *12*, 656–664, doi:10.1101/GR.229202.

[192] Pertea, G.; Pertea, M. GFF Utilities: GffRead and GffCompare. *F1000Res* **2020**, *9*, doi:10.12688/F1000RESEARCH.23297.2.

[193] Aparicio-Puerta, E.; Gómez-Martín, C.; Giannoukakos, S.; Medina, J.M.; Scheepbouwer, C.; García-Moreno, A.; Carmona-Saez, P.; Fromm, B.; Pegtel, M.; Keller, A.; et al. SRNAbench and SRNAtoolbox 2022 Update: Accurate MiRNA and SncRNA Profiling for Model and Non-Model Organisms. *Nucleic Acids Res* **2022**, *50*, W710–W717, doi:10.1093/NAR/GKAC363.

[194] Gulia-Nuss, M.; Nuss, A.B.; Meyer, J.M.; Sonenshine, D.E.; Roe, R.M.; Waterhouse, R.M.; Sattelle, D.B.; De La Fuente, J.; Ribeiro, J.M.; Megy, K.; et al. Genomic Insights into the Ixodes Scapularis Tick Vector of Lyme Disease. *Nature Communications 2016 7:1* **2016**, *7*, 1–13, doi:10.1038/ncomms10507.

[195] AW, C.; E, H.; AA, H.; VM, P.; J, V.; Ł, W.; I, B.; A, F.; V, O.; H, H.; et al. MirGeneDB 3.0: Improved Taxonomic Sampling, Uniform Nomenclature of Novel Conserved MicroRNA Families and Updated Covariance Models. *Nucleic Acids Res* **2025**, *53*, doi:10.1093/NAR/GKAE1094.

[196] Sayers, E.W.; Bolton, E.E.; Brister, J.R.; Canese, K.; Chan, J.; Comeau, D.C.; Connor, R.; Funk, K.; Kelly, C.; Kim, S.; et al. Database Resources of the National Center for Biotechnology Information. *Nucleic Acids Res* **2022**, *50*, D20–D26, doi:10.1093/nar/gkab1112.

[197] Grabherr, M.G.; Haas, B.J.; Yassour, M.; Levin, J.Z.; Thompson, D.A.; Amit, I.; Adiconis, X.; Fan, L.; Raychowdhury, R.; Zeng, Q.; et al. Trinity: Reconstructing a Full-Length Transcriptome without a Genome from RNA-Seq Data. *Nat Biotechnol* **2011**, *29*, 644, doi:10.1038/NBT.1883.

[198] Fu, L.; Niu, B.; Zhu, Z.; Wu, S.; Li, W. CD-HIT: Accelerated for Clustering the next-Generation Sequencing Data. *Bioinformatics* **2012**, *28*, 3150–3152, doi:10.1093/bioinformatics/bts565.

[199] Seppey, M.; Manni, M.; Zdobnov, E.M. BUSCO: Assessing Genome Assembly and Annotation Completeness. In *Methods in Molecular Biology*; Humana Press Inc., 2019; Vol. 1962, pp. 227–245.

[200] Dobin, A.; Davis, C.A.; Schlesinger, F.; Drenkow, J.; Zaleski, C.; Jha, S.; Batut, P.; Chaisson, M.; Gingeras, T.R. STAR: Ultrafast Universal RNA-Seq Aligner. *Bioinformatics* **2013**, *29*, 15, doi:10.1093/BIOINFORMATICS/BTS635.

[201] Haas, B.J.; Papanicolaou, A.; Yassour, M.; Grabherr, M.; Blood, P.D.; Bowden, J.; Couger, M.B.; Eccles, D.; Li, B.; Lieber, M.; et al. De Novo Transcript Sequence Reconstruction from RNA-Seq Using the Trinity Platform for Reference Generation and Analysis. *Nat Protoc* **2013**, *8*, 1494–1512, doi:10.1038/nprot.2013.084.

[202] Consortium, T.U. UniProt: A Worldwide Hub of Protein Knowledge. *Nucleic Acids Res* **2018**, *47*, D506–D515, doi:10.1093/nar/gky1049.

[203] Altschul, S.F.; Gish, W.; Miller, W.; Myers, E.W.; Lipman, D.J. Basic Local Alignment Search Tool. *J Mol Biol* **1990**, *215*, 403–410, doi:10.1016/S0022-2836(05)80360-2.

[204] Boutet, E.; Lieberherr, D.; Tognolli, M.; Schneider, M.; Bairoch, A. UniProtKB/Swiss-Prot. *Methods Mol Biol* **2007**, *406*, 89–112, doi:10.1007/978-1-59745-535-0_4.

[205] Suzek, B.E.; Wang, Y.; Huang, H.; McGarvey, P.B.; Wu, C.H. UniRef Clusters: A Comprehensive and Scalable Alternative for Improving Sequence Similarity Searches. *Bioinformatics* **2015**, *31*, 926, doi:10.1093/BIOINFORMATICS/BTU739.

[206] Ribeiro, J.M.C.; Mans, B.J. TickSialoFam (TSFam): A Database That Helps to Classify Tick Salivary Proteins, a Review on Tick Salivary Protein Function and Evolution, With Considerations on the Tick Sialome Switching Phenomenon. *Front Cell Infect Microbiol* **2020**, *10*, 374, doi:10.3389/fcimb.2020.00374.

[207] Götz, S.; García-Gómez, J.M.; Terol, J.; Williams, T.D.; Nagaraj, S.H.; Nueda, M.J.; Robles, M.; Talón, M.; Dopazo, J.; Conesa, A. High-Throughput Functional Annotation and Data Mining with the Blast2GO Suite. *Nucleic Acids Res* **2008**, *36*, 3420–3435, doi:10.1093/NAR/GKN176.

[208] Jones, P.; Binns, D.; Chang, H.Y.; Fraser, M.; Li, W.; McAnulla, C.; McWilliam, H.; Maslen, J.; Mitchell, A.; Nuka, G.; et al. InterProScan 5: Genome-Scale Protein Function Classification. *Bioinformatics* **2014**, *30*, 1236, doi:10.1093/BIOINFORMATICS/BTU031.

[209] Käll, L.; Krogh, A.; Sonnhammer, E.L.L. Advantages of Combined Transmembrane Topology and Signal Peptide Prediction-the Phobius Web Server. *Nucleic Acids Res* **2007**, *35*, doi:10.1093/nar/gkm256.

[210] Almagro Armenteros, J.J.; Tsirigos, K.D.; Sønderby, C.K.; Petersen, T.N.; Winther, O.; Brunak, S.; von Heijne, G.; Nielsen, H. SignalP 5.0 Improves Signal Peptide Predictions Using Deep Neural Networks. *Nat Biotechnol* **2019**, *37*, 420–423, doi:10.1038/s41587-019-0036-z.

[211] Krogh, A.; Larsson, B.; Von Heijne, G.; Sonnhammer, E.L.L. Predicting Transmembrane Protein Topology with a Hidden Markov Model: Application to Complete Genomes. *J Mol Biol* **2001**, *305*, 567–580, doi:10.1006/jmbi.2000.4315.

[212] Sturm, M.; Hackenberg, M.; Langenberger, D.; Frishman, D. TargetSpy: A Supervised Machine Learning Approach for MicroRNA Target Prediction. *BMC Bioinformatics* **2010**, *11*, doi:10.1186/1471-2105-11-292.

[213] Kertesz, M.; Iovino, N.; Unnerstall, U.; Gaul, U.; Segal, E. The Role of Site Accessibility in MicroRNA Target Recognition. *Nat Genet* **2007**, *39*, 1278–1284, doi:10.1038/ng2135.

[214] John, B.; Enright, A.J.; Aravin, A.; Tuschl, T.; Sander, C.; Marks, D.S. Human MicroRNA Targets. *PLoS Biol* **2004**, *2*, doi:10.1371/journal.pbio.0020363.

[215] Leclercq, M.; Diallo, A.B.; Blanchette, M. Prediction of Human MiRNA Target Genes Using Computationally Reconstructed Ancestral Mammalian Sequences. *Nucleic Acids Res* **2016**, *45*, 556, doi:10.1093/NAR/GKW1085.

[216] Rice, P.; Longden, I.; Bleasby, A. EMBOSS: The European Molecular Biology Open Software Suite. *Trends Genet* **2000**, *16*, 276–277, doi:10.1016/s0168-9525(00)02024-2.

[217] Babraham Bioinformatics Babraham Bioinformatics - Trim Galore Available online: https://www.bioinformatics.babraham.ac.uk/projects/trim_galore/ (accessed on 4 July 2018).

[218] Martin, M. Cutadapt Removes Adapter Sequences from High-Throughput Sequencing Reads. *EMBnet J* **2011**, *17*, 10, doi:10.14806/ej.17.1.200.

[219] Babraham Bioinformatics Babraham Bioinformatics - FastQC A Quality Control Tool for High Throughput Sequence Data Available online: https://www.bioinformatics.babraham.ac.uk/projects/fastqc/ (accessed on 4 July 2018).

[220] Ewels, P.; Magnusson, M.; Lundin, S.; Käller, M. MultiQC: Summarize Analysis Results for Multiple Tools and Samples in a Single Report. *Bioinformatics* **2016**, *32*, 3047–3048, doi:10.1093/bioinformatics/btw354.

[221] Li, B.; Dewey, C.N. RSEM: Accurate Transcript Quantification from RNA-Seq Data with or without a Reference Genome. *BMC Bioinformatics* **2011**, *12*, 323, doi:10.1186/1471-2105-12-323.

[222] Langmead, B.; Salzberg, S.L. Fast Gapped-Read Alignment with Bowtie 2. *Nature Methods 2012 9:4* **2012**, *9*, 357–359, doi:10.1038/nmeth.1923.

[223] Pedregosa, F.; Michel, V.; Grisel, O.; Blondel, M.; Prettenhofer, P.; Weiss, R.; Vanderplas, J.; Cournapeau, D.; Pedregosa, F.; Varoquaux, G.; et al. Scikit-Learn: Machine Learning in Python. *Journal of Machine Learning Research* **2011**, *12*, 2825–2830.

[224] Kolde, R. Pheatmap: Pretty Heatmaps 2018.

[225] Virtanen, P.; Gommers, R.; Oliphant, T.E.; Haberland, M.; Reddy, T.; Cournapeau, D.; Burovski, E.; Peterson, P.; Weckesser, W.; Bright, J.; et al. SciPy 1.0: Fundamental Algorithms for Scientific Computing in Python. *Nature Methods 2020 17:3* **2020**, *17*, 261–272, doi:10.1038/s41592-019-0686-2.

[226] R Core Team R: A Language and Environment for Statistical Computing 2025.

[227] Ward, J.H. Hierarchical Grouping to Optimize an Objective Function. *J Am Stat Assoc* **1963**, *58*, 236, doi:10.2307/2282967.

[228] Nueda, M.J.; Tarazona, S.; Conesa, A. Next MaSigPro: Updating MaSigPro Bioconductor Package for RNA-Seq Time Series. *Bioinformatics* **2014**, *30*, 2598, doi:10.1093/BIOINFORMATICS/BTU333.

[229] Robinson, M.D.; McCarthy, D.J.; Smyth, G.K. EdgeR: A Bioconductor Package for Differential Expression Analysis of Digital Gene Expression Data. *Bioinformatics* **2010**, *26*, 139, doi:10.1093/BIOINFORMATICS/BTP616.

[230] Varoquaux, N.; Purdom, E. A Pipeline to Analyse Time-Course Gene Expression Data. *F1000Res* **2020**, *9*, 1447, doi:10.12688/F1000RESEARCH.27262.1.

[231] Wang, M.; Zhao, Y.; Zhang, B. Efficient Test and Visualization of Multi-Set Intersections. *Sci Rep* **2015**, *5*, doi:10.1038/SREP16923.

[232] Yu, G.; Wang, L.-G.; Han, Y.; He, Q.-Y. ClusterProfiler: An R Package for Comparing Biological Themes among Gene Clusters. *OMICS* **2012**, *16*, 284–287, doi:10.1089/omi.2011.0118.

[233] Liberzon, A.; Birger, C.; Thorvaldsdóttir, H.; Ghandi, M.; Mesirov, J.P.; Tamayo, P. The Molecular Signatures Database (MSigDB) Hallmark Gene Set Collection. *Cell Syst* **2015**, *1*, 417–425, doi:10.1016/j.cels.2015.12.004.

[234] M, K.; Y, S.; M, K.; M, F.; M, T. KEGG as a Reference Resource for Gene and Protein Annotation. *Nucleic Acids Res* **2016**, *44*, doi:10.1093/NAR/GKV1070.

[235] Milacic, M.; Beavers, D.; Conley, P.; Gong, C.; Gillespie, M.; Griss, J.; Haw, R.; Jassal, B.; Matthews, L.; May, B.; et al. The Reactome Pathway Knowledgebase 2024. *Nucleic Acids Res* **2024**, *52*, D672–D678, doi:10.1093/nar/gkad1025.

[236] Agrawal, A.; Balcı, H.; Hanspers, K.; Coort, S.L.; Martens, M.; Slenter, D.N.; Ehrhart, F.; Digles, D.; Waagmeester, A.; Wassink, I.; et al. WikiPathways 2024: Next Generation Pathway Database. *Nucleic Acids Res* **2024**, *52*, D679–D689, doi:10.1093/nar/gkad960.

[237] SA, A.; J, B.; S, C.; JM, C.; HJ, D.; D, E.; M, F.; P, G.; NL, H.; DP, H.; et al. The Gene Ontology Knowledgebase in 2023. *Genetics* **2023**, *224*, doi:10.1093/GENETICS/IYAD031.

[238] G, E.; E, D.; S, A.; E, F.; A, S.; M, S.; J, W.; N, V.W.; JM, R.; J, W.; et al. Single-Nucleus Cross-Tissue Molecular Reference Maps toward Understanding Disease Gene Function. *Science* **2022**, *376*, doi:10.1126/SCIENCE.ABL4290.

[239] Szklarczyk, D.; Gable, A.L.; Nastou, K.C.; Lyon, D.; Kirsch, R.; Pyysalo, S.; Doncheva, N.T.; Legeay, M.; Fang, T.; Bork, P.; et al. The STRING Database in 2021: Customizable Protein-Protein Networks, and Functional Characterization of User-Uploaded Gene/Measurement Sets. *Nucleic Acids Res* **2021**, *49*, D605–D612, doi:10.1093/NAR/GKAA1074.

[240] Agrawal, R.; Mannila, H.; Srikant, R.; Toivonen, H.; Verkamo, a I. Fast Discovery of Association Rules. *Advances in knowledge discovery and data mining* **1996**, *12*, 307–328.

[241] Preusse, M.; Theis, F.J.; Mueller, N.S. MiTALOS v2: Analyzing Tissue Specific MicroRNA Function. *PLoS One* **2016**, *11*, doi:10.1371/JOURNAL.PONE.0151771.

[242] Vlachos, I.S.; Zagganas, K.; Paraskevopoulou, M.D.; Georgakilas, G.; Karagkouni, D.; Vergoulis, T.; Dalamagas, T.; Hatzigeorgiou, A.G. DIANA-MiRPath v3.0: Deciphering MicroRNA Function with Experimental Support. *Nucleic Acids Res* **2015**, *43*, W460–W466, doi:10.1093/NAR/GKV403.

[243] Shannon, P.; Markiel, A.; Ozier, O.; Baliga, N.S.; Wang, J.T.; Ramage, D.; Amin, N.; Schwikowski, B.; Ideker, T. Cytoscape: A Software Environment for Integrated Models of Biomolecular Interaction Networks. *Genome Res* **2003**, *13*, 2498–2504, doi:10.1101/gr.1239303.

[244] Szklarczyk, D.; Kirsch, R.; Koutrouli, M.; Nastou, K.; Mehryary, F.; Hachilif, R.; Gable, A.L.; Fang, T.; Doncheva, N.T.; Pyysalo, S.; et al. The STRING Database in 2023: Protein-Protein Association Networks and Functional Enrichment Analyses for Any Sequenced Genome of Interest. *Nucleic Acids Res* **2023**, *51*, D638–D646, doi:10.1093/nar/gkac1000.

[245] Scardoni, G.; Tosadori, G.; Faizan, M.; Spoto, F.; Fabbri, F.; Laudanna, C. Biological Network Analysis with CentiScaPe: Centralities and Experimental Dataset Integration. *F1000Res* **2014**, *3*, 139, doi:10.12688/f1000research.4477.2.

[246] Django Software Foundation Django 2019.

[247] Blanco-Míguez, A.; Fdez-Riverola, F.; Sánchez, B.; Lourenço, A. BlasterJS: A Novel Interactive JavaScript Visualisation Component for BLAST Alignment Results. *PLoS One* **2018**, *13*, e0205286, doi:10.1371/JOURNAL.PONE.0205286.

[248] Marcinkowska, M.; Szymanski, M.; Krzyzosiak, W.J.; Kozlowski, P. Copy Number Variation of MicroRNA Genes in the Human Genome. *BMC Genomics* **2011**, *12*, 183, doi:10.1186/1471-2164-12-183.

[249] Sun, J.; Liu, H.-P.; Deng, J.-E.; Zhou, M. Systematic Analysis of Genomic Organization and Heterogeneities of MiRNA Cluster in Vertebrates. *Mol Biol Rep* **2012**, *39*, 5143–5149, doi:10.1007/s11033-011-1310-4.

[250] Guo, L.; Zhao, Y.; Zhang, H.; Yang, S.; Chen, F. Integrated Evolutionary Analysis of Human MiRNA Gene Clusters and Families Implicates

Evolutionary Relationships. *Gene* **2014**, *534*, 24–32, doi:10.1016/j.gene.2013.10.037.

[251] Agarwal, V.; Bell, G.W.; Nam, J.W.; Bartel, D.P. Predicting Effective MicroRNA Target Sites in Mammalian MRNAs. *Elife* **2015**, *4*, doi:10.7554/ELIFE.05005.

[252] Pinzón, N.; Li, B.; Martinez, L.; Sergeeva, A.; Presumey, J.; Apparailly, F.; Seitz, H. MicroRNA Target Prediction Programs Predict Many False Positives. *Genome Res* **2017**, *27*, 234–245, doi:10.1101/GR.205146.116/-/DC1.

[253] Whyte, J.L.; Smith, A.A.; Helms, J.A. Wnt Signaling and Injury Repair. *Cold Spring Harb Perspect Biol* **2012**, *4*, a008078, doi:10.1101/CSHPERSPECT.A008078.

[254] Suzdaltseva, Y.; Selezneva, A.; Sergeev, N.; Kiselev, S.L. Initial WNT/β-Catenin or BMP Activation Modulates Inflammatory Response of Mesodermal Progenitors Derived from Human Induced Pluripotent Stem Cells. *Cells 2024, Vol. 13, Page 1820* **2024**, *13*, 1820, doi:10.3390/CELLS13211820.

[255] MO, L.; YY, W.; S, S.; AK, R.; RA, F. Transforming Growth Factor-Beta Regulation of Immune Responses. *Annu Rev Immunol* **2006**, *24*, doi:10.1146/ANNUREV.IMMUNOL.24.021605.090737.

[256] Zhong, X.-P.; Shin, J.; Gorentla, B.K.; O'Brien, T.; Srivatsan, S.; Xu, L.; Chen, Y.; Xie, D.; Pan, H. Receptor Signaling in Immune Cell Development and Function. *Immunol Res* **2011**, *49*, 109–123, doi:10.1007/s12026-010-8175-9.

[257] Canesin, G.; Hejazi, S.M.; Swanson, K.D.; Wegiel, B. Heme-Derived Metabolic Signals Dictate Immune Responses. *Front Immunol* **2020**, *11*, 509356, doi:10.3389/fimmu.2020.00066.

[258] Huang, C.-H.; Yang, T.-T.; Lin, K.-I. Mechanisms and Functions of SUMOylation in Health and Disease: A Review Focusing on Immune Cells. *J Biomed Sci* **2024**, *31*, 16, doi:10.1186/s12929-024-01003-y.

[259] Park, J.F.; Luo, Z.D. Calcium Channel Functions in Pain Processing. *Channels* **2010**, *4*, 510, doi:10.4161/CHAN.4.6.12869.

[260] J, D.; SM, G.; A, B.; P, J.; N, B.-B.; D, R.; H, L. Linking MECP2 and Pain Sensitivity: The Example of Rett Syndrome. *Am J Med Genet A* **2010**, *152A*, doi:10.1002/AJMG.A.33314.

[261] Damo, E.; Simonetti, M. Axon Guidance Molecules and Pain. *Cells* **2022**, *11*, 3143, doi:10.3390/cells11193143.

[262] Greenhalgh, D.G. The Role of Growth Factors in Wound Healing. *J Trauma* **1996**, *41*, 159–167, doi:10.1097/00005373-199607000-00029.

[263] MO, L.; YY, W.; S, S.; AK, R.; RA, F. Transforming Growth Factor-Beta Regulation of Immune Responses. *Annu Rev Immunol* **2006**, *24*, doi:10.1146/ANNUREV.IMMUNOL.24.021605.090737.

[264] K, I.; A, E.; S, A.; A, S. Control of Immunity and Allergy by Steroid Hormones. *Allergol Int* **2022**, *71*, doi:10.1016/J.ALIT.2022.07.006.

[265] Makhijani, P.; Basso, P.J.; Chan, Y.T.; Chen, N.; Baechle, J.; Khan, S.; Furman, D.; Tsai, S.; Winer, D.A. Regulation of the Immune System by the Insulin Receptor in Health and Disease. *Front Endocrinol (Lausanne)* **2023**, *14*, 1128622, doi:10.3389/fendo.2023.1128622.

[266] Ramirez-GarciaLuna, J.L.; Rangel-Berridi, K.; Bergeron, A.; Kolosovas-Machuca, E.S.; Wang, S.C.; Berry, G.K.; Martinez-Jimenez, M.A. Local Insulin Improves Wound Healing: A Systematic Review and Bayesian Network Meta-Analysis. *Plast Reconstr Surg* **2023**, doi:10.1097/PRS.0000000000010432.

[267] Z, L.; R, M.; J, T.; C, L.; Y, X.; X, Q.; S, J.; P, O.; Y, Z.; X, X.; et al. Hormonal Interventions in Skin Wounds - a Mini Review. *Mol Med* **2024**, *30*, doi:10.1186/S10020-024-00978-6.

[268] Paget, M.; Cadena, C.; Ahmad, S.; Wang, H.-T.; Jordan, T.X.; Kim, E.; Koo, B.; Lyons, S.M.; Ivanov, P.; tenOever, B.; et al. Stress Granules Are Shock Absorbers That Prevent Excessive Innate Immune Responses to DsRNA. *Mol Cell* **2023**, *83*, 1180-1196.e8, doi:10.1016/j.molcel.2023.03.010.

[269] EM, M. Human Natural Killer Cells: Form, Function, and Development. *J Allergy Clin Immunol* **2023**, *151*, doi:10.1016/J.JACI.2022.09.022.

[270] Bainbridge, P. Wound Healing and the Role of Fibroblasts. *J Wound Care* **2013**, *22*, 407–408, 410–412, doi:10.12968/jowc.2013.22.8.407.

[271] R, S.; JS, R.; M, K.; B, H. The Inflammatory Speech of Fibroblasts. *Immunol Rev* **2021**, *302*, doi:10.1111/IMR.12971.

[272] M, V.; B, D.C.; H, C.; AM, B.; C, C.; J, D.; J, V.; P, M.; G, D. Glypican-6, a New Member of the Glypican Family of Cell Surface Heparan Sulfate Proteoglycans. *J Biol Chem* **1999**, *274*, doi:10.1074/JBC.274.38.26968.

[273] Kataria, H.; Alizadeh, A.; Karimi-Abdolrezaee, S. Neuregulin-1/ErbB Network: An Emerging Modulator of Nervous System Injury and Repair. *Prog Neurobiol* **2019**, *180*, 101643, doi:10.1016/j.pneurobio.2019.101643.

[274] SM, K.; JH, K.; SY, W.; SJ, O.; IY, L.; YK, B.; KW, C.; BO, C.; B, P.; EJ, C.; et al. CEP41-Mediated Ciliary Tubulin Glutamylation Drives Angiogenesis through AURKA-Dependent Deciliation. *EMBO Rep* **2020**, *21*, doi:10.15252/EMBR.201948290.

[275] Yao, L.; Rathnakar, B.H.; Kwon, H.R.; Sakashita, H.; Kim, J.H.; Rackley, A.; Tomasek, J.J.; Berry, W.L.; Olson, L.E. Temporal Control of PDGFRα Regulates the Fibroblast-to-Myofibroblast Transition in Wound Healing. *Cell Rep* **2022**, *40*, 111192, doi:10.1016/j.celrep.2022.111192.

[276] Akbari, P.; Vuckovic, D.; Stefanucci, L.; Jiang, T.; Kundu, K.; Kreuzhuber, R.; Bao, E.L.; Collins, J.H.; Downes, K.; Grassi, L.; et al. A Genome-Wide Association Study of Blood Cell Morphology Identifies Cellular Proteins Implicated in Disease Aetiology. *Nat Commun* **2023**, *14*, 5023, doi:10.1038/s41467-023-40679-y.

[277] WJ, Q.; JJ, S.; RY, C.; CY, L.; YJ, L.; JF, L.; GJ, Y.; JF, C.; J, C. Curriculum Vitae of CUG Binding Protein 1 (CELF1) in Homeostasis and Diseases: A Systematic Review. *Cell Mol Biol Lett* **2024**, *29*, doi:10.1186/S11658-024-00556-Y.

[278] T, A.; D, B.; RF, D. A Network Approach to Wound Healing. *Adv Wound Care (New Rochelle)* **2013**, *2*, doi:10.1089/WOUND.2012.0386.

[279] Ye, X.; Ong, N.; An, H.; Zheng, Y. The Emerging Roles of NDR1/2 in Infection and Inflammation. *Front Immunol* **2020**, *11*, 534, doi:10.3389/fimmu.2020.00534.

[280] Erdoğan, Ö.; Xie, L.; Wang, L.; Wu, B.; Kong, Q.; Wan, Y.; Chen, X. Proteomic Dissection of LPS-Inducible, PHF8-Dependent Secretome Reveals Novel Roles of PHF8 in TLR4-Induced Acute Inflammation and T Cell Proliferation. *Sci Rep* **2016**, *6*, 24833, doi:10.1038/srep24833.

[281] K, H.; M, S.; A, I. Toll-like Receptor 9 Trafficking and Signaling for Type I Interferons Requires PIKfyve Activity. *Int Immunol* **2015**, *27*, doi:10.1093/INTIMM/DXV021.

[282] Dayam, R.M.; Sun, C.X.; Choy, C.H.; Mancuso, G.; Glogauer, M.; Botelho, R.J. The Lipid Kinase PIKfyve Coordinates the Neutrophil Immune Response through the Activation of the Rac GTPase. *J Immunol* **2017**, *199*, 2096–2105, doi:10.4049/jimmunol.1601466.

[283] Forwood, J.K.; Thakur, A.S.; Guncar, G.; Marfori, M.; Mouradov, D.; Meng, W.; Robinson, J.; Huber, T.; Kellie, S.; Martin, J.L.; et al. Structural Basis for Recruitment of Tandem Hotdog Domains in Acyl-CoA Thioesterase 7 and Its Role in Inflammation. *Proceedings of the National Academy of Sciences* **2007**, *104*, 10382–10387, doi:10.1073/pnas.0700974104.

[284] Hock, A.K.; Vigneron, A.M.; Vousden, K.H. Ubiquitin-Specific Peptidase 42 (USP42) Functions to Deubiquitylate Histones and Regulate Transcriptional Activity. *J Biol Chem* **2014**, *289*, 34862–34870, doi:10.1074/jbc.M114.589267.

[285] Tarcic, O.; Pateras, I.S.; Cooks, T.; Shema, E.; Kanterman, J.; Ashkenazi, H.; Boocholez, H.; Hubert, A.; Rotkopf, R.; Baniyash, M.; et al. RNF20 Links Histone H2B Ubiquitylation with Inflammation and Inflammation-Associated Cancer. *Cell Rep* **2016**, *14*, 1462–1476, doi:10.1016/j.celrep.2016.01.020.

[286] K, L.; Y, K.; SJ, L.; Y, Q.; D, L.; HW, L.; H, K.; HS, J.; TC, S.; J, K. MDGAs Interact Selectively with Neuroligin-2 but Not Other Neuroligins to Regulate Inhibitory Synapse Development. *Proc Natl Acad Sci U S A* **2013**, *110*, doi:10.1073/PNAS.1219987110.

[287] Liu, P.; Song, C.; Wang, C.; Li, Y.; Su, L.; Li, J.; Zhao, Q.; Wang, Z.; Shen, M.; Wang, G.; et al. Spinal SNAP-25 Regulates Membrane Trafficking of GluA1-

Containing AMPA Receptors in Spinal Injury-Induced Neuropathic Pain in Rats. *Neurosci Lett* **2020**, *715*, 134616, doi:10.1016/j.neulet.2019.134616.

[288] Jin, L.; Liu, Y.; Wu, Y.; Huang, Y.; Zhang, D. REST Is Not Resting: REST/NRSF in Health and Disease. *Biomolecules* **2023**, *13*, 1477, doi:10.3390/BIOM13101477.

[289] A, K.; J, M.; M, Ø.; A, M.; J, M.; F, L.; W, N.; TH, S.; JB, S. SNAP25 Disease Mutations Change the Energy Landscape for Synaptic Exocytosis Due to Aberrant SNARE Interactions. *Elife* **2024**, *12*, doi:10.7554/ELIFE.88619.

[290] Trager, W. Acquired Immunity to Ticks. *J Parasitol* **1939**, *25*, 57, doi:10.2307/3272160.

[291] Bateman, A.; Martin, M.J.; Orchard, S.; Magrane, M.; Ahmad, S.; Alpi, E.; Bowler-Barnett, E.H.; Britto, R.; Bye-A-Jee, H.; Cukura, A.; et al. UniProt: The Universal Protein Knowledgebase in 2023. *Nucleic Acids Res* **2023**, *51*, D523–D531, doi:10.1093/NAR/GKAC1052.

[292] Narasimhan, S.; Deponte, K.; Marcantonio, N.; Liang, X.; Royce, T.E.; Nelson, K.F.; Booth, C.J.; Koski, B.; Anderson, J.F.; Kantor, F.; et al. Immunity against Ixodes Scapularis Salivary Proteins Expressed within 24 Hours of Attachment Thwarts Tick Feeding and Impairs Borrelia Transmission. *PLoS One* **2007**, *2*, e451, doi:10.1371/journal.pone.0000451.

[293] Tirloni, L.; Lu, S.; Calvo, E.; Sabadin, G.; Di Maggio, L.S.; Suzuki, M.; Nardone, G.; da Silva Vaz, I.; Ribeiro, J.M.C. Integrated Analysis of Sialotranscriptome and Sialoproteome of the Brown Dog Tick Rhipicephalus Sanguineus (s.l.): Insights into Gene Expression during Blood Feeding. *J Proteomics* **2020**, *229*, 103899, doi:10.1016/j.jprot.2020.103899.

[294] Kotsyfakis, M.; Schwarz, A.; Erhart, J.; Ribeiro, J.M.C. Tissue- and Time-Dependent Transcription in Ixodes Ricinus Salivary Glands and Midguts When Blood Feeding on the Vertebrate Host. *Scientific Reports 2015 5:1* **2015**, *5*, 1–10, doi:10.1038/srep09103.

[295] Rosendale, A.J.; Dunlevy, M.E.; McCue, M.D.; Benoit, J.B. Progressive Behavioural, Physiological and Transcriptomic Shifts over the Course of Prolonged Starvation in Ticks. *Mol Ecol* **2019**, *28*, 49–65, doi:10.1111/MEC.14949.

[296] Mulenga, A.; Kim, T.; Ibelli, A.M.G. Amblyomma Americanum Tick Saliva Serine Protease Inhibitor 6 Is a Cross-Class Inhibitor of Serine Proteases and Papain-like Cysteine Proteases That Delays Plasma Clotting and Inhibits Platelet Aggregation. *Insect Mol Biol* **2013**, *22*, 306–319, doi:10.1111/IMB.12024.

[297] Vechtova, P.; Sterbova, J.; Sterba, J.; Vancova, M.; Rego, R.O.M.; Selinger, M.; Strnad, M.; Golovchenko, M.; Rudenko, N.; Grubhoffer, L. A Bite so Sweet: The Glycobiology Interface of Tick-Host-Pathogen Interactions. *Parasites & Vectors 2018 11:1* **2018**, *11*, 1–27, doi:10.1186/S13071-018-3062-7.

[298] Perner, J.; Kropáčková, S.; Kopáček, P.; Ribeiro, J.M.C. Sialome Diversity of Ticks Revealed by RNAseq of Single Tick Salivary Glands. *PLoS Negl Trop Dis* **2018**, *12*, doi:10.1371/journal.pntd.0006410.

[299] Gray, E.; Hogwood, J.; Mulloy, B. The Anticoagulant and Antithrombotic Mechanisms of Heparin. *Handb Exp Pharmacol* **2012**, *207*, 43–61, doi:10.1007/978-3-642-23056-1_3.

[300] Li, M.O.; Wan, Y.Y.; Sanjabi, S.; Robertson, A.K.L.; Flavell, R.A. Transforming Growth Factor-Beta Regulation of Immune Responses.

Annu Rev Immunol **2006**, *24*, 99–146, doi:10.1146/ANNUREV.IMMUNOL.24.021605.090737.

[301] Martínez, V.G.; Hernández-López, C.; Valencia, J.; Hidalgo, L.; Entrena, A.; Zapata, A.G.; Vicente, A.; Sacedón, R.; Varas, A. The Canonical BMP Signaling Pathway Is Involved in Human Monocyte-Derived Dendritic Cell Maturation. *Immunol Cell Biol* **2011**, *89*, 610–618, doi:10.1038/ICB.2010.135.

[302] MacDonald, L.A.; Cohen, A.; Baron, S.; Burchfiel, C.M. MacDonald et al. Respond to "Search for Preventable Causes of Cardiovascular Disease." *Am J Epidemiol* **2009**, *169*, 1426–1427, doi:10.1093/AJE/KWP080.

[303] Kim, M.; Choi, S.H.; Jin, Y.B.; Lee, H.J.; Ji, Y.H.; Kim, J.; Lee, Y.S.; Lee, Y.J. The Effect of Oxidized Low-Density Lipoprotein (Ox-LDL) on Radiation-Induced Endothelial-to-Mesenchymal Transition. *Int J Radiat Biol* **2013**, *89*, 356–363, doi:10.3109/09553002.2013.763193.

[304] Basson, M.D.; Sanders, M.A.; Gomez, R.; Hatfield, J.; VanderHeide, R.; Thamilselvan, V.; Zhang, J.; Walsh, M.F. Focal Adhesion Kinase Protein Levels in Gut Epithelial Motility. *Am J Physiol Gastrointest Liver Physiol* **2006**, *291*, doi:10.1152/AJPGI.00292.2005.

[305] Sheng, H.; Shao, J.; Townsend, C.M.; Evers, B.M. Phosphatidylinositol 3-Kinase Mediates Proliferative Signals in Intestinal Epithelial Cells. *Gut* **2003**, *52*, 1472–1478, doi:10.1136/GUT.52.10.1472.

[306] Chen, L.; Chi, H.; Kinashi, T. Editorial: Hippo Signaling in the Immune System. *Front Immunol* **2020**, *11*, 587514, doi:10.3389/FIMMU.2020.587514.

[307] Wang, Y.; Malik, A.B.; Sun, Y.; Hu, S.; Reynolds, A.B.; Minshall, R.D.; Hu, G. Innate Immune Function of the Adherens Junction Protein P120-

Catenin in Endothelial Response to Endotoxin. *J Immunol* **2011**, *186*, 3180, doi:10.4049/JIMMUNOL.1001252.

[308] Tian, E.; Ten Hagen, K.G. Recent Insights into the Biological Roles of Mucin-Type O-Glycosylation. *Glycoconj J* **2009**, *26*, 325–334, doi:10.1007/S10719-008-9162-4.

[309] Varki, A. Biological Roles of Glycans. *Glycobiology* **2017**, *27*, 3–49, doi:10.1093/GLYCOB/CWW086.

[310] Pinho, S.S.; Alves, I.; Gaifem, J.; Rabinovich, G.A. Immune Regulatory Networks Coordinated by Glycans and Glycan-Binding Proteins in Autoimmunity and Infection. *Cell Mol Immunol* **2023**, *20*, 1101–1113, doi:10.1038/s41423-023-01074-1.

[311] Sutherland, T.E.; Dyer, D.P.; Allen, J.E. The Extracellular Matrix and the Immune System: A Mutually Dependent Relationship. *Science* **2023**, *379*, eabp8964, doi:10.1126/science.abp8964.

[312] Nunes-Santos, C.J.; Uzel, G.; Rosenzweig, S.D. PI3K Pathway Defects Leading to Immunodeficiency and Immune Dysregulation. *J Allergy Clin Immunol* **2019**, *143*, 1676–1687, doi:10.1016/j.jaci.2019.03.017.

[313] Fridrich, A.; Hazan, Y.; Moran, Y. Too Many False Targets for MicroRNAs: Challenges and Pitfalls in Prediction of MiRNA Targets and Their Gene Ontology in Model and Non-Model Organisms. *Bioessays* **2019**, *41*, e1800169, doi:10.1002/bies.201800169.

[314] Wang, X.; El Naqa, I.M. Prediction of Both Conserved and Nonconserved MicroRNA Targets in Animals. *Bioinformatics* **2008**, *24*, 325–332, doi:10.1093/bioinformatics/btm595.

[315] Hwang, H.; Chang, H.R.; Baek, D. Determinants of Functional MicroRNA Targeting. *Mol Cells* **2023**, *46*, 21–32, doi:10.14348/molcells.2023.2157.

[316] Marth, J.D.; Grewal, P.K. Mammalian Glycosylation in Immunity. *Nat Rev Immunol* **2008**, *8*, 874–887, doi:10.1038/nri2417.

[317] Kobata, A. The N-Linked Sugar Chains of Human Immunoglobulin G: Their Unique Pattern, and Their Functional Roles. *Biochim Biophys Acta* **2008**, *1780*, 472–478, doi:10.1016/j.bbagen.2007.06.012.

[318] A, V.; RD, C.; JD, E.; HH, F.; P, S.; CR, B.; GW, H.; ME, E. *Essentials of Glycobiology*; 2009; ISBN 9780879697709.

[319] Williams, C.; Royo, F.; Aizpurua-Olaizola, O.; Pazos, R.; Boons, G.-J.; Reichardt, N.-C.; Falcon-Perez, J.M. Glycosylation of Extracellular Vesicles: Current Knowledge, Tools and Clinical Perspectives. *J Extracell Vesicles* **2018**, *7*, 1442985, doi:10.1080/20013078.2018.1442985.

[320] Brillante, S.; Volpe, M.; Indrieri, A. Advances in MicroRNA Therapeutics: From Preclinical to Clinical Studies. *Hum Gene Ther* **2024**, *35*, 628–648, doi:10.1089/hum.2024.113.

[321] Holjencin, C.; Jakymiw, A. MicroRNAs and Their Big Therapeutic Impacts: Delivery Strategies for Cancer Intervention. *Cells* **2022**, *11*, doi:10.3390/cells11152332.

[322] de la Fuente, J.; Canales, M.; Kocan, K.M. The Importance of Protein Glycosylation in Development of Novel Tick Vaccine Strategies. *Parasite Immunol* **2006**, *28*, 687–688, doi:10.1111/j.1365-3024.2006.00902.x.

[323] What Will It Take to Get MiRNA Therapies to Market? *Nat Biotechnol* **2024**, *42*, 1623–1624, doi:10.1038/s41587-024-02480-0.